Agenzia nazionale per le nuove tecnologie,
l'energia e lo sviluppo economico sostenibile

MINISTERO DELLO SVILUPPO ECONOMICO

Ricerca di Sistema elettrico

# BUGEND70.BOLIB - An ENEA-Bologna ENDF/B-VII.0 cross section library (47 n + 20 γ) in FIDO-ANISN format for LWR schielding and pressure vessel dosimetry applications

*M. Pescarini, V. Sinitsa, R. Orsi, M. Frisoni*

Report RdS/2013/056

# BUGENDF70.BOLIB - AN ENEA-BOLOGNA ENDF/B-VII.0 CROSS SECTION LIBRARY (47 n + 20 γ) IN FIDO-ANISN FORMAT FOR LWR SHIELDING AND PRESSURE VESSEL DOSIMETRY APPLICATIONS

M. Pescarini, R. Orsi, M. Frisoni (ENEA), V. Sinitsa (consultant IPPE-Obninsk)

Settembre 2013

Report Ricerca di Sistema Elettrico

Accordo di Programma Ministero dello Sviluppo Economico - ENEA
Piano Annuale di Realizzazione 2012
Area: Produzione di energia elettrica e protezione dell'ambiente
Progetto: Sviluppo competenze scientifiche nel campo della sicurezza nucleare e collaborazione ai programmi internazionali per il nucleare di IV Generazione
Obiettivo: Sviluppo competenze scientifiche nel campo della sicurezza nucleare
Responsabile del Progetto: Felice De Rosa, ENEA

**Titolo**

# BUGENDF70.BOLIB - An ENEA-Bologna ENDF/B-VII.0 Cross Section Library (47 n + 20 γ) in FIDO-ANISN Format for LWR Shielding and Pressure Vessel Dosimetry Applications

**Descrittori**

**Tipologia del documento:** Rapporto tecnico

**Collocazione contrattuale:** Accordo di programma ENEA-MSE su sicurezza nucleare e reattori di IV generazione

**Argomenti trattati:** Fisica nucleare, dati nucleari, fisica dei reattori nucleari

**Sommario**

The ENEA-Bologna Nuclear Data Group generated a broad-group coupled neutron and photon working cross section library in FIDO-ANISN format, dedicated to LWR shielding and pressure vessel dosimetry applications. This library, named BUGENDF70.BOLIB, was obtained in the neutron and photon energy group structures (47 n + 20 γ) of the ORNL BUGLE-96 similar library and it is based on the US ENDF/B-VII.0 library of evaluated nuclear data. BUGENDF70.BOLIB was produced through cross section collapsing of the ENEA-Bologna VITENDF70.BOLIB general-purpose library in AMPX format for nuclear fission applications using the updated and corrected ENEA-Bologna 2007 Revision of the ORNL SCAMPI nuclear data processing system. This library, based on the Bondarenko (f-factor) neutron resonance self-shielding method, has the same neutron and photon energy group structures (199 n + 42 γ) as the ORNL VITAMIN-B6 library in AMPX format (based on ENDF/B-VI.3 evaluated nuclear data) from which the BUGLE-96 library was generated at ORNL. A preliminary testing of the BUGENDF70.BOLIB library was performed through three-dimensional fixed source transport calculations with the TORT-3.2 discrete ordinates ($S_N$) code on the PCA-Replica 12/13 and VENUS-3 engineering neutron shielding benchmark experiments, specifically conceived to check the nuclear data and transport codes used in LWR radiation shielding and radiation damage analyses.

**Note**

Authors: Massimo PESCARINI, Valentin SINITSA*, Roberto ORSI, Manuela FRISONI

(*) ENEA Consultant, formerly at IPPE-Obninsk, Russian Federation.

**Copia n.** **In carico a:**

| | | | | | | |
|---|---|---|---|---|---|---|
| 2 | | | NOME | | | |
| | | | FIRMA | | | |
| 1 | | | NOME | | | |
| | | | FIRMA | | | |
| 0 | EMISSIONE | 04/06/2013 | NOME | M. Pescarini | F. Padoani | F. De Rosa |
| | | | FIRMA | M. Pescarini A. Padoani | | |
| REV. | DESCRIZIONE | DATA | | REDAZIONE | CONVALIDA | APPROVAZIONE |

INDEX

# BUGENDF70.BOLIB - An ENEA-Bologna ENDF/B-VII.0 Cross Section Library (47 n + 20 γ) in FIDO-ANISN Format for LWR Shielding and Pressure Vessel Dosimetry Applications

Massimo PESCARINI, Valentin SINITSA, Roberto ORSI, Manuela FRISONI

June 2013

## 1 - INTRODUCTION

Some years ago the ENEA-Bologna Nuclear Data Group started nuclear data processing and validation activities addressed to generate and/or to test broad-group coupled neutron/photon working cross section libraries, specifically dedicated to radiation shielding and radiation damage calculations for the light water nuclear fission reactors (LWRs) and, in particular, for the reactor pressure vessel (RPV) dosimetry analyses. The generation of working cross section libraries in ENEA-Bologna was initially /1/ and recently /2/ dedicated to the LWR radiation shielding and radiation damage applications since it was considered firstly important to produce working libraries for the most diffused types of nuclear power reactors all over the world. In fact about 81% of the 436 total world nuclear power reactor units are LWRs, i.e., 272 PWRs (about 62%) and 84 BWRs (about 19%), as reported in the June 3, 2013, updating of the IAEA-PRIS database.

It was considered useful (see in particular /3/) to offer new updated working cross section libraries specifically addressed, in particular, to improve the calculation accuracy of the radiation damage parameters like fast neutron flux, fast neutron fluence, iron displacement per atom rate (DPA/s) and total iron displacement per atom (DPA) in the structural components of the future and present operating LWRs. In fact in this kind of applications even more accuracy is required than in radiation shielding calculations where more conservative calculation approaches are usually applied. For example, in radiation damage calculations for the most important LWR component, the reactor pressure vessel, the calculation accuracy obtained is a fundamental parameter, directly linked with the RPV End-of-Life (EoL) prediction which is in its turn connected with well known fundamental nuclear safety aspects and relevant economic impacts.

The present technical report represents the user's manual of the ENEA-Bologna BUGENDF70.BOLIB broad-group coupled neutron/photon working cross section library in FIDO-ANISN /4/ format, dedicated to the previously cited LWR radiation shielding and radiation damage applications and, in particular, to the RPV dosimetry analyses. This library was obtained through problem-dependent cross section collapsing from the ENEA-Bologna VITENDF70.BOLIB /5/ fine-group cross section library for nuclear fission applications, based on the ENDF/B-VII.0 /6/ evaluated nuclear data library and on the Bondarenko /7/ (f-factor) method for the treatment of neutron resonance self-shielding and temperature effects. The VITENDF70.BOLIB library is a "pseudo-problem-independent" coupled neutron/photon library in AMPX format, i.e., a fine-group library prepared with enough detail in energy, temperatures and neutron resonance self-shielding so as to be applicable to a wide range of

physical systems. VITENDF70.BOLIB is characterized by the same neutron and photon energy group structures (199 neutron groups + 42 photon groups) as the ORNL DLC-0184/VITAMIN-B6 /8/ library in AMPX format, based on the ENDF/B-VI.3 /9/ evaluated data library. The BUGENDF70.BOLIB coupled working library adopts the neutron and photon energy group structures (47 neutron groups + 20 photon groups) of the ORNL DLC-0185/BUGLE-96 /8/ broad-group working library in FIDO-ANISN format, derived from the VITAMIN-B6 library and specifically conceived for the same previously cited applications in LWRs.

In particular broad-group working libraries, properly generated for the cited applications, are necessary to permit the use of the deterministic transport codes. The three-dimensional (3D) deterministic transport codes like, for example, the ORNL TORT /10/ discrete ordinates ($S_N$) code, can presently offer rigorous and reliable calculation solutions also for complex geometries, which could be described, up to few years ago, exclusively by the 3D stochastic transport codes like, for example, the LANL MCNP /11/ Monte Carlo code. In fact, if the 3D deterministic transport codes are properly assisted by dedicated pre/post-processor systems of programs (e.g., the ENEA-Bologna BOT3P /12/ /13/ /14/ /15/ and the Japanese TORTWARE /16/ systems) for the automatic generation and graphical verification of the spatial mesh grids of the reactor geometrical model, their performance can be highly competitive with that of the 3D Monte Carlo codes.

Despite the fact that, all over the world, the development of the 3D deterministic codes is going on and their use is increasingly appreciated also by the industrial organizations, it is not easy to find updated problem-dependent broad-group working cross section libraries for fission reactor shielding applications, free-released by the international distribution agencies (e.g., UNO-IAEA NDS, OECD-NEA Data Bank and ORNL-RSICC). In particular the packages of modular systems containing deterministic transport codes are distributed by the previously cited agencies without including working cross section libraries and this influences negatively the diffusion of the deterministic transport culture and expertise. This is mainly due to the fact that, in order to generate a problem-dependent broad-group working cross section library for the previously mentioned applications, it is necessary to collapse the fine-group cross sections of a multi-purpose library, as recommended by specific standards. This operation is performed using problem-dependent neutron and photon spectra for the various spatial regions of a specific type of reactor, pre-calculated with typical compositional, geometrical and temperature parameters. These data are very often considered confidential and this implies that these libraries are mainly produced for internal use and commercial purposes within the industrial organizations.

In this contribution, based on the compositional, geometrical and temperature parameters reported in the BUGLE-96 /8/ library user's manual for a typical PWR and a typical BWR, it was intentionally intended to follow the same data processing procedures and methodologies adopted at ORNL for the generation of the BUGLE-96 library which was widely and successfully used in LWR radiation shielding and radiation damage applications since 1996.
The LANL NJOY-99.259 /17/ and the ORNL SCAMPI /18/ nuclear data processing systems were selected and used to generate the group cross section libraries. NJOY-99.259 was employed, in particular, for the generation of the VITENDF70.BOLIB fine-group mother library. The so called ENEA-Bologna 2007 Revision /19/ of the SCAMPI system, an updated and corrected version specifically able, e.g., to process properly the recent nuclear data files

of the ENDF/B-VII.0 /6/ and JEFF-3.1.1 /20/ (see also /21/ and /22/) evaluated data libraries, was used to generate the BUGENDF70.BOLIB broad-group working library, through problem-dependent cross section collapsing. The AMPX format was adopted for the fine-group multi-purpose cross section library in order to have the compatibility with the AMPX-77 /23/ and SCAMPI nuclear data processing systems and with the SCALE-6 /24/ nuclear safety system, while the well known and diffused FIDO-ANISN format was selected for the broad-group working library.

A limited preliminary testing of the BUGENDF70.BOLIB library was successfully performed with the 3D TORT-3.2 discrete ordinates transport code on the PCA-Replica 12/13 /25/ /26/ (Winfrith, UK) and VENUS-3 /27/ (Mol, Belgium) engineering neutron shielding benchmark integral experiments, whose compositional and geometrical specifications were taken from the fission reactor shielding section of the ORNL-RSICC/ OECD-NEA Data Bank SINBAD /28/ /29/ international database of shielding benchmark experiments. It is underlined that the testing of the BUGENDF70.BOLIB library on the cited benchmark experiments is particularly meaningful since they were specifically conceived to verify and possibly to improve the accuracy of the calculation methodologies and nuclear data used in PWR radiation shielding and radiation damage calculations.

Finally, concerning the availability of similar recent libraries, it is stressed that the BUGENDF70.BOLIB and VITENDF70.BOLIB libraries, based on ENDF/B-VII.0 data, were respectively produced by the same data processing procedure employed to generate in parallel the similar BUGJEFF311.BOLIB /30/ and VITJEFF311.BOLIB /31/ ENEA-Bologna libraries, based on OECD-NEA Data Bank JEFF-3.1.1 data. The BUGJEFF311.BOLIB, VITJEFF311.BOLIB and VITENDF70.BOLIB libraries were already transferred for free distribution, in the reported chronological order, to OECD-NEA Data Bank and ORNL-RSICC. In addition, at the end of 2011 the BUGLE-B7 /32/ and VITAMIN-B7 /32/ ORNL libraries were diffused by ORNL-RSICC and then by OECD-NEA Data Bank. As the corresponding ENEA-Bologna counterparts, the BUGLE-B7 and VITAMIN-B7 libraries are based on ENDF/B-VII.0 data and adopt respectively the same neutron and photon group structures as the BUGLE-96 and VITAMIN-B6 libraries. On the other hand, differently from the ENEA-Bologna similar libraries processed with the cited NJOY and SCAMPI systems, the BUGLE-B7 and VITAMIN-B7 libraries were processed with the ORNL AMPX-6.1 nuclear data processing system not yet freely diffused.

## 1.1 - Background

Since many years, at the international level, a decrease of open activity was observed /33/ for debating production, features and performances of energy group-averaged working cross section libraries dedicated to radiation shielding and radiation damage applications in nuclear fission reactors.

This situation is unjustified, taking into account the actual increased performances of computers and 3D deterministic transport codes, the potential availability of collapsed and self-shielded group cross section libraries for different spectral, compositional and temperature conditions and, finally, the requirements of the nuclear safety authorities which encourage nuclear safety calculations possibly performed with transport codes based on different methods (stochastic and deterministic).

The methodology for the generation of energy group-averaged cross section libraries for nuclear radiation protection calculations for nuclear power plants, recommended by the ANSI/ANS-6.1.2-1999 (R2009) /34/ American National Standard and adopted in the present work, consists of a two stage process: 1) the processing of evaluated data files into a fine-group, pseudo-problem-independent library, followed by 2) the collapsing of the fine-group library cross sections into the broad-group, problem-dependent cross sections of the desired working library for the specific application. The problem-dependent library is then derived from the fine-group library by taking into account temperature and neutron resonance self-shielding specifications and collapsing into a smaller number of groups. As underlined in the VITAMIN-B6 and BUGLE-96 /8/ library user's manual, this approach removes from the end user the need to deal with the complex task of producing a group-averaged library from the evaluated data files, which contain a mix of point and functional data. This approach also reduces the user's responsibility to the operation of a finite number of well-defined processing codes. Hence a higher level of standardization and reliability is achieved since the user can focus only on those features which are special to his application.

In other words, following the previously cited standard, a working cross section library for a specific application should not be obtained directly in broad-group (tenths of groups) energy structures, using generic neutron and photon weighting fluxes derived from analytical functions (e.g., Maxwellian thermal neutron spectrum, 1/E neutron slowing-down spectrum, neutron fission spectrum, 1/E photon spectrum, etc.). In fact it is considered a more accurate approach to obtain the broad-group cross sections of the working libraries through proper cross section collapsing of fine-group (hundreds of groups) pseudo-problem independent cross section libraries, based, e.g., on the Bondarenko /7/ (f-factor) method for the treatment of neutron resonance self-shielding and temperature effects. It is recommendable, in particular, to collapse the fine-group cross sections using in-core and ex-core neutron and photon spectra, properly pre-calculated with a transport code for the specific compositional, geometrical and temperature data of the various spatial regions of a specific reactor type.

These libraries are required to run the deterministic transport codes which are, e.g., included in the following systems of deterministic codes: the US packages DOORS-3.2 /35/ and PARTISN-5.97 /36/ or the Russian package CNCSN 2009 /37/, distributed by the OECD-NEA Data Bank and ORNL-RSICC. On the other hand these packages, unlike those which include Monte Carlo codes like MCNP /11/, do not contain any working cross section library. The production of fine-group coupled neutron/photon pseudo-problem-independent libraries, based on the Bondarenko neutron resonance self-shielding method (e.g., of the type similar to the VITAMIN-B6 /8/ library) continues in several research institutes (ENEA, KAERI, ORNL, etc.). On the other hand, the free availability of derived broad-group working libraries of collapsed and self-shielded cross sections (e.g., of the type similar to the BUGLE-96 /8/, BUGJEFF311.BOLIB /30/, BUGLE-B7 /32/ or BUGENDF70.BOLIB libraries) is practically absent.

The previously cited decrease of open activity dedicated to the generation of broad-group working cross section libraries for fission reactor shielding applications is very probably due to the fact that it is traditionally considered highly convenient to perform 3D radiation shielding analyses for complex geometries with the combinatorial geometry approach included in the Monte Carlo codes (e.g., MCNP) using continuous-energy (point-wise)

processed cross section libraries, independent in practice from the specific neutron and photon spectral environment.

Differently from the 3D Monte Carlo codes using a single processed continuous-energy cross section library to treat the different spectral environments of interest, when deterministic transport codes are employed it is not practically meaningful to use only one broad-group spectrum-independent working cross section library for any kind of application.

As reported in the user's manual of the VITAMIN-B6 and BUGLE-96 libraries, the generation of group-averaged cross section libraries with broad-group energy structures is primarily justified for reasons of economy. Despite the impressive performance of modern supercomputers it is still often impractical to perform two and three-dimensional radiation transport analyses using point-wise data or finely structured multi-group data, especially if fine resolution is needed for the space or angular meshes. In particular the 3D deterministic transport codes, could have convergence problems when fine-group working libraries are used together with hundreds of thousands of volumetric spatial meshes, possibly needed to describe accurately complex in-core and ex-core reactor geometrical models used to perform radiation shielding and radiation damage analyses.
Even for one-dimensional analyses, it is often more efficient to use few-group data to perform the initial scoping analysis and then advance to finer group data as accuracy requirements become more stringent. The establishment of reference broad-group libraries is desirable to avoid duplication of effort, both in terms of the library generation and verification, and to assure a common database for comparisons among participants to a specific calculation program.

Taking into account this background and following the previously cited recommended methodology of generating a broad-group working cross section library dedicated to a specific reactor type, it is then necessary to know compositional, geometrical and temperature data, typical of the specific nuclear reactor, which are not normally freely released. These data, i.e., the typical homogenized atomic densities and the specific temperatures of the nuclide mixtures for the various in-core and ex-core spatial regions along the one-dimensional reactor radial geometry at the core midplane, are necessary for two fundamental reasons.

The first reason is that these data are necessary to pre-calculate the in-core and ex-core neutron and photon spectra in proper locations of each representative reactor zone of a specific reactor type in order to perform then a problem-dependent cross section collapsing of the fine-group cross sections of the pseudo-problem-independent mother library.

The second reason is that the mentioned data are necessary to calculate the correct problem-dependent neutron resonance self-shielding of the broad-group cross sections of the working library for a specific nuclear reactor type.

The fact that these data are still considered confidential by the industrial organizations implies that a wide and open data processing effort to produce this kind of libraries is not presently possible. This fact in its turn induces the risk that the culture and the technical expertise related to deterministic calculations may progressively disappear within the research and development organizations and university institutions whilst there is still the interest that they continue to be developed, within the industrial organizations, in a commercial and self-

referential perspective that does not guarantee, in general, a completely satisfactory approach to nuclear safety.

Moreover, despite the free availability of systems (e.g., NJOY/TRANSX /17/ /38/, AMPX-77 /23/, SCAMPI /18/ /19/, SCALE /24/, etc.) which permit the problem-dependent nuclear data processing in order to obtain broad-group working libraries of collapsed and self-shielded cross sections from fine-group general-purpose cross section libraries, the expertise about the nuclear data processing systems and methods is not generally widespread at the industrial level.

When, on the contrary, the industrial organizations are equipped with the necessary human resources and technical tools to perform detailed nuclear data processing addressed to generate multi-purpose fine-group libraries and derived collapsed working libraries of self-shielded cross sections for a specific type of fission reactor (the so called "custom-made" working cross section libraries), it is in any case necessary to follow the quality assurance approach.
This implies that, in order to reduce possible errors in the data entry during the problem-dependent data processing phase of a custom-made working library, it is in parallel recommended using of already processed working libraries dedicated to the same applications, with parameterized sets of self-shielded cross sections for a similar type of nuclear fission reactor.

In other words it is in any case important to verify and intercompare the results obtained with the custom-made working libraries together with the results obtained through working cross section libraries with parameterized sets of self-shielded cross sections, like for example BUGLE-96, BUGJEFF311.BOLIB, BUGLE-B7 or BUGENDF70.BOLIB, dedicated to LWR shielding and pressure vessel dosimetry.

Concerning the deterministic codes, it is really an upsetting fact that currently the 3D deterministic transport codes cannot be fully used due to the lack of broad-group working libraries also when their use should be strongly recommended and, in any case, competitive with the use of the 3D Monte Carlo stochastic codes. It is interesting to note that the industrial organizations continue to be interested in the use /39/ or even in the development /40/ of the 3D deterministic codes. Moreover they directly develop /41/ or outsource to external nuclear data processing working groups, under specific contracts, the generation of broad-group working cross section libraries for radiation shielding and radiation damage calculations with the deterministic transport codes. In fact they must fulfil quality assurance procedures with respect to the nuclear safety authority requirements and when deterministic codes are employed there is no need, as in the case of the Monte Carlo codes, to justify the validity of the statistics adopted since the deterministic codes are based on rigorous analytical solutions of the neutral particle transport equations. Moreover it is underlined that the 3D deterministic codes applied to radiation shielding and radiation damage analyses assure, with only a single run, a simultaneous and accurate average dose determination in every spatial position of the reactor geometrical model. It is then very important to underline that the deterministic transport codes permit reliable and effective sensitivity and uncertainty analyses, particularly recommended in the data validation activity and in a modern and rigorous approach to the industrial project of a nuclear reactor.

The 3D deterministic transport codes (e.g., the TORT /10/ code in the DOORS package, the PARTISN parallel code, etc.), which necessarily use the group-wise cross section libraries, increased in recent years their calculation performances in an impressive way and expanded their applicability to handle complex geometries, reaching in many cases the detail offered by the 3D Monte Carlo codes (e.g., MCNP). This result was achieved through the use of pre/post-processor systems of ancillary programs (e.g., the ENEA-Bologna BOT3P /12/ distributed by OECD-NEA Data Bank and ORNL-RSICC), dedicated to the 2D and 3D deterministic transport codes. In particular, with the support of BOT3P, based on combinatorial geometry algorithms, it is now easily possible to generate automatically detailed spatial mesh grids not only for the 2D and 3D transport codes of the DOORS system but also for any other possible transport code (through simple interfaces dedicated to manage the BOT3P binary output files), together with the graphical verification of the input data of the geometrical model.

During the last 10-15 years, the 3D discrete ordinates ($S_N$) transport codes increased their competitiveness with respect to the corresponding 3D Monte Carlo stochastic codes, obtaining comparable or even more convenient performances in terms of CPU times, with the same calculation precision, similar description capability of complex geometries and suitable simulation of different neutron and photon spectral conditions. Moreover 3D discrete ordinates codes like the US ATTILA /42/ commercial code, with unstructured spatial grids (finite elements) can now treat not only the neutral but also the charged particle transport as the more conventional discrete ordinates codes of the Russian CNCSN 2009 system of deterministic codes with structured spatial grids: the 1D code ROZ-6.6, the 2D codes KASKAD-S-2.5 (serial) and KASKAD-S-3.0 (parallel multi-threaded) and the 3D codes KATRIN-2.0 (serial) and KATRIN-2.5 (parallel multi-threaded).

Since deterministic transport codes are going to be employed in the analysis of the Generation IV nuclear reactor projects within the European Union research activities, it would be highly recommended that a specific interest dedicated to the generation of broad-group working cross section libraries should be promoted.

During the last years, the ENEA-Bologna Nuclear Data Group has performed several actions addressed to generate practical tools to increase, in particular, the performance and competitiveness of the 2D and 3D deterministic transport codes, following the recommendations proposed by the OECD-NEA Data Bank.

1. Several fine-group cross section libraries /2/ /5/ /30/ /31/ /43/ /44/ /45/ /46/ /47/ /48/ for nuclear fission applications were generated and are at present freely distributed by OECD-NEA Data Bank and ORNL-RSICC.

2. A pre/post-processor system /12/ /13/ /14/ /15/ of programs for the automatic spatial mesh generation, dedicated to the 2D and 3D deterministic transport codes, was developed and it is now freely distributed by OECD-NEA Data Bank and ORNL-RSICC.

3. Transport analyses dedicated to fission reactor neutron shielding benchmark experiments /1/ /2/ /49/ /50/ /51/ /52/ /53/ were performed also within the activities /51/ of the OECD-NEA Nuclear Science Committee TFRDD Task Force /3/ on nuclear fission reactor ageing problems.

4. The whole set of the IRDF-2002 /54/ dosimetry cross sections was processed /55/ in the 47 neutron group structure of the BUGLE-96 cross section library using a flat weighting neutron spectrum and neutron weighting spectra calculated with JEFF-3.1.1 and ENDF/B-VII.0 data, at one quarter of the thickness of a typical PWR pressure vessel: these data are partially included in the package of the present BUGENDF70.BOLIB library.

1.2 - ENDF/B-VII.0 Evaluated Nuclear Data Library

The cross section advances in the ENDF library support needs in a wide variety of applied technologies. Complete cross section evaluations are needed in radiation transport simulation codes that are used to model the neutronics, activation and nuclear transmutations, energy deposition and absorbed dose, etc.. The applications include advanced reactor design, nuclear waste transmutation and fuel cycles, nuclear criticality safety, fusion, medical applications (isotope production, external beam therapy, etc.), nonproliferation and national security, space physics, radiation protection and shielding.
The work performed for the ENDF/B-VII.0 /6/ library represented a coordinated effort for five years by researchers from many US institutions, organized by CSEWG (Cross Section Evaluation Working Group) which is the organization that oversees the development of this database. The principal advances were dictated by specific programmatic priorities set by several laboratories and by the Department of Energy (DOE). The DOE Office of Science, Office of Nuclear Physics' US Nuclear Data Program (USNDP) provided the bulk of the support for bringing the various capabilities developed at different laboratories together under CSEWG, and for the National Nuclear Data Center to maintain and archive the ENDF databases at Brookhaven National Laboratory. Most of the underlying research was supported by the DOE National Nuclear Security Agency's Advanced Simulation and Computing (ASC), Nuclear Criticality Safety and Nonproliferation Research and Engineering programs, in addition to the Office of Science. The DOE Nuclear Energy (NE) office supported work related to advanced fuel cycles and advanced reactors. Important support also came from the DOE Naval Reactor Laboratories and from the National Institute for Standards and Technology (NIST).

The development of complete, evaluated cross section data files depends upon a variety of expertises: nuclear experimentation; nuclear theory and model predictions; statistical analysis; radiation transport physics; computer code and database development; processing of nuclear data; and fundamental and integral validation against experiments that include criticality and neutron transmission (shielding) measurements. This effort has brought together scientists from these different disciplines to create the ENDF/B-VII.0 library.
A cross section library is developed not only for the purpose of providing accurate basic physics data, isotope-by-isotope, but also to perform well, as an ensemble, in applied simulations. This is particularly important for nuclear criticality applications, where for some critical assemblies the performance may depend sensitively upon H-1, O-16, U-235, U-238, etc. data. Since all cross sections are known only to a certain level of precision, significant attention was paid to ensure that the evaluated cross sections perform together well as a group in validation simulations of these critical assemblies.

The ENDF/B-VII.0 evaluated nuclear data library was developed in the period 2002-2006 and it was released (see /6/) in December 2006.
The ENDF/B-VII.0 library includes all the data in the internationally-accepted ENDF-6

format /56/. It contains 14 sublibraries ordered according to the NSUB sublibrary identification number, defined by the ENDF-6 format. The total number of materials in ENDF/B-VII.0 has increased considerably with respect to the previous (VI.8) version of the ENDF/B library, largely thanks to the new decay data sublibrary. Although the ENDF/B library is widely known for evaluated neutron cross sections, a considerable amount of non-neutron data are contained as well.
As discussed below, out of the total of 14 sublibraries, there are two new sublibraries, 7 sublibraries were considerably updated and extended, while the remaining 5 sublibraries were taken over from ENDF/B-VI.8 without any change:

1. The photonuclear sublibrary is entirely new. It contains evaluated cross sections for 163 materials (all isotopes) mostly up to 140 MeV. The sublibrary has been supplied by Los Alamos National Laboratory (LANL) and it is largely based on the IAEA-coordinated collaboration completed in 2000. This project mostly used the evaluation methodology and modelling tools for photonuclear reactions developed at LANL.

2. The photo-atomic sublibrary has been taken over from ENDF/B-VI.8. It contains data for photons from 10 eV up to 100 GeV interacting with atoms for 100 materials (all elements). The sublibrary has been supplied by Lawrence Livermore National Laboratory (LLNL).

3. The decay data sublibrary has been completely re-evaluated and considerably extended by the National Nuclear Data Center, Brookhaven National Laboratory (BNL).

4. The spontaneous fission yields were taken over from ENDF/B-VI.8. The data were supplied by LANL.

5. The atomic relaxation sublibrary was taken over from ENDF/B-VI.8. It contains data for 100 materials (all elements) supplied by LLNL.

6. The neutron reaction sublibrary represents the heart of the ENDF/B-VII.0 library. The sublibrary has been considerably updated and extended, with a number of entirely new evaluations. It contains 393 materials, including 390 isotopic evaluations and 3 elemental ones (C, V and Zn). These evaluations can be considered to be complete (the only exception is Es-253 that contains (n,γ) dosimetry cross sections) since they contain data for all important reaction channels including energy spectra and angular distributions for use in neutronics calculations. Important improvements were made to the actinide nuclides by LANL, often in collaboration with ORNL. Evaluations in the fission product range (Z = 31-68) have been entirely changed. ENDF/B-VII.0 contains fission product evaluations for 219 materials, with 71 materials evaluated by BNL, 2 by LLNL, 1 by LANL-BNL and the remaining 145 materials produced by the international project (OECD-NEA WPEC). Of the 393 materials, about 2/3 of the evaluations are based upon recent important contributions from the US evaluators. The remaining evaluations were adopted from other sources (mostly the JENDL-3.3 library). Livermore provided β-delayed γ-ray data for U-235 and Pu-239, for the first time in ENDF/B.

7. Neutron fission yields were taken over from ENDF/B-VI.8. The data were supplied by LANL.

8. The thermal neutron scattering sublibrary contains thermal scattering law data with 20 evaluations, largely supplied by LANL, with several important updates and extensions (in seven evaluations also based on the work /57/ by IKE Stuttgart, Germany). The remaining evaluations were taken over from the ENDF/B-VI.8 library.

9. The neutron cross section standards sublibrary is new. Although standards traditionally constituted part of the ENDF/B library, in the past these data were stored on a tape with a specific tape number. As the concept of tapes has been abandoned in ENDF/B-VII.0, the neutron cross sections standards sublibrary has been introduced. Out of 8 standards materials, 6 were newly evaluated, while the He-3(n,p) and C-nat(n,n) standards were taken over from ENDF/B-VI.8. The standard cross sections were completely adopted by the neutron reaction sublibrary except for the thermal cross section for U-235(n,f) where a slight difference occurs to satisfy thermal data testing. These new evaluations come from the international collaboration coordinated by the IAEA and OECD-NEA WPEC; the US effort was led by NIST and LANL.

10. The electro-atomic sublibrary was taken over from ENDF/B-VI.8. It contains data for 100 materials (all elements) supplied by LLNL.

11. The proton-induced reactions were supplied by LANL, the data being mostly to 150 MeV. There are several updates and several new evaluations.

12. The deuteron-induced reactions were supplied by LANL. This sublibrary contains 5 evaluations.

13. The triton-induced reactions were supplied by LANL. This sublibrary contains 3 evaluations.

14. Reactions induced with He-3 were supplied by LANL. This sublibrary contains 2 evaluations.

The major US laboratory contributors to the ENDF/B-VII.0 library are cited herewith. A dominant contributor to the evaluations is LANL, who provided the many actinide evaluations in the neutron reaction sublibrary, almost all the evaluations in the neutron thermal scattering sublibrary, many photonuclear and all the charged particle evaluations. BNL contributed the decay data sublibrary and many fission product evaluations in the neutron sublibrary; ORNL contributed neutron resonances for several actinides of key importance; LLNL contributed 3 atomic sublibraries (carried over from previous evaluations), and NIST played the leading role in developing neutron cross section standards. BNL performed Phase 1 testing (data verification), LANL was the leading laboratory in Phase 2 testing (data validation) and BNL is responsible for archival and dissemination of the library.

1.3 - Cross Section Processing and Testing

The calculation approach used to produce the BUGENDF70.BOLIB library, based on the ENDF/B-VII.0 /6/ evaluated nuclear data library, is consistent (see also 1.1) with the US ANS standard "Neutron and Gamma-Ray Cross Sections for Nuclear Radiation Protection Calculations for Nuclear Power Plants" (ANSI/ANS-6.1.2-1999 (R2009) /34/). Specifically the ENDF/B-VII.0 data were first processed into a fine-group cross section set (the VITENDF70.BOLIB /5/ library) similar to the VITAMIN-B6 /8/ pseudo-problem-independent library and then collapsed into a broad-group set (the BUGENDF70.BOLIB library) similar to the BUGLE-96 /8/ working library, derived from VITAMIN-B6.

The selected approach employs both the following modular nuclear data processing systems: the LANL NJOY-99.259 /17/ system and the ENEA-Bologna 2007 Revision /19/ of the ORNL SCAMPI /18/ system. Several modules of NJOY were used to process the neutron interaction, the photon production and the photon interaction data from the ENDF/B-VII.0 formats to a group-averaged format.
In order to process correctly modern evaluated nuclear data like the ENDF/B-VII.0 data files, it was necessary to develop an updated and corrected version of the SCAMPI system, originally developed at ORNL from the AMPX-77 /23/ system and already employed at ORNL to generate the BUGLE-96 library from the VITAMIN-B6 library. In particular, the previously cited so called "ENEA-Bologna 2007 Revision of SCAMPI", able to generate and to read data in AMPX format, was developed and was released to OECD-NEA Data Bank and ORNL-RSICC.
In particular the ENEA-Bologna 2007 Revision of SCAMPI, through the revised and corrected SMILER module, was employed to read the double-precision GENDF binary files from the NJOY-99.259 nuclear data processing system, to translate the intermediate NJOY file into the AMPX master format for the VITENDF70.BOLIB fine-group library and, finally, to calculate the total (prompt + delayed) neutron fission spectra and average numbers of neutrons emitted per fission, taking into account that their delayed neutron components could not be previously obtained with the original ORNL SMILER version of the SCAMPI system. The BONAMI module was used to self-shield the VITENDF70.BOLIB cross sections taking into account the compositional, geometrical and temperature specifications typical of PWR and BWR calculation models. These self-shielded cross sections in the VITENDF70.BOLIB neutron and photon fine-group energy structures were used in transport calculations to determine the problem-dependent weighting spectra employed to generate the BUGENDF70.BOLIB neutron and photon broad-group collapsed cross sections through the revised and corrected MALOCS module, which was used, in particular, to perform the cross section collapsing of the rectangular fission matrices.

A detailed description of the data processing performed for the generation of the VITENDF70.BOLIB fine-group library is given in Chapter 2 while the specifications and processing methods used to generate the BUGENDF70.BOLIB broad-group working library are described in Chapter 3. Finally, the results of a preliminary but important validation effort dedicated to the BUGENDF70.BOLIB library is presented in Chapter 4.

## 2 - VITENDF70.BOLIB FINE-GROUP LIBRARY SPECIFICATIONS

The VITENDF70.BOLIB /5/ library is a fine-group pseudo-problem-independent cross section library, based on the Bondarenko /7/ (f-factor) method for the treatment of neutron resonance self-shielding and temperature effects. This library, generated in ENEA-Bologna by the Nuclear Data Group, is a coupled neutron/photon library in AMPX format for nuclear fission applications, based on the US ENDF/B-VII.0 /6/ evaluated nuclear data library. It has the same neutron and photon energy group structures (199 neutron groups + 42 photon groups) and general basic features as the ORNL DLC-184/VITAMIN-B6 /8/ American library in AMPX format, based on the US ENDF/B-VI.3 /9/ evaluated nuclear data library.

The VITENDF70.BOLIB library was generated through an updated automatic calculation procedure based on the LANL NJOY-99.259 /17/ nuclear data processing system, with the updating "upnea049", and the ENEA-Bologna 2007 Revision /19/ of the ORNL SCAMPI /18/ nuclear data processing system. VITENDF70.BOLIB was extensively tested on many thermal, intermediate and fast neutron spectrum criticality safety benchmark experiments.

A revised version of the SMILER module of the ENEA-Bologna 2007 Revision of the SCAMPI system was used to translate the fine-group data from the GENDF format into the AMPX master library format of the VITENDF70.BOLIB library. In parallel, automatic multiplication of the term of $\ell$-th order of the Legendre polynomial ($P_\ell$) expansion of the scattering cross section matrix by the $(2\ell + 1)$ factor was performed by the SMILER module for all the processed data files of the nuclides contained in the library.

The cross section files of VITENDF70.BOLIB in AMPX format can be exclusively treated by the updated ENEA-Bologna 2007 Revision of the SCAMPI system which assures a high level of flexibility in the production of working cross section libraries and an evident consistency with the VITAMIN-B6 library generation methods. It is underlined, in particular, that the ENEA-Bologna revised version of the SMILER module, contained in the ENEA-Bologna 2007 Revision of the SCAMPI system, permits to obtain separately the prompt neutron fission spectrum (MF=6, MT=18), the delayed neutron fission spectrum (MF=5, MT=455) and the total neutron fission spectrum needed, e.g., in the fixed source transport calculations for reactor radiation shielding applications. On the contrary, from the original ORNL SMILER version (see /18/), used to generate VITAMIN-B6 and VITJEF22.BOLIB /48/, it is possible to obtain only the prompt neutron component of the fission spectrum.

At present, the availability of the VITENDF70.BOLIB library permits to obtain derived working libraries of collapsed and self-shielded cross sections, through the ENEA-Bologna 2007 Revision of the SCAMPI system. More specifically, the cross sections can be collapsed by the MALOCS module, can be self-shielded by the BONAMI module and finally can be generated in the AMPX or FIDO-ANISN /4/ format. The cross sections in AMPX format can be used by the XSDRNPM one-dimensional (1D) discrete ordinates transport code, included in the ORNL AMPX-77 /23/ and SCAMPI nuclear data processing systems, or in the ORNL SCALE-6 /24/ nuclear safety system. Concerning the cross sections in FIDO-ANISN format, they can be used by the discrete ordinates ($S_N$) deterministic codes ANISN-ORNL (1D), DORT (2D) and TORT (3D) of the DOORS /35/ system, by the PARTISN /36/ (1D, 2D and 3D) parallel time-dependent discrete ordinates system and, finally, by the MORSE /58/ 3D Monte Carlo stochastic code.

2.1 - Name

The fine-group pseudo-problem-independent library which generated the BUGENDF70.BOLIB broad-group working library is designated as VITENDF70.BOLIB /5/. "VIT" suggests that the main features of the library are similar to those of the ORNL VITAMIN-B6 /8/ library and to the ENEA fine-group libraries /31/ /44/ /48/ in AMPX format with the same neutron and photon energy group structures. The "ENDF70" designation conveniently reflects the origin of the evaluated data: the ENDF/B-VII.0 /6/ evaluated nuclear data library. Finally, "BOLIB" means BOlogna LIBrary and so it is indicative of the place of production of the library.

2.2 - Materials, Temperatures and Background Cross Sections

A set of 183 cross section files, derived from the ENDF/B-VII.0 /6/ evaluated nuclear data library, was processed for the VITENDF70.BOLIB /5/ fine-group library. In particular the complete list of the included nuclides is reported in TAB. 2.1 together with the corresponding Z atomic numbers, the ENDF/B-VII.0 MAT numbers, the AMPX identifiers and a flag (YES/NO) indicating the presence of gamma-ray production data in the specific evaluated nuclear data file. It is underlined that, in this set of processed data files, only two data files correspond to evaluated natural elements (C-nat and V-nat) whereas the other ones correspond to single isotope evaluated data files.

The Bondarenko /7/ (f-factor) method was used for handling neutron resonance self-shielding and temperature effects. As for VITAMIN-B6 /8/, all the 177 standard (not bound) nuclides were processed at the 4 temperatures of 300 °K, 600 °K, 1000 °K and 2100 °K and most materials were processed with 6 to 8 values for the background cross section $\sigma_0$. These parameters are indicated in detail in TAB. 2.2, where it is possible to verify that nearly all materials were processed with the following values of $\sigma_0$: 1, 10, 1.0E+2, 1.0E+3, 1.0E+4 and 1.0E+10 barns.

With respect to the $\sigma_0$ values used in the generation of the Fe-56 processed files in the VITAMIN-B6 (AMPX format), VITJEF22.BOLIB /48/ (AMPX format) and MATJEF22.BOLIB /47/ (MATXS format) older libraries, an additional $\sigma_0$ numerical value equal to 0.01 barns was used in the production of the Fe-56 processed file included in VITENDF70.BOLIB as it was done for the VITJEFF31.BOLIB /44/ (AMPX format) and VITJEFF311.BOLIB /31/ (AMPX format) libraries and for the MATJEFF31.BOLIB /43/ (MATXS format) library. This additional $\sigma_0$ numerical value improves further, through a more precise self-shielding factor interpolation, the neutron self-shielding of the Fe-56 cross sections in natural iron. Moreover the possibility of a more accurate self-shielding calculation for Fe-56 was considered useful also in LWR radiation damage analyses in the carbon steel of the pressure vessel and in the stainless steel of the reactor internals (see /8/ and /30/).
For consistency with most other similar libraries, it was decided to use infinitely dilute background cross sections ($\sigma_0$ = 1.0E+10 barns) for nuclides with the atomic number Z less than 7, with the exception of B-11. Hence, only a background cross section with a numerical value of 1.0E+10 barns was used for each of these nuclides.

Thermal scattering cross sections were produced for six additional bound nuclides which were processed at all the temperatures (see TAB. 2.3) available in the ENDF/B-VII.0 thermal

scattering law data file (see /6/): H-1 in light water, H-1 in polyethylene, H-1 in zirconium hydride (not contained in the VITAMIN-B6, VITJEF22.BOLIB and MATJEF22.BOLIB libraries), H-2 in heavy water, C in graphite and Be in beryllium metal.

Finally, it is important to note that in total reactor power and heating calculations, the corresponding results can be heavily affected by the lack of gamma production data in some ENDF/B-VII.0 evaluated data files. Concerning this, it is recommended to verify carefully if the ENDF/B-VII.0 data files of the nuclides involved in the calculations include gamma production data (see TAB. 2.1).

TAB. 2.1

ENDF/B-VII.0 Nuclides Processed for the VITENDF70.BOLIB Library.

| Z | Nuclide | ENDF/B-VII.0 MAT | AMPX Identifier | Gamma-Ray Production |
|---|---|---|---|---|
| 1 | H-$H_2O$ | 125/1 | 1001 | YES |
| | H-$CH_2$ | 125/37 | 1901 | YES |
| | H-ZrH | 125/7 | 1401 | YES |
| | D-$D_2O$ | 128/11 | 1002 | YES |
| | H-3 | 131 | 1003 | NO |
| 2 | He-3 | 225 | 2003 | NO |
| | He-4 | 228 | 2004 | NO |
| 3 | Li-6 | 325 | 3006 | YES |
| | Li-7 | 328 | 3007 | YES |
| 4 | Be-9 | 425 | 4009 | YES |
| | Be-9 (Thermal) | 425/26 | 4309 | YES |
| 5 | B-10 | 525 | 5010 | YES |
| | B-11 | 528 | 5011 | YES |
| 6 | C-nat | 600 | 6012 | YES |
| | C-nat (Graphite) | 600/31 | 6312 | YES |
| 7 | N-14 | 725 | 7014 | YES |
| | N-15 | 728 | 7015 | YES |
| 8 | O-16 | 825 | 8016 | YES |
| | O-17 | 828 | 8017 | NO |
| 9 | F-19 | 925 | 9019 | YES |
| 11 | Na-23 | 1125 | 11023 | YES |
| 12 | Mg-24 | 1225 | 12024 | YES |
| | Mg-25 | 1228 | 12025 | YES |
| | Mg-26 | 1231 | 12026 | YES |
| 13 | Al-27 | 1325 | 13027 | YES |
| 14 | Si-28 | 1425 | 14028 | YES |
| | Si-29 | 1428 | 14029 | YES |
| | Si-30 | 1431 | 14030 | YES |
| 15 | P-31 | 1525 | 15031 | YES |
| 16 | S-32 | 1625 | 16032 | YES |
| | S-33 | 1628 | 16033 | YES |
| | S-34 | 1631 | 16034 | YES |
| | S-36 | 1637 | 16036 | YES |
| 17 | Cl-35 | 1725 | 17035 | YES |
| | Cl-37 | 1731 | 17037 | YES |
| 19 | K-39 | 1925 | 19039 | YES |
| | K-40 | 1928 | 19040 | YES |
| | K-41 | 1931 | 19041 | YES |
| 20 | Ca-40 | 2025 | 20040 | YES |
| | Ca-42 | 2031 | 20042 | YES |
| | Ca-43 | 2034 | 20043 | YES |
| | Ca-44 | 2037 | 20044 | YES |
| | Ca-46 | 2043 | 20046 | YES |
| | Ca-48 | 2049 | 20048 | YES |
| 22 | Ti-46 | 2225 | 22046 | YES |
| | Ti-47 | 2228 | 22047 | YES |
| | Ti-48 | 2231 | 22048 | YES |
| | Ti-49 | 2234 | 22049 | YES |
| | Ti-50 | 2237 | 22050 | YES |

TAB. 2.1 Continued

ENDF/B-VII.0 Nuclides Processed for the VITENDF70.BOLIB Library.

| Z | Nuclide | ENDF/B-VII.0 MAT | AMPX Identifier | Gamma-Ray Production |
|---|---|---|---|---|
| 23 | V-nat | 2300 | 23000 | YES |
| 24 | Cr-50 | 2425 | 24050 | YES |
| | Cr-52 | 2431 | 24052 | YES |
| | Cr-53 | 2434 | 24053 | YES |
| | Cr-54 | 2437 | 24054 | YES |
| 25 | Mn-55 | 2525 | 25055 | YES |
| 26 | Fe-54 | 2625 | 26054 | YES |
| | Fe-56 | 2631 | 26056 | YES |
| | Fe-57 | 2634 | 26057 | YES |
| | Fe-58 | 2637 | 26058 | YES |
| 27 | Co-59 | 2725 | 27059 | YES |
| 28 | Ni-58 | 2825 | 28058 | YES |
| | Ni-60 | 2831 | 28060 | YES |
| | Ni-61 | 2834 | 28061 | YES |
| | Ni-62 | 2837 | 28062 | YES |
| | Ni-64 | 2843 | 28064 | YES |
| 29 | Cu-63 | 2925 | 29063 | YES |
| | Cu-65 | 2931 | 29065 | YES |
| 31 | Ga-69 | 3125 | 31069 | NO |
| | Ga-71 | 3131 | 31071 | NO |
| 39 | Y-89 | 3925 | 39089 | YES |
| 40 | Zr-90 | 4025 | 40090 | YES |
| | Zr-91 | 4028 | 40091 | YES |
| | Zr-92 | 4031 | 40092 | YES |
| | Zr-94 | 4037 | 40094 | YES |
| | Zr-96 | 4043 | 40096 | YES |
| 41 | Nb-93 | 4125 | 41093 | YES |
| 42 | Mo-92 | 4225 | 42092 | YES |
| | Mo-94 | 4231 | 42094 | YES |
| | Mo-95 | 4234 | 42095 | YES |
| | Mo-96 | 4237 | 42096 | YES |
| | Mo-97 | 4240 | 42097 | YES |
| | Mo-98 | 4243 | 42098 | YES |
| | Mo-100 | 4249 | 42100 | NO |
| 47 | Ag-107 | 4725 | 47107 | YES |
| | Ag-109 | 4731 | 47109 | YES |
| 48 | Cd-106 | 4825 | 48106 | YES |
| | Cd-108 | 4831 | 48108 | NO |
| | Cd-110 | 4837 | 48110 | NO |
| | Cd-111 | 4840 | 48111 | YES |
| | Cd-112 | 4843 | 48112 | NO |
| | Cd-113 | 4846 | 48113 | NO |
| | Cd-114 | 4849 | 48114 | NO |
| | Cd-115m | 4853 | 48115 | YES |
| | Cd-116 | 4855 | 48116 | NO |
| 49 | In-113 | 4925 | 49113 | NO |
| | In-115 | 4931 | 49115 | NO |
| 50 | Sn-112 | 5025 | 50112 | NO |
| | Sn-114 | 5031 | 50114 | NO |

TAB. 2.1 Continued

ENDF/B-VII.0 Nuclides Processed for the VITENDF70.BOLIB Library.

| Z | Nuclide | ENDF/B-VII.0 MAT | AMPX Identifier | Gamma-Ray Production |
|---|---|---|---|---|
| | Sn-115 | 5034 | 50115 | NO |
| | Sn-116 | 5037 | 50116 | NO |
| | Sn-117 | 5040 | 50117 | NO |
| | Sn-118 | 5043 | 50118 | NO |
| | Sn-119 | 5046 | 50119 | NO |
| | Sn-120 | 5049 | 50120 | NO |
| | Sn-122 | 5055 | 50122 | NO |
| | Sn-123 | 5058 | 50123 | NO |
| | Sn-124 | 5061 | 50124 | NO |
| | Sn-125 | 5064 | 50125 | YES |
| | Sn-126 | 5067 | 50126 | NO |
| 56 | Ba-138 | 5649 | 56138 | NO |
| 63 | Eu-151 | 6325 | 63151 | NO |
| | Eu-152 | 6328 | 63152 | NO |
| | Eu-153 | 6331 | 63153 | YES |
| | Eu-154 | 6334 | 63154 | NO |
| | Eu-155 | 6337 | 63155 | NO |
| 64 | Gd-152 | 6425 | 64152 | YES |
| | Gd-154 | 6431 | 64154 | YES |
| | Gd-155 | 6434 | 64155 | YES |
| | Gd-156 | 6437 | 64156 | YES |
| | Gd-157 | 6440 | 64157 | YES |
| | Gd-158 | 6443 | 64158 | YES |
| | Gd-160 | 6449 | 64160 | YES |
| 68 | Er-162 | 6825 | 68162 | YES |
| | Er-164 | 6831 | 68164 | YES |
| | Er-166 | 6837 | 68166 | YES |
| | Er-167 | 6840 | 68167 | YES |
| | Er-168 | 6843 | 68168 | YES |
| | Er-170 | 6849 | 68170 | YES |
| 72 | Hf-174 | 7225 | 72174 | NO |
| | Hf-176 | 7231 | 72176 | NO |
| | Hf-177 | 7234 | 72177 | NO |
| | Hf-178 | 7237 | 72178 | NO |
| | Hf-179 | 7240 | 72179 | NO |
| | Hf-180 | 7243 | 72180 | NO |
| 73 | Ta-181 | 7328 | 73181 | YES |
| | Ta-182 | 7331 | 73182 | NO |
| 74 | W-182 | 7431 | 74182 | YES |
| | W-183 | 7434 | 74183 | YES |
| | W-184 | 7437 | 74184 | YES |
| | W-186 | 7443 | 74186 | YES |
| 75 | Re-185 | 7525 | 75185 | NO |
| | Re-187 | 7531 | 75187 | NO |
| 79 | Au-197 | 7925 | 79197 | YES |
| 82 | Pb-204 | 8225 | 82204 | YES |
| | Pb-206 | 8231 | 82206 | YES |
| | Pb-207 | 8234 | 82207 | YES |
| | Pb-208 | 8237 | 82208 | YES |

TAB. 2.1 Continued

ENDF/B-VII.0 Nuclides Processed for the VITENDF70.BOLIB Library.

| Z | Nuclide | ENDF/B-VII.0 MAT | AMPX Identifier | Gamma-Ray Production |
|---|---|---|---|---|
| 83 | Bi-209 | 8325 | 83209 | YES |
| 90 | Th-230 | 9034 | 90230 | NO |
| | Th-232 | 9040 | 90232 | YES |
| 91 | Pa-231 | 9131 | 91231 | YES |
| | Pa-233 | 9137 | 91233 | YES |
| 92 | U-232 | 9219 | 92232 | YES |
| | U-233 | 9222 | 92233 | YES |
| | U-234 | 9225 | 92234 | YES |
| | U-235 | 9228 | 92235 | YES |
| | U-236 | 9231 | 92236 | YES |
| | U-237 | 9234 | 92237 | YES |
| | U-238 | 9237 | 92238 | YES |
| 93 | Np-237 | 9346 | 93237 | YES |
| | Np-238 | 9349 | 93238 | NO |
| | Np-239 | 9352 | 93239 | NO |
| 94 | Pu-236 | 9428 | 94236 | NO |
| | Pu-237 | 9431 | 94237 | NO |
| | Pu-238 | 9434 | 94238 | NO |
| | Pu-239 | 9437 | 94239 | YES |
| | Pu-240 | 9440 | 94240 | YES |
| | Pu-241 | 9443 | 94241 | YES |
| | Pu-242 | 9446 | 94242 | YES |
| | Pu-243 | 9449 | 94243 | YES |
| | Pu-244 | 9452 | 94244 | NO |
| 95 | Am-241 | 9543 | 95241 | YES |
| | Am-242 | 9546 | 95242 | NO |
| | Am-242m | 9547 | 95601 | NO |
| | Am-243 | 9549 | 95243 | YES |
| 96 | Cm-241 | 9628 | 96241 | NO |
| | Cm-242 | 9631 | 96242 | YES |
| | Cm-243 | 9634 | 96243 | NO |
| | Cm-244 | 9637 | 96244 | NO |
| | Cm-245 | 9640 | 96245 | NO |
| | Cm-246 | 9643 | 96246 | NO |
| | Cm-247 | 9646 | 96247 | NO |
| | Cm-248 | 9649 | 96248 | YES |

TAB. 2.2

Background Cross Sections Values at which Bondarenko Factors Are Tabulated
in the VITENDF70.BOLIB Library.
All Nuclides Were Processed at Four Temperatures: 300 °K, 600 °K, 1000 °K and 2100 °K.

| Nuclide | Background Cross Sections [barns] | | | | | | | | | | | Legendre |
|---|---|---|---|---|---|---|---|---|---|---|---|---|
| | 1.E+10 | 1.E+6 | 1.E+5 | 1.E+4 | 1000. | 300. | 100. | 50. | 10. | 1. | 0.01 | Order |
| H-1 | 1.E+10 | | | | | | | | | | | 7 |
| H-2 | 1.E+10 | | | | | | | | | | | 7 |
| H-3 | 1.E+10 | | | | | | | | | | | 7 |
| He-3 | 1.E+10 | | | | | | | | | | | 7 |
| He-4 | 1.E+10 | | | | | | | | | | | 7 |
| Li-6 | 1.E+10 | | | | | | | | | | | 7 |
| Li-7 | 1.E+10 | | | | | | | | | | | 7 |
| Be-9 | 1.E+10 | | | | | | | | | | | 7 |
| B-10 | 1.E+10 | | | | | | | | | | | 7 |
| B-11 | 1.E+10 | | | | 1000. | | 100. | | 10. | 1. | | 7 |
| C-nat | 1.E+10 | | | | | | | | | | | 7 |
| N-14 | 1.E+10 | | | | 1000. | | 100. | | 10. | 1. | | 7 |
| N-15 | 1.E+10 | | | | 1000. | | 100. | | 10. | 1. | | 7 |
| O-16 | 1.E+10 | | | | 1000. | | 100. | | 10. | 1. | | 7 |
| O-17 | 1.E+10 | | | | 1000. | | 100. | | 10. | 1. | | 7 |
| Fa-19 | 1.E+10 | | | | 1000. | | 100. | | 10. | 1. | | 7 |
| Na-23 | 1.E+10 | | | | 1000. | 300. | 100. | 50. | 10. | 1. | | 7 |
| Mg-24 | 1.E+10 | | 1.E+5 | 1.E+4 | 1000. | | 100. | | 10. | 1. | | 7 |
| Mg-25 | 1.E+10 | | 1.E+5 | 1.E+4 | 1000. | | 100. | | 10. | 1. | | 7 |
| Mg-26 | 1.E+10 | | 1.E+5 | 1.E+4 | 1000. | | 100. | | 10. | 1. | | 7 |
| Al-27 | 1.E+10 | | | 1.E+4 | 1000. | | 100. | 50. | 10. | 1. | | 7 |
| Si-28 | 1.E+10 | | 1.E+5 | 1.E+4 | 1000. | | 100. | | 10. | 1. | | 7 |
| Si-29 | 1.E+10 | | 1.E+5 | 1.E+4 | 1000. | | 100. | | 10. | 1. | | 7 |
| Si-30 | 1.E+10 | | 1.E+5 | 1.E+4 | 1000. | | 100. | | 10. | 1. | | 7 |
| P-31 | 1.E+10 | | | 1.E+4 | 1000. | | 100. | | 10. | 1. | | 7 |
| S-32 | 1.E+10 | | | 1.E+4 | 1000. | | 100. | | 10. | 1. | | 7 |
| S-33 | 1.E+10 | | | 1.E+4 | 1000. | | 100. | | 10. | 1. | | 7 |
| S-34 | 1.E+10 | | | 1.E+4 | 1000. | | 100. | | 10. | 1. | | 7 |
| S-36 | 1.E+10 | | | 1.E+4 | 1000. | | 100. | | 10. | 1. | | 7 |
| Cl-35 | 1.E+10 | | | 1.E+4 | 1000. | | 100. | | 10. | 1. | | 7 |
| Cl-37 | 1.E+10 | | | 1.E+4 | 1000. | | 100. | | 10. | 1. | | 7 |
| K-39 | 1.E+10 | | | 1.E+4 | 1000. | | 100. | | 10. | 1. | | 7 |
| K-40 | 1.E+10 | | | 1.E+4 | 1000. | | 100. | | 10. | 1. | | 7 |
| K-41 | 1.E+10 | | | 1.E+4 | 1000. | | 100. | | 10. | 1. | | 7 |
| Ca-40 | 1.E+10 | | 1.E+5 | 1.E+4 | 1000. | | 100. | | 10. | 1. | | 7 |
| Ca-42 | 1.E+10 | | 1.E+5 | 1.E+4 | 1000. | | 100. | | 10. | 1. | | 7 |
| Ca-43 | 1.E+10 | | 1.E+5 | 1.E+4 | 1000. | | 100. | | 10. | 1. | | 7 |
| Ca-44 | 1.E+10 | | 1.E+5 | 1.E+4 | 1000. | | 100. | | 10. | 1. | | 7 |
| Ca-46 | 1.E+10 | | 1.E+5 | 1.E+4 | 1000. | | 100. | | 10. | 1. | | 7 |
| Ca-48 | 1.E+10 | | 1.E+5 | 1.E+4 | 1000. | | 100. | | 10. | 1. | | 7 |
| Ti-46 | 1.E+10 | | 1.E+5 | 1.E+4 | 1000. | | 100. | | 10. | 1. | | 7 |
| Ti-47 | 1.E+10 | | 1.E+5 | 1.E+4 | 1000. | | 100. | | 10. | 1. | | 7 |
| Ti-48 | 1.E+10 | | 1.E+5 | 1.E+4 | 1000. | | 100. | | 10. | 1. | | 7 |
| Ti-49 | 1.E+10 | | 1.E+5 | 1.E+4 | 1000. | | 100. | | 10. | 1. | | 7 |
| Ti-50 | 1.E+10 | | 1.E+5 | 1.E+4 | 1000. | | 100. | | 10. | 1. | | 7 |
| V-nat | 1.E+10 | | | 1.E+4 | 1000. | | 100. | | 10. | 1. | | 7 |
| Cr-50 | 1.E+10 | | 1.E+5 | 1.E+4 | 1000. | | 100. | | 10. | 1. | | 7 |
| Cr-52 | 1.E+10 | | 1.E+5 | 1.E+4 | 1000. | | 100. | | 10. | 1. | | 7 |
| Cr-53 | 1.E+10 | | 1.E+5 | 1.E+4 | 1000. | | 100. | | 10. | 1. | | 7 |
| Cr-54 | 1.E+10 | | 1.E+5 | 1.E+4 | 1000. | | 100. | | 10. | 1. | | 7 |
| Mn-55 | 1.E+10 | | 1.E+5 | 1.E+4 | 1000. | | 100. | | 10. | 1. | | 7 |
| Fe-54 | 1.E+10 | | 1.E+5 | 1.E+4 | 1000. | | 100. | | 10. | 1. | | 7 |
| Fe-56 | 1.E+10 | | 1.E+5 | 1.E+4 | 1000. | | 100. | 50. | 10. | 1. | 0.01 | 7 |
| Fe-57 | 1.E+10 | | 1.E+5 | 1.E+4 | 1000. | | 100. | | 10. | 1. | | 7 |
| Fe-58 | 1.E+10 | | 1.E+5 | 1.E+4 | 1000. | | 100. | | 10. | 1. | | 7 |
| Co-59 | 1.E+10 | | 1.E+5 | 1.E+4 | 1000. | | 100. | | 10. | 1. | | 7 |
| Ni-58 | 1.E+10 | | 1.E+5 | 1.E+4 | 1000. | | 100. | 50. | 10. | 1. | | 7 |
| Ni-60 | 1.E+10 | | 1.E+5 | 1.E+4 | 1000. | | 100. | 50. | 10. | 1. | | 7 |
| Ni-61 | 1.E+10 | | 1.E+5 | 1.E+4 | 1000. | | 100. | | 10. | 1. | | 7 |

TAB. 2.2 Continued

Background Cross Sections Values at which Bondarenko Factors Are Tabulated
in the VITENDF70.BOLIB Library.
All Nuclides Were Processed at Four Temperatures: 300 °K, 600 °K, 1000 °K and 2100 °K.

| Nuclide | Background Cross Sections [barns] | | | | | | | | | | | Legendre |
|---|---|---|---|---|---|---|---|---|---|---|---|---|
| | 1.E+10 | 1.E+6 | 1.E+5 | 1.E+4 | 1000. | 300. | 100. | 50. | 10. | 1. | 0.01 | Order |
| Ni-62 | 1.E+10 | | 1.E+5 | 1.E+4 | 1000. | | 100. | | 10. | 1. | | 7 |
| Ni-64 | 1.E+10 | | 1.E+5 | 1.E+4 | 1000. | | 100. | | 10. | 1. | | 7 |
| Cu-63 | 1.E+10 | | 1.E+5 | 1.E+4 | 1000. | | 100. | | 10. | 1. | | 7 |
| Cu-65 | 1.E+10 | | 1.E+5 | 1.E+4 | 1000. | | 100. | | 10. | 1. | | 7 |
| Ga-69 | 1.E+10 | | 1.E+5 | 1.E+4 | 1000. | | 100. | | 10. | 1. | | 5 |
| Ga-71 | 1.E+10 | | 1.E+5 | 1.E+4 | 1000. | | 100. | | 10. | 1. | | 5 |
| Y-89 | 1.E+10 | | 1.E+5 | 1.E+4 | 1000. | | 100. | | 10. | 1. | | 5 |
| Zr-90 | 1.E+10 | | 1.E+5 | 1.E+4 | 1000. | | 100. | | 10. | 1. | | 5 |
| Zr-91 | 1.E+10 | | 1.E+5 | 1.E+4 | 1000. | | 100. | | 10. | 1. | | 5 |
| Zr-92 | 1.E+10 | | 1.E+5 | 1.E+4 | 1000. | | 100. | | 10. | 1. | | 5 |
| Zr-94 | 1.E+10 | | 1.E+5 | 1.E+4 | 1000. | | 100. | | 10. | 1. | | 5 |
| Zr-96 | 1.E+10 | | 1.E+5 | 1.E+4 | 1000. | | 100. | | 10. | 1. | | 5 |
| Nb-93 | 1.E+10 | | 1.E+5 | 1.E+4 | 1000. | | 100. | | 10. | 1. | | 5 |
| Mo-92 | 1.E+10 | | 1.E+5 | 1.E+4 | 1000. | | 100. | | | | | 5 |
| Mo-94 | 1.E+10 | | 1.E+5 | 1.E+4 | 1000. | | 100. | | | | | 5 |
| Mo-95 | 1.E+10 | | 1.E+5 | 1.E+4 | 1000. | | 100. | | | | | 5 |
| Mo-96 | 1.E+10 | | 1.E+5 | 1.E+4 | 1000. | | 100. | | | | | 5 |
| Mo-97 | 1.E+10 | | 1.E+5 | 1.E+4 | 1000. | | 100. | | | | | 5 |
| Mo-98 | 1.E+10 | | 1.E+5 | 1.E+4 | 1000. | | 100. | | | | | 5 |
| Mo-100 | 1.E+10 | | 1.E+5 | 1.E+4 | 1000. | | 100. | | | | | 5 |
| Ag-107 | 1.E+10 | | 1.E+5 | 1.E+4 | 1000. | | 100. | | 10. | 1. | | 5 |
| Ag-109 | 1.E+10 | | 1.E+5 | 1.E+4 | 1000. | | 100. | | 10. | 1. | | 5 |
| Cd-106 | 1.E+10 | | 1.E+5 | 1.E+4 | 1000. | | 100. | | 10. | 1. | | 5 |
| Cd-108 | 1.E+10 | | 1.E+5 | 1.E+4 | 1000. | | 100. | | 10. | 1. | | 5 |
| Cd-110 | 1.E+10 | | 1.E+5 | 1.E+4 | 1000. | | 100. | | 10. | 1. | | 5 |
| Cd-111 | 1.E+10 | | 1.E+5 | 1.E+4 | 1000. | | 100. | | 10. | 1. | | 5 |
| Cd-112 | 1.E+10 | | 1.E+5 | 1.E+4 | 1000. | | 100. | | 10. | 1. | | 5 |
| Cd-113 | 1.E+10 | | 1.E+5 | 1.E+4 | 1000. | | 100. | | 10. | 1. | | 5 |
| Cd-114 | 1.E+10 | | 1.E+5 | 1.E+4 | 1000. | | 100. | | 10. | 1. | | 5 |
| Cd-115m | 1.E+10 | | 1.E+5 | 1.E+4 | 1000. | | 100. | | 10. | 1. | | 5 |
| Cd-116 | 1.E+10 | | 1.E+5 | 1.E+4 | 1000. | | 100. | | 10. | 1. | | 5 |
| In-113 | 1.E+10 | | 1.E+5 | 1.E+4 | 1000. | | 100. | | 10. | 1. | | 5 |
| In-115 | 1.E+10 | | 1.E+5 | 1.E+4 | 1000. | | 100. | | 10. | 1. | | 5 |
| Sn-112 | 1.E+10 | | 1.E+5 | 1.E+4 | 1000. | | 100. | | 10. | 1. | | 5 |
| Sn-114 | 1.E+10 | | 1.E+5 | 1.E+4 | 1000. | | 100. | | 10. | 1. | | 5 |
| Sn-115 | 1.E+10 | | 1.E+5 | 1.E+4 | 1000. | | 100. | | 10. | 1. | | 5 |
| Sn-116 | 1.E+10 | | 1.E+5 | 1.E+4 | 1000. | | 100. | | 10. | 1. | | 5 |
| Sn-117 | 1.E+10 | | 1.E+5 | 1.E+4 | 1000. | | 100. | | 10. | 1. | | 5 |
| Sn-118 | 1.E+10 | | 1.E+5 | 1.E+4 | 1000. | | 100. | | 10. | 1. | | 5 |
| Sn-119 | 1.E+10 | | 1.E+5 | 1.E+4 | 1000. | | 100. | | 10. | 1. | | 5 |
| Sn-120 | 1.E+10 | | 1.E+5 | 1.E+4 | 1000. | | 100. | | 10. | 1. | | 5 |
| Sn-122 | 1.E+10 | | 1.E+5 | 1.E+4 | 1000. | | 100. | | 10. | 1. | | 5 |
| Sn-123 | 1.E+10 | | 1.E+5 | 1.E+4 | 1000. | | 100. | | 10. | 1. | | 5 |
| Sn-124 | 1.E+10 | | 1.E+5 | 1.E+4 | 1000. | | 100. | | 10. | 1. | | 5 |
| Sn-125 | 1.E+10 | | 1.E+5 | 1.E+4 | 1000. | | 100. | | 10. | 1. | | 5 |
| Sn-126 | 1.E+10 | | 1.E+5 | 1.E+4 | 1000. | | 100. | | 10. | 1. | | 5 |
| Ba-138 | 1.E+10 | | 1.E+5 | 1.E+4 | 1000. | | 100. | | 10. | 1. | | 5 |
| Eu-151 | 1.E+10 | | 1.E+5 | 1.E+4 | 1000. | | 100. | 50. | | | | 5 |
| Eu-152 | 1.E+10 | 1.E+6 | 1.E+5 | 1.E+4 | 1000. | | 100. | | | | | 5 |
| Eu-153 | 1.E+10 | | 1.E+5 | 1.E+4 | 1000. | | 100. | 50. | | | | 5 |
| Eu-154 | 1.E+10 | 1.E+6 | 1.E+5 | 1.E+4 | 1000. | | 100. | | | | | 5 |
| Eu-155 | 1.E+10 | 1.E+6 | 1.E+5 | 1.E+4 | 1000. | | 100. | | | | | 5 |
| Gd-152 | 1.E+10 | | 1.E+5 | 1.E+4 | 1000. | | 100. | | 10. | 1. | | 5 |
| Gd-154 | 1.E+10 | | 1.E+5 | 1.E+4 | 1000. | | 100. | | 10. | 1. | | 5 |
| Gd-155 | 1.E+10 | | 1.E+5 | 1.E+4 | 1000. | | 100. | | 10. | 1. | | 5 |
| Gd-156 | 1.E+10 | | 1.E+5 | 1.E+4 | 1000. | | 100. | | 10. | 1. | | 5 |
| Gd-157 | 1.E+10 | | 1.E+5 | 1.E+4 | 1000. | | 100. | | 10. | 1. | | 5 |
| Gd-158 | 1.E+10 | | 1.E+5 | 1.E+4 | 1000. | | 100. | | 10. | 1. | | 5 |
| Gd-160 | 1.E+10 | | 1.E+5 | 1.E+4 | 1000. | | 100. | | 10. | 1. | | 5 |

TAB. 2.2 Continued

Background Cross Sections Values at which Bondarenko Factors Are Tabulated
in the VITENDF70.BOLIB Library.
All Nuclides Were Processed at Four Temperatures: 300 °K, 600 °K, 1000 °K and 2100 °K.

| Nuclide | Background Cross Sections [barns] | | | | | | | | | | | Legendre |
|---|---|---|---|---|---|---|---|---|---|---|---|---|
| | 1.E+10 | 1.E+6 | 1.E+5 | 1.E+4 | 1000. | 300. | 100. | 50. | 10. | 1. | 0.01 | Order |
| Er-162 | 1.E+10 | | 1.E+5 | 1.E+4 | 1000. | | 100. | | 10. | 1. | | 5 |
| Er-164 | 1.E+10 | | 1.E+5 | 1.E+4 | 1000. | | 100. | | 10. | 1. | | 5 |
| Er-166 | 1.E+10 | | 1.E+5 | 1.E+4 | 1000. | | 100. | | 10. | 1. | | 5 |
| Er-167 | 1.E+10 | | 1.E+5 | 1.E+4 | 1000. | | 100. | | 10. | 1. | | 5 |
| Er-168 | 1.E+10 | | 1.E+5 | 1.E+4 | 1000. | | 100. | | 10. | 1. | | 5 |
| Er-170 | 1.E+10 | | 1.E+5 | 1.E+4 | 1000. | | 100. | | 10. | 1. | | 5 |
| Hf-174 | 1.E+10 | | 1.E+5 | 1.E+4 | 1000. | | 100. | | 10. | 1. | | 5 |
| Hf-176 | 1.E+10 | | 1.E+5 | 1.E+4 | 1000. | | 100. | | 10. | 1. | | 5 |
| Hf-177 | 1.E+10 | | 1.E+5 | 1.E+4 | 1000. | | 100. | 50. | | | | 5 |
| Hf-178 | 1.E+10 | | 1.E+5 | 1.E+4 | 1000. | | 100. | | 10. | 1. | | 5 |
| Hf-179 | 1.E+10 | | 1.E+5 | 1.E+4 | 1000. | | 100. | 50. | | | | 5 |
| Hf-180 | 1.E+10 | | 1.E+5 | 1.E+4 | 1000. | | 100. | | 10. | 1. | | 5 |
| Ta-181 | 1.E+10 | | 1.E+5 | 1.E+4 | 1000. | | 100. | 50. | | | | 5 |
| Ta-182 | 1.E+10 | | 1.E+5 | 1.E+4 | 1000. | | 100. | 50. | | | | 5 |
| W-182 | 1.E+10 | | 1.E+5 | 1.E+4 | 1000. | | 100. | | 10. | 1. | | 5 |
| W-183 | 1.E+10 | | 1.E+5 | 1.E+4 | 1000. | | 100. | 50. | | | | 5 |
| W-184 | 1.E+10 | | 1.E+5 | 1.E+4 | 1000. | | 100. | | 10. | 1. | | 5 |
| W-186 | 1.E+10 | | 1.E+5 | 1.E+4 | 1000. | | 100. | | 10. | 1. | | 5 |
| Re-185 | 1.E+10 | 1.E+6 | 1.E+5 | 1.E+4 | 1000. | | 100. | | | | | 5 |
| Re-187 | 1.E+10 | 1.E+6 | 1.E+5 | 1.E+4 | 1000. | | 100. | | | | | 5 |
| Au-197 | 1.E+10 | | 1.E+5 | 1.E+4 | 1000. | | 100. | | 10. | 1. | | 5 |
| Pb-204 | 1.E+10 | | 1.E+5 | 1.E+4 | 1000. | | 100. | | 10. | 1. | | 5 |
| Pb-206 | 1.E+10 | | 1.E+5 | 1.E+4 | 1000. | | 100. | | 10. | 1. | | 5 |
| Pb-207 | 1.E+10 | | 1.E+5 | 1.E+4 | 1000. | | 100. | | 10. | 1. | | 5 |
| Pb-208 | 1.E+10 | | 1.E+5 | 1.E+4 | 1000. | | 100. | | 10. | 1. | | 5 |
| Bi-209 | 1.E+10 | | 1.E+5 | 1.E+4 | 1000. | | 100. | | 10. | 1. | | 5 |
| Th-230 | 1.E+10 | 1.E+6 | 1.E+5 | 1.E+4 | 1000. | | 100. | | | | | 5 |
| Th-232 | 1.E+10 | | | 1.E+4 | 1000. | 300. | 100. | 50. | 10. | 1. | | 5 |
| Pa-231 | 1.E+10 | | 1.E+5 | 1.E+4 | 1000. | | 100. | 50. | | | | 5 |
| Pa-233 | 1.E+10 | | 1.E+5 | 1.E+4 | 1000. | | 100. | 50. | | | | 5 |
| U-232 | 1.E+10 | | 1.E+5 | 1.E+4 | 1000. | | 100. | 50. | | | | 5 |
| U-233 | 1.E+10 | | 1.E+5 | 1.E+4 | 1000. | | 100. | 50. | | | | 5 |
| U-234 | 1.E+10 | | 1.E+5 | 1.E+4 | 1000. | | 100. | | 10. | 1. | | 5 |
| U-235 | 1.E+10 | 1.E+6 | 1.E+5 | 1.E+4 | 1000. | | 100. | 50. | | | | 5 |
| U-236 | 1.E+10 | | 1.E+5 | 1.E+4 | 1000. | | 100. | | 10. | 1. | | 5 |
| U-237 | 1.E+10 | | 1.E+5 | 1.E+4 | 1000. | | 100. | 50. | | | | 5 |
| U-238 | 1.E+10 | | | 1.E+4 | 1000. | 300. | 100. | 50. | 10. | 1. | | 5 |
| N-237 | 1.E+10 | | 1.E+5 | 1.E+4 | 1000. | | 100. | | 10. | 1. | | 5 |
| Np-238 | 1.E+10 | | 1.E+5 | 1.E+4 | 1000. | | 100. | 50. | | | | 5 |
| Np-239 | 1.E+10 | | 1.E+5 | 1.E+4 | 1000. | | 100. | 50. | | | | 5 |
| Pu-236 | 1.E+10 | | 1.E+5 | 1.E+4 | 1000. | | 100. | | 10. | 1. | | 5 |
| Pu-237 | 1.E+10 | | 1.E+5 | 1.E+4 | 1000. | | 100. | 50. | | | | 5 |
| Pu-238 | 1.E+10 | | 1.E+5 | 1.E+4 | 1000. | | 100. | | 10. | 1. | | 5 |
| Pu-239 | 1.E+10 | | 1.E+5 | 1.E+4 | 1000. | | 100. | 50. | | | | 5 |
| Pu-240 | 1.E+10 | | 1.E+5 | 1.E+4 | 1000. | | 100. | | 10. | 1. | | 5 |
| Pu-241 | 1.E+10 | | 1.E+5 | 1.E+4 | 1000. | | 100. | 50. | | | | 5 |
| Pu-242 | 1.E+10 | | 1.E+5 | 1.E+4 | 1000. | | 100. | | 10. | 1. | | 5 |
| Pu-243 | 1.E+10 | | 1.E+5 | 1.E+4 | 1000. | | 100. | 50. | | | | 5 |
| Pu-244 | 1.E+10 | | 1.E+5 | 1.E+4 | 1000. | | 100. | | 10. | 1. | | 5 |
| Am-241 | 1.E+10 | | 1.E+5 | 1.E+4 | 1000. | | 100. | 50. | | | | 5 |
| Am-242 | 1.E+10 | | 1.E+5 | 1.E+4 | 1000. | | 100. | 50. | | | | 5 |
| Am-242m | 1.E+10 | | 1.E+5 | 1.E+4 | 1000. | | | | | | | 5 |
| Am-243 | 1.E+10 | | 1.E+5 | 1.E+4 | 1000. | | 100. | 50. | | | | 5 |
| Cm-241 | 1.E+10 | | 1.E+5 | 1.E+4 | 1000. | | 100. | 50. | | | | 5 |
| Cm-242 | 1.E+10 | | 1.E+5 | 1.E+4 | 1000. | | 100. | 50. | | | | 5 |
| Cm-243 | 1.E+10 | | 1.E+5 | 1.E+4 | 1000. | | 100. | 50. | | | | 5 |
| Cm-244 | 1.E+10 | | 1.E+5 | 1.E+4 | 1000. | | 100. | 50. | | | | 5 |
| Cm-245 | 1.E+10 | | 1.E+5 | 1.E+4 | 1000. | | 100. | 50. | | | | 5 |
| Cm-246 | 1.E+10 | | 1.E+5 | 1.E+4 | 1000. | | 100. | 50. | | | | 5 |

TAB. 2.2 Continued

Background Cross Sections Values at which Bondarenko Factors Are Tabulated
in the VITENDF70.BOLIB Library.
All Nuclides Were Processed at Four Temperatures: 300 °K, 600 °K, 1000 °K and 2100 °K.

| Nuclide | Background Cross Sections [barns] | | | | | | | | | | | Legendre |
|---|---|---|---|---|---|---|---|---|---|---|---|---|
| | 1.E+10 | 1.E+6 | 1.E+5 | 1.E+4 | 1000. | 300. | 100. | 50. | 10. | 1. | 0.01 | Order |
| Cm-247 | 1.E+10 | | 1.E+5 | 1.E+4 | 1000. | | 100. | 50. | | | | 5 |
| Cm-248 | 1.E+10 | | 1.E+5 | 1.E+4 | 1000. | | 100. | 50. | | | | 5 |

TAB. 2.3

Processed Thermal Scattering Data in the VITENDF70.BOLIB Library.

---

Thermal scattering cross sections for the following bound nuclides were produced, through the THERMR module of NJOY, from the scattering matrices S(α,β) at various temperatures, included in the original ENDF/B-VII.0 thermal scattering law data file:

H-1 in $H_2O$ (light water)
H-1 in $CH_2$ (polyethylene)
H-1 in ZrH (zirconium hydride)
H-2 in $D_2O$ (heavy water)
C (graphite)
Be (beryllium metal)

| Nuclide | Temperature [°K] |
|---|---|
| H-1 in $H_2O$ | 293.6 350. 400. 450. 500. 550. 600. 650. 800. |
| H-1 in $CH_2$ | 296. 350. |
| H-1 in ZrH | 296. 400. 500. 600. 700. 800. 1000. 1200. |
| H-2 in $D_2O$ | 293.6 350. 400. 450. 500. 550. 600. 650. |
| C | 296. 400. 500. 600. 700. 800. 1000. 1200. 1600. 2000. |
| Be | 296. 400. 500. 600. 700. 800. 1000. 1200. |

2.3 - Energy Group Structure

The VITENDF70.BOLIB library adopts the same neutron and photon energy group structures as the VITAMIN-B6 /8/ library with 199 neutron energy groups (see TAB. 2.4) and 42 photon energy groups (see TAB. 2.5). The neutron and photon energy ranges are respectively included within 1.0E-05 eV and 1.9640E+07 eV for neutrons and within 1.0E+03 eV and 3.0E+07 eV for photons.

As reported in the VITAMIN-B6 library user's manual, this 199 neutron group structure was constructed as a compromise and improvement over the 174 neutron group structure used for the VITAMIN-E /59/ fine-group library, primarily conceived to treat fast neutron spectrum applications, and the 27 neutron group structure of the 27-neutron-group library, included in the SCALE /24/ system, suitable to treat criticality safety problems and out-of-core radiation shielding applications. The 27-neutron-group library has, in particular, a favourable neutron group discretization in the thermal neutron energy range whilst the resolution in the fast neutron energy range above 0.1 MeV results to be inadequate. Therefore the choice of the 199 group structure permits to treat not only fast neutron spectrum applications, through the proper neutron group structure at higher energies typical of VITAMIN-E, but also to treat physical systems with thermal neutron spectra, through the adequate group structure at lower energies of the 27-neutron-group library. Like the VITAMIN-B6 library, the VITENDF70.BOLIB thermal neutron energy range, i.e. the range of the neutron energy groups which include upscatter, contains 36 groups and has 5.043 eV as the uppermost boundary. In particular, the thermal neutron group energy limits are listed in TAB. 2.6. As underlined in the VITAMIN-B6 library user's manual, by combining the best features of the VITAMIN-E with the 27-group neutron energy grids, the best options were obtained for creating a problem-independent energy grid for a variety of reactor designs, including thermal (water or graphite-moderated) and fast reactor systems. Consequently, problem-dependent cross section libraries can be easily derived from VITENDF70.BOLIB, through the ENEA-Bologna 2007 Revision /19/ of the SCAMPI /18/ data processing system, without having to repeat the multi-group averaging directly from the ENDF/B-VII.0 /6/ data files.

The full VITENDF70.BOLIB library neutron energy group structure given in TAB. 2.4 is identical to the corresponding structure of the VITAMIN-B6 library. The 199 group energy limits are based on the 175 groups in VITAMIN-J /60/ (an OECD-NEA Data Bank library based on the VITAMIN-C /61/ and VITAMIN-E structures) with an expanded number of thermal groups as discussed above. At higher energies, the boundaries are almost identical with the earlier VITAMIN libraries, which consist of a basic 100-group-mesh of equal lethargy width plus numerous additional boundaries to resolve resonance minima that are important for radiation shielding calculations.

The full VITENDF70.BOLIB library photon energy group structure given in TAB. 2.5 is identical to the corresponding structure of the VITAMIN-B6 library. It is based on a combination of the 42 photon groups in the VITAMIN-J structure and the 18 group structure in the SCALE shielding library. The top energy group extends to 30 MeV, which allows proper representation of high energy gamma-rays from neutron capture at high energies. Although the cross section for capture at neutron energies between 20 and 30 MeV is small, such a reaction in some materials can produce gamma-rays with energies between 20 and 30 MeV, as reported in the VITAMIN-B6 library user's manual.

TAB. 2.4

Neutron Group Energy Boundaries for the VITENDF70.BOLIB Library.

| Group | Upper Energy [eV] | Energy Width [eV] | Upper Lethargy | Lethargy Width |
|---|---|---|---|---|
| 1 | 1.9640E+07 | 2.3080E+06 | -6.7498E-01 | 0.1250 |
| 2 | 1.7332E+07 | 4.2700E+05 | -5.4997E-01 | 0.0249 |
| 3 | 1.6905E+07 | 4.1800E+05 | -5.2502E-01 | 0.0250 |
| 4 | 1.6487E+07 | 8.0400E+05 | -4.9999E-01 | 0.0500 |
| 5 | 1.5683E+07 | 7.6500E+05 | -4.4999E-01 | 0.0500 |
| 6 | 1.4918E+07 | 3.6800E+05 | -3.9998E-01 | 0.0250 |
| 7 | 1.4550E+07 | 3.5900E+05 | -3.7501E-01 | 0.0250 |
| 8 | 1.4191E+07 | 3.5100E+05 | -3.5002E-01 | 0.0250 |
| 9 | 1.3840E+07 | 3.4100E+05 | -3.2498E-01 | 0.0249 |
| 10 | 1.3499E+07 | 6.5900E+05 | -3.0003E-01 | 0.0501 |
| 11 | 1.2840E+07 | 3.1700E+05 | -2.4998E-01 | 0.0250 |
| 12 | 1.2523E+07 | 3.0900E+05 | -2.2498E-01 | 0.0250 |
| 13 | 1.2214E+07 | 5.9600E+05 | -2.0000E-01 | 0.0500 |
| 14 | 1.1618E+07 | 5.6600E+05 | -1.4997E-01 | 0.0499 |
| 15 | 1.1052E+07 | 5.3900E+05 | -1.0003E-01 | 0.0500 |
| 16 | 1.0513E+07 | 5.1300E+05 | -5.0027E-02 | 0.0500 |
| 17 | 1.0000E+07 | 4.8770E+05 | 0.0000E+00 | 0.0500 |
| 18 | 9.5123E+06 | 4.6390E+05 | 4.9999E-02 | 0.0500 |
| 19 | 9.0484E+06 | 4.4130E+05 | 9.9997E-02 | 0.0500 |
| 20 | 8.6071E+06 | 4.1980E+05 | 1.5000E-01 | 0.0500 |
| 21 | 8.1873E+06 | 3.9930E+05 | 2.0000E-01 | 0.0500 |
| 22 | 7.7880E+06 | 3.7980E+05 | 2.5000E-01 | 0.0500 |
| 23 | 7.4082E+06 | 3.6130E+05 | 3.0000E-01 | 0.0500 |
| 24 | 7.0469E+06 | 3.4370E+05 | 3.5000E-01 | 0.0500 |
| 25 | 6.7032E+06 | 1.1080E+05 | 4.0000E-01 | 0.0167 |
| 26 | 6.5924E+06 | 2.1610E+05 | 4.1667E-01 | 0.0333 |
| 27 | 6.3763E+06 | 3.1100E+05 | 4.5000E-01 | 0.0500 |
| 28 | 6.0653E+06 | 2.9580E+05 | 5.0000E-01 | 0.0500 |
| 29 | 5.7695E+06 | 2.8140E+05 | 5.5000E-01 | 0.0500 |
| 30 | 5.4881E+06 | 2.6760E+05 | 6.0000E-01 | 0.0500 |
| 31 | 5.2205E+06 | 2.5460E+05 | 6.4999E-01 | 0.0500 |
| 32 | 4.9659E+06 | 2.4220E+05 | 6.9999E-01 | 0.0500 |
| 33 | 4.7237E+06 | 2.3040E+05 | 7.4999E-01 | 0.0500 |
| 34 | 4.4933E+06 | 4.2760E+05 | 8.0000E-01 | 0.1000 |
| 35 | 4.0657E+06 | 3.8690E+05 | 9.0000E-01 | 0.1000 |
| 36 | 3.6788E+06 | 3.5010E+05 | 1.0000E+00 | 0.1000 |
| 37 | 3.3287E+06 | 1.6230E+05 | 1.1000E+00 | 0.0500 |
| 38 | 3.1664E+06 | 1.5450E+05 | 1.1500E+00 | 0.0500 |
| 39 | 3.0119E+06 | 1.4680E+05 | 1.2000E+00 | 0.0500 |
| 40 | 2.8651E+06 | 1.3980E+05 | 1.2500E+00 | 0.0500 |
| 41 | 2.7253E+06 | 1.3290E+05 | 1.3000E+00 | 0.0500 |
| 42 | 2.5924E+06 | 1.2640E+05 | 1.3500E+00 | 0.0500 |
| 43 | 2.4660E+06 | 8.0800E+04 | 1.4000E+00 | 0.0333 |
| 44 | 2.3852E+06 | 1.9900E+04 | 1.4333E+00 | 0.0084 |
| 45 | 2.3653E+06 | 1.9600E+04 | 1.4417E+00 | 0.0083 |
| 46 | 2.3457E+06 | 3.8800E+04 | 1.4500E+00 | 0.0167 |
| 47 | 2.3069E+06 | 7.5600E+04 | 1.4667E+00 | 0.0333 |
| 48 | 2.2313E+06 | 1.0880E+05 | 1.5000E+00 | 0.0500 |
| 49 | 2.1225E+06 | 1.0350E+05 | 1.5500E+00 | 0.0500 |

TAB. 2.4 Continued

Neutron Group Energy Boundaries for the VITENDF70.BOLIB Library.

| Group | Upper Energy [eV] | Energy Width [eV] | Upper Lethargy | Lethargy Width |
|---|---|---|---|---|
| 50 | 2.0190E+06 | 9.8500E+04 | 1.6000E+00 | 0.0500 |
| 51 | 1.9205E+06 | 9.3700E+04 | 1.6500E+00 | 0.0500 |
| 52 | 1.8268E+06 | 8.9100E+04 | 1.7000E+00 | 0.0500 |
| 53 | 1.7377E+06 | 8.4700E+04 | 1.7500E+00 | 0.0500 |
| 54 | 1.6530E+06 | 8.0600E+04 | 1.8000E+00 | 0.0500 |
| 55 | 1.5724E+06 | 7.6700E+04 | 1.8500E+00 | 0.0500 |
| 56 | 1.4957E+06 | 7.3000E+04 | 1.9000E+00 | 0.0500 |
| 57 | 1.4227E+06 | 6.9300E+04 | 1.9500E+00 | 0.0500 |
| 58 | 1.3534E+06 | 6.6000E+04 | 2.0000E+00 | 0.0500 |
| 59 | 1.2874E+06 | 6.2800E+04 | 2.0500E+00 | 0.0500 |
| 60 | 1.2246E+06 | 5.9800E+04 | 2.1000E+00 | 0.0500 |
| 61 | 1.1648E+06 | 5.6800E+04 | 2.1500E+00 | 0.0500 |
| 62 | 1.1080E+06 | 1.0540E+05 | 2.2000E+00 | 0.1000 |
| 63 | 1.0026E+06 | 4.0960E+04 | 2.3000E+00 | 0.0417 |
| 64 | 9.6164E+05 | 5.4460E+04 | 2.3417E+00 | 0.0583 |
| 65 | 9.0718E+05 | 4.4240E+04 | 2.4000E+00 | 0.0500 |
| 66 | 8.6294E+05 | 4.2090E+04 | 2.4500E+00 | 0.0500 |
| 67 | 8.2085E+05 | 4.0030E+04 | 2.5000E+00 | 0.0500 |
| 68 | 7.8082E+05 | 3.8080E+04 | 2.5500E+00 | 0.0500 |
| 69 | 7.4274E+05 | 3.6230E+04 | 2.6000E+00 | 0.0500 |
| 70 | 7.0651E+05 | 3.4450E+04 | 2.6500E+00 | 0.0500 |
| 71 | 6.7206E+05 | 3.2780E+04 | 2.7000E+00 | 0.0500 |
| 72 | 6.3928E+05 | 3.1180E+04 | 2.7500E+00 | 0.0500 |
| 73 | 6.0810E+05 | 2.9660E+04 | 2.8000E+00 | 0.0500 |
| 74 | 5.7844E+05 | 2.8210E+04 | 2.8500E+00 | 0.0500 |
| 75 | 5.5023E+05 | 2.6830E+04 | 2.9000E+00 | 0.0500 |
| 76 | 5.2340E+05 | 2.5530E+04 | 2.9500E+00 | 0.0500 |
| 77 | 4.9787E+05 | 4.7380E+04 | 3.0000E+00 | 0.1000 |
| 78 | 4.5049E+05 | 4.2870E+04 | 3.1000E+00 | 0.1000 |
| 79 | 4.0762E+05 | 1.9880E+04 | 3.2000E+00 | 0.0500 |
| 80 | 3.8774E+05 | 1.8910E+04 | 3.2500E+00 | 0.0500 |
| 81 | 3.6883E+05 | 3.5100E+04 | 3.3000E+00 | 0.1000 |
| 82 | 3.3373E+05 | 3.1760E+04 | 3.4000E+00 | 0.1000 |
| 83 | 3.0197E+05 | 3.4800E+03 | 3.5000E+00 | 0.0116 |
| 84 | 2.9849E+05 | 1.2800E+03 | 3.5116E+00 | 0.0043 |
| 85 | 2.9721E+05 | 2.6900E+03 | 3.5159E+00 | 0.0091 |
| 86 | 2.9452E+05 | 7.2700E+03 | 3.5250E+00 | 0.0250 |
| 87 | 2.8725E+05 | 1.4010E+04 | 3.5500E+00 | 0.0500 |
| 88 | 2.7324E+05 | 2.6000E+04 | 3.6000E+00 | 0.1000 |
| 89 | 2.4724E+05 | 1.2060E+04 | 3.7000E+00 | 0.0500 |
| 90 | 2.3518E+05 | 1.1470E+04 | 3.7500E+00 | 0.0500 |
| 91 | 2.2371E+05 | 1.0910E+04 | 3.8000E+00 | 0.0500 |
| 92 | 2.1280E+05 | 1.0380E+04 | 3.8500E+00 | 0.0500 |
| 93 | 2.0242E+05 | 9.8700E+03 | 3.9000E+00 | 0.0500 |
| 94 | 1.9255E+05 | 9.3900E+03 | 3.9500E+00 | 0.0500 |
| 95 | 1.8316E+05 | 8.9400E+03 | 4.0000E+00 | 0.0500 |
| 96 | 1.7422E+05 | 8.4900E+03 | 4.0500E+00 | 0.0500 |
| 97 | 1.6573E+05 | 8.0900E+03 | 4.1000E+00 | 0.0500 |
| 98 | 1.5764E+05 | 7.6800E+03 | 4.1500E+00 | 0.0500 |

TAB. 2.4 Continued

Neutron Group Energy Boundaries for the VITENDF70.BOLIB Library.

| Group | Upper Energy [eV] | Energy Width [eV] | Upper Lethargy | Lethargy Width |
|---|---|---|---|---|
| 99 | 1.4996E+05 | 7.3200E+03 | 4.2000E+00 | 0.0500 |
| 100 | 1.4264E+05 | 6.9500E+03 | 4.2500E+00 | 0.0500 |
| 101 | 1.3569E+05 | 6.6200E+03 | 4.3000E+00 | 0.0500 |
| 102 | 1.2907E+05 | 6.3000E+03 | 4.3500E+00 | 0.0500 |
| 103 | 1.2277E+05 | 5.9800E+03 | 4.4000E+00 | 0.0500 |
| 104 | 1.1679E+05 | 5.7000E+03 | 4.4500E+00 | 0.0500 |
| 105 | 1.1109E+05 | 1.3053E+04 | 4.5000E+00 | 0.1250 |
| 106 | 9.8037E+04 | 1.1520E+04 | 4.6250E+00 | 0.1250 |
| 107 | 8.6517E+04 | 4.0140E+03 | 4.7500E+00 | 0.0475 |
| 108 | 8.2503E+04 | 3.0040E+03 | 4.7975E+00 | 0.0371 |
| 109 | 7.9499E+04 | 7.5010E+03 | 4.8346E+00 | 0.0991 |
| 110 | 7.1998E+04 | 4.6190E+03 | 4.9337E+00 | 0.0663 |
| 111 | 6.7379E+04 | 1.0817E+04 | 5.0000E+00 | 0.1750 |
| 112 | 5.6562E+04 | 4.0870E+03 | 5.1750E+00 | 0.0750 |
| 113 | 5.2475E+04 | 6.1660E+03 | 5.2500E+00 | 0.1250 |
| 114 | 4.6309E+04 | 5.4410E+03 | 5.3750E+00 | 0.1250 |
| 115 | 4.0868E+04 | 6.5610E+03 | 5.5000E+00 | 0.1750 |
| 116 | 3.4307E+04 | 2.4790E+03 | 5.6750E+00 | 0.0750 |
| 117 | 3.1828E+04 | 3.3270E+03 | 5.7500E+00 | 0.1104 |
| 118 | 2.8501E+04 | 1.5010E+03 | 5.8604E+00 | 0.0541 |
| 119 | 2.7000E+04 | 9.4200E+02 | 5.9145E+00 | 0.0355 |
| 120 | 2.6058E+04 | 1.2700E+03 | 5.9500E+00 | 0.0500 |
| 121 | 2.4788E+04 | 6.1200E+02 | 6.0000E+00 | 0.0250 |
| 122 | 2.4176E+04 | 5.9700E+02 | 6.0250E+00 | 0.0250 |
| 123 | 2.3579E+04 | 1.7040E+03 | 6.0500E+00 | 0.0750 |
| 124 | 2.1875E+04 | 2.5700E+03 | 6.1250E+00 | 0.1250 |
| 125 | 1.9305E+04 | 4.2710E+03 | 6.2500E+00 | 0.2500 |
| 126 | 1.5034E+04 | 3.3250E+03 | 6.5000E+00 | 0.2500 |
| 127 | 1.1709E+04 | 1.1140E+03 | 6.7500E+00 | 0.1000 |
| 128 | 1.0595E+04 | 1.4762E+03 | 6.8500E+00 | 0.1500 |
| 129 | 9.1188E+03 | 2.0171E+03 | 7.0000E+00 | 0.2500 |
| 130 | 7.1017E+03 | 1.5709E+03 | 7.2500E+00 | 0.2500 |
| 131 | 5.5308E+03 | 1.2234E+03 | 7.5000E+00 | 0.2500 |
| 132 | 4.3074E+03 | 6.0000E+02 | 7.7500E+00 | 0.1500 |
| 133 | 3.7074E+03 | 3.5280E+02 | 7.9000E+00 | 0.1000 |
| 134 | 3.3546E+03 | 3.1920E+02 | 8.0000E+00 | 0.1000 |
| 135 | 3.0354E+03 | 2.8890E+02 | 8.1000E+00 | 0.1000 |
| 136 | 2.7465E+03 | 1.3390E+02 | 8.2000E+00 | 0.0500 |
| 137 | 2.6126E+03 | 1.2740E+02 | 8.2500E+00 | 0.0500 |
| 138 | 2.4852E+03 | 2.3650E+02 | 8.3000E+00 | 0.1000 |
| 139 | 2.2487E+03 | 2.1400E+02 | 8.4000E+00 | 0.1000 |
| 140 | 2.0347E+03 | 4.5010E+02 | 8.5000E+00 | 0.2500 |
| 141 | 1.5846E+03 | 3.5050E+02 | 8.7500E+00 | 0.2500 |
| 142 | 1.2341E+03 | 2.7298E+02 | 9.0000E+00 | 0.2500 |
| 143 | 9.6112E+02 | 2.1260E+02 | 9.2500E+00 | 0.2500 |
| 144 | 7.4852E+02 | 1.6557E+02 | 9.5000E+00 | 0.2500 |
| 145 | 5.8295E+02 | 1.2895E+02 | 9.7500E+00 | 0.2500 |
| 146 | 4.5400E+02 | 1.0043E+02 | 1.0000E+01 | 0.2500 |
| 147 | 3.5357E+02 | 7.8210E+01 | 1.0250E+01 | 0.2500 |

TAB. 2.4 Continued

Neutron Group Energy Boundaries for the VITENDF70.BOLIB Library.

| Group | Upper Energy [eV] | Energy Width [eV] | Upper Lethargy | Lethargy Width |
|---|---|---|---|---|
| 148 | 2.7536E+02 | 6.0910E+01 | 1.0500E+01 | 0.2500 |
| 149 | 2.1445E+02 | 4.7430E+01 | 1.0750E+01 | 0.2500 |
| 150 | 1.6702E+02 | 3.6950E+01 | 1.1000E+01 | 0.2500 |
| 151 | 1.3007E+02 | 2.8770E+01 | 1.1250E+01 | 0.2500 |
| 152 | 1.0130E+02 | 2.2407E+01 | 1.1500E+01 | 0.2500 |
| 153 | 7.8893E+01 | 1.7451E+01 | 1.1750E+01 | 0.2500 |
| 154 | 6.1442E+01 | 1.3591E+01 | 1.2000E+01 | 0.2500 |
| 155 | 4.7851E+01 | 1.0585E+01 | 1.2250E+01 | 0.2500 |
| 156 | 3.7266E+01 | 8.2430E+00 | 1.2500E+01 | 0.2500 |
| 157 | 2.9023E+01 | 6.4200E+00 | 1.2750E+01 | 0.2500 |
| 158 | 2.2603E+01 | 4.9990E+00 | 1.3000E+01 | 0.2500 |
| 159 | 1.7604E+01 | 3.8940E+00 | 1.3250E+01 | 0.2500 |
| 160 | 1.3710E+01 | 3.0330E+00 | 1.3500E+01 | 0.2500 |
| 161 | 1.0677E+01 | 2.3617E+00 | 1.3750E+01 | 0.2500 |
| 162 | 8.3153E+00 | 1.8393E+00 | 1.4000E+01 | 0.2500 |
| 163 | 6.4760E+00 | 1.4325E+00 | 1.4250E+01 | 0.2500 |
| 164 | 5.0435E+00 | 1.1156E+00 | 1.4500E+01 | 0.2500 |
| 165 | 3.9279E+00 | 8.6890E-01 | 1.4750E+01 | 0.2500 |
| 166 | 3.0590E+00 | 6.7660E-01 | 1.5000E+01 | 0.2500 |
| 167 | 2.3824E+00 | 5.2700E-01 | 1.5250E+01 | 0.2500 |
| 168 | 1.8554E+00 | 4.1040E-01 | 1.5500E+01 | 0.2500 |
| 169 | 1.4450E+00 | 1.4500E-01 | 1.5750E+01 | 0.1060 |
| 170 | 1.3000E+00 | 1.7470E-01 | 1.5856E+01 | 0.1440 |
| 171 | 1.1253E+00 | 4.5300E-02 | 1.6000E+01 | 0.0410 |
| 172 | 1.0800E+00 | 4.0000E-02 | 1.6041E+01 | 0.0380 |
| 173 | 1.0400E+00 | 4.0000E-02 | 1.6079E+01 | 0.0390 |
| 174 | 1.0000E+00 | 1.2357E-01 | 1.6118E+01 | 0.1320 |
| 175 | 8.7643E-01 | 7.6430E-02 | 1.6250E+01 | 0.0910 |
| 176 | 8.0000E-01 | 1.1744E-01 | 1.6341E+01 | 0.1590 |
| 177 | 6.8256E-01 | 5.7500E-02 | 1.6500E+01 | 0.0880 |
| 178 | 6.2506E-01 | 9.3480E-02 | 1.6588E+01 | 0.1620 |
| 179 | 5.3158E-01 | 3.1580E-02 | 1.6750E+01 | 0.0610 |
| 180 | 5.0000E-01 | 8.6010E-02 | 1.6811E+01 | 0.1890 |
| 181 | 4.1399E-01 | 4.7190E-02 | 1.7000E+01 | 0.1210 |
| 182 | 3.6680E-01 | 4.1800E-02 | 1.7121E+01 | 0.1210 |
| 183 | 3.2500E-01 | 5.0000E-02 | 1.7242E+01 | 0.1670 |
| 184 | 2.7500E-01 | 5.0000E-02 | 1.7409E+01 | 0.2010 |
| 185 | 2.2500E-01 | 4.1000E-02 | 1.7610E+01 | 0.2010 |
| 186 | 1.8400E-01 | 3.4000E-02 | 1.7811E+01 | 0.2040 |
| 187 | 1.5000E-01 | 2.5000E-02 | 1.8015E+01 | 0.1830 |
| 188 | 1.2500E-01 | 2.5000E-02 | 1.8198E+01 | 0.2230 |
| 189 | 1.0000E-01 | 3.0000E-02 | 1.8421E+01 | 0.3560 |
| 190 | 7.0000E-02 | 2.0000E-02 | 1.8777E+01 | 0.3370 |
| 191 | 5.0000E-02 | 1.0000E-02 | 1.9114E+01 | 0.2230 |
| 192 | 4.0000E-02 | 1.0000E-02 | 1.9337E+01 | 0.2880 |
| 193 | 3.0000E-02 | 9.0000E-03 | 1.9625E+01 | 0.3560 |
| 194 | 2.1000E-02 | 6.5000E-03 | 1.9981E+01 | 0.3710 |
| 195 | 1.4500E-02 | 4.5000E-03 | 2.0352E+01 | 0.3710 |
| 196 | 1.0000E-02 | 5.0000E-03 | 2.0723E+01 | 0.6930 |

TAB. 2.4 Continued

Neutron Group Energy Boundaries for the VITENDF70.BOLIB Library.

| Group | Upper Energy [eV] | Energy Width [eV] | Upper Lethargy | Lethargy Width |
|---|---|---|---|---|
| 197 | 5.0000E-03 | 3.0000E-03 | 2.1416E+01 | 0.9170 |
| 198 | 2.0000E-03 | 1.5000E-03 | 2.2333E+01 | 1.3860 |
| 199 | 5.0000E-04 | 4.9000E-04 | 2.3719E+01 | 3.9120 |
| | Lower Energy | | Lower Lethargy | |
| | 1.0000E-05 | | 2.7631E+01 | |

TAB. 2.5

Photon Group Energy Boundaries for the VITENDF70.BOLIB Library.

| Group | Upper Energy [eV] | Energy Width [eV] | Upper Lethargy | Lethargy Width |
|---|---|---|---|---|
| 1 | 3.0000E+07 | 1.0000E+07 | -1.0986E+00 | 0.4055 |
| 2 | 2.0000E+07 | 6.0000E+06 | -6.9315E-01 | 0.3567 |
| 3 | 1.4000E+07 | 2.0000E+06 | -3.3647E-01 | 0.1542 |
| 4 | 1.2000E+07 | 2.0000E+06 | -1.8232E-01 | 0.1823 |
| 5 | 1.0000E+07 | 2.0000E+06 | 0.0000E+00 | 0.2231 |
| 6 | 8.0000E+06 | 5.0000E+05 | 2.2314E-01 | 0.0645 |
| 7 | 7.5000E+06 | 5.0000E+05 | 2.8768E-01 | 0.0690 |
| 8 | 7.0000E+06 | 5.0000E+05 | 3.5667E-01 | 0.0741 |
| 9 | 6.5000E+06 | 5.0000E+05 | 4.3078E-01 | 0.0800 |
| 10 | 6.0000E+06 | 5.0000E+05 | 5.1083E-01 | 0.0870 |
| 11 | 5.5000E+06 | 5.0000E+05 | 5.9784E-01 | 0.0953 |
| 12 | 5.0000E+06 | 5.0000E+05 | 6.9315E-01 | 0.1054 |
| 13 | 4.5000E+06 | 5.0000E+05 | 7.9851E-01 | 0.1178 |
| 14 | 4.0000E+06 | 5.0000E+05 | 9.1629E-01 | 0.1335 |
| 15 | 3.5000E+06 | 5.0000E+05 | 1.0498E+00 | 0.1542 |
| 16 | 3.0000E+06 | 5.0000E+05 | 1.2040E+00 | 0.1823 |
| 17 | 2.5000E+06 | 5.0000E+05 | 1.3863E+00 | 0.2231 |
| 18 | 2.0000E+06 | 3.4000E+05 | 1.6094E+00 | 0.1863 |
| 19 | 1.6600E+06 | 1.6000E+05 | 1.7958E+00 | 0.1014 |
| 20 | 1.5000E+06 | 1.6000E+05 | 1.8971E+00 | 0.1128 |
| 21 | 1.3400E+06 | 1.0000E+04 | 2.0099E+00 | 0.0075 |
| 22 | 1.3300E+06 | 3.3000E+05 | 2.0174E+00 | 0.2852 |
| 23 | 1.0000E+06 | 2.0000E+05 | 2.3026E+00 | 0.2231 |
| 24 | 8.0000E+05 | 1.0000E+05 | 2.5257E+00 | 0.1335 |
| 25 | 7.0000E+05 | 1.0000E+05 | 2.6593E+00 | 0.1542 |
| 26 | 6.0000E+05 | 8.8000E+04 | 2.8134E+00 | 0.1586 |
| 27 | 5.1200E+05 | 2.0000E+03 | 2.9720E+00 | 0.0039 |
| 28 | 5.1000E+05 | 6.0000E+04 | 2.9759E+00 | 0.1252 |
| 29 | 4.5000E+05 | 5.0000E+04 | 3.1011E+00 | 0.1178 |
| 30 | 4.0000E+05 | 1.0000E+05 | 3.2189E+00 | 0.2877 |
| 31 | 3.0000E+05 | 1.0000E+05 | 3.5066E+00 | 0.4055 |
| 32 | 2.0000E+05 | 5.0000E+04 | 3.9120E+00 | 0.2877 |
| 33 | 1.5000E+05 | 5.0000E+04 | 4.1997E+00 | 0.4055 |
| 34 | 1.0000E+05 | 2.5000E+04 | 4.6052E+00 | 0.2877 |
| 35 | 7.5000E+04 | 5.0000E+03 | 4.8929E+00 | 0.0690 |
| 36 | 7.0000E+04 | 1.0000E+04 | 4.9618E+00 | 0.1542 |
| 37 | 6.0000E+04 | 1.5000E+04 | 5.1160E+00 | 0.2877 |
| 38 | 4.5000E+04 | 5.0000E+03 | 5.4037E+00 | 0.1178 |
| 39 | 4.0000E+04 | 1.0000E+04 | 5.5215E+00 | 0.2877 |
| 40 | 3.0000E+04 | 1.0000E+04 | 5.8091E+00 | 0.4055 |
| 41 | 2.0000E+04 | 1.0000E+04 | 6.2146E+00 | 0.6931 |
| 42 | 1.0000E+04 | 9.0000E+03 | 6.9078E+00 | 2.3026 |
| | Lower Energy | | Lower Lethargy | |
| | 1.0000E+03 | | 9.2103E+00 | |

TAB. 2.6

VITENDF70.BOLIB Library Thermal Neutron Energy Range.

| Group | Upper Energy [eV] | Lethargy Width | Group | Upper Energy [eV] | Lethargy Width |
|---|---|---|---|---|---|
| 164 | 5.04350 | 0.250 | 182 | 0.36680 | 0.121 |
| 165 | 3.92790 | 0.250 | 183 | 0.32500 | 0.167 |
| 166 | 3.05900 | 0.250 | 184 | 0.27500 | 0.201 |
| 167 | 2.38240 | 0.250 | 185 | 0.22500 | 0.201 |
| 168 | 1.85540 | 0.250 | 186 | 0.18400 | 0.204 |
| 169 | 1.44500 | 0.106 | 187 | 0.15000 | 0.183 |
| 170 | 1.30000 | 0.144 | 188 | 0.12500 | 0.223 |
| 171 | 1.12530 | 0.041 | 189 | 0.10000 | 0.356 |
| 172 | 1.08000 | 0.038 | 190 | 0.07000 | 0.337 |
| 173 | 1.04000 | 0.039 | 191 | 0.05000 | 0.223 |
| 174 | 1.00000 | 0.132 | 192 | 0.04000 | 0.288 |
| 175 | 0.87643 | 0.091 | 193 | 0.03000 | 0.356 |
| 176 | 0.80000 | 0.159 | 194 | 0.02100 | 0.371 |
| 177 | 0.68256 | 0.088 | 195 | 0.01450 | 0.371 |
| 178 | 0.62506 | 0.162 | 196 | 0.01000 | 0.693 |
| 179 | 0.53158 | 0.061 | 197 | 0.00500 | 0.917 |
| 180 | 0.50000 | 0.189 | 198 | 0.00200 | 1.386 |
| 181 | 0.41399 | 0.121 | 199 | 0.00050 | 3.912 |
| | | | | Lower Energy 0.00001 | |

2.4 - Weighting Function

The neutron and photon weighting functions used to produce the VITENDF70.BOLIB /5/ library cross sections are the same as those employed in the generation of the VITAMIN-B6 /8/ cross sections.
The neutron weighting function is of the form typically chosen for fission reactor shielding problems, i.e. it consists of a smoothly varying combination of a Maxwellian thermal spectrum, a fission spectrum, and a "l/E" slowing down spectrum. This corresponds to the IWT=4 option in the GROUPR module of the NJOY /17/ system. The breakpoint energies for the 3-region spectrum are similar to those used in VITAMIN-C /61/. The breakpoint energy between the Maxwellian and l/E shapes is 0.125 eV. The fission temperature has been adjusted to better reflect the neutron spectrum in a thermal reactor ($\theta$ = 1.273 MeV). The use of a large number of energy groups should make the exact functional form and energy break points less important compared to generating a broad-group library directly from ENDF/B data. The functional form of the weighting spectrum is given by the following:

| Functional Form | Energy Limits | Groups |
|---|---|---|
| 1. Maxwellian Thermal Spectrum (kT = 0.025 eV) | | |
| $W_1(E) = C_1 E e^{-E/kT}$ | 1.0E-5 eV to 0.125 eV | 188-199 |
| 2. "l/E" Slowing-Down Spectrum | | |
| $W_2(E) = C_2/E$ | 0.125 eV to 820.8 keV | 67-187 |
| 3. Fission Spectrum ($\theta$ = 1.273 MeV) | | |
| $W_3(E) = C_3 E^{1/2} e^{-E/\theta}$ | 820.8 keV to 20 MeV | 1-66 |

A continuous weighting spectrum is achieved with the following constants: $C_1 = 9498.4\ eV^{-2}$, $C_2 = 1.0$ and $C_3 = 2.5625\ MeV^{-1.5}$. The neutron weighting function is shown in FIG. 2.1 and listed in TAB. 2.7 in a 199 group representation.

The photon weighting spectrum consists of a l/E spectrum with a "roll-off" of the spectrum at lower energies to represent photoelectric absorption and a similar drop-off of the spectrum at higher energies corresponding to the Q-value for neutron capture. This corresponds to the IWT=3 input option in the GAMINR module of the NJOY system. The photon weighting function is shown in FIG. 2.2 and listed in TAB. 2.8 in a 42 group representation.

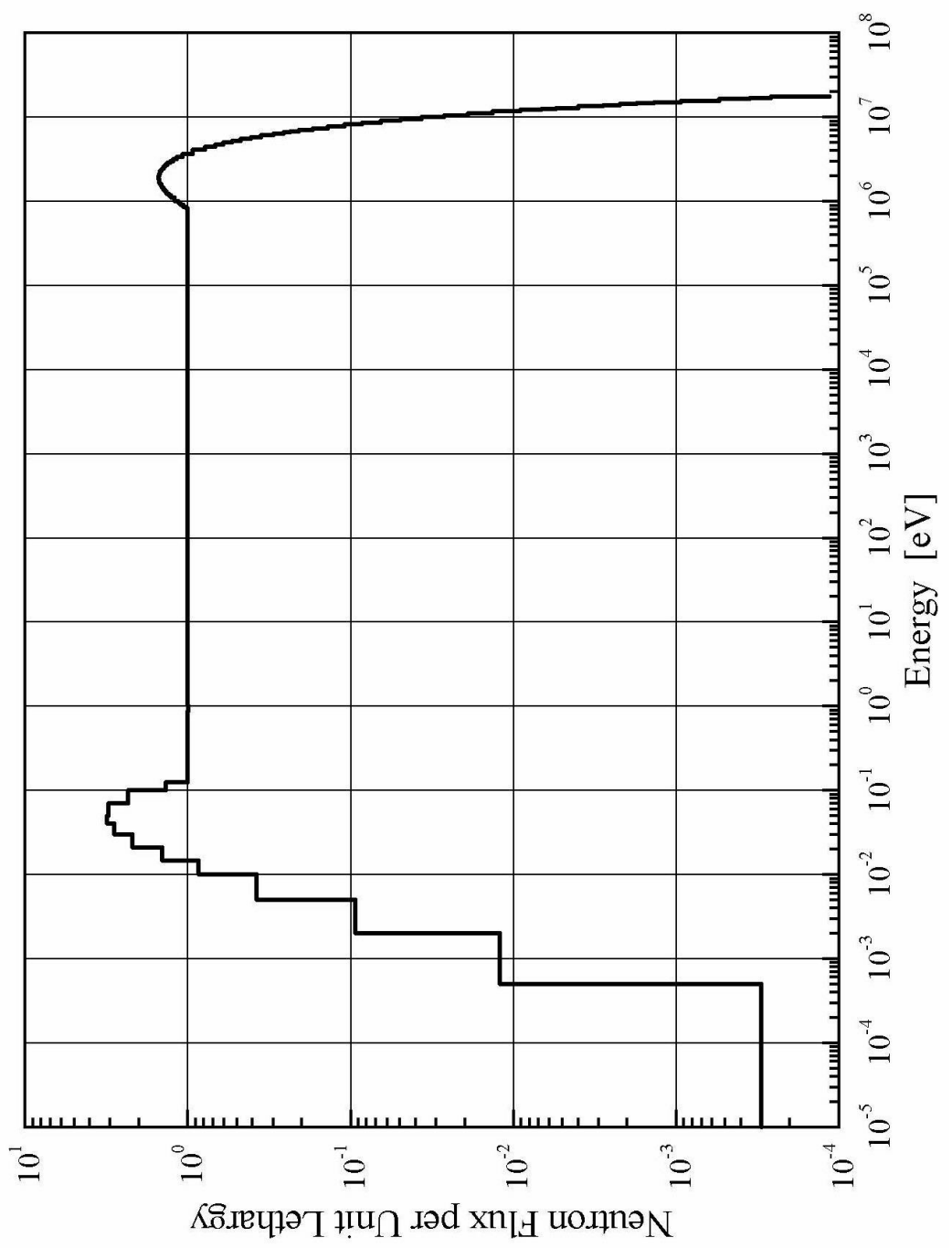


FIG. 2.1 199 Group Representation of Standard Weighting Spectrum Used to Create VITENDF70.BOLIB Neutron Cross Sections from ENDF/B-VII.0 Point-Wise Data.

TAB. 2.7

Neutron Energy Weighting Spectrum for the VITENDF70.BOLIB Library.

| Group | Weight | Group | Weight | Group | Weight |
|---|---|---|---|---|---|
| 1 | 1.423E-05 | 51 | 7.543E-02 | 101 | 5.002E-02 |
| 2 | 6.578E-06 | 52 | 7.516E-02 | 102 | 5.004E-02 |
| 3 | 8.861E-06 | 53 | 7.461E-02 | 103 | 4.994E-02 |
| 4 | 2.733E-05 | 54 | 7.389E-02 | 104 | 5.004E-02 |
| 5 | 4.690E-05 | 55 | 7.295E-02 | 105 | 1.250E-01 |
| 6 | 3.419E-05 | 56 | 7.181E-02 | 106 | 1.250E-01 |
| 7 | 4.380E-05 | 57 | 7.031E-02 | 107 | 4.751E-02 |
| 8 | 5.590E-05 | 58 | 6.888E-02 | 108 | 3.709E-02 |
| 9 | 7.036E-05 | 59 | 6.723E-02 | 109 | 9.911E-02 |
| 10 | 1.991E-04 | 60 | 6.552E-02 | 110 | 6.631E-02 |
| 11 | 1.368E-04 | 61 | 6.354E-02 | 111 | 1.750E-01 |
| 12 | 1.684E-04 | 62 | 1.211E-01 | 112 | 7.500E-02 |
| 13 | 4.576E-04 | 63 | 4.809E-02 | 113 | 1.250E-01 |
| 14 | 6.684E-04 | 64 | 6.474E-02 | 114 | 1.250E-01 |
| 15 | 9.574E-04 | 65 | 5.321E-02 | 115 | 1.750E-01 |
| 16 | 1.342E-03 | 66 | 5.108E-02 | 116 | 7.500E-02 |
| 17 | 1.843E-03 | 67 | 5.000E-02 | 117 | 1.104E-01 |
| 18 | 2 482E-03 | 68 | 5.000E-02 | 118 | 5.410E-02 |
| 19 | 3.285E-03 | 69 | 5.001E-02 | 119 | 3.551E-02 |
| 20 | 4.272E-03 | 70 | 4.999E-02 | 120 | 4.997E-02 |
| 21 | 5.465E-03 | 71 | 5.001E-02 | 121 | 2.500E-02 |
| 22 | 6.882E-03 | 72 | 5.000E-02 | 122 | 2.500E-02 |
| 23 | 8.540E-03 | 73 | 5.000E-02 | 123 | 7.501E-02 |
| 24 | 1.045E-02 | 74 | 5.000E-02 | 124 | 1.250E-01 |
| 25 | 3.951E-03 | 75 | 4.999E-02 | 125 | 2.501E-01 |
| 26 | 8.659E-03 | 76 | 5.001E-02 | 126 | 2.500E-01 |
| 27 | 1.503E-02 | 77 | 1.000E-01 | 127 | 9.998E-02 |
| 28 | 1.769E-02 | 78 | 1.000E-01 | 128 | 1.500E-01 |
| 29 | 2.058E-02 | 79 | 5.000E-02 | 129 | 2.500E-01 |
| 30 | 2.368E-02 | 80 | 5.000E-02 | 130 | 2.500E-01 |
| 31 | 2.697E-02 | 81 | 1.000E-01 | 131 | 2.500E-01 |
| 32 | 3.041E-02 | 82 | 1.000E-01 | 132 | 1.500E-01 |
| 33 | 3.397E-02 | 83 | 1.159E-02 | 133 | 1.000E-01 |
| 34 | 7.885E-02 | 84 | 4.297E-03 | 134 | 9.999E-02 |
| 35 | 9.338E-02 | 85 | 9.092E-03 | 135 | 1.000E-01 |
| 36 | 1.073E-01 | 86 | 2.499E-02 | 136 | 4.998E-02 |
| 37 | 5.848E-02 | 87 | 5.000E-02 | 137 | 4.999E-02 |
| 38 | 6.148E-02 | 88 | 9.999E-02 | 138 | 1.000E-01 |
| 39 | 6.413E-02 | 89 | 5.001E-02 | 139 | 1.000E-01 |
| 40 | 6.666E-02 | 90 | 5.000E-02 | 140 | 2.500E-01 |
| 41 | 6.879E-02 | 91 | 5.000E-02 | 141 | 2.500E-01 |
| 42 | 7.065E-02 | 92 | 5.001E-02 | 142 | 2.500E-01 |
| 43 | 4.797E-02 | 93 | 4.999E-02 | 143 | 2.500E-01 |
| 44 | 1.216E-02 | 94 | 5.000E-02 | 144 | 2.500E-01 |
| 45 | 1.212E-02 | 95 | 5.004E-02 | 145 | 2.500E-01 |
| 46 | 2.439E-02 | 96 | 4.996E-02 | 146 | 2.500E-01 |
| 47 | 4.909E-02 | 97 | 5.005E-02 | 147 | 2.500E-01 |
| 48 | 7.440E-02 | 98 | 4.995E-02 | 148 | 2.500E-01 |
| 49 | 7.503E-02 | 99 | 5.004E-02 | 149 | 2.500E-01 |
| 50 | 7.539E-02 | 100 | 4.995E-02 | 150 | 2.500E-01 |

TAB. 2.7 Continued

Neutron Energy Weighting Spectrum for the VITENDF70.BOLIB Library.

| Group | Weight | Group | Weight | Group | Weight |
|---|---|---|---|---|---|
| 151 | 2.500E-01 | 168 | 2.500E-01 | 185 | 2.012E-01 |
| 152 | 2.500E-01 | 169 | 1.057E-01 | 186 | 2.043E-01 |
| 153 | 2.500E-01 | 170 | 1.443E-01 | 187 | 1.823E-01 |
| 154 | 2.500E-01 | 171 | 4.109E-02 | 188 | 3.037E-01 |
| 155 | 2.500E-01 | 172 | 3.774E-02 | 189 | 8.282E-01 |
| 156 | 2.500E-01 | 173 | 3.922E-02 | 190 | 1.038E+00 |
| 157 | 2.500E-01 | 174 | 1.319E-01 | 191 | 7.060E-01 |
| 158 | 2.500E-01 | 175 | 9.125E-02 | 192 | 8.174E-01 |
| 159 | 2.500E-01 | 176 | 1.588E-01 | 193 | 7.820E-01 |
| 160 | 2.500E-01 | 177 | 8.800E-02 | 194 | 5.360E-01 |
| 161 | 2.500E-01 | 178 | 1.620E-01 | 195 | 3.194E-01 |
| 162 | 2.500E-01 | 179 | 6.125E-02 | 196 | 2.614E-01 |
| 163 | 2.500E-01 | 180 | 1.888E-01 | 197 | 8.601E-02 |
| 164 | 2.500E-01 | 181 | 1.210E-01 | 198 | 1.684E-02 |
| 165 | 2.500E-01 | 182 | 1.210E-01 | 199 | 1.171E-03 |
| 166 | 2.500E-01 | 183 | 1.671E-01 | | |
| 167 | 2.500E-01 | 184 | 2.007E-01 | | |

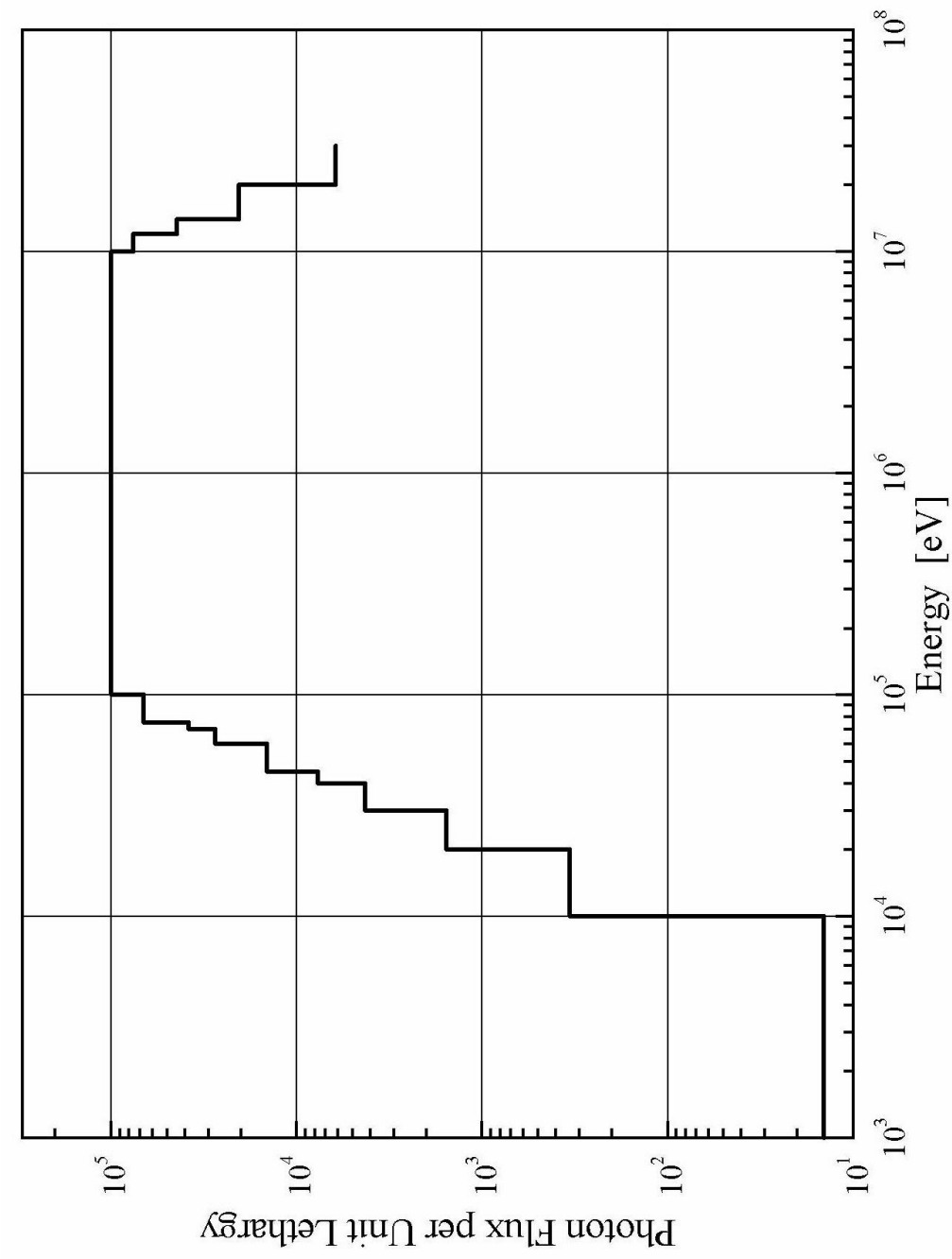


FIG. 2.2 42 Group Representation of Standard Weighting Spectrum Used to Create VITENDF70.BOLIB Photon Cross Sections from ENDF/B-VII.0 Point-Wise Data.

TAB. 2.8

Photon Energy Weighting Spectrum for the VITENDF70.BOLIB Library.

| Group | Weight | Group | Weight | Group | Weight |
|---|---|---|---|---|---|
| 1 | 2.498E+03 | 15 | 1.542E+04 | 29 | 1.178E+04 |
| 2 | 7.298E+03 | 16 | 1.824E+04 | 30 | 2.877E+04 |
| 3 | 6.824E+03 | 17 | 2.232E+04 | 31 | 4.055E+04 |
| 4 | 1.387E+04 | 18 | 1.864E+04 | 32 | 2.877E+04 |
| 5 | 2.232E+04 | 19 | 1.014E+04 | 33 | 4.055E+04 |
| 6 | 6.455E+03 | 20 | 1.128E+04 | 34 | 1.927E+04 |
| 7 | 6.901E+03 | 21 | 7.491E+02 | 35 | 2.629E+03 |
| 8 | 7.413E+03 | 22 | 2.852E+04 | 36 | 4.233E+03 |
| 9 | 8.006E+03 | 23 | 2.232E+04 | 37 | 4.163E+03 |
| 10 | 8.703E+03 | 24 | 1.335E+04 | 38 | 9.042E+02 |
| 11 | 9.534E+03 | 25 | 1.542E+04 | 39 | 1.233E+03 |
| 12 | 1.054E+04 | 26 | 1.586E+04 | 40 | 6.333E+02 |
| 13 | 1.178E+04 | 27 | 3.914E+02 | 41 | 2.333E+02 |
| 14 | 1.336E+04 | 28 | 1.252E+04 | 42 | 3.330E+01 |

2.5 - Legendre Order of Scattering

The order of scattering used for both neutrons and photons is $P_7$, for nuclides with Z=l through Z=29 (copper) and $P_5$ for the remainder of the nuclides. In particular, the previous values corresponding to L=ℓ-max, the maximum order of the Legendre polynomial ($P_\ell$) expansion of the scattering cross section matrix, available for each nuclide of the library, are listed in TAB. 2.2.
Most calculations are likely to be done with $P_3$ scattering, but for some problems, e.g., when single scatter events dominate, higher orders may be required as stated in the VITAMIN-B6 /8/ library user's manual. For the same nuclide, an identical order of scattering for both neutrons and photons was adopted in the generation of the VITAMIN-B6, VITENDF70.BOLIB /5/, VITJEFF311.BOLIB /31/, MATJEFF31.BOLIB /43/, VITJEFF31.BOLIB /44/, MATJEF22.BOLIB /47/ and VITJEF22.BOLIB /48/ cross sections.

2.6 - Convergence Parameters

The following numerical values of the fractional error tolerances were chosen as input parameters in NJOY /17/ to generate the libraries VITENDF70.BOLIB /5/, VITJEFF311.BOLIB /31/, MATJEFF31.BOLIB /43/ and VITJEFF31.BOLIB /44/: 0.1% for resolved resonance reconstruction and for linearization in RECONR and 0.1% for thinning in BROADR. These data have reduced numerical values with respect to the 0.2% corresponding error tolerance values used to generate VITAMIN-B6 /8/, MATJEF22.BOLIB /47/ and VITJEF22.BOLIB /48/, chosen on the basis of the ORNL experience with the VITAMIN libraries and the experience of the NJOY users.

2.7 - Processing Codes and Procedures

The NJOY-99.259 /17/ nuclear data processing system and the ENEA-Bologna 2007 Revision /19/ of the SCAMPI /18/ nuclear data processing system were used on a Personal Computer (CPU INTEL Pentium III, 448 MB of RAM; FSF-g77 version 0.5.26 FORTRAN compiler for NJOY and f77 Absoft version 5.0 FORTRAN 77 compiler for SCAMPI) with the Linux Red Hat 7.1 operating system to generate the VITENDF70.BOLIB /5/ library. The following modules of NJOY were used to process neutron interaction (n-n), photon production (n-γ) and photon interaction (γ-γ) data into the GENDF format, from the ENDF/B-VII.0 incident neutron and photo-atomic data in ENDF-6 /56/ format. Specifically, the MODER, RECONR, BROADR, THERMR, HEATR, GASPR, PURR, GROUPR modules were used for the incident neutron data while the MODER, RECONR and GAMINR modules were used for the photo-atomic data. Then the ENEA-Bologna revised version of the SMILER module, contained in the ENEA-Bologna 2007 Revision of SCAMPI, was used to translate the fine-group data from the GENDF format into the AMPX master library format of VITENDF70.BOLIB. The RADE module of SCAMPI was used to check and screen the data for internal consistency and "sanity", i.e. the data values are physical and within expected bounds. Then the module AIM of SCAMPI was used to convert the master cross section libraries for the standard and bound nuclide cross section files from binary to BCD format.
A brief description of the function of the NJOY and SCAMPI modules is presented in TAB. 2.9. A schematic diagram illustrating the VITENDF70.BOLIB processing procedure to produce the standard nuclide cross section files is given in FIG. 2.3, while the procedure to produce the bound nuclide cross section files is reported in FIG. 2.4.

TAB. 2.9

Modules from the NJOY-99.259 and SCAMPI
Nuclear Data Processing Systems Used to Process VITENDF70.BOLIB.

NJOY-99.259 System

| Module | Function |
|---|---|
| MODER | Converts between ENDF/B standard coded mode and the NJOY blocked binary mode. |
| RECONR | Reconstructs point-wise cross sections from ENDF/B resonance parameters and interpolation schemes. |
| BROADR | Doppler-broadens and thins point-wise cross sections. |
| THERMR | Produces cross sections and energy-to-energy matrices for free or bound scatterers in the thermal energy range. |
| HEATR | Generates heat production cross sections (KERMA factors) and damage-energy production. |
| GASPR | Computes gas production cross sections. |
| PURR | Computes probability tables and effective point-wise self-shielded cross sections in the unresolved energy range. |
| GROUPR | Generates self-shielded multi-group cross sections and group-to-group scattering and photon production matrices in GENDF format. |
| GAMINR | Computes multi-group photo-atomic cross sections, KERMA factors, group-to-group photon scattering matrices. |

SCAMPI System (ENEA-Bologna 2007 Revision)

| Module | Function |
|---|---|
| SMILER | Translates GENDF files produced by NJOY into AMPX master interface format. |
| RADE | Performs sanity and consistency tests on multi-group libraries. |
| AIM | Converts master cross section libraries from binary format to BCD (or vice-versa). |

FIG. 2.3 Procedure for Generating the VITENDF70.BOLIB Library in AMPX Format from ENDF/B-VII.0.

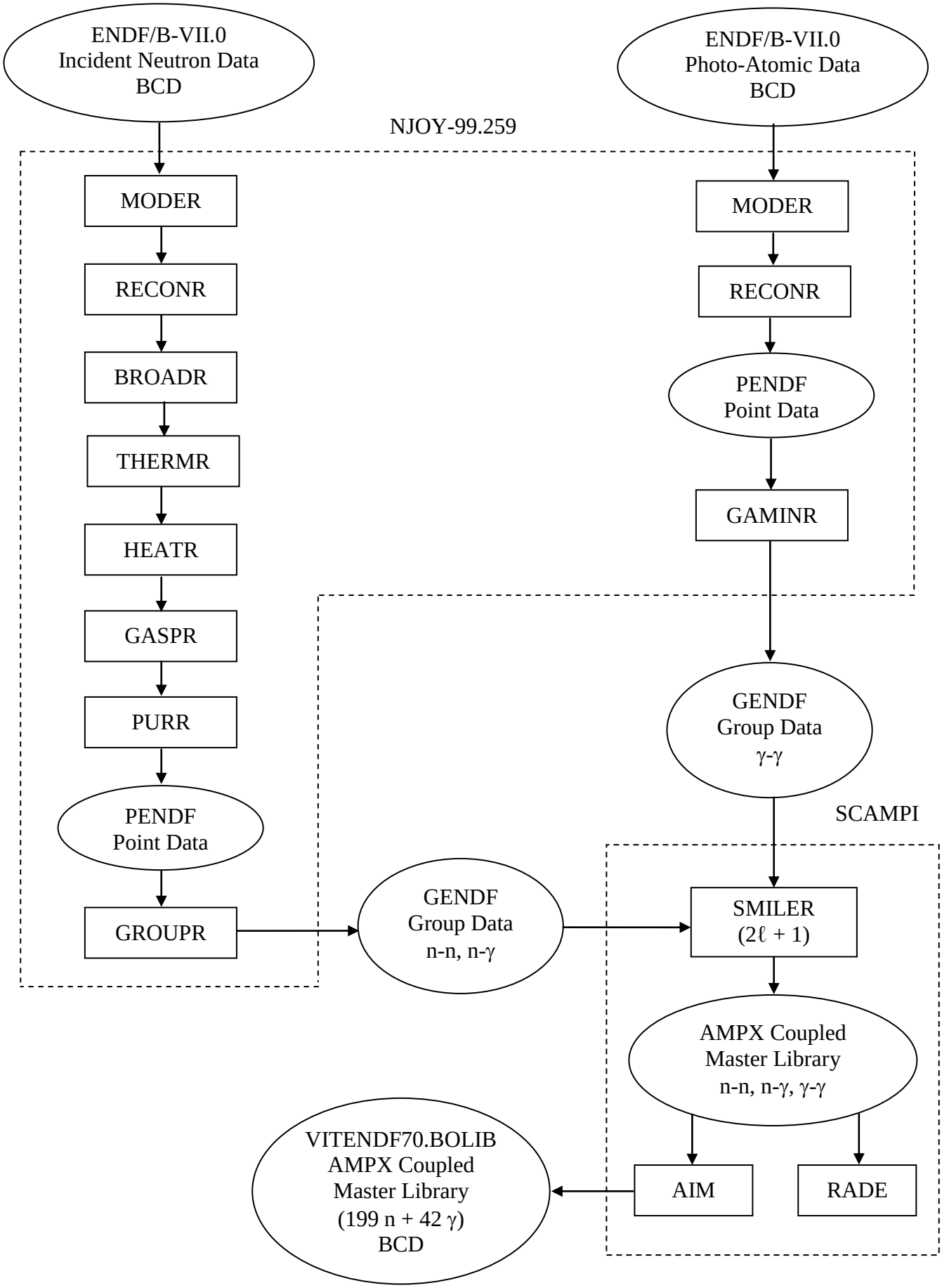

FIG. 2.4 Procedure for Generating the VITENDF70.BOLIB Bound Nuclides in AMPX Format from ENDF/B-VII.0.

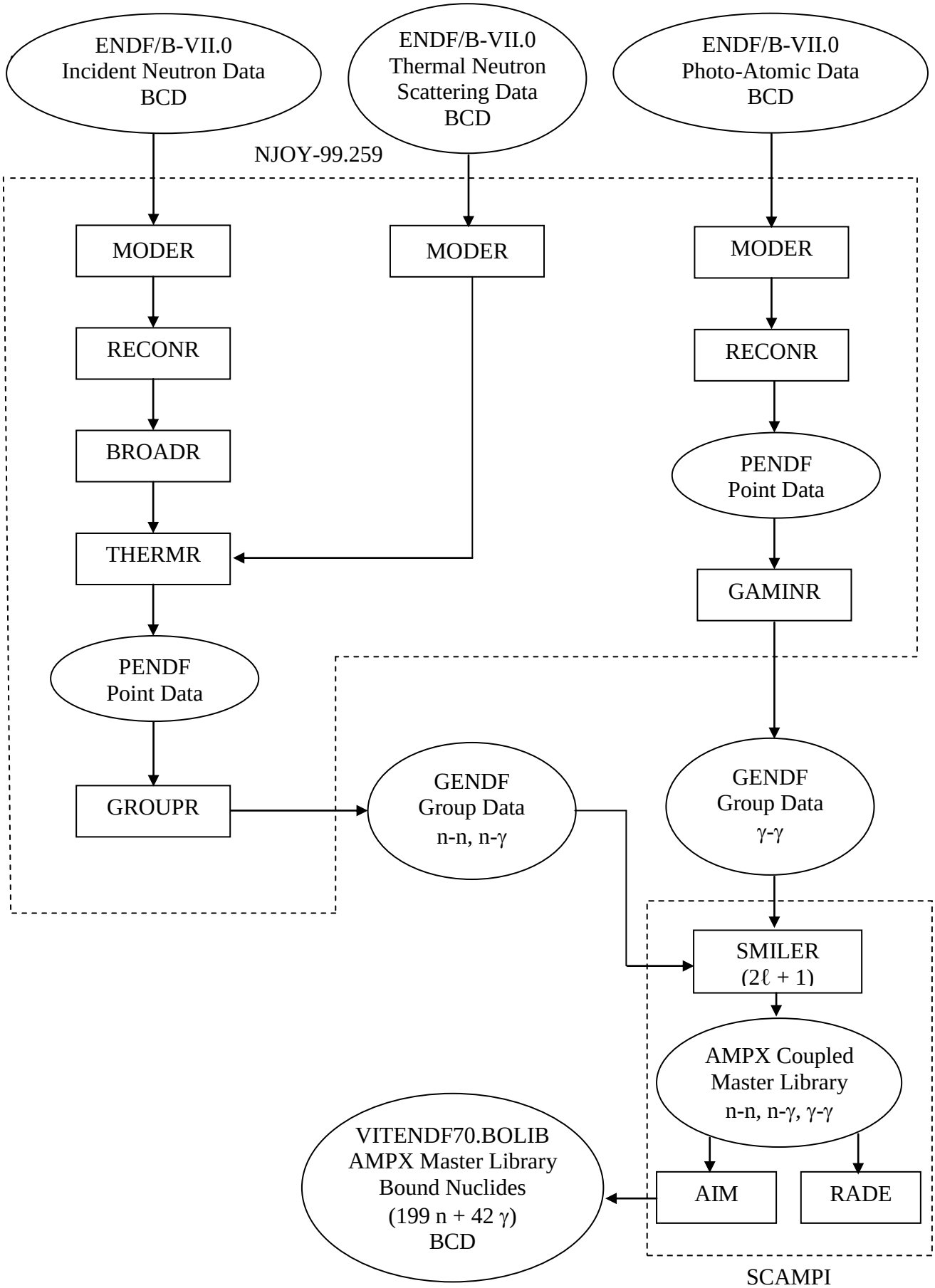

2.8 - Response Functions

At present only the following "response" functions are included in tabulated form in the VITENDF70.BOLIB /5/ library package: neutron and photon group energy boundaries, neutron and photon group energy widths, neutron and photon group lethargy boundaries, neutron and photon group lethargy widths, total (prompt + delayed) neutron fission spectra ($\chi$) for the U-235, U-238 and Pu-239 nuclides.

The total neutron fission spectra ($\chi$) were obtained through the ENEA-Bologna 2007 Revision /19/ of the SCAMPI /18/ system which allows processing of delayed neutron spectra. In particular the BONAMI and NITAWL modules were firstly used to generate an AMPX working file for each fissile nuclide, containing infinitely dilute cross sections (background cross section $\sigma_0$ = 1.0E+10 barns) at the temperature of 300 °K. Then the fine-group $\chi$-vectors were calculated by the ICE module with the KOPT=4 option (nuclide-dependent spectrum option) in the 1$$ array, i.e. using the neutron flux spectrum derived from the weighting functions corresponding to the IWT=4 option in GROUPR (see 2.4), always provided in each nuclide data file of an AMPX working library.

Then the normalization of the total neutron fission spectra ($\chi$) to one neutron per fission was performed since the ICE module with the KOPT=4 option does not ensure a proper normalization (see /18/).

The resulting total neutron fission spectra for the U-235, U-238 and Pu-239 nuclides are reported in TAB. 2.10.

A 199 group representation of the U-235, U-238 and Pu-239 total neutron fission spectra are shown in FIG. 2.5.

TAB. 2.10

VITENDF70.BOLIB Library Total Neutron Fission Spectra for U-235, U-238 and Pu-239.

| Group | Upper Energy [eV] | U-235 X | U-238 X | Pu-239 X |
|---|---|---|---|---|
| 1 | 1.9640E+07 | 4.48487E-06 | 3.96812E-06 | 8.08940E-06 |
| 2 | 1.7332E+07 | 1.78036E-06 | 1.61066E-06 | 3.04165E-06 |
| 3 | 1.6905E+07 | 2.53075E-06 | 2.20345E-06 | 4.24039E-06 |
| 4 | 1.6487E+07 | 7.81808E-06 | 6.95344E-06 | 1.28221E-05 |
| 5 | 1.5683E+07 | 1.38041E-05 | 1.22533E-05 | 2.20075E-05 |
| 6 | 1.4918E+07 | 1.04142E-05 | 9.08987E-06 | 1.62518E-05 |
| 7 | 1.4550E+07 | 1.34914E-05 | 1.17857E-05 | 2.07938E-05 |
| 8 | 1.4191E+07 | 1.67525E-05 | 1.52045E-05 | 2.55743E-05 |
| 9 | 1.3840E+07 | 2.22662E-05 | 1.93326E-05 | 3.34426E-05 |
| 10 | 1.3499E+07 | 6.20470E-05 | 5.55362E-05 | 9.17669E-05 |
| 11 | 1.2840E+07 | 4.44299E-05 | 3.86555E-05 | 6.44415E-05 |
| 12 | 1.2523E+07 | 5.48109E-05 | 4.79983E-05 | 7.86931E-05 |
| 13 | 1.2214E+07 | 1.47656E-04 | 1.32016E-04 | 2.08738E-04 |
| 14 | 1.1618E+07 | 2.20844E-04 | 1.95609E-04 | 3.05587E-04 |
| 15 | 1.1052E+07 | 3.19935E-04 | 2.83836E-04 | 4.33535E-04 |
| 16 | 1.0513E+07 | 4.49962E-04 | 4.02938E-04 | 5.98666E-04 |
| 17 | 1.0000E+07 | 5.99349E-04 | 5.58856E-04 | 7.85270E-04 |
| 18 | 9.5123E+06 | 8.15877E-04 | 7.61601E-04 | 1.04929E-03 |
| 19 | 9.0484E+06 | 1.09028E-03 | 1.01902E-03 | 1.37736E-03 |
| 20 | 8.6071E+06 | 1.43116E-03 | 1.33946E-03 | 1.77749E-03 |
| 21 | 8.1873E+06 | 1.84627E-03 | 1.73067E-03 | 2.25656E-03 |
| 22 | 7.7880E+06 | 2.34208E-03 | 2.19927E-03 | 2.82002E-03 |
| 23 | 7.4082E+06 | 2.92318E-03 | 2.75017E-03 | 3.47132E-03 |
| 24 | 7.0469E+06 | 3.59131E-03 | 3.38571E-03 | 4.21079E-03 |
| 25 | 6.7032E+06 | 1.36042E-03 | 1.28433E-03 | 1.58274E-03 |
| 26 | 6.5924E+06 | 2.98418E-03 | 2.82034E-03 | 3.45219E-03 |
| 27 | 6.3763E+06 | 5.18167E-03 | 4.90604E-03 | 5.94099E-03 |
| 28 | 6.0653E+06 | 6.09432E-03 | 5.78236E-03 | 6.91861E-03 |
| 29 | 5.7695E+06 | 7.07797E-03 | 6.72959E-03 | 7.96166E-03 |
| 30 | 5.4881E+06 | 8.12031E-03 | 7.73577E-03 | 9.05525E-03 |
| 31 | 5.2205E+06 | 9.21823E-03 | 8.79774E-03 | 1.01951E-02 |
| 32 | 4.9659E+06 | 1.03591E-02 | 9.90336E-03 | 1.13661E-02 |
| 33 | 4.7237E+06 | 1.15317E-02 | 1.10417E-02 | 1.25555E-02 |
| 34 | 4.4933E+06 | 2.66534E-02 | 2.55783E-02 | 2.86918E-02 |
| 35 | 4.0657E+06 | 3.14418E-02 | 3.02593E-02 | 3.33648E-02 |
| 36 | 3.6788E+06 | 3.60420E-02 | 3.47873E-02 | 3.77335E-02 |
| 37 | 3.3287E+06 | 1.96141E-02 | 1.89743E-02 | 2.03429E-02 |
| 38 | 3.1664E+06 | 2.06016E-02 | 1.99625E-02 | 2.12414E-02 |
| 39 | 3.0119E+06 | 2.14605E-02 | 2.08363E-02 | 2.20036E-02 |
| 40 | 2.8651E+06 | 2.22674E-02 | 2.16613E-02 | 2.27134E-02 |
| 41 | 2.7253E+06 | 2.29212E-02 | 2.23406E-02 | 2.32705E-02 |
| 42 | 2.5924E+06 | 2.34670E-02 | 2.29205E-02 | 2.37220E-02 |
| 43 | 2.4660E+06 | 1.58833E-02 | 1.55410E-02 | 1.60031E-02 |
| 44 | 2.3852E+06 | 4.01958E-03 | 3.93646E-03 | 4.04369E-03 |
| 45 | 2.3653E+06 | 4.00129E-03 | 3.92024E-03 | 4.02276E-03 |
| 46 | 2.3457E+06 | 8.04429E-03 | 7.88599E-03 | 8.08050E-03 |
| 47 | 2.3069E+06 | 1.61487E-02 | 1.58471E-02 | 1.61953E-02 |
| 48 | 2.2313E+06 | 2.43563E-02 | 2.39476E-02 | 2.43645E-02 |
| 49 | 2.1225E+06 | 2.44031E-02 | 2.40480E-02 | 2.43438E-02 |

TAB. 2.10 Continued

VITENDF70.BOLIB Library Total Neutron Fission Spectra for U-235, U-238 and Pu-239.

| Group | Upper Energy [eV] | U-235 X | U-238 X | Pu-239 X |
|---|---|---|---|---|
| 50 | 2.0190E+06 | 2.43446E-02 | 2.40485E-02 | 2.42247E-02 |
| 51 | 1.9205E+06 | 2.41644E-02 | 2.39299E-02 | 2.39929E-02 |
| 52 | 1.8268E+06 | 2.38759E-02 | 2.36894E-02 | 2.36599E-02 |
| 53 | 1.7377E+06 | 2.34973E-02 | 2.33656E-02 | 2.32394E-02 |
| 54 | 1.6530E+06 | 2.30653E-02 | 2.29788E-02 | 2.27713E-02 |
| 55 | 1.5724E+06 | 2.25743E-02 | 2.25411E-02 | 2.22444E-02 |
| 56 | 1.4957E+06 | 2.20394E-02 | 2.20779E-02 | 2.16740E-02 |
| 57 | 1.4227E+06 | 2.14035E-02 | 2.14608E-02 | 2.10102E-02 |
| 58 | 1.3534E+06 | 2.07889E-02 | 2.08802E-02 | 2.03799E-02 |
| 59 | 1.2874E+06 | 2.01424E-02 | 2.02639E-02 | 1.97095E-02 |
| 60 | 1.2246E+06 | 1.95105E-02 | 1.96781E-02 | 1.90497E-02 |
| 61 | 1.1648E+06 | 1.88028E-02 | 1.89854E-02 | 1.83262E-02 |
| 62 | 1.1080E+06 | 3.54943E-02 | 3.59530E-02 | 3.45146E-02 |
| 63 | 1.0026E+06 | 1.39988E-02 | 1.42192E-02 | 1.35762E-02 |
| 64 | 9.6164E+05 | 1.87557E-02 | 1.90732E-02 | 1.81574E-02 |
| 65 | 9.0718E+05 | 1.53248E-02 | 1.55992E-02 | 1.48163E-02 |
| 66 | 8.6294E+05 | 1.46545E-02 | 1.49572E-02 | 1.41468E-02 |
| 67 | 8.2085E+05 | 1.39821E-02 | 1.42882E-02 | 1.34708E-02 |
| 68 | 7.8082E+05 | 1.33466E-02 | 1.36751E-02 | 1.28294E-02 |
| 69 | 7.4274E+05 | 1.27009E-02 | 1.30335E-02 | 1.21924E-02 |
| 70 | 7.0651E+05 | 1.20706E-02 | 1.24073E-02 | 1.15671E-02 |
| 71 | 6.7206E+05 | 1.14668E-02 | 1.18034E-02 | 1.09706E-02 |
| 72 | 6.3928E+05 | 1.08914E-02 | 1.12478E-02 | 1.03949E-02 |
| 73 | 6.0810E+05 | 1.03235E-02 | 1.06967E-02 | 9.84075E-03 |
| 74 | 5.7844E+05 | 9.76520E-03 | 1.01484E-02 | 9.29471E-03 |
| 75 | 5.5023E+05 | 9.22553E-03 | 9.60066E-03 | 8.76171E-03 |
| 76 | 5.2340E+05 | 8.72337E-03 | 9.11924E-03 | 8.26667E-03 |
| 77 | 4.9787E+05 | 1.59481E-02 | 1.67150E-02 | 1.50931E-02 |
| 78 | 4.5049E+05 | 1.40613E-02 | 1.47590E-02 | 1.32947E-02 |
| 79 | 4.0762E+05 | 6.40656E-03 | 6.74257E-03 | 6.04067E-03 |
| 80 | 3.8774E+05 | 6.02002E-03 | 6.35863E-03 | 5.66889E-03 |
| 81 | 3.6883E+05 | 1.08842E-02 | 1.15143E-02 | 1.02493E-02 |
| 82 | 3.3373E+05 | 9.52454E-03 | 1.00995E-02 | 8.95953E-03 |
| 83 | 3.0197E+05 | 1.02262E-03 | 1.08605E-03 | 9.61614E-04 |
| 84 | 2.9849E+05 | 3.75182E-04 | 3.98718E-04 | 3.52722E-04 |
| 85 | 2.9721E+05 | 7.86566E-04 | 8.36010E-04 | 7.39444E-04 |
| 86 | 2.9452E+05 | 2.11344E-03 | 2.24788E-03 | 1.98634E-03 |
| 87 | 2.8725E+05 | 4.02252E-03 | 4.28495E-03 | 3.77777E-03 |
| 88 | 2.7324E+05 | 7.26811E-03 | 7.74599E-03 | 6.82012E-03 |
| 89 | 2.4724E+05 | 3.27331E-03 | 3.49017E-03 | 3.06853E-03 |
| 90 | 2.3518E+05 | 3.05036E-03 | 3.25667E-03 | 2.85961E-03 |
| 91 | 2.2371E+05 | 2.84389E-03 | 3.03769E-03 | 2.66514E-03 |
| 92 | 2.1280E+05 | 2.64960E-03 | 2.83138E-03 | 2.48324E-03 |
| 93 | 2.0242E+05 | 2.46704E-03 | 2.64182E-03 | 2.31239E-03 |
| 94 | 1.9255E+05 | 2.30370E-03 | 2.47644E-03 | 2.15560E-03 |
| 95 | 1.8316E+05 | 2.15113E-03 | 2.31750E-03 | 2.00998E-03 |
| 96 | 1.7422E+05 | 2.00153E-03 | 2.15774E-03 | 1.86855E-03 |
| 97 | 1.6573E+05 | 1.86740E-03 | 2.01254E-03 | 1.74253E-03 |
| 98 | 1.5764E+05 | 1.73463E-03 | 1.86757E-03 | 1.61862E-03 |

TAB. 2.10 Continued

VITENDF70.BOLIB Library Total Neutron Fission Spectra for U-235, U-238 and Pu-239.

| Group | Upper Energy [eV] | U-235 X | U-238 X | Pu-239 X |
|---|---|---|---|---|
| 99 | 1.4996E+05 | 1.61776E-03 | 1.74049E-03 | 1.50952E-03 |
| 100 | 1.4264E+05 | 1.50372E-03 | 1.61996E-03 | 1.40221E-03 |
| 101 | 1.3569E+05 | 1.40184E-03 | 1.51244E-03 | 1.30638E-03 |
| 102 | 1.2907E+05 | 1.30530E-03 | 1.41228E-03 | 1.21556E-03 |
| 103 | 1.2277E+05 | 1.21089E-03 | 1.31028E-03 | 1.12779E-03 |
| 104 | 1.1679E+05 | 1.12782E-03 | 1.22064E-03 | 1.05046E-03 |
| 105 | 1.1109E+05 | 2.48174E-03 | 2.68071E-03 | 2.31195E-03 |
| 106 | 9.8037E+04 | 2.07246E-03 | 2.24412E-03 | 1.92774E-03 |
| 107 | 8.6517E+04 | 6.93576E-04 | 7.53783E-04 | 6.44999E-04 |
| 108 | 8.2503E+04 | 5.09006E-04 | 5.53796E-04 | 4.73142E-04 |
| 109 | 7.9499E+04 | 1.23035E-03 | 1.34208E-03 | 1.14311E-03 |
| 110 | 7.1998E+04 | 7.27543E-04 | 7.87821E-04 | 6.76125E-04 |
| 111 | 6.7379E+04 | 1.60973E-03 | 1.73204E-03 | 1.49606E-03 |
| 112 | 5.6562E+04 | 5.72664E-04 | 6.15820E-04 | 5.31977E-04 |
| 113 | 5.2475E+04 | 8.24983E-04 | 8.91338E-04 | 7.65589E-04 |
| 114 | 4.6309E+04 | 6.86850E-04 | 7.45611E-04 | 6.36411E-04 |
| 115 | 4.0868E+04 | 7.71330E-04 | 8.38078E-04 | 7.14334E-04 |
| 116 | 3.4307E+04 | 2.74573E-04 | 2.99190E-04 | 2.53852E-04 |
| 117 | 3.1828E+04 | 3.54298E-04 | 3.87604E-04 | 3.26313E-04 |
| 118 | 2.8501E+04 | 1.54479E-04 | 1.69722E-04 | 1.41650E-04 |
| 119 | 2.7000E+04 | 9.49637E-05 | 1.04482E-04 | 8.69987E-05 |
| 120 | 2.6058E+04 | 1.25548E-04 | 1.38323E-04 | 1.14918E-04 |
| 121 | 2.4788E+04 | 5.94622E-05 | 6.55945E-05 | 5.43843E-05 |
| 122 | 2.4176E+04 | 5.73442E-05 | 6.33113E-05 | 5.24194E-05 |
| 123 | 2.3579E+04 | 1.60003E-04 | 1.76954E-04 | 1.46105E-04 |
| 124 | 2.1875E+04 | 2.31266E-04 | 2.57489E-04 | 2.10222E-04 |
| 125 | 1.9305E+04 | 3.56542E-04 | 4.03479E-04 | 3.20453E-04 |
| 126 | 1.5034E+04 | 2.48177E-04 | 2.84193E-04 | 2.21343E-04 |
| 127 | 1.1709E+04 | 7.67522E-05 | 8.87156E-05 | 6.80352E-05 |
| 128 | 1.0595E+04 | 9.28095E-05 | 1.04500E-04 | 8.39487E-05 |
| 129 | 9.1188E+03 | 1.12799E-04 | 1.24855E-04 | 1.03421E-04 |
| 130 | 7.1017E+03 | 7.82429E-05 | 8.75073E-05 | 7.13475E-05 |
| 131 | 5.5308E+03 | 5.43256E-05 | 6.14618E-05 | 4.92361E-05 |
| 132 | 4.3074E+03 | 2.42788E-05 | 2.77521E-05 | 2.18829E-05 |
| 133 | 3.7074E+03 | 1.34838E-05 | 1.55175E-05 | 1.21085E-05 |
| 134 | 3.3546E+03 | 1.16632E-05 | 1.34976E-05 | 1.04417E-05 |
| 135 | 3.0354E+03 | 1.00942E-05 | 1.17498E-05 | 9.00811E-06 |
| 136 | 2.7465E+03 | 4.52318E-06 | 5.28900E-06 | 4.02638E-06 |
| 137 | 2.6126E+03 | 4.20916E-06 | 4.93689E-06 | 3.74048E-06 |
| 138 | 2.4852E+03 | 7.56126E-06 | 8.90970E-06 | 6.70189E-06 |
| 139 | 2.2487E+03 | 6.54719E-06 | 7.76442E-06 | 5.78204E-06 |
| 140 | 2.0347E+03 | 1.27876E-05 | 1.53378E-05 | 1.12198E-05 |
| 141 | 1.5846E+03 | 8.94093E-06 | 1.09171E-05 | 7.76302E-06 |
| 142 | 1.2341E+03 | 6.26443E-06 | 7.79748E-06 | 5.37656E-06 |
| 143 | 9.6112E+02 | 4.39888E-06 | 5.58861E-06 | 3.72765E-06 |
| 144 | 7.4852E+02 | 3.09549E-06 | 4.01912E-06 | 2.58669E-06 |
| 145 | 5.8295E+02 | 2.18380E-06 | 2.90106E-06 | 1.79711E-06 |
| 146 | 4.5400E+02 | 1.54473E-06 | 2.10179E-06 | 1.25015E-06 |
| 147 | 3.5357E+02 | 1.09569E-06 | 1.52832E-06 | 8.70805E-07 |

TAB. 2.10 Continued

VITENDF70.BOLIB Library Total Neutron Fission Spectra for U-235, U-238 and Pu-239.

| Group | Upper Energy [eV] | U-235 X | U-238 X | Pu-239 X |
|---|---|---|---|---|
| 148 | 2.7536E+02 | 7.79591E-07 | 1.11567E-06 | 6.07561E-07 |
| 149 | 2.1445E+02 | 5.56391E-07 | 8.17495E-07 | 4.24569E-07 |
| 150 | 1.6702E+02 | 3.98609E-07 | 6.01613E-07 | 2.97383E-07 |
| 151 | 1.3007E+02 | 2.86418E-07 | 4.44212E-07 | 2.08611E-07 |
| 152 | 1.0130E+02 | 2.06642E-07 | 3.29365E-07 | 1.46736E-07 |
| 153 | 7.8893E+01 | 1.49629E-07 | 2.45099E-07 | 1.03450E-07 |
| 154 | 6.1442E+01 | 1.08761E-07 | 1.83045E-07 | 7.31235E-08 |
| 155 | 4.7851E+01 | 7.93633E-08 | 1.37177E-07 | 5.18335E-08 |
| 156 | 3.7266E+01 | 5.81324E-08 | 1.03129E-07 | 3.68484E-08 |
| 157 | 2.9023E+01 | 4.27526E-08 | 7.77828E-08 | 2.62821E-08 |
| 158 | 2.2603E+01 | 3.15557E-08 | 5.88235E-08 | 1.88039E-08 |
| 159 | 1.7604E+01 | 2.33884E-08 | 4.46235E-08 | 1.35056E-08 |
| 160 | 1.3710E+01 | 1.73974E-08 | 3.39341E-08 | 9.73426E-09 |
| 161 | 1.0677E+01 | 1.28576E-08 | 2.57326E-08 | 6.91964E-09 |
| 162 | 8.3153E+00 | 9.32006E-09 | 1.93467E-08 | 4.72477E-09 |
| 163 | 6.4760E+00 | 6.82789E-09 | 1.46367E-08 | 3.26711E-09 |
| 164 | 5.0435E+00 | 5.05610E-09 | 1.11373E-08 | 2.29406E-09 |
| 165 | 3.9279E+00 | 3.77951E-09 | 8.51593E-09 | 1.63493E-09 |
| 166 | 3.0590E+00 | 2.84692E-09 | 6.53510E-09 | 1.18103E-09 |
| 167 | 2.3824E+00 | 2.15915E-09 | 5.03183E-09 | 8.64046E-10 |
| 168 | 1.8554E+00 | 1.64607E-09 | 3.88314E-09 | 6.39000E-10 |
| 169 | 1.4450E+00 | 5.74175E-10 | 1.36455E-09 | 2.18677E-10 |
| 170 | 1.3000E+00 | 6.86647E-10 | 1.63892E-09 | 2.58550E-10 |
| 171 | 1.1253E+00 | 1.77133E-10 | 4.23951E-10 | 6.61649E-11 |
| 172 | 1.0800E+00 | 1.56095E-10 | 3.74040E-10 | 5.81233E-11 |
| 173 | 1.0400E+00 | 1.55801E-10 | 3.73750E-10 | 5.78416E-11 |
| 174 | 1.0000E+00 | 4.79449E-10 | 1.15297E-09 | 1.76907E-10 |
| 175 | 8.7643E-01 | 2.95142E-10 | 7.11677E-10 | 1.08074E-10 |
| 176 | 8.0000E-01 | 4.51413E-10 | 1.09150E-09 | 1.64059E-10 |
| 177 | 6.8256E-01 | 2.20092E-10 | 5.33446E-10 | 7.94394E-11 |
| 178 | 6.2506E-01 | 3.56516E-10 | 8.65988E-10 | 1.27905E-10 |
| 179 | 5.3158E-01 | 1.20077E-10 | 2.92169E-10 | 4.28619E-11 |
| 180 | 5.0000E-01 | 3.26108E-10 | 7.94870E-10 | 1.15846E-10 |
| 181 | 4.1399E-01 | 1.78344E-10 | 4.35521E-10 | 6.30065E-11 |
| 182 | 3.6680E-01 | 1.57631E-10 | 3.85441E-10 | 5.54824E-11 |
| 183 | 3.2500E-01 | 1.88132E-10 | 4.60640E-10 | 6.59624E-11 |
| 184 | 2.7500E-01 | 1.87673E-10 | 4.60189E-10 | 6.55222E-11 |
| 185 | 2.2500E-01 | 1.53549E-10 | 3.76999E-10 | 5.33996E-11 |
| 186 | 1.8400E-01 | 1.27099E-10 | 3.12384E-10 | 4.40581E-11 |
| 187 | 1.5000E-01 | 9.33193E-11 | 2.29148E-10 | 3.22658E-11 |
| 188 | 1.2500E-01 | 9.32044E-11 | 2.29009E-10 | 3.21557E-11 |
| 189 | 1.0000E-01 | 1.11694E-10 | 2.74792E-10 | 3.84416E-11 |
| 190 | 7.0000E-02 | 7.43700E-11 | 1.83174E-10 | 2.55395E-11 |
| 191 | 5.0000E-02 | 3.71573E-11 | 9.15869E-11 | 1.27432E-11 |
| 192 | 4.0000E-02 | 3.71390E-11 | 9.15868E-11 | 1.27257E-11 |
| 193 | 3.0000E-02 | 3.34095E-11 | 8.24281E-11 | 1.14381E-11 |
| 194 | 2.1000E-02 | 2.41198E-11 | 5.95314E-11 | 8.25198E-12 |
| 195 | 1.4500E-02 | 1.66938E-11 | 4.12140E-11 | 5.70857E-12 |
| 196 | 1.0000E-02 | 1.85443E-11 | 4.57934E-11 | 6.33868E-12 |

TAB. 2.10 Continued

VITENDF70.BOLIB Library Total Neutron Fission Spectra for U-235, U-238 and Pu-239.

| Group | Upper Energy [eV] | U-235 X | U-238 X | Pu-239 X |
|---|---|---|---|---|
| 197 | 5.0000E-03 | 1.11244E-11 | 2.74760E-11 | 3.80110E-12 |
| 198 | 2.0000E-03 | 5.56158E-12 | 1.37380E-11 | 1.89996E-12 |
| 199 | 5.0000E-04 | 1.85377E-12 | 4.57934E-12 | 6.33231E-13 |
| | Lower Energy 1.0000E-05 | | | |

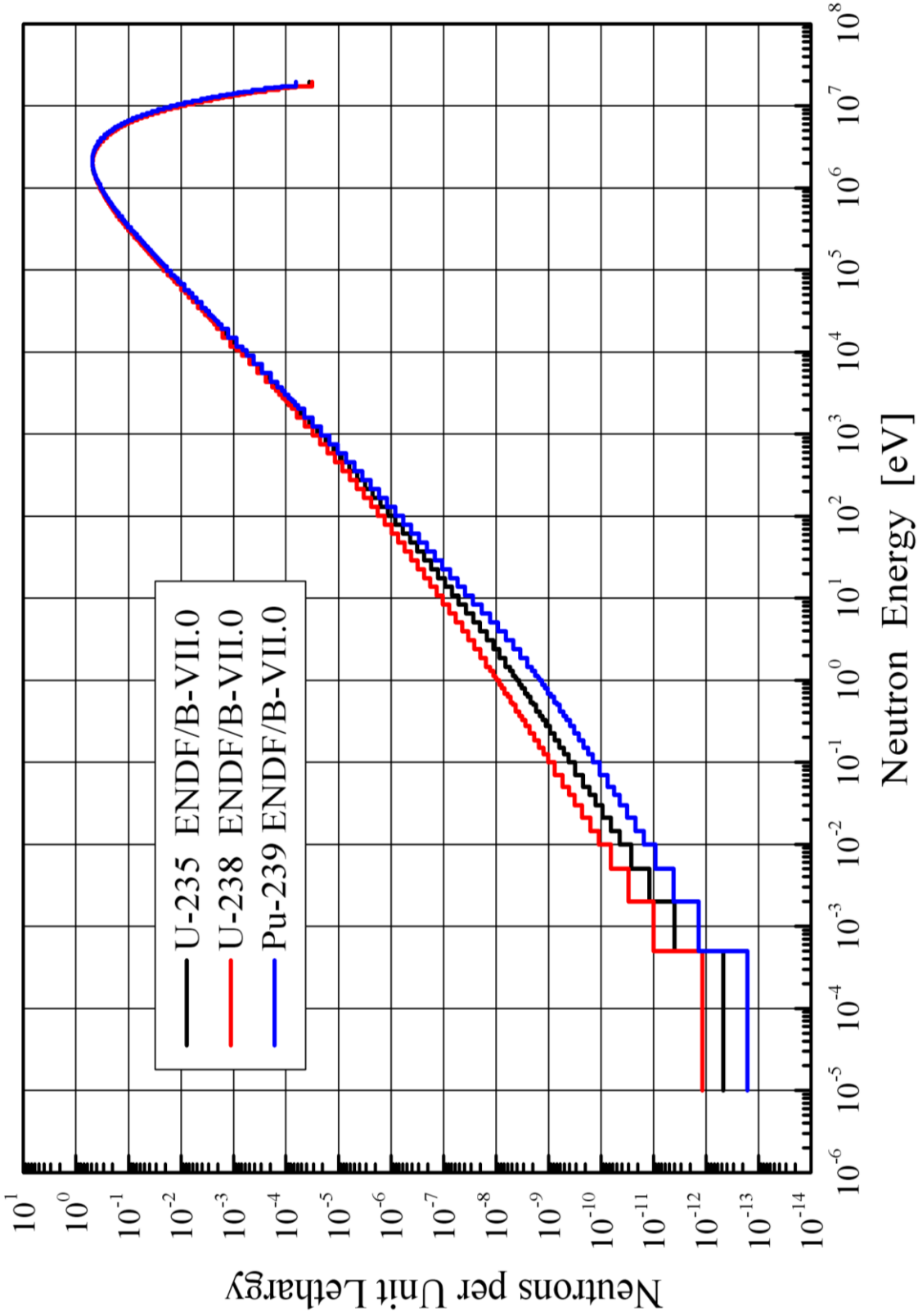


FIG. 2.5 199 Group Representation of the Total (Prompt + Delayed) Neutron Fission Spectrum for the U-235, U-238 and Pu-239 Processed Files Included in the VITENDF70.BOLIB Library. Spectra Averaged on Incident Neutron Energies and Normalized to 1 Neutron per Fission.

2.9 - Library Validation

The VITENDF70.BOLIB /5/ library was extensively tested on about 80, thermal, intermediate and fast neutron spectrum criticality safety benchmark experiments, taking the compositional and geometrical data for the transport calculations exclusively from the ICSBEP handbook (2004 Edition) /62/ of benchmark specifications.
The k-effective ($k_{eff}$) results obtained with the VITENDF70.BOLIB library were compared with the results previously obtained in ENEA-Bologna with the VITJEFF311.BOLIB /31/ library.
The ENEA-Bologna 2007 Revision /19/ of the SCAMPI /18/ system was used to prepare, through the BONAMI module, the working libraries of neutron self-shielded cross sections for the one-dimensional (1D) and two-dimensional (2D) transport calculations, respectively performed with the XSDRNPM 1D discrete ordinates transport code of the SCAMPI system and the DORT 2D discrete ordinates transport code, included in the DOORS-3.2 /35/ system.

Following the denominations reported in the ICSBEP handbook, the k-effective ($k_{eff}$) results obtained in the 1D and 2D transport calculations with the VITENDF70.BOLIB library refer to HEU (Highly Enriched Uranium) benchmark experiments (TAB. 2.11), to IEU (Intermediate Enrichement Uranium) benchmark experiments (TAB. 2.12), to LEU (Low Enriched Uranium) benchmark experiments (TAB. 2.13), to a MIX (MIXed Plutonium-Uranium) benchmark experiment (TAB. 2.14), to U-233 benchmark experiments (TAB. 2.15) and to Pu-239 benchmark experiments (TAB. 2.16). The following acronyms are used in the cited tables: NU (natural uranium), DU (depleted uranium) and WC (wolfram carbide or tungsten carbide).
The k-effective ($k_{eff}$) results obtained with the VITENDF70.BOLIB library are compared in the cited tables with the corresponding results obtained with the VITJEFF311.BOLIB library.
It is underlined that in the ICSBEP Handbook it is considered usually reasonable the assumption of a normal probability distribution for the $k_{eff}$ values of the "experimental or benchmark-model" configurations. Consequently the $k_{eff}$ values reported in TABs. 2.11÷2.16 are the mean values of the assumed normal distributions and their associated uncertainties correspond to one standard deviation (± sigma) which represents a 68% confidence level.

The one-dimensional transport calculations in spherical geometry were performed with the XSDRNPM code, module of the SCAMPI system, in the $P_5$-$S_{16}$ approximation: $P_5$ corresponds to L=ℓ-max, the maximum order of the Legendre polynomial ($P_\ell$) expansion of the scattering cross section matrices and $S_{16}$ represents the order of the flux angular discretization. The DORT 2D discrete ordinates code, included in the DOORS-3.2 system, was exclusively employed in the simulation of the IEU-MET-FAST-007 (BIG TEN) (see TAB. 2.12) fast neutron spectrum benchmark experiment with a 2D (R,Z) cylindrical geometry calculation in the $P_3$-$S_8$ approximation.

It is noted that the most part of the results obtained with the VITENDF70.BOLIB library on the U-233 benchmark experiments fall within the experimental or benchmark-model k-effective errors whereas the corresponding results obtained with the VITJEFF311.BOLIB library are always outside the cited experimental errors.

At present no testing of the VITENDF70.BOLIB library was performed on integral shielding benchmark experiments.

TAB. 2.11

VITENDF70.BOLIB and VITJEFF311.BOLIB Criticality Calculation Results
for Highly Enriched Uranium (HEU) Benchmark Experiments.

| ICSBEP Handbook Benchmark Name | Reflector | Experimental or Benchmark-Model $k_{eff} \pm \Delta k_{eff}$ (pcm) | Geometry/ $P_L$ - $S_N$ | VITENDF70 $k_{eff}$ | VITJEFF311 $k_{eff}$ |
|---|---|---|---|---|---|
| Thermal Neutron Spectrum | | | | | |
| HEU-SOL-THERM-009-001 | H2O | 0.99900 ± (430) | 1D Sph./ P5-S16 | 1.00378 | 1.00189 |
| HEU-SOL-THERM-009-002 | H2O | 1.00000 ± (390) | 1D Sph./ P5-S16 | 1.00425 | 1.00236 |
| HEU-SOL-THERM-009-003 | H2O | 1.00000 ± (360) | 1D Sph./ P5-S16 | 1.00342 | 1.00166 |
| HEU-SOL-THERM-009-004 | H2O | 0.99860 ± (350) | 1D Sph./ P5-S16 | 0.99737 | 0.99591 |
| HEU-SOL-THERM-010-001 | H2O | 1.00000 ± (290) | 1D Sph./ P5-S16 | 1.00192 | 1.00123 |
| HEU-SOL-THERM-010-002 | H2O | 1.00000 ± (290) | 1D Sph./ P5-S16 | 1.00255 | 1.00185 |
| HEU-SOL-THERM-010-003 | H2O | 1.00000 ± (290) | 1D Sph./ P5-S16 | 1.00123 | 1.00044 |
| HEU-SOL-THERM-010-004 | H2O | 0.99920 ± (290) | 1D Sph./ P5-S16 | 0.99989 | 0.99906 |
| HEU-SOL-THERM-011-001 | H2O | 1.00000 ± (230) | 1D Sph./ P5-S16 | 1.00517 | 1.00523 |
| HEU-SOL-THERM-011-002 | H2O | 1.00000 ± (230) | 1D Sph./ P5-S16 | 1.00129 | 1.00137 |
| HEU-SOL-THERM-012-001 | H2O | 0.99990 ± (580) | 1D Sph./ P5-S16 | 1.00071 | 1.00111 |
| HEU-SOL-THERM-013-001 (ORNL-1) | -- | 1.00120 ± (260) | 1D Sph./ P5-S16 | 0.99832 | 0.99892 |
| HEU-SOL-THERM-013-002 (ORNL-2) | -- | 1.00070 ± (360) | 1D Sph./ P5-S16 | 0.99749 | 0.99797 |
| HEU-SOL-THERM-013-003 (ORNL-3) | -- | 1.00090 ± (360) | 1D Sph./ P5-S16 | 0.99406 | 0.99442 |
| HEU-SOL-THERM-013-004 (ORNL-4) | -- | 1.00030 ± (360) | 1D Sph./ P5-S16 | 0.99568 | 0.99599 |
| HEU-SOL-THERM-032 (ORNL-10) | -- | 1.00150 ± (260) | 1D Sph./ P5-S16 | 0.99893 | 0.99878 |
| Intermediate Neutron Spectrum | | | | | |
| ICSBEP Handbook Benchmark Name | Reflector | Experimental or Benchmark-Model $k_{inf} \pm \Delta k_{inf}$ (pcm) | Geometry/ $P_L$ - $S_N$ | VITENDF70 $k_{inf}$ | VITJEFF311 $k_{inf}$ |
| HEU-COMP-INTER-004 | -- | 1.00000 ± (400) | Inf. Homogeneous/ P5-S16 | 1.00970 | 1.00807 |

TAB. 2.11 Continued

VITENDF70.BOLIB and VITJEFF311.BOLIB Criticality Calculation Results
for Highly Enriched Uranium (HEU) Benchmark Experiments.

| ICSBEP Handbook Benchmark Name | Reflector | Experimental or Benchmark-Model $k_{eff} \pm \Delta k_{eff}$ (pcm) | Geometry/ $P_L$ - $S_N$ | VITENDF70 $k_{eff}$ | VITJEFF311 $k_{eff}$ |
|---|---|---|---|---|---|
| Fast Neutron Spectrum | | | | | |
| HEU-MET-FAST-001-001 (GODIVA) | -- | 1.00000 ± (100) | 1D Sph./ P5-S16 | 0.99954 | 0.99533 |
| HEU-MET-FAST-002-001 (TOPSY) | NU | 1.00000 ± (300) | 1D Sph./ P5-S16 | 1.00266 | 1.00095 |
| HEU-MET-FAST-003-001 | NU (2in) | 1.00000 ± (500) | 1D Sph./ P5-S16 | 0.99576 | 0.99373 |
| HEU-MET-FAST-003-002 | NU (3in) | 1.00000 ± (500) | 1D Sph./ P5-S16 | 0.99544 | 0.99345 |
| HEU-MET-FAST-003-003 | NU (4in) | 1.00000 ± (500) | 1D Sph./ P5-S16 | 1.00027 | 0.99825 |
| HEU-MET-FAST-003-004 | NU (5in) | 1.00000 ± (300) | 1D Sph./ P5-S16 | 0.99843 | 0.99643 |
| HEU-MET-FAST-003-005 | NU (7in) | 1.00000 ± (300) | 1D Sph./ P5-S16 | 1.00251 | 1.00071 |
| HEU-MET-FAST-003-006 | NU (8in) | 1.00000 ± (300) | 1D Sph./ P5-S16 | 1.00262 | 1.00092 |
| HEU-MET-FAST-003-007 | NU (11in) | 1.00000 ± (300) | 1D Sph./ P5-S16 | 1.00299 | 1.00148 |
| HEU-MET-FAST-003-008 | WC (1.9in) | 1.00000 ± (500) | 1D Sph./ P5-S16 | 1.00962 | 1.00146 |
| HEU-MET-FAST-003-009 | WC (2.9in) | 1.00000 ± (500) | 1D Sph./ P5-S16 | 1.01093 | 1.00364 |
| HEU-MET-FAST-003-010 | WC (4.5in) | 1.00000 ± (500) | 1D Sph./ P5-S16 | 1.01379 | 1.00897 |
| HEU-MET-FAST-003-011 | WC (6.5in) | 1.00000 ± (500) | 1D Sph./ P5-S16 | 1.01733 | 1.01416 |
| HEU-MET-FAST-003-012 | Ni (8in) | 1.00000 ± (500) | 1D Sph./ P5-S16 | 1.01600 | 1.00922 |
| HEU-MET-FAST-022-001 | Al | 1.00000 ± (190) | 1D Sph./ P5-S16 | 0.99941 | 0.99527 |
| HEU-MET-FAST-027-001 | Pb | 1.00000 ± (250) | 1D Sph./ P5-S16 | 1.00019 | 1.00052 |
| HEU-MET-FAST-028-001 (FLATTOP-25) | NU | 1.00000 ± (300) | 1D Sph./ P5-S16 | 1.00397 | 1.00218 |
| HEU-MET-FAST-057-001 | Pb | 1.00000 ± (200) | 1D Sph./ P5-S16 | 0.98979 | 0.99425 |
| HEU-MET-FAST-057-002 | Pb | 1.00000 ± (230) | 1D Sph./ P5-S16 | 0.99788 | 1.00122 |

TAB. 2.12

VITENDF70.BOLIB and VITJEFF311.BOLIB Criticality Calculation Results
for Intermediate Enrichment Uranium (IEU) Benchmark Experiments.

| ICSBEP Handbook Benchmark Name | Reflector | Experimental or Benchmark-Model $k_{eff} \pm \Delta k_{eff}$ (pcm) | Geometry/ $P_L$ - $S_N$ | VITENDF70 $k_{eff}$ | VITJEFF311 $k_{eff}$ |
|---|---|---|---|---|---|
| Fast Neutron Spectrum | | | | | |
| IEU-MET-FAST-007 (BIG TEN) Simplified Model | DU | 1.00450 ± (70) | 2D Cyl./ P3-S8 | 1.00416 | 0.99714 |
| IEU-MET-FAST-007 (BIG TEN) Two Zone Model | DU | 0.99480 ± (130) | 2D Cyl./ P3-S8 | 0.99705 | 0.99039 |

TAB. 2.13

VITENDF70.BOLIB and VITJEFF311.BOLIB Criticality Calculation Results
for Low Enriched Uranium (LEU) Benchmark Experiments.

| ICSBEP Handbook Benchmark Name | Reflector | Experimental or Benchmark-Model $k_{eff} \pm \Delta k_{eff}$ (pcm) | Geometry/ $P_L$ - $S_N$ | VITENDF70 $k_{eff}$ | VITJEFF311 $k_{eff}$ |
|---|---|---|---|---|---|
| Thermal Neutron Spectrum | | | | | |
| LEU-SOL-THERM-003-003 | -- | 0.99950 ± (420) | 1D Sph./ P5-S16 | 1.00163 | 1.00358 |
| LEU-SOL-THERM-003-006 | -- | 0.99990 ± (490) | 1D Sph./ P5-S16 | 0.99869 | 1.00088 |
| LEU-SOL-THERM-003-009 | -- | 0.99960 ± (520) | 1D Sph./ P5-S16 | 0.99757 | 0.99942 |

TAB. 2.14

VITENDF70.BOLIB and VITJEFF311.BOLIB Criticality Calculation Results
for Mixed Plutonium-Uranium (MIX) Benchmark Experiments.

| ICSBEP Handbook Benchmark Name | Reflector | Experimental or Benchmark-Model $k_{eff} \pm \Delta k_{eff}$ (pcm) | Geometry/ $P_L - S_N$ | VITENDF70 $k_{eff}$ | VITJEFF311 $k_{eff}$ |
|---|---|---|---|---|---|
| Fast Neutron Spectrum | | | | | |
| MIX-MET-FAST-001-001 | -- | 1.00000 ± (160) | 1D Sph./ P5-S16 | 0.99923 | 0.99740 |

TAB. 2.15

VITENDF70.BOLIB and VITJEFF311.BOLIB Criticality Calculation Results
for U-233 Benchmark Experiments.

| ICSBEP Handbook Benchmark Name | Reflector | Experimental or Benchmark-Model $k_{eff} \pm \Delta k_{eff}$ (pcm) | Geometry/ $P_L - S_N$ | VITENDF70 $k_{eff}$ | VITJEFF311 $k_{eff}$ |
|---|---|---|---|---|---|
| Fast Neutron Spectrum | | | | | |
| U233-MET-FAST-001-001 (JEZEBEL-233) | -- | 1.00000 ± (100) | 1D Sph./.P5-S16 | 1.00065 | 1.00383 |
| U233-MET-FAST-002-001 | HEU | 1.00000 ± (100) | 1D Sph./.P5-S16 | 1.00020 | 1.00257 |
| U233-MET-FAST-002-002 | HEU | 1.00000 ± (110) | 1D Sph./.P5-S16 | 1.00174 | 1.00342 |
| U233-MET-FAST-003-001 | NU | 1.00000 ± (100) | 1D Sph./.P5-S16 | 1.00087 | 1.00575 |
| U233-MET-FAST-003-002 | NU | 1.00000 ± (100) | 1D Sph./.P5-S16 | 1.00184 | 1.00719 |
| U233-MET-FAST-006-001 (FLATTOP-23) | NU | 1.00000 ± (140) | 1D Sph./.P5-S16 | 1.00138 | 1.00665 |

TAB. 2.16

VITENDF70.BOLIB and VITJEFF311.BOLIB Criticality Calculation Results for Plutonium Benchmark Experiments.

| ICSBEP Handbook Benchmark Name | Reflector | Experimental or Benchmark-Model $k_{eff} \pm \Delta k_{eff}$ (pcm) | Geometry/ $P_L$ - $S_N$ | VITENDF70 $k_{eff}$ | VITJEFF311 $k_{eff}$ |
|---|---|---|---|---|---|
| Thermal Neutron Spectrum | | | | | |
| PU-SOL-THERM-006-001 | H2O | 1.00000 ± (350) | 1D Sph./ P5-S16 | 1.00095 | 0.99716 |
| PU-SOL-THERM-006-002 | H2O | 1.00000 ± (350) | 1D Sph./ P5-S16 | 1.00223 | 0.99843 |
| PU-SOL-THERM-006-003 | H2O | 1.00000 ± (350) | 1D Sph./ P5-S16 | 1.00181 | 0.99800 |
| PU-SOL-THERM-011-001 | -- | 1.00000 ± (520) | 1D Sph./ P5-S16 | 1.01017 | 1.00721 |
| PU-SOL-THERM-011-002 | -- | 1.00000 ± (520) | 1D Sph./ P5-S16 | 1.01489 | 1.01190 |
| PU-SOL-THERM-011-003 | -- | 1.00000 ± (520) | 1D Sph./ P5-S16 | 1.01697 | 1.01397 |
| PU-SOL-THERM-011-004 | -- | 1.00000 ± (520) | 1D Sph./ P5-S16 | 1.00951 | 1.00656 |
| PU-SOL-THERM-011-005 (PNL-5R) | -- | 1.00000 ± (520) | 1D Sph./ P5-S16 | 1.00659 | 1.00364 |
| PU-SOL-THERM-011-006 (PNL-3R) | -- | 1.00000 ± (520) | 1D Sph./ P5-S16 | 0.99453 | 0.99165 |
| PU-SOL-THERM-011-007 | -- | 1.00000 ± (520) | 1D Sph./ P5-S16 | 1.00052 | 0.99760 |
| PU-SOL-THERM-011-008 | -- | 1.00000 ± (520) | 1D Sph./ P5-S16 | 0.99712 | 0.99421 |
| PU-SOL-THERM-011-009 | -- | 1.00000 ± (520) | 1D Sph./ P5-S16 | 0.99376 | 0.99088 |
| PU-SOL-THERM-011-010 | -- | 1.00000 ± (520) | 1D Sph./ P5-S16 | 1.00378 | 1.00083 |
| PU-SOL-THERM-011-011 (PNL-4R) | -- | 1.00000 ± (520) | 1D Sph./ P5-S16 | 1.00043 | 0.99752 |
| PU-SOL-THERM-011-012 | -- | 1.00000 ± (520) | 1D Sph./ P5-S16 | 0.99993 | 0.99702 |
| PU-SOL-THERM-021-007 (PNL-1) | -- | 1.00000 ± (320) | 1D Sph./ P5-S16 | 1.00699 | 1.00412 |
| PU-SOL-THERM-021-008 (PNL-2) | -- | 1.00000 ± (650) | 1D Sph./ P5-S16 | 1.00424 | 1.00226 |
| PU-SOL-THERM-021-009 | -- | 1.00000 ± (320) | 1D Sph./ P5-S16 | 1.00748 | 1.00461 |
| Intermediate Neutron Spectrum | | | | | |
| ICSBEP Handbook Benchmark Name | Reflector | Experimental or Benchmark-Model $k_{eff} \pm \Delta k_{eff}$ (pcm) | Geometry/ $P_L$ - $S_N$ | VITENDF70 $k_{eff}$ | VITJFF311 $k_{eff}$ |
| PU-COMP-INTER-001 | -- | 1.00000 ± (1100) | Inf. Homogeneous/ P5-S16 | 1.00517 | 1.00110 |

TAB. 2.16 Continued

VITENDF70.BOLIB and VITJEFF311.BOLIB Criticality Calculation Results for Plutonium Benchmark Experiments.

| ICSBEP Handbook Benchmark Name | Reflector | Experimental or Benchmark-Model $k_{eff} \pm \Delta k_{eff}$ (pcm) | Geometry/ $P_L$ - $S_N$ | VITENDF70 $k_{eff}$ | VITJEFF311 $k_{eff}$ |
|---|---|---|---|---|---|
| Fast Neutron Spectrum | | | | | |
| PU-MET-FAST-001-001 (JEZEBEL) | -- | 1.00000 ± (200) | 1D Sph./ P5-S16 | 0.99924 | 0.99889 |
| PU-MET-FAST-002-001 (JEZEBEL-240) | -- | 1.00000 ± (200) | 1D Sph./ P5-S16 | 0.99966 | 1.00277 |
| PU-MET-FAST-006-001 (FLATTOP-PU) | NU | 1.00000 ± (300) | 1D Sph./ P5-S16 | 1.00163 | 1.00305 |
| PU-MET-FAST-008-001 (THOR) | Th | 1.00000 ± (60) | 1D Sph./ P5-S16 | 0.99848 | 1.00124 |
| PU-MET-FAST-009-001 | Al | 1.00000 ± (270) | 1D Sph./ P5-S16 | 1.00492 | 1.00401 |
| PU-MET-FAST-010-001 | NU | 1.00000 ± (180) | 1D Sph./ P5-S16 | 0.99971 | 1.00091 |
| PU-MET-FAST-011-001 | H2O | 1.00000 ± (100) | 1D Sph./ P5-S16 | 1.00262 | 0.99943 |
| PU-MET-FAST-018-001 | Be | 1.00000 ± (300) | 1D Sph./ P5-S16 | 0.99705 | 1.00200 |
| PU-MET-FAST-023-001 | Graphite | 1.00000 ± (230) | 1D Sph./ P5-S16 | 1.00008 | 0.99850 |
| PU-MET-FAST-024-001 | Polyethylene | 1.00000 ± (200) | 1D Sph./ P5-S16 | 1.00192 | 0.99948 |
| PU-MET-FAST-030-001 | Graphite | 1.00000 ± (210) | 1D Sph./ P5-S16 | 1.00377 | 1.00395 |
| PU-MET-FAST-031-001 | Polyethylene | 1.00000 ± (210) | 1D Sph./ P5-S16 | 1.00530 | 1.00385 |

## 3 - BUGENDF70.BOLIB BROAD-GROUP LIBRARY SPECIFICATIONS

The ENEA-Bologna Nuclear Data Group generated the BUGENDF70.BOLIB broad-group coupled neutron/photon working cross section library in FIDO-ANISN /4/ format, based on the US ENDF/B-VII.0 /6/ evaluated nuclear data library. This BUGLE-type library has features similar to the ORNL DLC-0185/BUGLE-96 /8/ broad-group working library and the same neutron and photon energy group structures (47 n + 20 γ) with the 47 neutron energy groups covering the energy range 1.0E-05 eV - 1.7332E+07 eV and the 20 photon groups included within the energy range 1.0E+04 - 1.4E+07 eV.

As previously performed at ORNL, where BUGLE-96 was obtained through proper cross section collapsing with the ORNL SCAMPI /18/ nuclear data processing system from the ORNL DLC-0184/VITAMIN-B6 /8/ (ENDF/B-VI.3 /9/) fine-group (199 n + 42 γ) library, the ENEA-Bologna BUGENDF70.BOLIB library was generated with the same methodology and reactor models previously used to produce the BUGLE-96 library. It was obtained through cross section collapsing from the recently produced ENEA-Bologna VITENDF70.BOLIB /5/ fine-group library (see Chapter 2), based on ENDF/B-VII.0 data and characterized by the same neutron and photon energy group structure as VITAMIN-B6.

In order to perform this task an updating was required to the original SCAMPI, developed at ORNL from the AMPX-77 /23/ system and already employed to generate BUGLE-96. In particular, the so called "ENEA-Bologna 2007 Revision of SCAMPI" /19/ was developed (see 1.3) and released to the OECD-NEA Data Bank and ORNL-RSICC.

### 3.1 - Name

The present problem-dependent broad-group working cross section library, derived through proper cross section collapsing of the ENEA-Bologna VITENDF70.BOLIB /5/ fine-group mother library, is designated as BUGENDF70.BOLIB.
"BUG" suggests that the main features of the library are similar to those of the BUGLE-96 /8/ library, generated at ORNL. The "ENDF70" designation in both ENEA-Bologna libraries conveniently reflects the origin of the evaluated data, i.e. the US ENDF/B-VII.0 /6/ evaluated nuclear data library (see 1.2). Finally, "BOLIB" means BOlogna LIBrary and so it is indicative of the place of production of the library.

### 3.2 - Materials, Legendre Order of Scattering and Energy Group Structure

The BUGENDF70.BOLIB library contains all the 183 nuclides, based on the the US ENDF/B-VII.0 /6/ evaluated nuclear data library, available in the VITENDF70.BOLIB /5/ fine-group mother library, as listed in TAB. 2.1. Some nuclides appear several times due to the inclusion of different resonance self-shielding and energy weighting options for key fuel and structural materials.

The Legendre order of scattering of the cross sections contained in BUGENDF70.BOLIB is the same as available in the VITENDF70.BOLIB library: $P_7$ for both neutrons and photons for nuclides with Z=l through Z=29 (copper) and $P_5$ for the remainder of the nuclides (see TAB. 2.2).

The BUGENDF70.BOLIB library, as previously reported, has the same neutron and photon energy group structures (47 neutron groups + 20 photon groups) as the ORNL BUGLE-96 /8/ library with 47 neutron groups covering the energy range 1.0E-05 eV - 1.7332E+07 eV and 20 photon groups included within the energy range 1.0E+04 eV - 1.4E+07 eV. The energy boundaries for the 47 neutron groups are given in TAB. 3.1 along with the corresponding VITENDF70.BOLIB group numbers which were collapsed to form the BUGENDF70.BOLIB groups. Similarly, the 20 photon group structure is given in TAB. 3.2.
With respect to the neutron energy range covered by the VITENDF70.BOLIB library, it is underlined that in the BUGENDF70.BOLIB neutron energy group structure (see TAB. 3.1), the contribution of the highest neutron energy group (neutron fine-group No.1 in the energy range 1.7332E+07 eV - 1.9640E+07 eV; see TAB. 2.4) of the VITENDF70.BOLIB neutron group structure is omitted. Concerning the photon energy range covered by the VITENDF70.BOLIB library, the contributions of the two highest photon energy groups (photon fine-group No.1 in the energy range 2.0E+07 eV - 3.0E+07 eV and No. 2 in the energy range 1.4E+07 eV - 2.0E+07 eV; see TAB. 2.5) and that of the lowest photon energy group (photon fine-group No. 42 in the energy range 1.0E+03 eV - 1.0E+04 eV; see TAB. 2.5) of the VITENDF70.BOLIB photon group structure are omitted in the BUGENDF70.BOLIB photon energy group structure (see TAB. 3.2).
The BUGENDF70.BOLIB thermal neutron energy range below 5.0435 eV, i.e. the energy range containing the neutron groups which include upscatter in the BUGENDF70T.BOLIB version of the library (see also 3.5), has only five neutron groups (see TAB. 3.1) with respect to the 36 neutron groups of the VITENDF70.BOLIB library in the same energy range (see TAB. 2.4).

TAB. 3.1

Neutron Group Energy Boundaries for the BUGENDF70.BOLIB Library.

| Broad Group | Upper Energy [eV] | Upper Lethargy | VITENDF70 Groups |
|---|---|---|---|
| 1 | 1.7332E+07 | -5.4997E-01 | 2-7 |
| 2 | 1.4191E+07 | -3.5002E-01 | 8-12 |
| 3 | 1.2214E+07 | -2.0000E-01 | 13-16 |
| 4 | 1.0000E+07 | 0.0000E+00 | 17-19 |
| 5 | 8.6071E+06 | 1.5000E-01 | 20-22 |
| 6 | 7.4082E+06 | 3.0000E-01 | 23-27 |
| 7 | 6.0653E+06 | 5.0000E-01 | 28-31 |
| 8 | 4.9659E+06 | 7.0000E-01 | 32-35 |
| 9 | 3.6788E+06 | 1.0000E+00 | 36-38 |
| 10 | 3.0119E+06 | 1.2000E+00 | 39-40 |
| 11 | 2.7253E+06 | 1.3000E+00 | 41-42 |
| 12 | 2.4660E+06 | 1.4000E+00 | 43-44 |
| 13 | 2.3653E+06 | 1.4417E+00 | 45 |
| 14 | 2.3457E+06 | 1.4500E+00 | 46-47 |
| 15 | 2.2313E+06 | 1.5000E+00 | 48-50 |
| 16 | 1.9205E+06 | 1.6500E+00 | 51-53 |
| 17 | 1.6530E+06 | 1.8000E+00 | 54-57 |
| 18 | 1.3534E+06 | 2.0000E+00 | 58-62 |
| 19 | 1.0026E+06 | 2.3000E+00 | 63-66 |
| 20 | 8.2085E+05 | 2.5000E+00 | 67-68 |
| 21 | 7.4274E+05 | 2.6000E+00 | 69-72 |
| 22 | 6.0810E+05 | 2.8000E+00 | 73-76 |
| 23 | 4.9787E+05 | 3.0000E+00 | 77-80 |
| 24 | 3.6883E+05 | 3.3000E+00 | 81-84 |
| 25 | 2.9721E+05 | 3.5159E+00 | 85-94 |
| 26 | 1.8316E+05 | 4.0000E+00 | 95-104 |
| 27 | 1.1109E+05 | 4.5000E+00 | 105-110 |
| 28 | 6.7379E+04 | 5.0000E+00 | 111-114 |
| 29 | 4.0868E+04 | 5.5000E+00 | 115-116 |
| 30 | 3.1828E+04 | 5.7500E+00 | 117-119 |
| 31 | 2.6058E+04 | 5.9500E+00 | 120-121 |
| 32 | 2.4176E+04 | 6.0250E+00 | 122-123 |
| 33 | 2.1875E+04 | 6.1250E+00 | 124-125 |
| 34 | 1.5034E+04 | 6.5000E+00 | 126-129 |
| 35 | 7.1017E+03 | 7.2500E+00 | 130-133 |
| 36 | 3.3546E+03 | 8.0000E+00 | 134-140 |
| 37 | 1.5846E+03 | 8.7500E+00 | 141-145 |
| 38 | 4.5400E+02 | 1.0000E+01 | 146-148 |
| 39 | 2.1445E+02 | 1.0750E+01 | 149-151 |
| 40 | 1.0130E+02 | 1.1500E+01 | 152-155 |
| 41 | 3.7266E+01 | 1.2500E+01 | 156-160 |
| 42 | 1.0677E+01 | 1.3750E+01 | 161-163 |
| 43 | 5.0435E+00 | 1.4500E+01 | 164-167 |
| 44 | 1.8554E+00 | 1.5500E+01 | 168-174 |
| 45 | 8.7643E-01 | 1.6250E+01 | 175-180 |
| 46 | 4.1399E-01 | 1.7000E+01 | 181-188 |
| 47 | 1.0000E-01 | 1.8421E+01 | 189-199 |
| | 1.0000E-05 | 2.7631E+01 | |

TAB. 3.2

Photon Group Energy Boundaries for the BUGENDF70.BOLIB Library.

| Broad Group | Upper Energy [eV] | VITENDF70 Groups |
|---|---|---|
| 1 | 1.4000E+07 | 3-4 |
| 2 | 1.0000E+07 | 5 |
| 3 | 8.0000E+06 | 6-7 |
| 4 | 7.0000E+06 | 8-9 |
| 5 | 6.0000E+06 | 10-11 |
| 6 | 5.0000E+06 | 12-13 |
| 7 | 4.0000E+06 | 14-15 |
| 8 | 3.0000E+06 | 16-17 |
| 9 | 2.0000E+06 | 18-19 |
| 10 | 1.5000E+06 | 20-22 |
| 11 | 1.0000E+06 | 23 |
| 12 | 8.0000E+05 | 24 |
| 13 | 7.0000E+05 | 25 |
| 14 | 6.0000E+05 | 26-29 |
| 15 | 4.0000E+05 | 30-31 |
| 16 | 2.0000E+05 | 32-33 |
| 17 | 1.0000E+05 | 34-36 |
| 18 | 6.0000E+04 | 37-39 |
| 19 | 3.0000E+04 | 40 |
| 20 | 2.0000E+04 | 41 |
| | 1.0000E+04 | |

3.3 - Self-Shielding, Weighting Spectra and Collapsing

As reported in the BUGLE-96 /8/ library user's manual, the accuracy of the results from a radiation transport calculation which uses broad-group cross section data can be significantly affected by the energy-dependent weighting spectrum used to collapse the data from point-wise or fine-group data. It is important to use a weighting spectrum which is sufficiently prototypical to provide the desired accuracy. In general, a broad-group library is useful only for the range of problems represented by the specific weighting functions. For BUGENDF70.BOLIB, this range includes in-vessel and reactor cavity analyses for light-water-cooled reactors (PWR and BWR). For other applications, the validity of the BUGENDF70.BOLIB data will need to be explicitly demonstrated. Even for LWR applications, it is important that the proper data sets be used for specific regions of the reactor geometry to insure sufficiently accurate results.

The cross section sets contained in the BUGENDF70.BOLIB library were produced in two phases. The first phase was dedicated 1) to properly self-shield the cross sections and 2) to calculate problem-dependent BWR- and PWR-specific neutron/photon weighting spectra. In the second phase, infinitely dilute (not self-shielded) and self-shielded cross section sets, derived from the VITENDF70.BOLIB /5/ fine-group library, were collapsed to generate the BUGENDF70.BOLIB broad-group cross section sets, using the neutron/photon weighting spectra, pre-calculated in the first phase of the data processing. It is underlined that the BUGENDF70.BOLIB broad-group cross sections were generated from the VITENDF70.BOLIB fine-group cross sections with the same methodology and reactor models previously used to produce the ORNL BUGLE-96 library. All the compositional, geometrical and temperature data needed for the cross section self-shielding, the BWR and PWR neutron/photon weighting spectra calculation methodology and the cross section collapsing procedure were consistently taken from the BUGLE-96 library user's manual, respectively from the corresponding ORNL data processing inputs which generated BUGLE-96.

In particular in the first phase, five different neutron/photon weighting spectra in the VITENDF70.BOLIB neutron and photon energy group structures were calculated with a one-dimensional transport code in order to permit, in the second phase, problem-dependent cross section collapsing from the VITENDF70.BOLIB neutron and photon fine-group energy structures into the BUGENDF70.BOLIB neutron and photon broad-group energy structures.

In order to determine the BWR- and PWR-specific neutron/photon weighting spectra, one-dimensional fixed source transport calculations were performed introducing the same compositional/geometrical reactor models used to obtain BUGLE-96: the former representing a typical BWR plant and the latter representing a typical PWR plant. These reactor models, which correspond exactly to those described in the BUGLE-96 library user's manual, are shown in FIG. 3.1. The atomic densities for the various reactor regions, used in the transport calculations to determine the neutron and photon weighting spectra, are given in TAB. 3.3.

The atomic densities used in the transport calculations (see in particular 3.4 for the calculation details) were always directly taken from the transport code input examples reported in the BUGLE-96 library user's manual (see /8/, APPENDIX A). On the other hand in certain cases, e.g., for the magnesium, silicon, potassium, calcium and zirconium isotopes, contained in

VITENDF70.BOLIB and involved in the transport calculations, it was necessary to determine their atomic densities which are not available in the BUGLE-96 library user's manual. In fact these isotopes are constituents of the natural elements included as corresponding data files in the VITAMIN-B6 /8/ library since the relative component isotopes were not available in the ENDF/B-VI.3 /9/ evaluated data library. The atomic densities of these isotopes were calculated on the basis of the natural isotopic abundances (see TAB. 3.3), taken from the BNL-NNDC database /63/.

The 1D fixed source transport calculations were performed using as volumetric source spectra the same fine-group neutron source spectrum data set for both types of reactors. These data were taken from the BUGLE-96 library user's manual (see /8/, APPENDIX A, TAB. A.6 and TAB. A.7).

Neutron and photon flux spectra from five representative spatial locations within the previously cited BWR and PWR models (see FIG. 3.1) were then selected corresponding to: 1) off-center in the BWR core region (spatial mesh interval #57 in the BWR model), 2) off-center in the PWR core region (spatial mesh interval #37 in the PWR model), 3) the downcomer region (spatial mesh interval #69 in the PWR model), 4) within the pressure vessel at a depth of one-fourth of the total thickness (spatial mesh interval #82 in the PWR model) and 5) within the concrete shield surrounding the reactor pressure vessel (spatial mesh interval #106 in the PWR model).
The midpoints of the one-dimensional spatial mesh intervals, where the selected neutron and photon flux spectra were calculated, are located at the following distances, respectively from the BWR and PWR core centers (see FIG. 3.1): at about 217.50 cm in the interval #57 in the BWR core region, at about 140.58 cm in the interval #37 in the PWR core region, at about 203.52 cm in the interval #69 in the PWR downcomer, at about 226.28 cm in the interval #82 at a depth of one-fourth of the total thickness of the PWR pressure vessel and at about 270.83 cm in the interval #106 within the concrete shield surrounding the PWR pressure vessel.
The calculated neutron flux spectra are compared graphically in FIG. 3.2 and listed in TAB. 3.4 while the corresponding photon flux spectra are compared in FIG. 3.3 and reported in TAB. 3.5.

The cross sections used in the transport calculations, dedicated to the determination of the five different neutron/photon weighting spectra, were previously separately self-shielded using the BWR and PWR compositional/geometrical models and the specific operating temperatures of the nuclides involved in the calculations. In particular, the proper cross section self-shielding factors were determined on the basis of the specific background cross sections and temperatures of the single nuclides constituting the various material mixtures of the reactor model spatial regions.

In the BWR and PWR core regions, the cross sections of the nuclides involved were self-shielded using the corresponding fuel-clad-moderator pin models. The key compositional, geometrical and temperature parameters for the BWR and PWR pin cell models are given in TAB. 3.6.

In the steel regions, the cross sections of the nuclides that are constituents of steels were separately self-shielded for carbon steel (A533-B), used for the BWR and PWR pressure vessels, and for stainless steel (SS-304), employed for the BWR and PWR core barrels, using

the atomic densities given in TAB. 3.7. As in the case of the BUGLE-96 library, the cross sections of the constituents of carbon steel and stainless steel were self-shielded at the temperature of 600 °K.
It is underlined that, as performed for BUGLE-96, the self-shielding of the cross sections of the nuclides constituting steel was performed following an approach that contained only steel instead of a 50%-50% mixture of water and stainless steel, which was the approach previously followed for similar ORNL working cross section libraries. The present choice using only steel constituents, adopted originally for BUGLE-96, permitted to obtain a significant improvement in the agreement of the results coming from one-dimensional transport calculations using ENDF/B-VI.3 nuclear data and the dosimeter experimental data relative to the ANO-1 (Arkansas Nuclear One) commercial nuclear power reactor, as reported in the BUGLE-96 library user's manual.

The cross section self-shielding for the nuclides of the iron-water mixture representing the PWR downcomer was calculated at the temperature of 590 °K.

Finally, concerning the nuclides constituting the concrete shields, their cross section self-shielding was performed at the temperature of 300 °K.

Although it was decided to use, as much as possible, the input data given in the BUGLE-96 library user's manual, it seems proper to make a few remarks.
The atomic densities of the concrete constituents used in the cross section self-shielding and spectrum calculations, except that of carbon, present different values in TAB. 3.3 (spectrum calculations) and in TAB. 3.7 (self-shielding calculations). The different numerical values reported were respectively taken from the BUGLE-96 library user's manual (see /8/, respectively from page 31, TAB. 3.3 and from page A.8 of APPENDIX A, TAB. A.5), although both concrete compositions are labelled with "Type 04".
The atomic densities of the iron isotopes used in the cross section self-shielding calculations for the carbon and stainless steel components were calculated with a different set of natural atomic abundances with respect to the set of atomic abundances of the iron isotopes reported in TAB. 3.3. In particular, in this case, the following atomic abundances were used to determine the atomic densities of the iron isotopes: 5.8% for Fe-54, 91.8% for Fe-56, 2.1% for Fe-57 (identical to the numerical value reported in TAB. 3.3) and 0.3% for Fe-58.
Silicon is present in the carbon and stainless steel material compositions (see TAB. 3.3) used in the spectrum calculations whilst it is not included, as steel constituent, in the corresponding material compositions employed in the cross section self-shielding calculations.

The second phase of the data processing was dedicated, as previously reported, to the cross section collapsing of infinitely dilute (not-self-shielded) and self-shielded cross sections, using the neutron/photon weighting spectra, pre-calculated in the first phase of the data processing.

Concerning the self-shielded cross sections, six sets of collapsed and self-shielded cross sections were generated using the five pre-calculated neutron/photon weighting spectra: in particular there is 1) a set of cross sections for the PWR core materials collapsed with the PWR core flux spectra using a fuel-clad-moderator pin model, 2) a set of cross sections for an iron-water mixture of structural and coolant materials collapsed with the PWR downcomer flux spectra, 3) a set of cross sections for the carbon steel pressure vessel materials collapsed

with the PWR flux spectra at the one-quarter thickness (T) position in the pressure vessel (1/4 T PV), 4) a set of cross sections for the biological shield concrete materials collapsed with the PWR flux spectra in the concrete biological shield, 5) a set of cross sections for the carbon and stainless steel materials collapsed with the PWR pressure vessel flux spectra at the one quarter thickness (T) position in the pressure vessel (1/4 T PV) and, finally, 6) a set of cross sections for the BWR core materials collapsed with the BWR core flux spectra using a fuel-clad-moderator pin model.

Finally, a cross section set of collapsed and infinitely dilute (not self-shielded) cross sections was generated for all the 183 materials contained in the VITENDF70.BOLIB fine-group library. In particular the VITENDF70.BOLIB fine-group cross sections, processed at the infinite dilution background cross section ($\sigma_0$ = 1.0E+10 barns) and at the temperature of 300 °K, were collapsed using the neutron/photon weighting spectrum, pre-calculated in the concrete PWR biological shield during the first phase of the data processing.

FIG. 3.1

One-Dimensional PWR and BWR Radial Geometry and Composition Models[a] Adopted to Calculate the Specific Flux Spectra for Collapsing the VITENDF70.BOLIB Library Fine-Group Cross Sections into the BUGENDF70.BOLIB Broad-Group Library.

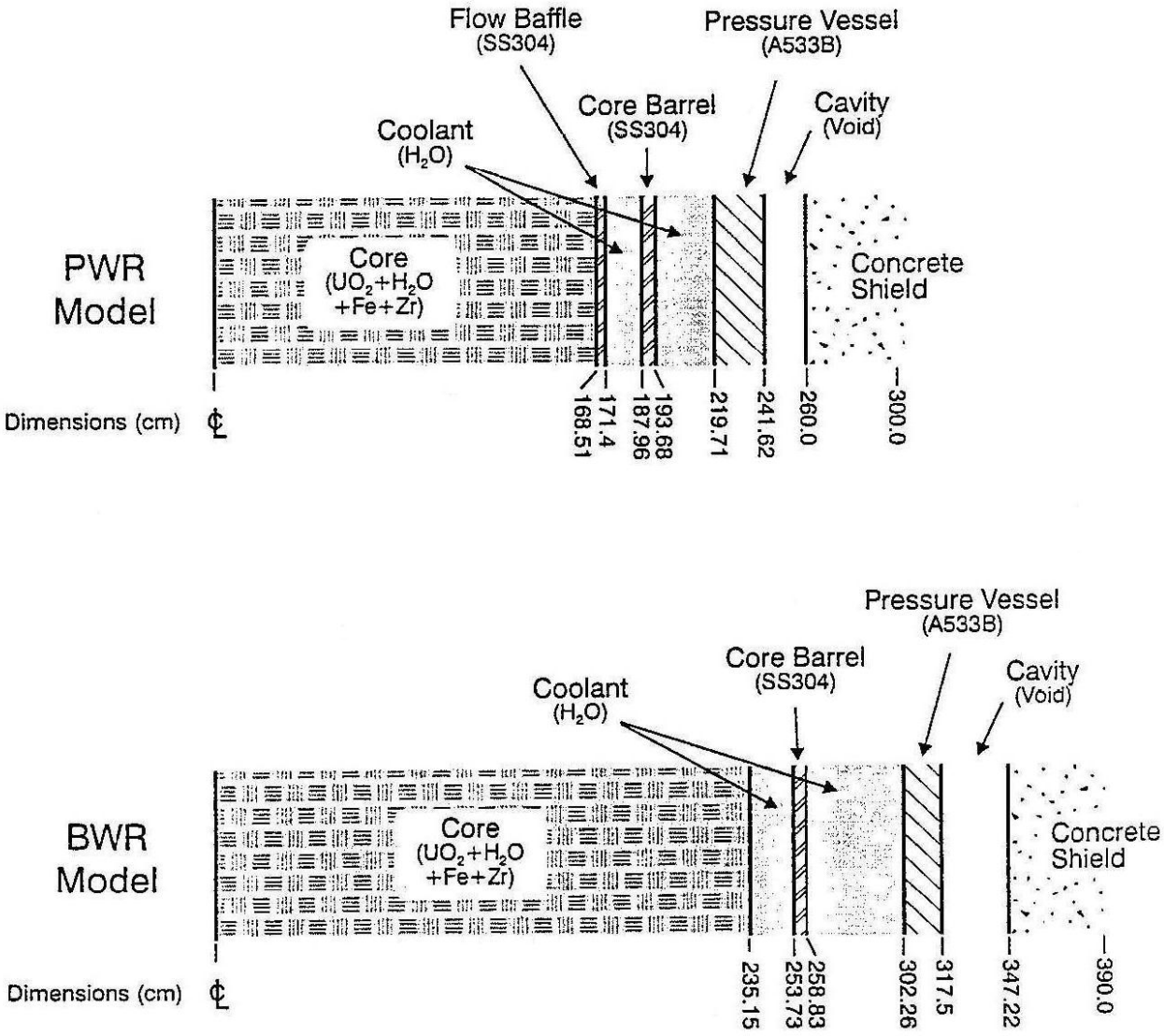


([a]) Figure taken from reference /8/.

TAB. 3.3

Atomic Densities[a] and Natural Isotopic Abundances Used in BWR and PWR Models for Spectrum Calculations.

| | HOMOGENEOUS CORES | | COOLANT | |
|---|---|---|---|---|
| | BWR | PWR | BWR | PWR |
| Hydrogen | 1.5354-2[b] | 2.768-2 | 4.950-2 | 4.714-2 |
| Oxygen | 7.6770-3 | 1.384-2 | 2.475-2 | 2.357-2 |
| Boron-10 | 0.0 | 2.466-6 | 0.0 | 4.200-6 |
| Zirconium | 5.7645-3 | 4.257-3 | | |
| Iron | 2.0030-5 | 1.444-5 | | |
| U-235 | 1.2125-4 | 1.903-4 | | |
| U-238 | 5.3220-3 | 6.515-3 | | |
| Fuel Oxygen | 1.0884-2 | 1.343-2 | | |

| | STEELS | | CONCRETE | |
|---|---|---|---|---|
| | SS-304 | A533-B | | Type 04 |
| Carbon | 2.37-4 | 9.81-4 | Hydrogen | 7.77-3 |
| Silicon | 8.93-4 | 3.71-4 | Carbon | 1.15-4 |
| Chromium | 1.74-2 | 1.27-4 | Oxygen | 4.38-2 |
| Manganese | 1.52-3 | 1.12-3 | Sodium | 1.05-3 |
| Iron | 5.83-2 | 8.19-2 | Magnesium | 1.48-4 |
| Nickel | 8.55-3 | 4.44-4 | Aluminum | 2.39-3 |
| | | | Silicon | 1.58-2 |
| | | | Potassium | 6.93-4 |
| | | | Calcium | 2.92-3 |
| | | | Iron | 3.13-4 |

NATURAL ISOTOPIC ABUNDANCES (%)

| | | | | | | | |
|---|---|---|---|---|---|---|---|
| Mg-24 | 78.99 | Ca-40 | 96.941 | Fe-54 | 5.90 | Zr-90 | 51.45 |
| Mg-25 | 10.00 | Ca-42 | 0.647 | Fe-56 | 91.72 | Zr-91 | 11.22 |
| Mg-26 | 11.01 | Ca-43 | 0.135 | Fe-57 | 2.10 | Zr-92 | 17.15 |
| | | Ca-44 | 2.086 | Fe-58 | 0.28 | Zr-94 | 17.38 |
| Si-28 | 92.23 | Ca-46 | 0.004 | | | Zr-96 | 2.80 |
| Si-29 | 4.67 | Ca-48 | 0.187 | Ni-58 | 68.27 | | |
| Si-30 | 3.10 | | | Ni-60 | 26.10 | | |
| | | Cr-50 | 4.345 | Ni-61 | 1.13 | | |
| K-39 | 93.2581 | Cr-52 | 83.790 | Ni-62 | 3.59 | | |
| K-40 | 0.0117 | Cr-53 | 9.500 | Ni-64 | 0.91 | | |
| K-41 | 6.7302 | Cr-54 | 2.365 | | | | |

([a]) In units of [Atoms·$b^{-1}$·$cm^{-1}$].
([b]) Read as 1.535 × $10^{-2}$.

FIG. 3.2

Comparison of Five BWR- and PWR-Specific Neutron Flux Spectra Calculated with VITENDF70.BOLIB and Used to Generate BUGENDF70.BOLIB.

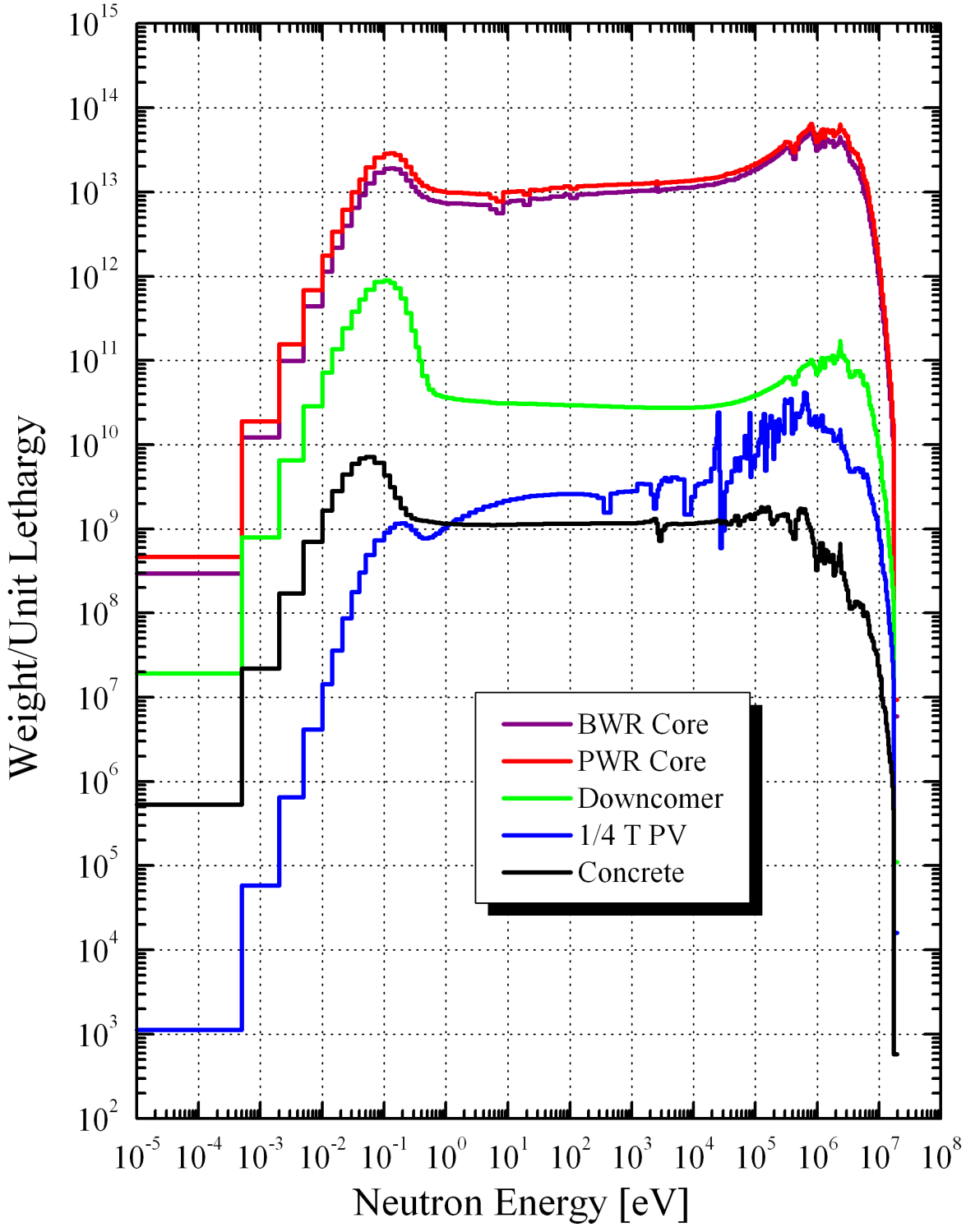

TAB. 3.4

Neutron Weighting Spectra from BWR/PWR Models for BUGENDF70.BOLIB.

| Fine Group | BWR Core (Int#57)[a] | PWR Core (Int#37) | Downcomer (Int#69) | 1/4T PV (Int#82) | Concrete (Int#106) |
|---|---|---|---|---|---|
| 1 | 7.4025E+05 | 1.1650E+06 | 1.3681E+04 | 1.9829E+03 | 7.2935E+01 |
| 2 | 2.8344E+08 | 4.3732E+08 | 3.4919E+06 | 4.1242E+05 | 1.1586E+04 |
| 3 | 3.1895E+08 | 4.9820E+08 | 5.1200E+06 | 6.7457E+05 | 2.1681E+04 |
| 4 | 1.0540E+09 | 1.6352E+09 | 1.5493E+07 | 2.0141E+06 | 6.3887E+04 |
| 5 | 1.7353E+09 | 2.6794E+09 | 2.3249E+07 | 2.8672E+06 | 8.4498E+04 |
| 6 | 1.2326E+09 | 1.8982E+09 | 1.5689E+07 | 1.8794E+06 | 5.3272E+04 |
| 7 | 1.5787E+09 | 2.4352E+09 | 2.0222E+07 | 2.4034E+06 | 6.6498E+04 |
| 8 | 1.9934E+09 | 3.0749E+09 | 2.5329E+07 | 2.9897E+06 | 8.2439E+04 |
| 9 | 2.4647E+09 | 3.7946E+09 | 3.0381E+07 | 3.5418E+06 | 9.7269E+04 |
| 10 | 6.7907E+09 | 1.0424E+10 | 7.9651E+07 | 9.1051E+06 | 2.4442E+05 |
| 11 | 5.0385E+09 | 7.7162E+09 | 5.6097E+07 | 6.2370E+06 | 1.6663E+05 |
| 12 | 5.2022E+09 | 7.9780E+09 | 6.0622E+07 | 6.8338E+06 | 1.8527E+05 |
| 13 | 1.4365E+10 | 2.1795E+10 | 1.4048E+08 | 1.4959E+07 | 3.8123E+05 |
| 14 | 2.0358E+10 | 3.0758E+10 | 1.8456E+08 | 1.8735E+07 | 4.6472E+05 |
| 15 | 3.0729E+10 | 4.6948E+10 | 3.1251E+08 | 3.2336E+07 | 8.4425E+05 |
| 16 | 4.0256E+10 | 6.0828E+10 | 3.5875E+08 | 3.6853E+07 | 9.0218E+05 |
| 17 | 5.5066E+10 | 8.3265E+10 | 4.8258E+08 | 4.8687E+07 | 1.1949E+06 |
| 18 | 7.4769E+10 | 1.1330E+11 | 6.5470E+08 | 6.4793E+07 | 1.6253E+06 |
| 19 | 9.4934E+10 | 1.4287E+11 | 7.5753E+08 | 7.3318E+07 | 1.7966E+06 |
| 20 | 1.1927E+11 | 1.7846E+11 | 8.5884E+08 | 7.9709E+07 | 1.8592E+06 |
| 21 | 1.5511E+11 | 2.3299E+11 | 1.1213E+09 | 1.0024E+08 | 2.3023E+06 |
| 22 | 1.9220E+11 | 2.8797E+11 | 1.3209E+09 | 1.1607E+08 | 2.5888E+06 |
| 23 | 2.3228E+11 | 3.4643E+11 | 1.4707E+09 | 1.2590E+08 | 2.7770E+06 |
| 24 | 2.9495E+11 | 4.4205E+11 | 1.9059E+09 | 1.6005E+08 | 3.5921E+06 |
| 25 | 1.1263E+11 | 1.6888E+11 | 7.1923E+08 | 5.9867E+07 | 1.3883E+06 |
| 26 | 2.5109E+11 | 3.7728E+11 | 1.6246E+09 | 1.3483E+08 | 3.1291E+06 |
| 27 | 4.2900E+11 | 6.4242E+11 | 2.6630E+09 | 2.2099E+08 | 5.1044E+06 |
| 28 | 4.7310E+11 | 7.0154E+11 | 2.5633E+09 | 2.0711E+08 | 4.6616E+06 |
| 29 | 5.3208E+11 | 7.8528E+11 | 2.6366E+09 | 2.0468E+08 | 4.6376E+06 |
| 30 | 6.4626E+11 | 9.6078E+11 | 3.3740E+09 | 2.5206E+08 | 6.2127E+06 |
| 31 | 7.0482E+11 | 1.0394E+12 | 3.2420E+09 | 2.3668E+08 | 5.8666E+06 |
| 32 | 8.1178E+11 | 1.2003E+12 | 3.7464E+09 | 2.6199E+08 | 6.5265E+06 |
| 33 | 8.5524E+11 | 1.2552E+12 | 3.6537E+09 | 2.6398E+08 | 6.4087E+06 |
| 34 | 1.9380E+12 | 2.8285E+12 | 7.4621E+09 | 5.2357E+08 | 1.3612E+07 |
| 35 | 2.0777E+12 | 2.9845E+12 | 6.6285E+09 | 4.8303E+08 | 1.1927E+07 |
| 36 | 2.2946E+12 | 3.2600E+12 | 6.4338E+09 | 4.7984E+08 | 1.1327E+07 |
| 37 | 1.3610E+12 | 1.9340E+12 | 3.7556E+09 | 2.6389E+08 | 7.0245E+06 |
| 38 | 1.6108E+12 | 2.3018E+12 | 4.8742E+09 | 3.2914E+08 | 9.4467E+06 |
| 39 | 1.6242E+12 | 2.3025E+12 | 4.9815E+09 | 3.8294E+08 | 1.0614E+07 |
| 40 | 1.7505E+12 | 2.4736E+12 | 5.2546E+09 | 4.1381E+08 | 1.2350E+07 |
| 41 | 1.9177E+12 | 2.7026E+12 | 5.7523E+09 | 4.7559E+08 | 1.4992E+07 |
| 42 | 1.9309E+12 | 2.7058E+12 | 5.6134E+09 | 4.5358E+08 | 1.5056E+07 |
| 43 | 1.3379E+12 | 1.8736E+12 | 4.2366E+09 | 3.5808E+08 | 1.3768E+07 |
| 44 | 3.6298E+11 | 5.1074E+11 | 1.3052E+09 | 1.1056E+08 | 4.2041E+06 |
| 45 | 3.7055E+11 | 5.2120E+11 | 1.4330E+09 | 1.2531E+08 | 5.5247E+06 |
| 46 | 7.2864E+11 | 1.0174E+12 | 2.4624E+09 | 2.0268E+08 | 9.0900E+06 |
| 47 | 1.3276E+12 | 1.8267E+12 | 4.3032E+09 | 4.3066E+08 | 1.5808E+07 |
| 48 | 1.8676E+12 | 2.5477E+12 | 5.6674E+09 | 5.9945E+08 | 1.9770E+07 |
| 49 | 1.8159E+12 | 2.4620E+12 | 5.3213E+09 | 5.7117E+08 | 1.8312E+07 |

TAB. 3.4 Continued

Neutron Weighting Spectra from BWR/PWR Models for BUGENDF70.BOLIB.

| Fine Group | BWR Core (Int#57) | PWR Core (Int#37) | Downcomer (Int#69) | 1/4T PV (Int#82) | Concrete (Int#106) |
|---|---|---|---|---|---|
| 50 | 1.7712E+12 | 2.3882E+12 | 5.1294E+09 | 5.5517E+08 | 1.5470E+07 |
| 51 | 1.7046E+12 | 2.2821E+12 | 4.6683E+09 | 5.5953E+08 | 1.4093E+07 |
| 52 | 2.0163E+12 | 2.6983E+12 | 5.7639E+09 | 6.8998E+08 | 2.4411E+07 |
| 53 | 1.9684E+12 | 2.6035E+12 | 5.4552E+09 | 7.4713E+08 | 2.2057E+07 |
| 54 | 1.9173E+12 | 2.5228E+12 | 5.1200E+09 | 7.0477E+08 | 2.0303E+07 |
| 55 | 2.0023E+12 | 2.6265E+12 | 5.3461E+09 | 7.4303E+08 | 2.4541E+07 |
| 56 | 2.0994E+12 | 2.7362E+12 | 5.3784E+09 | 7.1658E+08 | 2.7119E+07 |
| 57 | 2.0558E+12 | 2.6585E+12 | 5.2690E+09 | 7.7057E+08 | 2.8179E+07 |
| 58 | 1.7185E+12 | 2.2083E+12 | 4.1096E+09 | 7.9652E+08 | 1.9622E+07 |
| 59 | 2.1403E+12 | 2.7533E+12 | 5.2114E+09 | 7.2592E+08 | 2.8771E+07 |
| 60 | 2.1484E+12 | 2.7329E+12 | 5.3577E+09 | 1.1106E+09 | 3.4043E+07 |
| 61 | 1.9986E+12 | 2.5266E+12 | 4.8505E+09 | 1.0250E+09 | 3.3681E+07 |
| 62 | 3.2928E+12 | 4.1553E+12 | 7.5622E+09 | 1.6827E+09 | 4.1824E+07 |
| 63 | 1.2885E+12 | 1.6233E+12 | 2.8558E+09 | 6.7115E+08 | 1.3501E+07 |
| 64 | 2.1579E+12 | 2.6957E+12 | 4.7982E+09 | 1.2668E+09 | 2.7517E+07 |
| 65 | 2.0821E+12 | 2.5685E+12 | 4.4274E+09 | 8.9787E+08 | 3.3896E+07 |
| 66 | 2.4020E+12 | 2.9288E+12 | 4.8970E+09 | 9.9559E+08 | 3.9284E+07 |
| 67 | 2.6645E+12 | 3.2113E+12 | 5.0958E+09 | 8.6835E+08 | 4.7241E+07 |
| 68 | 2.5535E+12 | 3.0399E+12 | 4.7796E+09 | 8.9582E+08 | 5.2384E+07 |
| 69 | 2.3812E+12 | 2.8179E+12 | 4.5917E+09 | 1.2883E+09 | 5.7828E+07 |
| 70 | 2.2965E+12 | 2.7103E+12 | 4.4619E+09 | 1.5289E+09 | 6.4702E+07 |
| 71 | 2.2354E+12 | 2.6305E+12 | 4.4037E+09 | 2.0346E+09 | 7.5256E+07 |
| 72 | 2.1748E+12 | 2.5534E+12 | 4.2915E+09 | 2.0964E+09 | 8.5677E+07 |
| 73 | 2.1148E+12 | 2.4791E+12 | 4.2134E+09 | 1.4932E+09 | 8.6573E+07 |
| 74 | 2.0546E+12 | 2.4056E+12 | 4.0731E+09 | 1.2887E+09 | 7.8635E+07 |
| 75 | 1.9945E+12 | 2.3332E+12 | 3.9408E+09 | 1.1903E+09 | 8.6643E+07 |
| 76 | 1.9159E+12 | 2.2412E+12 | 3.7898E+09 | 1.0762E+09 | 8.2136E+07 |
| 77 | 3.1947E+12 | 3.7665E+12 | 6.4588E+09 | 2.3416E+09 | 1.2779E+08 |
| 78 | 2.4517E+12 | 2.9366E+12 | 5.1998E+09 | 1.5393E+09 | 7.5982E+07 |
| 79 | 1.4389E+12 | 1.7255E+12 | 3.0302E+09 | 6.7941E+08 | 4.4420E+07 |
| 80 | 1.4435E+12 | 1.7202E+12 | 3.0189E+09 | 1.7453E+09 | 4.6671E+07 |
| 81 | 3.2825E+12 | 3.8576E+12 | 6.4294E+09 | 3.1689E+09 | 1.2326E+08 |
| 82 | 3.3472E+12 | 3.8868E+12 | 6.3418E+09 | 3.3188E+09 | 1.4833E+08 |
| 83 | 3.7436E+11 | 4.3218E+11 | 7.0686E+08 | 4.0089E+08 | 1.7291E+07 |
| 84 | 1.3765E+11 | 1.5890E+11 | 2.6038E+08 | 1.3103E+08 | 6.4723E+06 |
| 85 | 2.8939E+11 | 3.3410E+11 | 5.4772E+08 | 2.1106E+08 | 1.3308E+07 |
| 86 | 7.8517E+11 | 9.0673E+11 | 1.4859E+09 | 3.4030E+08 | 3.5818E+07 |
| 87 | 1.5310E+12 | 1.7670E+12 | 2.8986E+09 | 7.3878E+08 | 7.4432E+07 |
| 88 | 2.9125E+12 | 3.3579E+12 | 5.5531E+09 | 1.6753E+09 | 1.4511E+08 |
| 89 | 1.3910E+12 | 1.6025E+12 | 2.6728E+09 | 9.9618E+08 | 7.1569E+07 |
| 90 | 1.3458E+12 | 1.5528E+12 | 2.6098E+09 | 5.5194E+08 | 7.1090E+07 |
| 91 | 1.3094E+12 | 1.5124E+12 | 2.5595E+09 | 9.4950E+08 | 6.3929E+07 |
| 92 | 1.2787E+12 | 1.4781E+12 | 2.5128E+09 | 5.6124E+08 | 6.2548E+07 |
| 93 | 1.2463E+12 | 1.4420E+12 | 2.4627E+09 | 3.3807E+08 | 5.9170E+07 |
| 94 | 1.2123E+12 | 1.4033E+12 | 2.4088E+09 | 7.8682E+08 | 5.6633E+07 |
| 95 | 1.1828E+12 | 1.3699E+12 | 2.3635E+09 | 1.0948E+09 | 6.5219E+07 |
| 96 | 1.1522E+12 | 1.3356E+12 | 2.3120E+09 | 8.7232E+08 | 8.0572E+07 |
| 97 | 1.1274E+12 | 1.3078E+12 | 2.2737E+09 | 7.9015E+08 | 9.1186E+07 |
| 98 | 1.0995E+12 | 1.2768E+12 | 2.2307E+09 | 4.6712E+08 | 8.8392E+07 |

TAB. 3.4 Continued

Neutron Weighting Spectra from BWR/PWR Models for BUGENDF70.BOLIB.

| Fine Group | BWR Core (Int#57) | PWR Core (Int#37) | Downcomer (Int#69) | 1/4T PV (Int#82) | Concrete (Int#106) |
|---|---|---|---|---|---|
| 99 | 1.0762E+12 | 1.2506E+12 | 2.1904E+09 | 2.4586E+08 | 8.0999E+07 |
| 100 | 1.0484E+12 | 1.2186E+12 | 2.1435E+09 | 1.1577E+09 | 8.7814E+07 |
| 101 | 1.0256E+12 | 1.1927E+12 | 2.1063E+09 | 5.3322E+08 | 8.0647E+07 |
| 102 | 1.0036E+12 | 1.1679E+12 | 2.0703E+09 | 9.3379E+08 | 9.1300E+07 |
| 103 | 9.8044E+11 | 1.1418E+12 | 2.0304E+09 | 5.8425E+08 | 7.9655E+07 |
| 104 | 9.6292E+11 | 1.1223E+12 | 2.0014E+09 | 5.4552E+08 | 8.0802E+07 |
| 105 | 2.3257E+12 | 2.7150E+12 | 4.8712E+09 | 9.3612E+08 | 1.9055E+08 |
| 106 | 2.2150E+12 | 2.5934E+12 | 4.6988E+09 | 6.8193E+08 | 1.6574E+08 |
| 107 | 8.2918E+11 | 9.6431E+11 | 1.7429E+09 | 1.9615E+08 | 6.2988E+07 |
| 108 | 6.1907E+11 | 7.3185E+11 | 1.3524E+09 | 8.8029E+08 | 5.5013E+07 |
| 109 | 1.6596E+12 | 1.9364E+12 | 3.5290E+09 | 6.8452E+08 | 1.4179E+08 |
| 110 | 1.0548E+12 | 1.2482E+12 | 2.3137E+09 | 8.4874E+08 | 9.2748E+07 |
| 111 | 2.7528E+12 | 3.2174E+12 | 5.9301E+09 | 1.2309E+09 | 2.1758E+08 |
| 112 | 1.1311E+12 | 1.3292E+12 | 2.4706E+09 | 3.7243E+08 | 8.3527E+07 |
| 113 | 1.8220E+12 | 2.1529E+12 | 4.0400E+09 | 8.5631E+08 | 1.7870E+08 |
| 114 | 1.7431E+12 | 2.0797E+12 | 3.9484E+09 | 6.1176E+08 | 1.5677E+08 |
| 115 | 2.4629E+12 | 2.8747E+12 | 5.3922E+09 | 6.2555E+08 | 1.9862E+08 |
| 116 | 1.0157E+12 | 1.1949E+12 | 2.2672E+09 | 2.0745E+08 | 9.1546E+07 |
| 117 | 1.4688E+12 | 1.7299E+12 | 3.2920E+09 | 1.0548E+08 | 1.3643E+08 |
| 118 | 7.0453E+11 | 8.3382E+11 | 1.5980E+09 | 3.2175E+07 | 6.3577E+07 |
| 119 | 4.6046E+11 | 5.4382E+11 | 1.0518E+09 | 1.7269E+08 | 4.3907E+07 |
| 120 | 6.4522E+11 | 7.6127E+11 | 1.4763E+09 | 1.2049E+09 | 6.2143E+07 |
| 121 | 3.1605E+11 | 3.7628E+11 | 7.3564E+08 | 5.7570E+08 | 3.1617E+07 |
| 122 | 3.1412E+11 | 3.7486E+11 | 7.3123E+08 | 3.0336E+08 | 3.1203E+07 |
| 123 | 9.5770E+11 | 1.1290E+12 | 2.1815E+09 | 6.8175E+08 | 9.2597E+07 |
| 124 | 1.5343E+12 | 1.8373E+12 | 3.5964E+09 | 6.4926E+08 | 1.5176E+08 |
| 125 | 3.0795E+12 | 3.6361E+12 | 7.0884E+09 | 9.1839E+08 | 2.9877E+08 |
| 126 | 2.9748E+12 | 3.5358E+12 | 7.0057E+09 | 8.5943E+08 | 2.9525E+08 |
| 127 | 1.1683E+12 | 1.3928E+12 | 2.7841E+09 | 3.2580E+08 | 1.1708E+08 |
| 128 | 1.7235E+12 | 2.0641E+12 | 4.1556E+09 | 3.6134E+08 | 1.7262E+08 |
| 129 | 2.8168E+12 | 3.3900E+12 | 6.8869E+09 | 3.7098E+08 | 2.8972E+08 |
| 130 | 2.8211E+12 | 3.3656E+12 | 6.8714E+09 | 9.7704E+08 | 2.8522E+08 |
| 131 | 2.7564E+12 | 3.3118E+12 | 6.8639E+09 | 1.0207E+09 | 2.8834E+08 |
| 132 | 1.6357E+12 | 1.9700E+12 | 4.1202E+09 | 5.5460E+08 | 1.6989E+08 |
| 133 | 1.0920E+12 | 1.3134E+12 | 2.7502E+09 | 4.0239E+08 | 1.0925E+08 |
| 134 | 1.0751E+12 | 1.3002E+12 | 2.7518E+09 | 3.7764E+08 | 9.7316E+07 |
| 135 | 1.0480E+12 | 1.2835E+12 | 2.7537E+09 | 3.3342E+08 | 7.2631E+07 |
| 136 | 5.0889E+11 | 6.3085E+11 | 1.3763E+09 | 1.4598E+08 | 4.4271E+07 |
| 137 | 5.8229E+11 | 6.7608E+11 | 1.3764E+09 | 1.1990E+08 | 5.8126E+07 |
| 138 | 1.0474E+12 | 1.2724E+12 | 2.7545E+09 | 1.7415E+08 | 1.3097E+08 |
| 139 | 1.0786E+12 | 1.2995E+12 | 2.7647E+09 | 2.5730E+08 | 1.2594E+08 |
| 140 | 2.6055E+12 | 3.1734E+12 | 6.9350E+09 | 8.5098E+08 | 3.0503E+08 |
| 141 | 2.5966E+12 | 3.1630E+12 | 6.9602E+09 | 8.6365E+08 | 2.9589E+08 |
| 142 | 2.5920E+12 | 3.1596E+12 | 6.9873E+09 | 7.0385E+08 | 2.9220E+08 |
| 143 | 2.5431E+12 | 3.1156E+12 | 7.0265E+09 | 6.9478E+08 | 2.9132E+08 |
| 144 | 2.5105E+12 | 3.0858E+12 | 7.0657E+09 | 6.8514E+08 | 2.9110E+08 |
| 145 | 2.4829E+12 | 3.0622E+12 | 7.1059E+09 | 6.5879E+08 | 2.9104E+08 |
| 146 | 2.4619E+12 | 3.0460E+12 | 7.1387E+09 | 3.9369E+08 | 2.9048E+08 |
| 147 | 2.4376E+12 | 3.0268E+12 | 7.1951E+09 | 5.8702E+08 | 2.9046E+08 |

TAB. 3.4 Continued

Neutron Weighting Spectra from BWR/PWR Models for BUGENDF70.BOLIB.

| Fine Group | BWR Core (Int#57) | PWR Core (Int#37) | Downcomer (Int#69) | 1/4T PV (Int#82) | Concrete (Int#106) |
|---|---|---|---|---|---|
| 148 | 2.3888E+12 | 2.9775E+12 | 7.2380E+09 | 6.2524E+08 | 2.9031E+08 |
| 149 | 2.3793E+12 | 2.9701E+12 | 7.2795E+09 | 6.4008E+08 | 2.9003E+08 |
| 150 | 2.3388E+12 | 2.9344E+12 | 7.3247E+09 | 6.4699E+08 | 2.8979E+08 |
| 151 | 2.1458E+12 | 2.7419E+12 | 7.3664E+09 | 6.4964E+08 | 2.8931E+08 |
| 152 | 2.3391E+12 | 2.9344E+12 | 7.4102E+09 | 6.4970E+08 | 2.8881E+08 |
| 153 | 2.2210E+12 | 2.8141E+12 | 7.4538E+09 | 6.4740E+08 | 2.8822E+08 |
| 154 | 2.2189E+12 | 2.8154E+12 | 7.4973E+09 | 6.4278E+08 | 2.8756E+08 |
| 155 | 2.1194E+12 | 2.7234E+12 | 7.5407E+09 | 6.3575E+08 | 2.8681E+08 |
| 156 | 2.0757E+12 | 2.6612E+12 | 7.5829E+09 | 6.2611E+08 | 2.8596E+08 |
| 157 | 2.0970E+12 | 2.6979E+12 | 7.6255E+09 | 6.1385E+08 | 2.8505E+08 |
| 158 | 1.7727E+12 | 2.3430E+12 | 7.6657E+09 | 5.9864E+08 | 2.8398E+08 |
| 159 | 1.9864E+12 | 2.5867E+12 | 7.7081E+09 | 5.8077E+08 | 2.8292E+08 |
| 160 | 1.9629E+12 | 2.5544E+12 | 7.7495E+09 | 5.5997E+08 | 2.8175E+08 |
| 161 | 1.9056E+12 | 2.4937E+12 | 7.7879E+09 | 5.3615E+08 | 2.8039E+08 |
| 162 | 1.4209E+12 | 1.9508E+12 | 7.8266E+09 | 5.0967E+08 | 2.7896E+08 |
| 163 | 1.5632E+12 | 2.1429E+12 | 7.8646E+09 | 4.8065E+08 | 2.7741E+08 |
| 164 | 1.7667E+12 | 2.3686E+12 | 8.0790E+09 | 4.5846E+08 | 2.8195E+08 |
| 165 | 1.7654E+12 | 2.3648E+12 | 8.1582E+09 | 4.2600E+08 | 2.7939E+08 |
| 166 | 1.7985E+12 | 2.4083E+12 | 8.2906E+09 | 3.9176E+08 | 2.8043E+08 |
| 167 | 1.8091E+12 | 2.4260E+12 | 8.4443E+09 | 3.5763E+08 | 2.8162E+08 |
| 168 | 1.8363E+12 | 2.4657E+12 | 8.6332E+09 | 3.2496E+08 | 2.8338E+08 |
| 169 | 7.8247E+11 | 1.0523E+12 | 3.7184E+09 | 1.2998E+08 | 1.2052E+08 |
| 170 | 1.0577E+12 | 1.4259E+12 | 5.1534E+09 | 1.6670E+08 | 1.6536E+08 |
| 171 | 2.9892E+11 | 4.0369E+11 | 1.4849E+09 | 4.5682E+07 | 4.7270E+07 |
| 172 | 2.7673E+11 | 3.7384E+11 | 1.3719E+09 | 4.1031E+07 | 4.3518E+07 |
| 173 | 2.8985E+11 | 3.9160E+11 | 1.4338E+09 | 4.1570E+07 | 4.5302E+07 |
| 174 | 9.8816E+11 | 1.3354E+12 | 4.8897E+09 | 1.3292E+08 | 1.5316E+08 |
| 175 | 6.9429E+11 | 9.3886E+11 | 3.4553E+09 | 8.6494E+07 | 1.0679E+08 |
| 176 | 1.2307E+12 | 1.6660E+12 | 6.2108E+09 | 1.4024E+08 | 1.8786E+08 |
| 177 | 6.9636E+11 | 9.4391E+11 | 3.6098E+09 | 7.3289E+07 | 1.0538E+08 |
| 178 | 1.3164E+12 | 1.7878E+12 | 7.2811E+09 | 1.2808E+08 | 1.9670E+08 |
| 179 | 5.1247E+11 | 6.9767E+11 | 3.1396E+09 | 4.7224E+07 | 7.5258E+07 |
| 180 | 1.6524E+12 | 2.2605E+12 | 1.2479E+10 | 1.4556E+08 | 2.3486E+08 |
| 181 | 1.1415E+12 | 1.5758E+12 | 1.2025E+10 | 9.7862E+07 | 1.5284E+08 |
| 182 | 1.2376E+12 | 1.7255E+12 | 1.7533E+10 | 1.0592E+08 | 1.5547E+08 |
| 183 | 1.9273E+12 | 2.7244E+12 | 3.7689E+10 | 1.6285E+08 | 2.2264E+08 |
| 184 | 2.7615E+12 | 3.9718E+12 | 7.3416E+10 | 2.1894E+08 | 2.9323E+08 |
| 185 | 3.2933E+12 | 4.8142E+12 | 1.0991E+11 | 2.3383E+08 | 3.5464E+08 |
| 186 | 3.7588E+12 | 5.5695E+12 | 1.4708E+11 | 2.3378E+08 | 4.7690E+08 |
| 187 | 3.4997E+12 | 5.2436E+12 | 1.5298E+11 | 1.8988E+08 | 5.7698E+08 |
| 188 | 4.2030E+12 | 6.3482E+12 | 1.9970E+11 | 2.0264E+08 | 9.6933E+08 |
| 189 | 5.9818E+12 | 9.0880E+12 | 3.0709E+11 | 2.6093E+08 | 2.1738E+09 |
| 190 | 4.2990E+12 | 6.5668E+12 | 2.3551E+11 | 1.6614E+08 | 2.4183E+09 |
| 191 | 2.0674E+12 | 3.1727E+12 | 1.1820E+11 | 6.8152E+07 | 1.5432E+09 |
| 192 | 1.8770E+12 | 2.8910E+12 | 1.1067E+11 | 5.1387E+07 | 1.7120E+09 |
| 193 | 1.4298E+12 | 2.2092E+12 | 8.6786E+10 | 3.0769E+07 | 1.5764E+09 |
| 194 | 8.1302E+11 | 1.2596E+12 | 5.0573E+10 | 1.3344E+07 | 1.0479E+09 |
| 195 | 4.2302E+11 | 6.5686E+11 | 2.6799E+10 | 5.3192E+06 | 6.1017E+08 |
| 196 | 3.0798E+11 | 4.7920E+11 | 1.9815E+10 | 2.8752E+06 | 4.8914E+08 |

TAB. 3.4 Continued

Neutron Weighting Spectra from BWR/PWR Models for BUGENDF70.BOLIB.

| Fine Group | BWR Core (Int#57) | PWR Core (Int#37) | Downcomer (Int#69) | 1/4T PV (Int#82) | Concrete (Int#106) |
|---|---|---|---|---|---|
| 197 | 9.1598E+10 | 1.4284E+11 | 5.9694E+09 | 5.9519E+05 | 1.5778E+08 |
| 198 | 1.6924E+10 | 2.6443E+10 | 1.1073E+09 | 8.0640E+04 | 3.0367E+07 |
| 199 | 1.1616E+09 | 1.8146E+09 | 7.5093E+07 | 4.4219E+03 | 2.0797E+06 |

(a) Spatial mesh interval number from BWR or PWR model.

FIG. 3.3

Comparison of Five BWR- and PWR-Specific Photon Flux Spectra Calculated with VITENDF70.BOLIB and Used to Generate BUGENDF70.BOLIB.

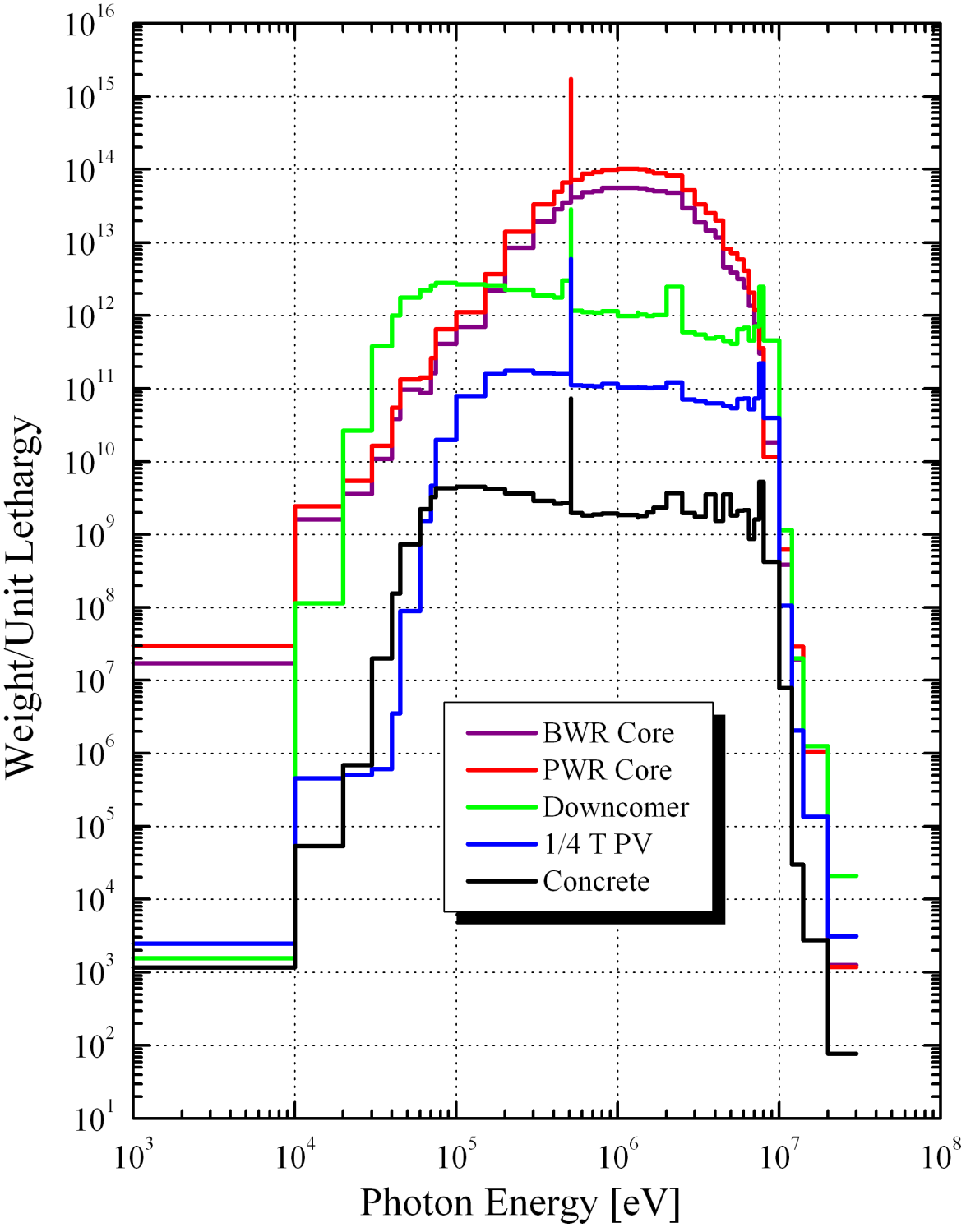

TAB. 3.5

Photon Weighting Spectra from BWR/PWR Models for BUGENDF70.BOLIB.

| Fine Group | BWR Core (Int#57)[a] | PWR Core (Int#37) | Downcomer (Int#69) | 1/4T PV (Int#82) | Concrete (Int#106) |
|---|---|---|---|---|---|
| 1 | 5.0831E+02 | 4.7579E+02 | 8.4498E+03 | 1.2571E+03 | 3.1569E+01 |
| 2 | 3.7694E+05 | 3.7200E+05 | 4.4996E+05 | 4.8458E+04 | 9.7961E+02 |
| 3 | 3.0268E+06 | 4.4810E+06 | 3.0968E+06 | 3.1593E+05 | 4.5927E+03 |
| 4 | 7.0618E+07 | 1.1422E+08 | 2.1045E+08 | 1.9307E+07 | 1.4377E+06 |
| 5 | 4.0943E+09 | 2.5728E+09 | 1.0245E+11 | 8.8636E+09 | 9.4421E+07 |
| 6 | 1.9559E+10 | 2.3127E+10 | 1.6051E+11 | 1.4383E+10 | 3.4197E+08 |
| 7 | 5.2925E+10 | 8.2212E+10 | 4.9206E+10 | 5.0388E+09 | 1.1117E+08 |
| 8 | 1.0202E+11 | 1.5424E+11 | 3.4018E+10 | 3.8711E+09 | 6.4852E+07 |
| 9 | 1.9498E+11 | 3.3225E+11 | 5.4957E+10 | 5.8388E+09 | 1.7398E+08 |
| 10 | 2.7683E+11 | 5.1668E+11 | 5.7308E+10 | 6.3157E+09 | 1.8695E+08 |
| 11 | 3.6997E+11 | 6.8588E+11 | 3.9351E+10 | 5.1544E+09 | 1.7388E+08 |
| 12 | 4.8631E+11 | 8.7940E+11 | 4.7738E+10 | 6.0964E+09 | 3.7584E+08 |
| 13 | 1.3960E+12 | 2.3874E+12 | 5.9884E+10 | 7.4714E+09 | 1.8088E+08 |
| 14 | 1.9476E+12 | 3.4046E+12 | 6.5392E+10 | 8.4386E+09 | 4.7368E+08 |
| 15 | 2.9568E+12 | 5.2194E+12 | 8.5624E+10 | 1.0517E+10 | 2.7088E+08 |
| 16 | 5.4447E+12 | 9.5553E+12 | 1.0798E+11 | 1.3083E+10 | 3.5783E+08 |
| 17 | 1.0914E+13 | 1.8747E+13 | 5.5500E+11 | 2.7052E+10 | 8.2641E+08 |
| 18 | 9.5225E+12 | 1.6400E+13 | 1.9002E+11 | 1.9322E+10 | 4.3624E+08 |
| 19 | 5.3084E+12 | 9.3930E+12 | 1.0054E+11 | 1.0354E+10 | 2.0389E+08 |
| 20 | 6.3114E+12 | 1.1238E+13 | 1.1785E+11 | 1.1682E+10 | 2.0200E+08 |
| 21 | 4.2783E+11 | 7.6895E+11 | 8.2900E+09 | 7.8064E+08 | 1.2838E+07 |
| 22 | 1.6108E+13 | 2.8830E+13 | 2.8454E+11 | 2.9384E+10 | 5.2851E+08 |
| 23 | 1.2663E+13 | 2.2108E+13 | 2.5647E+11 | 2.6136E+10 | 4.3557E+08 |
| 24 | 6.8405E+12 | 1.2188E+13 | 1.4764E+11 | 1.4399E+10 | 2.5304E+08 |
| 25 | 7.6465E+12 | 1.3453E+13 | 1.7390E+11 | 1.6908E+10 | 2.8238E+08 |
| 26 | 6.7136E+12 | 1.1628E+13 | 1.8504E+11 | 1.7764E+10 | 3.1078E+08 |
| 27 | 3.9479E+12 | 6.7828E+12 | 1.1279E+11 | 2.3433E+10 | 2.8651E+08 |
| 28 | 4.5021E+12 | 8.3713E+12 | 3.8318E+11 | 1.9838E+10 | 3.4318E+08 |
| 29 | 3.3960E+12 | 5.8816E+12 | 2.0955E+11 | 1.8771E+10 | 3.1205E+08 |
| 30 | 5.6062E+12 | 9.6218E+12 | 5.4689E+11 | 4.7279E+10 | 8.3220E+08 |
| 31 | 3.4419E+12 | 5.7994E+12 | 9.2405E+11 | 7.1730E+10 | 1.4764E+09 |
| 32 | 6.3753E+11 | 1.0640E+12 | 7.5135E+11 | 4.5429E+10 | 1.2139E+09 |
| 33 | 2.8459E+11 | 4.5112E+11 | 1.0959E+12 | 3.2370E+10 | 1.8432E+09 |
| 34 | 1.1787E+11 | 1.8856E+11 | 8.1626E+11 | 5.6941E+09 | 1.2420E+09 |
| 35 | 1.1243E+10 | 1.8074E+10 | 1.8049E+11 | 3.2265E+08 | 2.2553E+08 |
| 36 | 1.3505E+10 | 2.1843E+10 | 3.4414E+11 | 2.3976E+08 | 3.4320E+08 |
| 37 | 2.8056E+10 | 3.8614E+10 | 5.1195E+11 | 2.5808E+07 | 2.1135E+08 |
| 38 | 4.5300E+09 | 6.4259E+09 | 1.1805E+11 | 4.1726E+05 | 1.8241E+07 |
| 39 | 3.1269E+09 | 4.7548E+09 | 1.0912E+11 | 1.7638E+05 | 5.7579E+06 |
| 40 | 1.4622E+09 | 2.2175E+09 | 1.0788E+10 | 2.0522E+05 | 2.7980E+05 |
| 41 | 1.1260E+09 | 1.6856E+09 | 7.9699E+07 | 3.1495E+05 | 3.7504E+04 |
| 42 | 3.9691E+07 | 6.8888E+07 | 3.5751E+03 | 5.6930E+03 | 2.6790E+03 |

([a]) Spatial mesh interval number from BWR or PWR model.

TAB. 3.6

Key Parameters for BWR and PWR Pin Cells in Self-Shielding Calculations.

| | BWR | PWR |
|---|---|---|
| Inner radius clad [cm] | 0.53213 | 0.41783 |
| Outer radius clad [cm] | 0.6134 | 0.47498 |
| Outer radius cell [cm] | 0.9174 | 0.71079 |
| Region temperature [°K] | | |
| Pellet | 921 | 921 |
| Clad | 672 | 672 |
| Moderator | 551 | 583 |
| Pellet nuclear density [Atoms·b$^{-1}$·cm$^{-1}$] | | |
| U-235 | 4.959-4[a] | 6.325-4 |
| U-238 | 2.177-2 | 2.166-2 |
| Oxygen | 4.455-2 | 4.465-2 |
| Moderator density [Atoms·b$^{-1}$·cm$^{-1}$] | | |
| Hydrogen | 2.475-2 | 4.714-2 |
| Oxygen | 1.2375-2 | 2.357-2 |
| Boron-10 | 0.0 | 4.200-6 |
| Zircaloy-4 density [Atoms·b$^{-1}$·cm$^{-1}$] | | |
| Cromium | 7.64-5 | 7.64-5 |
| Iron | 1.45-4 | 1.45-4 |
| Nickel | 8.77-4 | 8.77-4 |
| Zirconium | 4.27-2 | 4.27-2 |

([a]) Read as $4.959 \times 10^{-4}$.

TAB. 3.7

Atomic Densities[a] Used for Steel and Concrete Constituents in Self-Shielding Calculations.

| | STEELS | | CONCRETE | |
|---|---|---|---|---|
| | Stainless Steel | Carbon Steel | | Type 04 |
| Carbon | 2.37-4[b] | 9.81-4 | Hydrogen | 8.60-3 |
| Chromium | 1.74-2 | 1.27-4 | Carbon | 1.15-4 |
| Manganese | 1.52-3 | 1.12-3 | Oxygen | 4.33-2 |
| Iron | 5.83-2 | 8.19-2 | Sodium | 9.64-4 |
| Nickel | 8.55-3 | 4.44-4 | Magnesium | 1.24-4 |
| | | | Aluminum | 1.74-4 |
| | | | Silicon | 1.66-3 |
| | | | Potassium | 4.60-4 |
| | | | Calcium | 1.50-3 |
| | | | Iron | 3.45-4 |

([a]) In units of [Atoms·$b^{-1}$·$cm^{-1}$].
([b]) Read as 2.37 × $10^{-4}$.

3.4 - Processing Codes and Procedures

All the computational tools used to self-shield, temperature correct, and collapse the VITENDF70.BOLIB /5/ fine-group cross sections into the BUGENDF70.BOLIB broad-group cross sections were modules of the ENEA-Bologna 2007 Revision /19/ of the SCAMPI /18/ nuclear data processing system which was used on a Personal Computer (CPU INTEL Pentium III, 448 MB of RAM; f77 Absoft version 5.0 FORTRAN 77 compiler) with the Linux Red Hat 7.1 operating system. The names and a brief description of the primary SCAMPI modules used are given in TAB. 3.8.

The first part of the data processing procedure, dedicated to the generation of the BUGENDF70.BOLIB library, is given in FIG. 3.4 which diagrams the sequence of steps needed to select and self-shield specific sets of cross sections and to perform the BWR and PWR one-dimensional transport calculations addressed to obtain five neutron/photon flux weighting spectra, employed in the second part of the data processing procedure for a proper cross section collapsing.

Starting from the VITENDF70.BOLIB binary AMPX master library, it was necessary to perform one-dimensional transport calculations with the XSDRNPM module of SCAMPI, using proper fine-group working cross sections self-shielded with the BONAMI module, to obtain BWR- and PWR-specific neutron/photon flux weighting spectra to collapse the fine-group cross sections of the VITENDF70.BOLIB mother library. In particular, five different fine-group neutron/photon flux weighting spectra in the VITENDF70.BOLIB (or VITAMIN-B6 /8/) neutron and photon energy group structures were calculated (see also 3.3) with two XSDRNPM fixed source transport calculations simulating the simplified in-vessel and ex-vessel one-dimensional radial geometries and compositions at the reactor core midplanes, typical of the BWR and PWR models. The same fine-group neutron source spectrum data set was introduced in both BWR and PWR spectrum calculations in the 31** volumetric source spectra array of XSDRNPM. These data, taken from the BUGLE-96 library user's manual (see /8/, APPENDIX A, TAB. A.6 and TAB. A.7), are normalized to the unity. The XNF normalization factor numerical value, in the 5** array of XSDRNPM, permits respectively to obtain the BWR and the PWR total neutron source (XNF = 7.46419E+17 in the BWR case and XNF = 7.2676E+17 in the PWR case). The calculation of these BWR- and PWR-specific neutron/photon flux weighting spectra permitted the problem-dependent collapsing of the VITENDF70.BOLIB cross sections in the second part of the data processing procedure. The complete detailed listings of the 199 group values of the neutron flux weighting spectra is reported in TAB. 3.4 and graphically represented in FIG. 3.2 while the corresponding 42 group photon spectra are respectively inserted in TAB. 3.5 and shown in FIG. 3.3.

The second part of the data processing procedure is diagrammed in FIG. 3.5. The starting point of this sequence is represented by the AMPX master library of fine-group self-shielded cross sections, previously calculated during the first part of the data processing procedure. Then the MALOCS module was used to perform the collapsing of the self-shielded cross sections from the VITENDF70.BOLIB neutron and photon fine-group energy structures into the respective broad-group energy structures of the BUGENDF70.BOLIB (or BUGLE-96 /8/) library.

In particular the five neutron/photon flux weighting spectra, previously calculated with the XSDRNPM module in the first part of the data processing procedure, were used in the MALOCS module to obtain six cross section sets of self-shielded cross sections which were included in the BUGENDF70.BOLIB library.

The ANISN /4/ code methodology was selected in the MALOCS module for removal of the upscatter transfer matrix in the thermal energy range.
As reported in the BUGLE-96 library user's manual, removing upscatter is done for purposes of economy, since it eliminates the need to perform outer (source) iterations during flux convergence. However, removing the upscatter terms does require a non-physical adjustment to the cross sections, since in reality, low-energy neutrons can increase their kinetic energy by scattering off low-Z nuclei such as hydrogen. For most shielding problems, this is an acceptable approximation because the leading shielding issues are frequently dominated by the transport of higher-energy neutrons and an accurate transport of the thermal neutrons is relatively unimportant.
The approach used for removing the upscatter terms in BUGENDF70.BOLIB and BUGLE-96 is the same as implemented in the ANISN code. Conceptually, the upscatter between two groups is set to zero and the downscatter is reduced by an equivalent amount to preserve the net transfer reaction rate between the two groups. The within-group scatter terms of both groups are increased by a corresponding amount to preserve the total scatter reaction rate.
While this yields an acceptable solution in most circumstances, it can cause the generation of negative downscatter terms if the upscatter is greater than the downscatter between two groups. This highlights the importance of using a particular cross section set only for the type of application for which it was intended.

A final collapsing sequence within the second part of the data processing procedure is diagrammed in FIG. 3.6.

In particular, starting from the VITENDF70.BOLIB binary AMPX master library, a set of infinitely dilute cross sections at 300 °K, for the whole set of 183 materials contained in the VITENDF70.BOLIB fine-group library, were collapsed with the MALOCS module introducing in input the neutron/photon weighting spectrum for concrete, previously calculated during the first part of the data processing procedure. A set of infinitely dilute (not self-shielded) broad-group cross sections was generated and included in the BUGENDF70.BOLIB library. These data can be used for general purposes and for cases where the problem-specific self-shielded/weighted data sets are not appropriate.

In both the collapsing procedures, for self-shielded (see FIG. 3.5) and infinitely dilute (not self-shielded) (see FIG. 3.6) cross sections, the NITAWL and ALPO modules were used for format conversion, respectively from the AMPX master to the AMPX working format and from the AMPX working to the FIDO-ANISN /4/ format.

The complete BUGENDF70.BOLIB library actually contains three distinct types of data: 1) the infinitely dilute (not self-shielded) cross section set for all the 183 materials contained in the VITENDF70.BOLIB library, 2) six sets of self-shielded and energy weighted cross sections for nuclides specific to BWR and PWR models, and 3) a set of response functions and KERMA factors.

TAB. 3.8

Modules of the SCAMPI Nuclear Data Processing System (ENEA-Bologna 2007 Revision)
Used to Produce the BUGENDF70.BOLIB Library.

| Module | Function |
|---|---|
| AIM | Converts master libraries from binary-to-BCD (or vice-versa). |
| ALPO | Produces ANISN library from AMPX working library format. |
| AJAX | Merges and deletes nuclides from master libraries. |
| BONAMI | Performs interpolation on Bondarenko factors to self-shield reaction cross sections. |
| MALOCS | Collapses energy group structure of master library. |
| NITAWL | Converts master library to working library format. |
| XSDRNPM | Performs a one-dimensional discrete ordinates or diffusion theory calculation using cross sections in an AMPX working library. Performs spatial cross section weighting. |

FIG. 3.4 Procedure for Calculating BWR- and PWR-Specific Flux Spectra Using the VITENDF70.BOLIB Library.

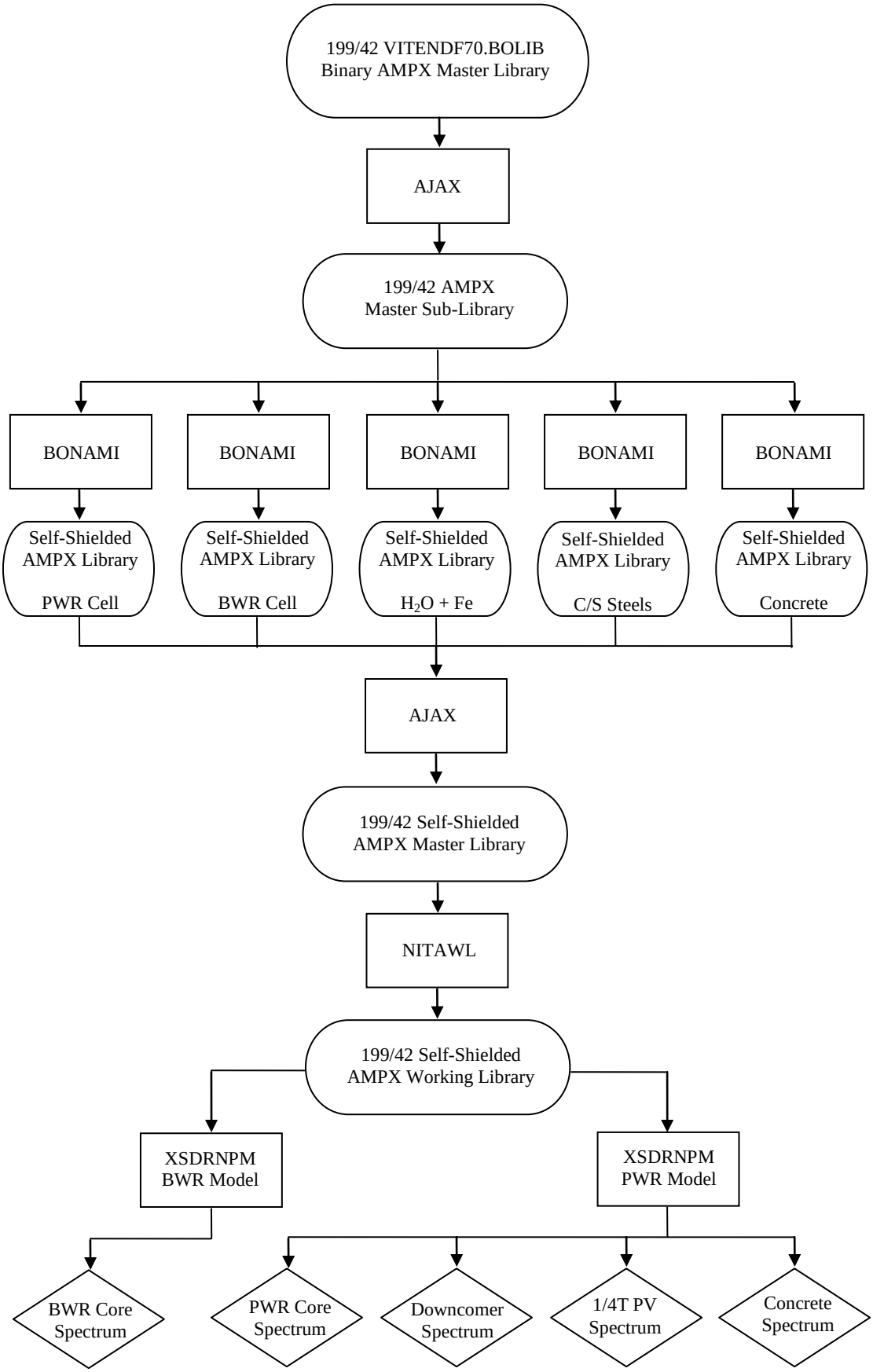

FIG. 3.5 Procedure for Generating the BUGENDF70.BOLIB Library Self-Shielded and Collapsed Cross Sections Using BWR- and PWR-Specific Flux Spectra.

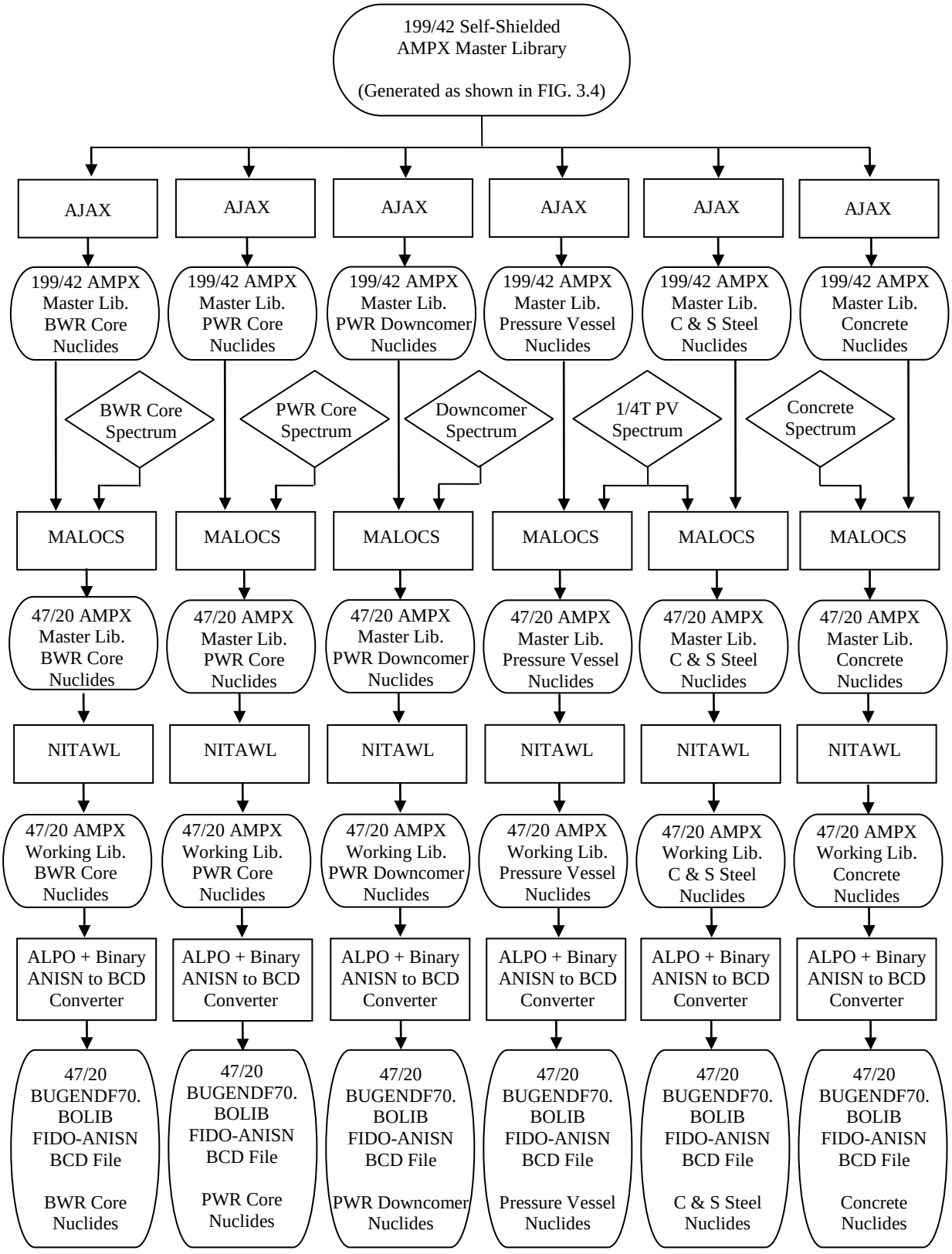

FIG. 3.6 Procedure for Generating the BUGENDF70.BOLIB Library Infinitely Dilute and Collapsed Cross Sections at 300 °K Using Concrete Flux Spectrum.

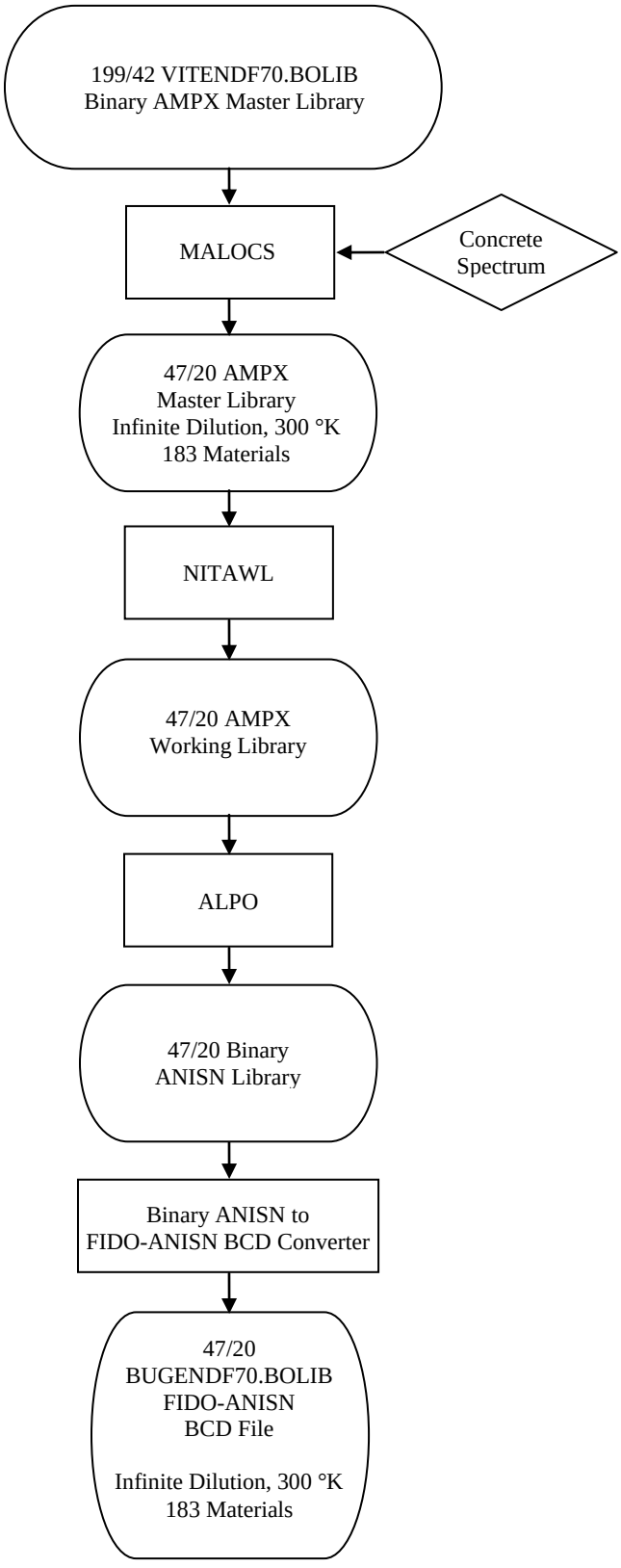

3.5 - Library Format and Content

The BUGENDF70.BOLIB library package consists of two major parts:

BUGENDF70.BOLIB - including the self-shielded and infinitely dilute cross section sets;

BUGENDF70T.BOLIB - including the same cross sections as BUGENDF70.BOLIB with the thermal neutron upscattering cross sections retained in the thermal neutron energy region below 5.0435 eV.

The BUGENDF70.BOLIB broad-group data library package is available in ANISN /4/ card image format for direct use, e.g., in the ORNL deterministic radiation transport codes ANISN (1D), DORT (2D) and TORT (3D) included in the DOORS /35/ system or in the ORNL Monte Carlo code MORSE (3D) /58/.

For BUGENDF70.BOLIB, the Carlson table width is 67 (total number of 47 neutron + 20 photon groups) and the table length is 70 (total number of groups plus 3). For BUGENDF70T.BOLIB, the Carlson table width is 67 (total number of groups) and the table length is 74 (total number of groups plus 3 plus 4 upscatter groups).

In the BUGENDF70.BOLIB library, the cross section table positions 1 through 4 are defined as:

1. absorption cross section ($\sigma_a$);
2. fission cross section times the number of neutrons produced per fission ($\nu\sigma_f$);
3. total cross section ($\sigma_t$);
4. within-group scattering cross section ($\sigma_{g\rightarrow g}$).

These positions are followed by the standard downscatter transfer matrix. As mentioned in 3.4, the upscatter transfer matrix was removed using the ANISN methodology option in the MALOCS module of the ENEA-Bologna 2007 Revision /19/ of the SCAMPI /18/ system for the BUGENDF70.BOLIB library.
In the case of the BUGENDF70T.BOLIB library, the upscatter cross sections for the four lower energy neutron groups in each cross section matrix occupy the cross section table positions from 4 to 7 and consequently, in this case, the within-group scattering cross section ($\sigma_{g\rightarrow g}$) takes up the position 8.

Each cross section matrix (67×70 cross section data in BUGENDF70.BOLIB without upscatter and 67×74 in BUGENDF70T.BOLIB with upscatter) is preceded by a title card containing four integer parameters and an alpha/numeric descriptor. The integer parameters (4I6 format) include: 1) the number of columns in the cross section table (total number of energy groups), 2) the number of rows in the table (normally equals the number of columns plus 3), 3) a control code which is generally not used and 4) a unique identification (ANISN identifier or ANISN-ID) number. The 36-character descriptor field (36H format) can contain any pertinent information, but usually includes the order of the Legendre polynomial ($P_\ell$) expansion of the scattering cross section matrix, the specific isotope or element and special processing treatments such as self-shielding or energy weighting in the specific BWR or PWR spatial region.

On the first step, the collapsing procedure outlined in FIG. 3.5 generated the self-shielded cross sections without thermal upscattering data for the BUGENDF70.BOLIB library. The collapsing procedure was then repeated for the six MALOCS cases to produce self-shielded cross sections with upscattering data. On this second step a new library with upscattering data, designated as BUGENDF70T.BOLIB, was created.

The difference between the production of the collapsed data for BUGENDF70.BOLIB and BUGENDF70T.BOLIB depends on a single parameter (IOPT7) of the 3$$ array in the MALOCS module input: IOPT7=0 (no upscatter) for BUGENDF70.BOLIB or IOPT7=2 (with upscatter, according to the "ANISN" scheme) for BUGENDF70T.BOLIB.

Listings of the library contents for BUGENDF70.BOLIB are given in the TABs. 3.9 and 3.10. TAB. 3.9 lists all the 183 materials included in the "standard weighted" library, i.e. the collection of materials which were processed as infinitely dilute and collapsed using the neutron and photon flux spectra for concrete. TAB. 3.10 lists the "special weighted" library, i.e. the collection of materials which were processed with specific self-shielding compositions and collapsed using the BWR and PWR neutron and photon flux spectra. As in the case of the corresponding BUGLE-96 special weighted library, the self-shielded cross sections of the carbon steel constituents in the "Carbon & Stainless Steel" cross section set are the same as those included in the pressure vessel cross section set, designated as "PWR 1/4 T in Pressure Vessel".
In both TABs. 3.9 and 3.10, the range of the ANISN identifiers (ANISN-IDs) for each nuclide are for the $P_0$ through $P_L$ components, where L=ℓ-max is either 5 or 7 (see 3.2).

TAB. 3.9

Nuclides in the BUGENDF70.BOLIB Library which are Infinitely Dilute and Weighted with a Concrete Flux Spectrum.

| Entry | Nuclide | ANISN-ID | Entry | Nuclide | ANISN-ID |
|---|---|---|---|---|---|
| 1 | Ag-107 | 1-6 | 49 | Er-162 | 333-338 |
| 2 | Ag-109 | 7-12 | 50 | Er-164 | 339-344 |
| 3 | Al-27 | 13-20 | 51 | Er-166 | 345-350 |
| 4 | Am-241 | 21-26 | 52 | Er-167 | 351-356 |
| 5 | Am-242 | 27-32 | 53 | Er-168 | 357-362 |
| 6 | Am-242m | 33-38 | 54 | Er-170 | 363-368 |
| 7 | Am-243 | 39-44 | 55 | Eu-151 | 369-374 |
| 8 | Au-197 | 45-50 | 56 | Eu-152 | 375-380 |
| 9 | B-10 | 51-58 | 57 | Eu-153 | 381-386 |
| 10 | B-11 | 59-66 | 58 | Eu-154 | 387-392 |
| 11 | Ba-138 | 67-72 | 59 | Eu-155 | 393-398 |
| 12 | Be-9 | 73-80 | 60 | F-19 | 399-406 |
| 13 | Be-9 (Thermal) | 81-88 | 61 | Fe-54 | 407-414 |
| 14 | Bi-209 | 89-94 | 62 | Fe-56 | 415-422 |
| 15 | C-nat | 95-102 | 63 | Fe-57 | 423-430 |
| 16 | C-nat(Graphite) | 103-110 | 64 | Fe-58 | 431-438 |
| 17 | Ca-40 | 111-118 | 65 | Ga-69 | 439-444 |
| 18 | Ca-42 | 119-126 | 66 | Ga-71 | 445-450 |
| 19 | Ca-43 | 127-134 | 67 | Gd-152 | 451-456 |
| 20 | Ca-44 | 135-142 | 68 | Gd-154 | 457-462 |
| 21 | Ca-46 | 143-150 | 69 | Gd-155 | 463-468 |
| 22 | Ca-48 | 151-158 | 70 | Gd-156 | 469-474 |
| 23 | Cd-106 | 159-164 | 71 | Gd-157 | 475-480 |
| 24 | Cd-108 | 165-170 | 72 | Gd-158 | 481-486 |
| 25 | Cd-110 | 171-176 | 73 | Gd-160 | 487-492 |
| 26 | Cd-111 | 177-182 | 74 | H-1($H_2O$) | 493-500 |
| 27 | Cd-112 | 183-188 | 75 | H-1($CH_2$) | 501-508 |
| 28 | Cd-113 | 189-194 | 76 | H-1(ZrH) | 509-516 |
| 29 | Cd-114 | 195-200 | 77 | H-2($D_2O$) | 517-524 |
| 30 | Cd-115m | 201-206 | 78 | H-3 | 525-532 |
| 31 | Cd-116 | 207-212 | 79 | He-3 | 533-540 |
| 32 | Cl-35 | 213-220 | 80 | He-4 | 541-548 |
| 33 | Cl-37 | 221-228 | 81 | Hf-174 | 549-554 |
| 34 | Cm-241 | 229-234 | 82 | Hf-176 | 555-560 |
| 35 | Cm-242 | 235-240 | 83 | Hf-177 | 561-566 |
| 36 | Cm-243 | 241-246 | 84 | Hf-178 | 567-572 |
| 37 | Cm-244 | 247-252 | 85 | Hf-179 | 573-578 |
| 38 | Cm-245 | 253-258 | 86 | Hf-180 | 579-584 |
| 39 | Cm-246 | 259-264 | 87 | In-113 | 585-590 |
| 40 | Cm-247 | 265-270 | 88 | In-115 | 591-596 |
| 41 | Cm-248 | 271-276 | 89 | K-39 | 597-604 |
| 42 | Co-59 | 277-284 | 90 | K-40 | 605-612 |
| 43 | Cr-50 | 285-292 | 91 | K-41 | 613-620 |
| 44 | Cr-52 | 293-300 | 92 | Li-6 | 621-628 |
| 45 | Cr-53 | 301-308 | 93 | Li-7 | 629-636 |
| 46 | Cr-54 | 309-316 | 94 | Mg-24 | 637-644 |
| 47 | Cu-63 | 317-324 | 95 | Mg-25 | 645-652 |
| 48 | Cu-65 | 325-332 | 96 | Mg-26 | 653-660 |

TAB. 3.9 Continued

Nuclides in the BUGENDF70.BOLIB Library which are Infinitely Dilute and Weighted with a Concrete Flux Spectrum.

| Entry | Nuclide | ANISN-ID | Entry | Nuclide | ANISN-ID |
|---|---|---|---|---|---|
| 97 | Mn-55 | 661-668 | 141 | Si-28 | 957-964 |
| 98 | Mo-92 | 669-674 | 142 | Si-29 | 965-972 |
| 99 | Mo-94 | 675-680 | 143 | Si-30 | 973-980 |
| 100 | Mo-95 | 681-686 | 144 | Sn-112 | 981-986 |
| 101 | Mo-96 | 687-692 | 145 | Sn-114 | 987-992 |
| 102 | Mo-97 | 693-698 | 146 | Sn-115 | 993-998 |
| 103 | Mo-98 | 699-704 | 147 | Sn-116 | 999-1004 |
| 104 | Mo-100 | 705-710 | 148 | Sn-117 | 1005-1010 |
| 105 | N-14 | 711-718 | 149 | Sn-118 | 1011-1016 |
| 106 | N-15 | 719-726 | 150 | Sn-119 | 1017-1022 |
| 107 | Na-23 | 727-734 | 151 | Sn-120 | 1023-1028 |
| 108 | Nb-93 | 735-740 | 152 | Sn-122 | 1029-1034 |
| 109 | Ni-58 | 741-748 | 153 | Sn-123 | 1035-1040 |
| 110 | Ni-60 | 749-756 | 154 | Sn-124 | 1041-1046 |
| 111 | Ni-61 | 757-764 | 155 | Sn-125 | 1047-1052 |
| 112 | Ni-62 | 765-772 | 156 | Sn-126 | 1053-1058 |
| 113 | Ni-64 | 773-780 | 157 | Ta-181 | 1059-1064 |
| 114 | Np-237 | 781-786 | 158 | Ta-182 | 1065-1070 |
| 115 | Np-238 | 787-792 | 159 | Th-230 | 1071-1076 |
| 116 | Np-239 | 793-798 | 160 | Th-232 | 1077-1082 |
| 117 | O-16 | 799-806 | 161 | Ti-46 | 1083-1090 |
| 118 | O-17 | 807-814 | 162 | Ti-47 | 1091-1098 |
| 119 | P-31 | 815-822 | 163 | Ti-48 | 1099-1106 |
| 120 | Pa-231 | 823-828 | 164 | Ti-49 | 1107-1114 |
| 121 | Pa-233 | 829-834 | 165 | Ti-50 | 1115-1122 |
| 122 | Pb-204 | 835-840 | 166 | U-232 | 1123-1128 |
| 123 | Pb-206 | 841-846 | 167 | U-233 | 1129-1134 |
| 124 | Pb-207 | 847-852 | 168 | U-234 | 1135-1140 |
| 125 | Pb-208 | 853-858 | 169 | U-235 | 1141-1146 |
| 126 | Pu-236 | 859-864 | 170 | U-236 | 1147-1152 |
| 127 | Pu-237 | 865-870 | 171 | U-237 | 1153-1158 |
| 128 | Pu-238 | 871-876 | 172 | U-238 | 1159-1164 |
| 129 | Pu-239 | 877-882 | 173 | V | 1165-1172 |
| 130 | Pu-240 | 883-888 | 174 | W-182 | 1173-1178 |
| 131 | Pu-241 | 889-894 | 175 | W-183 | 1179-1184 |
| 132 | Pu-242 | 895-900 | 176 | W-184 | 1185-1190 |
| 133 | Pu-243 | 901-906 | 177 | W-186 | 1191-1196 |
| 134 | Pu-244 | 907-912 | 178 | Y-89 | 1197-1202 |
| 135 | Re-185 | 913-918 | 179 | Zr-90 | 1203-1208 |
| 136 | Re-187 | 919-924 | 180 | Zr-91 | 1209-1214 |
| 137 | S-32 | 925-932 | 181 | Zr-92 | 1215-1220 |
| 138 | S-33 | 933-940 | 182 | Zr-94 | 1221-1226 |
| 139 | S-34 | 941-948 | 183 | Zr-96 | 1227-1232 |
| 140 | S-36 | 949-956 | | | |

TAB. 3.10

Nuclides in the BUGENDF70.BOLIB Library which are Self-Shielded and Weighted with BWR- and PWR-Specific Flux Spectra.

| Nuclide | ANISN-ID | Description |
|---|---|---|
| B-10 | 2001-2008 | PWR Core Coolant |
| Cr-50 | 2009-2016 | PWR Core Clad |
| Cr-52 | 2017-2024 | PWR Core Clad |
| Cr-53 | 2025-2032 | PWR Core Clad |
| Cr-54 | 2033-2040 | PWR Core Clad |
| Fe-54 | 2041-2048 | PWR Core Clad |
| Fe-56 | 2049-2056 | PWR Core Clad |
| Fe-57 | 2057-2064 | PWR Core Clad |
| Fe-58 | 2065-2072 | PWR Core Clad |
| H-1($H_2O$) | 2073-2080 | PWR Core Coolant |
| Ni-58 | 2081-2088 | PWR Core Clad |
| Ni-60 | 2089-2096 | PWR Core Clad |
| Ni-61 | 2097-2104 | PWR Core Clad |
| Ni-62 | 2105-2112 | PWR Core Clad |
| Ni-64 | 2113-2120 | PWR Core Clad |
| O-16 | 2121-2128 | PWR Core Coolant |
| O-16 | 2129-2136 | PWR Core Fuel |
| U-235 | 2137-2142 | PWR Core Fuel |
| U-238 | 2143-2148 | PWR Core Fuel |
| Zr-90 | 2149-2154 | PWR Core Clad |
| Zr-91 | 2155-2160 | PWR Core Clad |
| Zr-92 | 2161-2166 | PWR Core Clad |
| Zr-94 | 2167-2172 | PWR Core Clad |
| Zr-96 | 2173-2178 | PWR Core Clad |
| | | |
| H-1($H_2O$) | 3001-3008 | PWR Downcomer |
| O-16 | 3009-3016 | PWR Downcomer |
| C-nat | 3017-3024 | PWR Downcomer |
| Cr-50 | 3025-3032 | PWR Downcomer |
| Cr-52 | 3033-3040 | PWR Downcomer |
| Cr-53 | 3041-3048 | PWR Downcomer |
| Cr-54 | 3049-3056 | PWR Downcomer |
| Fe-54 | 3057-3064 | PWR Downcomer |
| Fe-56 | 3065-3072 | PWR Downcomer |
| Fe-57 | 3073-3080 | PWR Downcomer |
| Fe-58 | 3081-3088 | PWR Downcomer |
| Mn-55 | 3089-3096 | PWR Downcomer |
| Ni-58 | 3097-3104 | PWR Downcomer |
| Ni-60 | 3105-3112 | PWR Downcomer |
| Ni-61 | 3113-3120 | PWR Downcomer |
| Ni-62 | 3121-3128 | PWR Downcomer |
| Ni-64 | 3129-3136 | PWR Downcomer |

TAB. 3.10 Continued

Nuclides in the BUGENDF70.BOLIB Library which are Self-Shielded and Weighted with BWR- and PWR-Specific Flux Spectra.

| Nuclide | ANISN-ID | Description |
|---|---|---|
| C-nat | 4001-4008 | PWR 1/4 T in Pressure Vessel |
| Cr-50 | 4009-4016 | PWR 1/4 T in Pressure Vessel |
| Cr-52 | 4017-4024 | PWR 1/4 T in Pressure Vessel |
| Cr-53 | 4025-4032 | PWR 1/4 T in Pressure Vessel |
| Cr-54 | 4033-4040 | PWR 1/4 T in Pressure Vessel |
| Fe-54 | 4041-4048 | PWR 1/4 T in Pressure Vessel |
| Fe-56 | 4049-4056 | PWR 1/4 T in Pressure Vessel |
| Fe-57 | 4057-4064 | PWR 1/4 T in Pressure Vessel |
| Fe-58 | 4065-4072 | PWR 1/4 T in Pressure Vessel |
| Mn-55 | 4073-4080 | PWR 1/4 T in Pressure Vessel |
| Ni-58 | 4081-4088 | PWR 1/4 T in Pressure Vessel |
| Ni-60 | 4089-4096 | PWR 1/4 T in Pressure Vessel |
| Ni-61 | 4097-4104 | PWR 1/4 T in Pressure Vessel |
| Ni-62 | 4105-4112 | PWR 1/4 T in Pressure Vessel |
| Ni-64 | 4113-4120 | PWR 1/4 T in Pressure Vessel |
| Al-27 | 5001-5008 | Concrete Type 04 |
| C-nat | 5009-5016 | Concrete Type 04 |
| Ca-40 | 5017-5024 | Concrete Type 04 |
| Ca-42 | 5025-5032 | Concrete Type 04 |
| Ca-43 | 5033-5040 | Concrete Type 04 |
| Ca-44 | 5041-5048 | Concrete Type 04 |
| Ca-46 | 5049-5056 | Concrete Type 04 |
| Ca-48 | 5057-5064 | Concrete Type 04 |
| Fe-54 | 5065-5072 | Concrete Type 04 |
| Fe-56 | 5073-5080 | Concrete Type 04 |
| Fe-57 | 5081-5088 | Concrete Type 04 |
| Fe-58 | 5089-5096 | Concrete Type 04 |
| H-1($H_2O$) | 5097-5104 | Concrete Type 04 |
| K-39 | 5105-5112 | Concrete Type 04 |
| K-40 | 5113-5120 | Concrete Type 04 |
| K-41 | 5121-5128 | Concrete Type 04 |
| Mg-24 | 5129-5136 | Concrete Type 04 |
| Mg-25 | 5137-5144 | Concrete Type 04 |
| Mg-26 | 5145-5152 | Concrete Type 04 |
| Na-23 | 5153-5160 | Concrete Type 04 |
| O-16 | 5161-5168 | Concrete Type 04 |
| Si-28 | 5169-5176 | Concrete Type 04 |
| Si-29 | 5177-5184 | Concrete Type 04 |
| Si-30 | 5185-5192 | Concrete Type 04 |

TAB. 3.10 Continued

Nuclides in the BUGENDF70.BOLIB Library which are Self-Shielded and Weighted with BWR- and PWR-Specific Flux Spectra.

| Nuclide | ANISN-ID | Description |
|---|---|---|
| C-nat | 6001-6008 | Carbon Steel |
| C-nat | 6009-6016 | Stainless Steel |
| Cr-50 | 6017-6024 | Carbon Steel |
| Cr-50 | 6025-6032 | Stainless Steel |
| Cr-52 | 6033-6040 | Carbon Steel |
| Cr-52 | 6041-6048 | Stainless Steel |
| Cr-53 | 6049-6056 | Carbon Steel |
| Cr-53 | 6057-6064 | Stainless Steel |
| Cr-54 | 6065-6072 | Carbon Steel |
| Cr-54 | 6073-6080 | Stainless Steel |
| Fe-54 | 6081-6088 | Carbon Steel |
| Fe-54 | 6089-6096 | Stainless Steel |
| Fe-56 | 6097-6104 | Carbon Steel |
| Fe-56 | 6105-6112 | Stainless Steel |
| Fe-57 | 6113-6120 | Carbon Steel |
| Fe-57 | 6121-6128 | Stainless Steel |
| Fe-58 | 6129-6136 | Carbon Steel |
| Fe-58 | 6137-6144 | Stainless Steel |
| Mn-55 | 6145-6152 | Carbon Steel |
| Mn-55 | 6153-6160 | Stainless Steel |
| Ni-58 | 6161-6168 | Carbon Steel |
| Ni-58 | 6169-6176 | Stainless Steel |
| Ni-60 | 6177-6184 | Carbon Steel |
| Ni-60 | 6185-6192 | Stainless Steel |
| Ni-61 | 6193-6200 | Carbon Steel |
| Ni-61 | 6201-6208 | Stainless Steel |
| Ni-62 | 6209-6216 | Carbon Steel |
| Ni-62 | 6217-6224 | Stainless Steel |
| Ni-64 | 6225-6232 | Carbon Steel |
| Ni-64 | 6233-6240 | Stainless Steel |
| Fe-54 | 7001-7008 | BWR Core Clad |
| Fe-56 | 7009-7016 | BWR Core Clad |
| Fe-57 | 7017-7024 | BWR Core Clad |
| Fe-58 | 7025-7032 | BWR Core Clad |
| H-1($H_2O$) | 7033-7040 | BWR Core Coolant |
| O-16 | 7041-7048 | BWR Core Coolant |
| O-16 | 7049-7056 | BWR Core Fuel |
| U-235 | 7057-7062 | BWR Core Fuel |
| U-238 | 7063-7068 | BWR Core Fuel |
| Zr-90 | 7069-7074 | BWR Core Clad |
| Zr-91 | 7075-7080 | BWR Core Clad |
| Zr-92 | 7081-7086 | BWR Core Clad |
| Zr-94 | 7087-7092 | BWR Core Clad |
| Zr-96 | 7093-7098 | BWR Core Clad |

3.6 - Response Functions

The package of the BUGENDF70.BOLIB library contains many response functions in the neutron and photon energy group structures of the library. Following the designation adopted also in the BUGLE-96 /8/ library package, it is underlined that, for the sake of simplicity, the term "response functions" is intended here not only for the group dosimeter cross sections or the group KERMA factors available in the package, which can be properly considered in a strict physical sense as "response functions". This denomination is in fact also extended to the group total neutron fission spectra and to the group total neutrons per fission as well as to useful general neutron data as, for example, the neutron group energy boundaries, the midpoint values of the energy groups, etc.. In particular the following four types of broad-group response functions are included in the package.

1. General neutron response functions in the BUGENDF70.BOLIB 47 neutron energy group structure (see TAB. 3.11): group energy boundaries, group energy intervals (widths), group lethargy intervals (widths), midpoint values of the energy groups (E-mid), square-roots of the E-mid values and, finally, the multiplicative factors of the group neutron fluxes to obtain the total neutron flux, the neutron fluxes above 1.0 MeV and 0.1 MeV and the neutron flux below 0.414 eV.

2. Neutron fission spectra ($\chi$) in the BUGENDF70.BOLIB 47 neutron energy group structure are included (see TAB. 3.11) for only 34 fissionable nuclides since the neutron fission spectrum of Am-242 cannot be calculated because MF=4, MT=18 is missing in the corresponding ENDF/B-VII.0 evaluated data file. For each fissionable nuclide, when the delayed component (MF=5, MT=455) of the neutron fission spectrum is available in the corresponding evaluated data file, the total (prompt + delayed) neutron fission spectrum is included, otherwise only the prompt component is given.
   Total (prompt + delayed) neutrons per fission ($\nu$) in the BUGENDF70.BOLIB 47 neutron energy group structure are included for 35 fissionable nuclides (see TAB. 3.12).

3. Dosimetry cross sections for 71 nuclear reactions, processed (see /55/) from the IAEA International Reactor Dosimetry File /54/ (IRDF-2002) in the BUGENDF70.BOLIB 47 neutron energy group structure.

4. Total neutron and photon KERMA factors for 183 materials (all the materials available in the library) in the BUGENDF70.BOLIB 47 neutron and 20 photon energy group structures (see respectively TAB. 3.1 and TAB. 3.2).

The list of the available general neutron response functions is reported in TAB. 3.11 together with the list of the fissionable nuclides for which the neutron fission spectra are included in the package.

Concerning the total neutron fission spectra, it is underlined that the ENEA-Bologna 2007 Revision /19/ of the SCAMPI /18/ nuclear data processing system permitted to process (see the procedure described in 2.8) delayed neutron fission spectra to obtain the total (prompt + delayed) neutron fission spectra ($\chi$) in the VITENDF70.BOLIB /5/ 199 neutron fine-group energy structure (see TAB. 2.4).

The normalized fine-group (total or prompt) neutron fission spectra ($\chi$) were calculated with the procedure described in 2.8, using the BONAMI, NITAWL and ICE modules. For example, a 199 group graphical representation of the U-235, U-238 and Pu-239 total neutron fission spectra is shown in FIG. 2.5 while the total neutron fission spectrum fine-group $\chi$ values for U-235, U-238 and Pu-239 are listed in TAB. 2.10.
Then the fine-group $\chi$ values were summed up to obtain the corresponding broad-group $\chi$ value and this operation was obviously repeated for each broad-group.
In this procedure the small contribution of the first fine-group between 17.332 MeV and 19.640 MeV (see TAB. 2.4 and TAB. 3.1) was neglected and so a new normalization to one neutron per fission of the broad-group $\chi$ values was needed.
It is worth of note that the fissionable nuclides included in the BUGLE-96 library contain only the prompt neutron fission spectrum. Differently from the previous case, the total neutron fission spectrum was obtained for all the fissionable nuclides included in the BUGENDF70.BOLIB library which have both prompt and delayed neutron fission spectra in the corresponding ENDF/B-VII.0 evaluated data files.

Total (prompt + delayed) neutrons per fission ($\nu$) data are available for the 35 fissionable nuclides (TAB. 3.12) included in the BUGENDF70.BOLIB library. These data were obtained through collapsing of the corresponding data contained in the VITENDF70.BOLIB library, processed at the infinite dilution background cross section and at the temperature of 300 °K. The data collapsing was performed with the MALOCS module of the ENEA-Bologna Revision 2007 of the SCAMPI nuclear data processing system, using alternatively the "flat weighting" neutron spectrum and the "1/4 T PV weighting" neutron spectrum.

The whole set of point-wise dosimetry cross sections for 71 nuclear reactions (see TAB. 3.13), included in IRDF-2002, was processed through the GROUPIE program of the PREPRO 2007 /64/ nuclear data processing system into the BUGENDF70.BOLIB 47 neutron energy group structure.

The KERMA factors for neutrons and photons were originally generated respectively with the HEATR and GAMINR modules of the NJOY-99.259 /17/ system in the VITENDF70.BOLIB neutron and photon fine-group energy structures with 199 neutron groups and 42 photon groups. These data, contained in the VITENDF70.BOLIB library and processed at the infinite dilution background cross section and at the temperature of 300 °K, were then collapsed with the MALOCS module of the ENEA-Bologna 2007 Revision /19/ of the SCAMPI /18/ system, into the 47 neutron and 20 photon broad-group energy structures of the BUGENDF70.BOLIB library.
The neutron and photon weighting spectra for concrete (see respectively TAB. 3.4 and TAB. 3.5), calculated in a PWR biological shield, were used to perform the collapsing of the neutron and photon KERMA factors.
The neutron KERMA factors were obtained for all the 183 nuclides (see TAB. 3.14) contained in the VITENDF70.BOLIB library (see TAB. 2.1) and in the infinite dilution cross section set of the BUGENDF70.BOLIB library (see TAB. 3.9).
In TAB. 3.14, 15 nuclides (labelled with *) with negative group values of the neutron KERMA factors and 56 nuclides (labelled with #) without photon production data (see also TAB. 2.1) are indicated. If the processed files of ENDF/B-VII.0 nuclides presented one or more negative neutron KERMA factor group values, all the corresponding 47 neutron

KERMA factor group values were set to zero, following the same procedure adopted for the BUGLE-96 library.
Anyway, the generation of negative group values for the neutron KERMA factors of the 15 previously cited isotopes is almost certainly due to problems in the corresponding ENDF/B-VII.0 evaluated data files rather than in their data processing.
Moreover it is important to note that, in total reactor power and heating calculations, the results can be heavily affected by the lack of photon production data in some important ENDF/B-VII.0 evaluated data files. Concerning this, it is recommended to check carefully if the ENDF/B-VII.0 data files of the nuclides involved in the specific calculations include photon production data, as it is easily possible to verify in TAB. 3.14.
The elements for which the photon KERMA factors are available are listed in TAB. 3.15: the photon KERMA factors are the same for all the isotopes of each element.

TAB. 3.11

Response Functions Included with BUGENDF70.BOLIB.
General Neutron Responses and Total (Prompt + Delayed) Neutron Fission Spectra (χ).

| | General Neutron Response | | General Neutron Response |
|---|---|---|---|
| 1 | Group upper energy [MeV] | 6 | Total neutron flux |
| 2 | Group energy width [MeV] | 7 | E > 1.0 MeV neutron flux |
| 3 | Group lethargy width | 8 | E > 0.1 MeV neutron flux |
| 4 | Midpoint energy (E-mid) [MeV] | 9 | E < 0.414 eV neutron flux |
| 5 | Square-root (E-mid) [$MeV^{1/2}$] | | |

| | Total Fission Spectrum (χ) | | Total Fission Spectrum (χ) |
|---|---|---|---|
| 1 | Th-230 Fission spectrum (χ)* | 19 | Pu-240 Fission spectrum (χ) |
| 2 | Th-232 Fission spectrum (χ) | 20 | Pu-241 Fission spectrum (χ) |
| 3 | Pa-231 Fission spectrum (χ) | 21 | Pu-242 Fission spectrum (χ) |
| 4 | Pa-233 Fission spectrum (χ) | 22 | Pu-243 Fission spectrum (χ)* |
| 5 | U-232 Fission spectrum (χ)* | 23 | Pu-244 Fission spectrum (χ)* |
| 6 | U-233 Fission spectrum (χ) | 24 | Am-241 Fission spectrum (χ) |
| 7 | U-234 Fission spectrum (χ) | 25 | Am-242 Fission spectrum (χ)# |
| 8 | U-235 Fission spectrum (χ) | 26 | Am-242m Fission spectrum (χ)* |
| 9 | U-236 Fission spectrum (χ) | 27 | Am-243 Fission spectrum (χ) |
| 10 | U-237 Fission spectrum (χ) | 28 | Cm-241 Fission spectrum (χ)* |
| 11 | U-238 Fission spectrum (χ) | 29 | Cm-242 Fission spectrum (χ) |
| 12 | Np-237 Fission spectrum (χ) | 30 | Cm-243 Fission spectrum (χ)* |
| 13 | Np-238 Fission spectrum (χ)* | 31 | Cm-244 Fission spectrum (χ)* |
| 14 | Np-239 Fission spectrum (χ)* | 32 | Cm-245 Fission spectrum (χ) |
| 15 | Pu-236 Fission spectrum (χ)* | 33 | Cm-246 Fission spectrum (χ)* |
| 16 | Pu-237 Fission spectrum (χ)* | 34 | Cm-247 Fission spectrum (χ)* |
| 17 | Pu-238 Fission spectrum (χ) | 35 | Cm-248 Fission spectrum (χ)* |
| 18 | Pu-239 Fission spectrum (χ) | | |

(*) The neutron fission spectrum contains only the prompt component because the delayed component (MF=5, MT=455) is not available in the corresponding ENDF/B-VII.0 evaluated data file.
(#) The neutron fission spectrum of Am-242 cannot be calculated by NJOY because MF=4, MT=18 is missing in the corresponding ENDF/B-VII.0 evaluated data file.

TAB. 3.12

Response Functions Included with BUGENDF70.BOLIB.
Total (Prompt + Delayed) Neutrons per Fission (ν) Collapsed Using
Flat Weighting and 1/4 T PV Weighting.

| Neutrons per Fission (ν) | | Neutrons per Fission (ν) | |
|---|---|---|---|
| 1 | Th-230 Neutrons per fission (ν) | 19 | Pu-240 Neutrons per fission (ν) |
| 2 | Th-232 Neutrons per fission (ν) | 20 | Pu-241 Neutrons per fission (ν) |
| 3 | Pa-231 Neutrons per fission (ν) | 21 | Pu-242 Neutrons per fission (ν) |
| 4 | Pa-233 Neutrons per fission (ν) | 22 | Pu-243 Neutrons per fission (ν) |
| 5 | U-232 Neutrons per fission (ν) | 23 | Pu-244 Neutrons per fission (ν) |
| 6 | U-233 Neutrons per fission (ν) | 24 | Am-241 Neutrons per fission (ν) |
| 7 | U-234 Neutrons per fission (ν) | 25 | Am-242 Neutrons per fission (ν) |
| 8 | U-235 Neutrons per fission (ν) | 26 | Am-242m Neutrons per fission (ν) |
| 9 | U-236 Neutrons per fission (ν) | 27 | Am-243 Neutrons per fission (ν) |
| 10 | U-237 Neutrons per fission (ν) | 28 | Cm-241 Neutrons per fission (ν) |
| 11 | U-238 Neutrons per fission (ν) | 29 | Cm-242 Neutrons per fission (ν) |
| 12 | Np-237 Neutrons per fission (ν) | 30 | Cm-243 Neutrons per fission (ν) |
| 13 | Np-238 Neutrons per fission (ν) | 31 | Cm-244 Neutrons per fission (ν) |
| 14 | Np-239 Neutrons per fission (ν) | 32 | Cm-245 Neutrons per fission (ν) |
| 15 | Pu-236 Neutrons per fission (ν) | 33 | Cm-246 Neutrons per fission (ν) |
| 16 | Pu-237 Neutrons per fission (ν) | 34 | Cm-247 Neutrons per fission (ν) |
| 17 | Pu-238 Neutrons per fission (ν) | 35 | Cm-248 Neutrons per fission (ν) |
| 18 | Pu-239 Neutrons per fission (ν) | | |

TAB. 3.13

Response Functions Included with BUGENDF70.BOLIB.
IRDF-2002 Neutron Dosimeter Cross Sections [barns] Collapsed Using
Flat Weighting and 1/4 T PV Weighting.

| | Dosimeter | | Dosimeter |
|---|---|---|---|
| 1 | Li-6 (n,t) | 37 | Zn-64 (n,p) |
| 2 | B-10 (n,α) | 38 | As-75 (n,2n) |
| 3 | F-19 (n,2n) | 39 | Y-89 (n,2n) |
| 4 | Na-23 (n,γ) | 40 | Zr-90 (n,2n) |
| 5 | Na-23 (n,2n) | 41 | Nb-93 (n,2n) |
| 6 | Mg-24 (n,p) | 42 | Nb-93 (n,n') |
| 7 | Al-27 (n,p) | 43 | Nb-93 (n,γ) |
| 8 | Al-27 (n,α) | 44 | Rh-103 (n,n') |
| 9 | P-31 (n,p) | 45 | Ag-109 (n,γ) |
| 10 | S-32 (n,p) | 46 | In-115 (n,2n) |
| 11 | Sc-45 (n,γ) | 47 | In-115 (n,n') |
| 12 | Ti-46 (n,2n) | 48 | In-115 (n,γ) |
| 13 | Ti-46 (n,p) | 49 | I-127 (n,2n) |
| 14 | Ti-47 (n,x) | 50 | La-139 (n,γ) |
| 15 | Ti-47 (n,p) | 51 | Pr-141 (n,2n) |
| 16 | Ti-48 (n,x) | 52 | Tm-169 (n,2n) |
| 17 | Ti-48 (n,p) | 53 | Ta-181 (n,γ) |
| 18 | Ti-49 (n,x) | 54 | W-186 (n,γ) |
| 19 | V-51 (n,α) | 55 | Au-197 (n,2n) |
| 20 | Cr-52 (n,2n) | 56 | Au-197 (n,γ) |
| 21 | Mn-55 (n,γ) | 57 | Hg-199 (n,n') |
| 22 | Fe-54 (n,2n) | 58 | Pb-204 (n,n') |
| 23 | Fe-54 (n,α) | 59 | Th-232 (n,γ) |
| 24 | Fe-54 (n,p) | 60 | Th-232 (n,f) |
| 25 | Fe-56 (n,p) | 61 | U-235 (n,f) |
| 26 | Fe-58 (n,γ) | 62 | U-238 (n,f) |
| 27 | Co-59 (n,2n) | 63 | U-238 (n,γ) |
| 28 | Co-59 (n,α) | 64 | Np-237 (n,f) |
| 29 | Co-59 (n,γ) | 65 | Pu-239 (n,f) |
| 30 | Ni-58 (n,2n) | 66 | Am-241 (n,f) |
| 31 | Ni-58 (n,p) | 67 | B-nat (n,disap) |
| 32 | Ni-60 (n,p) | 68 | B-nat (n,γ) |
| 33 | Cu-63 (n,2n) | 69 | B-nat (n,α) |
| 34 | Cu-63 (n,γ) | 70 | Cd-nat (n,γ) |
| 35 | Cu-63 (n,α) | 71 | Gd-nat (n,γ) |
| 36 | Cu-65 (n,2n) | | |

TAB. 3.14

Response Functions Included with BUGENDF70.BOLIB.
Neutron KERMA Factor Data [eV·b] Collapsed Using Concrete Weighting Spectrum.

| | Nuclide | | Nuclide | | Nuclide | | Nuclide |
|---|---|---|---|---|---|---|---|
| 1 | Ag-107 | 47 | Cu-63 | 93 | Li-7 | 139 | S-34 |
| 2 | Ag-109 | 48 | Cu-65 | 94 | Mg-24 | 140 | S-36* |
| 3 | Al-27 | 49 | Er-162 | 95 | Mg-25 | 141 | Si-28 |
| 4 | Am-241 | 50 | Er-164 | 96 | Mg-26 | 142 | Si-29 |
| 5 | Am-242# | 51 | Er-166* | 97 | Mn-55 | 143 | Si-30 |
| 6 | Am-242m# | 52 | Er-167 | 98 | Mo-92* | 144 | Sn-112# |
| 7 | Am-243 | 53 | Er-168 | 99 | Mo-94* | 145 | Sn-114# |
| 8 | Au-197* | 54 | Er-170 | 100 | Mo-95 | 146 | Sn-115# |
| 9 | B-10 | 55 | Eu-151# | 101 | Mo-96* | 147 | Sn-116# |
| 10 | B-11 | 56 | Eu-152# | 102 | Mo-97* | 148 | Sn-117# |
| 11 | Ba-138# | 57 | Eu-153 | 103 | Mo-98* | 149 | Sn-118# |
| 12 | Be-9 | 58 | Eu-154# | 104 | Mo-100# | 150 | Sn-119# |
| 13 | Be-9 (Thermal) | 59 | Eu-155# | 105 | N-14 | 151 | Sn-120# |
| 14 | Bi-209* | 60 | F-19 | 106 | N-15 | 152 | Sn-122# |
| 15 | C-nat | 61 | Fe-54 | 107 | Na-23 | 153 | Sn-123# |
| 16 | C (Graphite) | 62 | Fe-56 | 108 | Nb-93* | 154 | Sn-124# |
| 17 | Ca-40 | 63 | Fe-57 | 109 | Ni-58 | 155 | Sn-125* |
| 18 | Ca-42 | 64 | Fe-58 | 110 | Ni-60 | 156 | Sn-126# |
| 19 | Ca-43 | 65 | Ga-69# | 111 | Ni-61 | 157 | Ta-181* |
| 20 | Ca-44 | 66 | Ga-71# | 112 | Ni-62 | 158 | Ta-182# |
| 21 | Ca-46 | 67 | Gd-152 | 113 | Ni-64 | 159 | Th-230# |
| 22 | Ca-48 | 68 | Gd-154 | 114 | Np-237 | 160 | Th-232 |
| 23 | Cd-106 | 69 | Gd-155 | 115 | Np-238# | 161 | Ti-46 |
| 24 | Cd-108# | 70 | Gd-156 | 116 | Np-239# | 162 | Ti-47* |
| 25 | Cd-110# | 71 | Gd-157 | 117 | O-16 | 163 | Ti-48 |
| 26 | Cd-111 | 72 | Gd-158 | 118 | O-17# | 164 | Ti-49 |
| 27 | Cd-112# | 73 | Gd-160 | 119 | P-31 | 165 | Ti-50 |
| 28 | Cd-113# | 74 | H-1 ($H_2O$) | 120 | Pa-231 | 166 | U-232 |
| 29 | Cd-114# | 75 | H-1 ($CH_2$) | 121 | Pa-233 | 167 | U-233 |
| 30 | Cd-115m* | 76 | H-1 (ZrH) | 122 | Pb-204 | 168 | U-234 |
| 31 | Cd-116# | 77 | H-2 ($D_2O$) | 123 | Pb-206 | 169 | U-235 |
| 32 | Cl-35 | 78 | H-3# | 124 | Pb-207 | 170 | U-236 |
| 33 | Cl-37 | 79 | He-3# | 125 | Pb-208 | 171 | U-237 |
| 34 | Cm-241# | 80 | He-4# | 126 | Pu-236# | 172 | U-238 |
| 35 | Cm-242 | 81 | Hf-174# | 127 | Pu-237# | 173 | V-nat |
| 36 | Cm-243# | 82 | Hf-176# | 128 | Pu-238# | 174 | W-182 |
| 37 | Cm-244# | 83 | Hf-177# | 129 | Pu-239 | 175 | W-183 |
| 38 | Cm-245# | 84 | Hf-178# | 130 | Pu-240 | 176 | W-184 |
| 39 | Cm-246# | 85 | Hf-179# | 131 | Pu-241 | 177 | W-186 |
| 40 | Cm-247# | 86 | Hf-180# | 132 | Pu-242 | 178 | Y-89 |
| 41 | Cm-248 | 87 | In-113# | 133 | Pu-243 | 179 | Zr-90 |
| 42 | Co-59 | 88 | In-115# | 134 | Pu-244# | 180 | Zr-91 |
| 43 | Cr-50 | 89 | K-39 | 135 | Re-185# | 181 | Zr-92 |
| 44 | Cr-52 | 90 | K-40 | 136 | Re-187# | 182 | Zr-94 |
| 45 | Cr-53 | 91 | K-41 | 137 | S-32 | 183 | Zr-96* |
| 46 | Cr-54 | 92 | Li-6 | 138 | S-33 | | |

TAB. 3.14 Continued

Response Functions Included with BUGENDF70.BOLIB.
Neutron KERMA Factor Data [eV·b] Collapsed Using Concrete Weighting Spectrum.

**(*) The KERMA factors of this nuclide are set to zero in all the neutron groups.**
**(#) The photon production data of this nuclide are not available.**
**All photon energy is deposited locally and this is consistent with the fact that there will be no contribution to the photon transport source from this nuclide.**

TAB. 3.15

Response Functions Included with BUGENDF70.BOLIB.
Photon KERMA Factor Data[a] [eV·b] Collapsed Using Concrete Weighting Spectrum.

| | Z | Element | | Z | Element | | Z | Element |
|---|---|---|---|---|---|---|---|---|
| 1 | 1 | H | 19 | 22 | Ti | 37 | 63 | Eu |
| 2 | 2 | He | 20 | 23 | V | 38 | 64 | Gd |
| 3 | 3 | Li | 21 | 24 | Cr | 39 | 68 | Er |
| 4 | 4 | Be | 22 | 25 | Mn | 40 | 72 | Hf |
| 5 | 5 | B | 23 | 26 | Fe | 41 | 73 | Ta |
| 6 | 6 | C | 24 | 27 | Co | 42 | 74 | W |
| 7 | 7 | N | 25 | 28 | Ni | 43 | 75 | Re |
| 8 | 8 | O | 26 | 29 | Cu | 44 | 79 | Au |
| 9 | 9 | F | 27 | 31 | Ga | 45 | 82 | Pb |
| 10 | 11 | Na | 28 | 39 | Y | 46 | 83 | Bi |
| 11 | 12 | Mg | 29 | 40 | Zr | 47 | 90 | Th |
| 12 | 13 | Al | 30 | 41 | Nb | 48 | 91 | Pa |
| 13 | 14 | Si | 31 | 42 | Mo | 49 | 92 | U |
| 14 | 15 | P | 32 | 47 | Ag | 50 | 93 | Np |
| 15 | 16 | S | 33 | 48 | Cd | 51 | 94 | Pu |
| 16 | 17 | Cl | 34 | 49 | In | 52 | 95 | Am |
| 17 | 19 | K | 35 | 50 | Sn | 53 | 96 | Cm |
| 18 | 20 | Ca | 36 | 56 | Ba | | | |

([a]) The photon KERMA factors are the same for all the isotopes of each element.

## 4 - BUGENDF70.BOLIB PRELIMINARY VALIDATION

The BUGENDF70.BOLIB library was preliminarily tested on two low-flux engineering neutron shielding benchmark experiments, specifically dedicated to improve the accuracy of the neutron fluence calculations in the structural components of the pressurized light water reactors (PWRs), whose geometrical and compositional specifications were contained in the SINBAD /28/ (see also /29/) international database of fission reactor neutron shielding benchmark experiments.
The PCA-Replica 12/13 /25/ (see also /26/) (Winfrith, United Kingdom) and the VENUS-3 /27/ (Mol, Belgium) neutron shielding benchmark experiments were simulated with three-dimensional fixed source transport calculations using the ORNL TORT-3.2 /10/ discrete ordinates deterministic code. The automatic generation and the graphical verification of the benchmark experiment geometrical models for TORT-3.2 were performed through the ENEA-Bologna BOT3P-5.3 /12/ pre/post-processor system.
The BUGENDF70.BOLIB library was alternatively used in the transport calculations with the BUGLE-96 /8/ library, which was specifically employed to obtain corresponding reference dosimetric results. Group-organized files of macroscopic cross sections, requested by TORT-3.2 and derived from the cited working libraries in FIDO-ANISN format, were prepared through the GIP /35/ program, specifically dedicated to the transport codes (ANISN-ORNL, DORT, TORT) of the DOORS /35/ system. The ENEA-Bologna ADEFTA-4.1 /65/ program was used to calculate the atomic densities for the benchmark experiment compositional models and to handle them properly in order to automatically prepare the macroscopic cross section sets of the compositional model material mixtures in the format required by GIP.
The IRDF-2002 /54/ flat weighting dosimeter cross sections /55/ in the 47 neutron energy group structure (see TAB. 3.1) were used in both the calculations for the PCA-Replica 12/13 and VENUS-3 benchmark experiments with the BUGENDF70.BOLIB and BUGLE-96 libraries.

### 4.1 - PCA-Replica 12/13 Neutron Shielding Benchmark

#### 4.1.1 - PCA-Replica 12/13 Experimental Details

The PCA-Replica 12/13 /25/ low-flux neutron shielding benchmark experiment (Winfrith, United Kingdom) is a water/iron benchmark experiment including PWR thermal shield and pressure vessel simulators. The source of neutrons was a thin fission plate (whose dimensions are 63.5 cm × 40.2 cm × 0.6 cm) of highly enriched uranium (93.0 w% in U-235), irradiated by the NESTOR low-power experimental reactor through a graphite thermal column (total thickness 43.91 cm). Beyond the fission plate, the PCA-Replica shielding array (12/13 experimental configuration with two water gaps of about 12 cm and 13 cm) was arranged in a large parallelepiped steel tank (square section; side 180.0 cm) filled with water. After a first water gap (12.1 cm), there was the stainless steel thermal shield simulator (5.9 cm), the second water gap (12.7 cm), the mild steel pressure vessel simulator (thickness T = 22.5 cm) and a void box made of a thin layer of aluminium simulating the air cavity between the pressure vessel and the biological shield in a real PWR.
The fission plate, the thermal shield, the pressure vessel and the void box were perfectly orthogonally aligned and centred along an imaginary line Z (horizontal or nuclear axis) passing through the centre of the fission plate. Along this nuclear axis three types of threshold detectors were located in ten positions and gave the integral measurements.

The Rh-103(n,n')Rh-103m, In-115(n,n')In-115m and S-32(n,p)P-32 threshold dosimeters were employed in the PCA-Replica experiment. The corresponding typical parameters in a light water material testing reactor (MTR) spectrum (see /66/), similar to that of PCA-Replica, are reported in TAB. 4.1 to help in the analysis of the calculated results.
In practice the results coming from Rh-103(n,n') and In-115(n,n') are comparable with neutron fluxes above about 1.0 MeV and the results from S-32(n,p) with neutron fluxes above about 3.0 MeV.
Moreover spectral measurements were performed in two positions: in the one-quarter thickness (T) of the reactor pressure vessel (RPV 1/4 T) simulator and in the void box. Two kinds of spectrometer were used. The spherical hydrogen-filled proportional counters employed were of type SP-2 of internal diameter 40.0 mm. Individual counters with gas fillings of approximately 0.5, 1.0, 3.0 and 10.0 atmospheres were used in combination, to cover the energy range from 50.0 keV to 1.2 MeV. The neutron fluxes between 1.0 and 10.0 MeV were determined with a spherical 3.5 ml organic liquid (NE213) scintillator.

TAB. 4.1

PCA-Replica - Dosimeter Parameters in a Light Water MTR Neutron Spectrum.

| Dosimeter | Effective Energy Threshold [MeV] | 90% Response Energy Range [MeV] | Median Energy [MeV] |
|---|---|---|---|
| Rh-103(n,n') | 0.69 | 0.53 – 5.4 | 1.9 |
| In-115(n,n') | 1.30 | 1.0 – 5.6 | 2.4 |
| S-32(n,p) | 2.70 | 2.2 – 7.4 | 3.9 |

4.1.2 - PCA-Replica 12/13 Analysis and Results

The BUGENDF70.BOLIB and the BUGLE-96 /8/ libraries were alternatively used to simulate the PCA-Replica 12/13 /25/ engineering neutron shielding benchmark experiment. The whole PCA-Replica 12/13 experimental array was reproduced with the TORT-3.2 /10/ code, using the BOT3P-5.3 /12/ system for the preparation of the input of the geometrical model and the ADEFTA-4.1 /65/ program for the calculation of the atomic densities of the isotopes involved in the compositional model, on the basis of the atomic abundances reported in the BNL-NNDC database /67/. In fact the atomic densities indicated in the official description /25/ of the PCA-Replica experiment are given for natural element except for two uranium isotopes, i.e. U-235 and U-238. All the calculations were performed only with the 29 neutron groups (see TAB. 3.1) above 3.1828E+04 eV since all the energy thresholds of the employed dosimeters are above this energy value.

It was decided to reproduce the whole three-dimensional PCA-Replica experimental array in the (X,Y,Z) cartesian geometry in order to assure a detailed description of the spatial heterogeneity of the neutron source emitted by the fission plate. The origin of the cartesian co-ordinate system was taken in the centre of the fission plate.
In particular a parallelepiped geometry (whose dimensions were 185.08 cm × 180.0 cm × 180.0 cm, respectively along the X, Y and Z axis) was described with a 65X×63Y×182Z fine

spatial mesh grid (see the horizontal section at the height Y=0.0 cm in FIG. 4.1), where Z is the horizontal nuclear axis on which the detector positions are located. Along this axis, in order to obtain the best accuracy in the calculations, volumetric meshes with sides always inferior to 0.5 cm were described. Both infinitely dilute and self-shielded cross sections were selected. Self-shielded cross sections from the library package were used when available: in particular it is underlined that the thermal shield (stainless steel) and the pressure vessel (mild steel) components of the PCA-Replica experiment were characterized by atomic densities quite similar to those used to determine the background cross sections employed in the self-shielding of the BUGENDF70.BOLIB cross sections.
Fixed source transport calculations with one source (outer) iteration were performed using fully symmetrical quadrature sets. The $P_3$-$S_8$ approximation was adopted: $P_3$ corresponds to the order of the expansion in Legendre polynomials of the scattering cross section matrix and $S_8$ represents the order of the flux angular discretization. Further calculations in the $P_5$-$S_{16}$ approximation did not give significant differences in the integral dosimetric results.
The theta-weighted difference approximation was selected for the flux extrapolation model. In all the calculations the same numerical value (1.0E-03) for the point-wise flux convergence criterion was employed. The vacuum boundary condition was selected at the left, right, inside, outside, bottom and top geometrical boundaries.
As previously reported, a precise heterogeneous fission neutron source distribution in the fission plate was adopted, following the recommended official specifications (see /25/, page 55, TAB. A6 and page 57, FIG. A1).
The distributed (or volumetric) fission neutron sources used in the calculations with the BUGENDF70.BOLIB library and the BUGLE-96 library were obtained using, respectively, the BUGENDF70.BOLIB U-235 total (prompt + delayed) neutron fission spectrum ($\chi$) data and the BUGLE-96 U-235 prompt neutron fission spectrum ($\chi$) data (see /8/, page 58, TAB. 3.14), since the total neutron fission spectrum data are not available in the BUGLE-96 library. In order to determine the volumetric neutron source, the value of $\bar{\nu}$(U-235) = 2.437 was used for the average number of neutrons produced per U-235 thermal fission, as suggested in the official description (see /25/, page 49) of the PCA-Replica experiment.

The IRDF-2002 /54/ “flat weighting” dosimeter cross sections /55/ in the 47 neutron energy group structure (see TAB. 3.1) for the Rh-103(n,n’)Rh-103m, In-115(n,n’)In-115m and S-32(n,p)P-32 nuclear reactions were used in the calculations with the BUGENDF70.BOLIB and BUGLE-96 libraries to determine the detector activities in both water and steel locations. The use of the IRDF-2002 “1/4T PV weighting” dosimeter cross sections, to be used more properly in measurement positions located in steel, gave negligible differences in the pressure vessel simulator reaction rate results with respect to the corresponding results obtained with the IRDF-2002 flat weighting dosimeter cross sections. The reaction rate integral results obtained with the flat weighting dosimeter cross sections are reported in TAB. 4.2 and FIG. 4.2 for Rh-103(n,n’)Rh-103m, in TAB. 4.3 and FIG. 4.3 for In-115(n,n’)In-115m and in TAB. 4.4 and FIG. 4.4 for S-32(n,p)P-32. It is underlined that the calculated reaction rates for both the libraries are practically within the desired target accuracy of ±10%.
The spectral results are reported in FIGs. 4.5÷4.6 for the 1/4 T reactor pressure vessel (RPV 1/4 T) position and in FIGs. 4.7÷4.8 for the void box position.

FIG. 4.1

PCA-Replica Model with TORT-3.2 (X,Y,Z), Horizontal Section at Y=0.0 cm.
Dosimeter Locations "×", 65X×63Y×182Z Spatial Meshes.

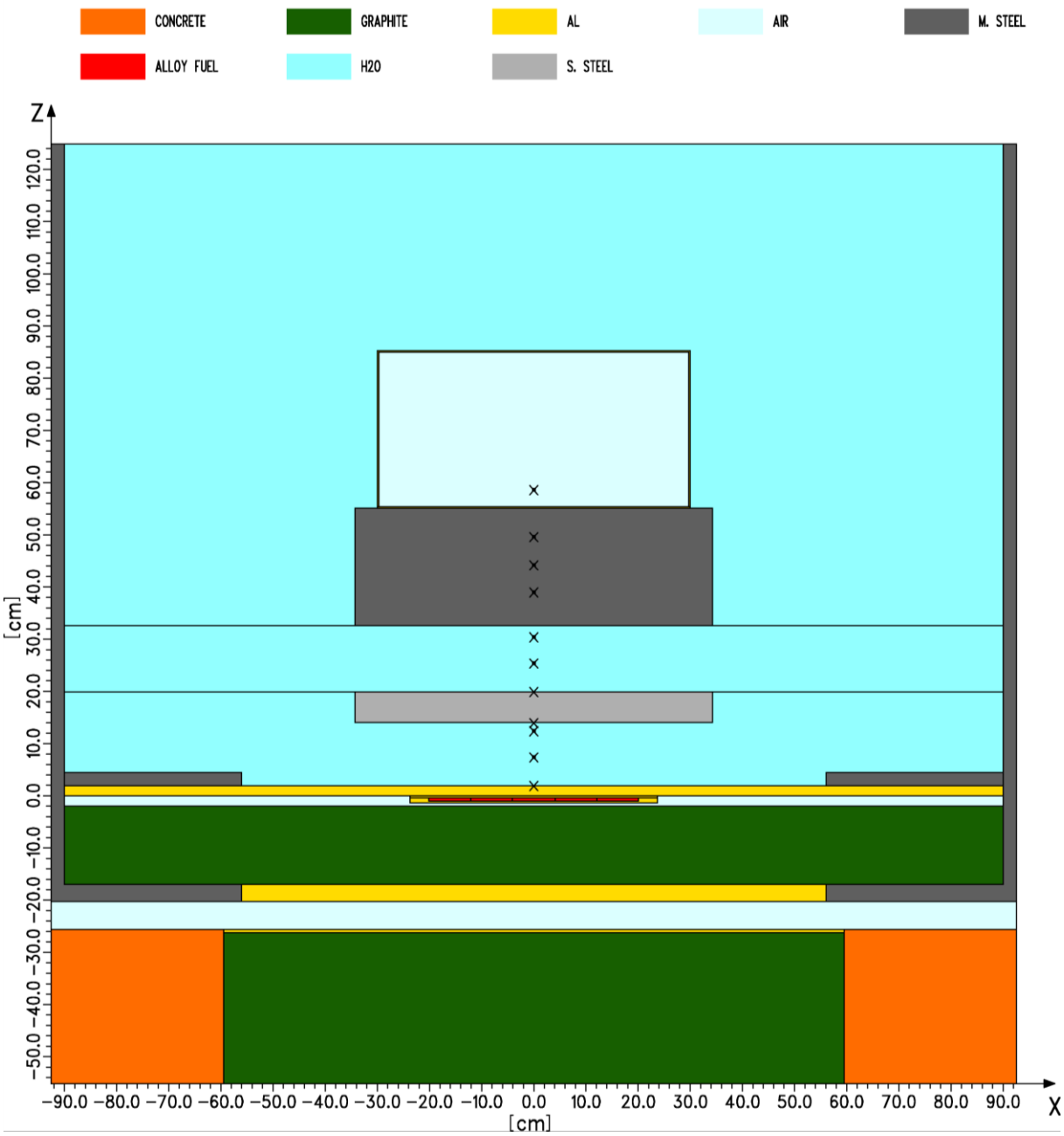

TAB. 4.2

PCA-Replica - Summary of Experimental (E) and Calculated (C) Rh-103(n,n') Reaction Rates[a] per NESTOR Reactor Watt along the Z Horizontal Axis.

| Detec. Pos. | Distance from Fission Plate [cm] | Experimental. Reaction Rates ± Random Error (1σ) (E) Systematic Error ± 3.0% | BUGENDF70.BOLIB Calculation | | BUGLE-96 Calculation | | Reference Location |
|---|---|---|---|---|---|---|---|
| | | | Calculated Reaction Rates (C) | C/E[b] | Calculated Reaction Rates (C) | C/E[b] | |
| 1 | 1.91 | 1.69E-20 ± 3.0% | 1.81E-20 | 1.09 | 1.82E-20 | 1.10 | 12 cm Water Gap |
| 2 | 7.41 | 3.78E-21 ± 3.0% | 3.44E-21 | 0.93 | 3.44E-21 | 0.93 | |
| 3 | 12.41 | 1.40E-21 ± 3.0% | 1.31E-21 | 0.95 | 1.30E-21 | 0.95 | |
| 4 | 14.01 | 1.27E-21 ± 3.0% | 1.16E-21 | 0.93 | 1.15E-21 | 0.93 | |
| 5 | 19.91 | 4.23E-22 ± 3.0% | 4.17E-22 | 1.00 | 4.11E-22 | 0.99 | 13 cm Water Gap |
| 6 | 25.41 | 1.15E-22 ± 4.0% | 1.02E-22 | 0.91 | 1.01E-22 | 0.89 | |
| 7 | 30.41 | 4.73E-23 ± 4.0% | 4.13E-23 | 0.89 | 4.06E-23 | 0.88 | |
| 8 | 39.01 | 2.07E-23 ± 1.0% | 2.02E-23 | 1.01 | 1.98E-23 | 1.00 | RPV (1/4 T) |
| 9 | 49.61 | 5.53E-24 ± 1.9% | 5.59E-24 | 1.05 | 5.45E-24 | 1.03 | RPV (3/4 T) |
| 10 | 58.61 | 1.80E-24 ± 1.6% | 1.66E-24 | 0.96 | 1.59E-24 | 0.92 | Void Box |

Note: The total experimental error (1σ level) should be calculated as the square root of the quadratic sum of the random error listed with each measurement and the systematic error indicated at the head of the column of the experimental results, as indicated on page 12 of reference /25/.

([a]) Reaction rates are in units of reactions/(s·atom·NESTOR Watt).
([b]) Experimental results contain a contribution from the NESTOR core background. Calculated results refer only to the neutrons produced in the fission plate for 1 Watt of NESTOR power. As indicated on page 10 of reference /25/, the E values, in the C/E ratios, are reduced by 4% in the RPV and Void Box and by 2% in the Water Gaps.

TAB. 4.3

PCA-Replica - Summary of Experimental (E) and Calculated (C) In-115(n,n') Reaction Rates[a] per NESTOR Reactor Watt along the Z Horizontal Axis.

| Detec. Pos. | Distance from Fission Plate [cm] | Experimental. Reaction Rates ± Random Error (1σ) (E) Systematic Error ± 2.0% | BUGENDF70.BOLIB Calculation | | BUGLE-96 Calculation | | Reference Location |
|---|---|---|---|---|---|---|---|
| | | | Calculated Reaction Rates (C) | C/E[b] | Calculated Reaction Rates (C) | C/E[b] | |
| 1 | 1.91 | -- | -- | -- | -- | -- | 12 cm Water Gap |
| 2 | 7.41 | -- | -- | -- | -- | -- | |
| 3 | 12.41 | -- | -- | -- | -- | -- | |
| 4 | 14.01 | -- | -- | -- | -- | -- | |
| 5 | 19.91 | -- | -- | -- | -- | -- | 13 cm Water Gap |
| 6 | 25.41 | -- | -- | -- | -- | -- | |
| 7 | 30.41 | -- | -- | -- | -- | -- | |
| 8 | 39.01 | 3.93E-24 ± 0.9% | 3.87E-24 | 1.03 | 3.81E-24 | 1.01 | RPV (1/4 T) |
| 9 | 49.61 | 8.23E-25 ± 1.4% | 7.76E-25 | 0.98 | 7.58E-25 | 0.96 | RPV (3/4 T) |
| 10 | 58.61 | 2.31E-25 ± 1.5% | 2.16E-25 | 0.97 | 2.09E-25 | 0.94 | Void Box |

Note: The total experimental error (1σ level) should be calculated as the square root of the quadratic sum of the random error listed with each measurement and the systematic error indicated at the head of the column of the experimental results, as indicated on page 12 of reference /25/.

([a]) Reaction rates are in units of reactions/(s·atom·NESTOR Watt).
([b]) Experimental results contain a contribution from the NESTOR core background. Calculated results refer only to the neutrons produced in the fission plate for 1 Watt of NESTOR power. As indicated on page 10 of reference /25/, the E values, in the C/E ratios, are reduced by 4% in the RPV and Void Box and by 2% in the Water Gaps.

TAB. 4.4

PCA-Replica - Summary of Experimental (E) and Calculated (C) S-32(n,p) Reaction Rates[a] per NESTOR Reactor Watt along the Z Horizontal Axis.

| Detec. Pos. | Distance from Fission Plate [cm] | Experimental. Reaction Rates ± Random Error (1σ) (E)<br>Systematic Error ± 4.0% | BUGENDF70.BOLIB Calculation | | BUGLE-96 Calculation | | Reference Location |
|---|---|---|---|---|---|---|---|
| | | | Calculated Reaction Rates (C) | C/E[b] | Calculated Reaction Rates (C) | C/E[b] | |
| 1 | 1.91 | -- | -- | -- | -- | -- | 12 cm Water Gap |
| 2 | 7.41 | -- | -- | -- | -- | -- | |
| 3 | 12.41 | -- | -- | -- | -- | -- | |
| 4 | 14.01 | -- | -- | -- | -- | -- | |
| 5 | 19.91 | -- | -- | -- | -- | -- | 13 cm Water Gap |
| 6 | 25.41 | -- | -- | -- | -- | -- | |
| 7 | 30.41 | -- | -- | -- | -- | -- | |
| 8 | 39.01 | 1.08E-24 ± 1.5% | 9.78E-25 | 0.94 | 9.67E-25 | 0.93 | RPV (1/4 T) |
| 9 | 49.61 | 1.46E-25 ± 1.9% | 1.35E-25 | 0.97 | 1.34E-25 | 0.95 | RPV (3/4 T) |
| 10 | 58.61 | 3.73E-26 ± 1.3% | 3.57E-26 | 1.00 | 3.52E-26 | 0.98 | Void Box |

Note: The total experimental error (1σ level) should be calculated as the square root of the quadratic sum of the random error listed with each measurement and the systematic error indicated at the head of the column of the experimental results, as indicated on page 12 of reference /25/.

([a]) Reaction rates are in units of reactions/(s·atom·NESTOR Watt).
([b]) Experimental results contain a contribution from the NESTOR core background. Calculated results refer only to the neutrons produced in the fission plate for 1 Watt of NESTOR power. As indicated on page 10 of reference /25/, the E values, in the C/E ratios, are reduced by 4% in the RPV and Void Box and by 2% in the Water Gaps.

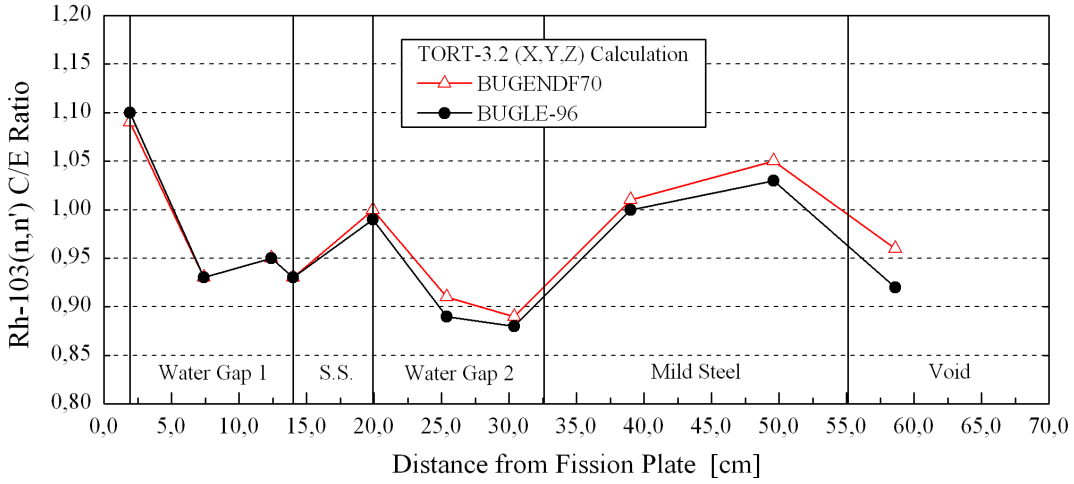


FIG. 4.2 PCA-Replica - Rh-103(n,n') Reaction Rate Ratios (Calculated/Experimental).

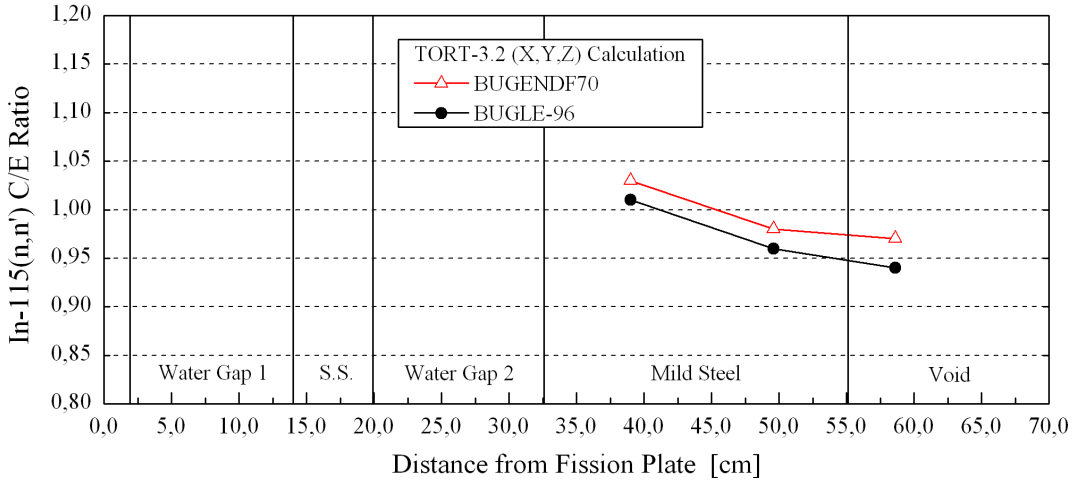


FIG. 4.3 PCA-Replica - In-115(n,n') Reaction Rate Ratios (Calculated/Experimental).

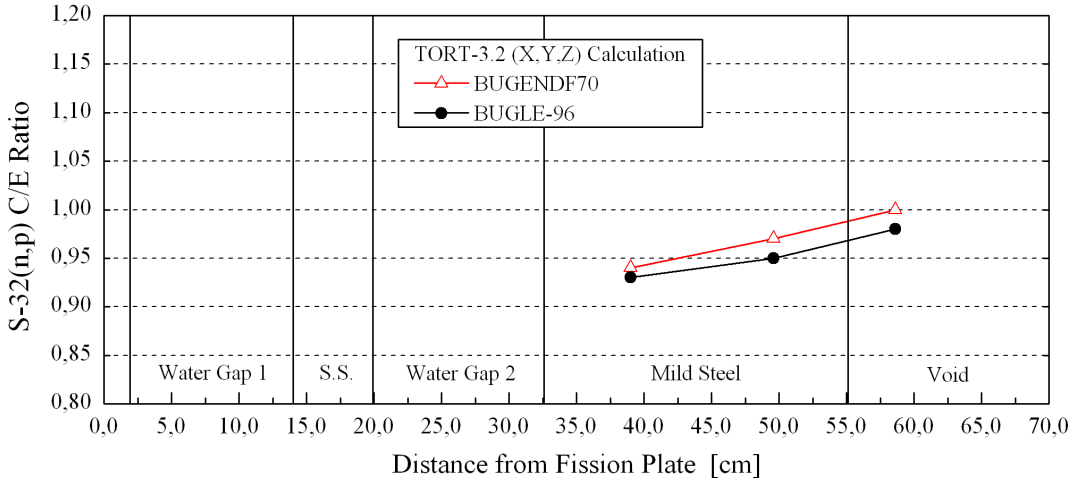


FIG. 4.4 PCA-Replica - S-32(n,p) Reaction Rate Ratios (Calculated/Experimental).

FIG. 4.5

PCA-Replica - Comparison of Experimental and Calculated Neutron Fluxes in the RPV 1/4 T Position (Mild Steel).

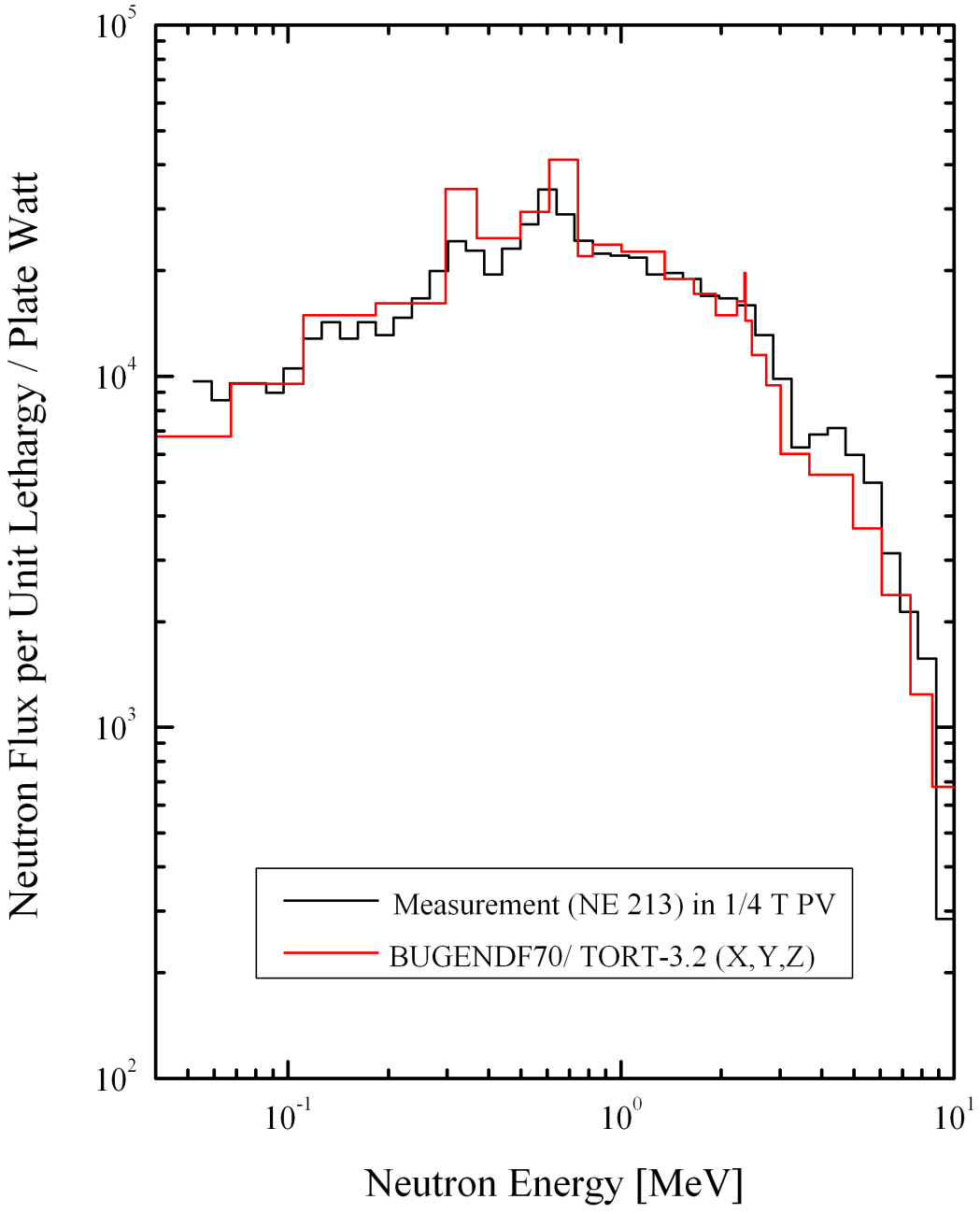

FIG. 4.6

PCA-Replica - Comparison of Experimental and Calculated Neutron Fluxes in the RPV 1/4 T Position (Mild Steel).

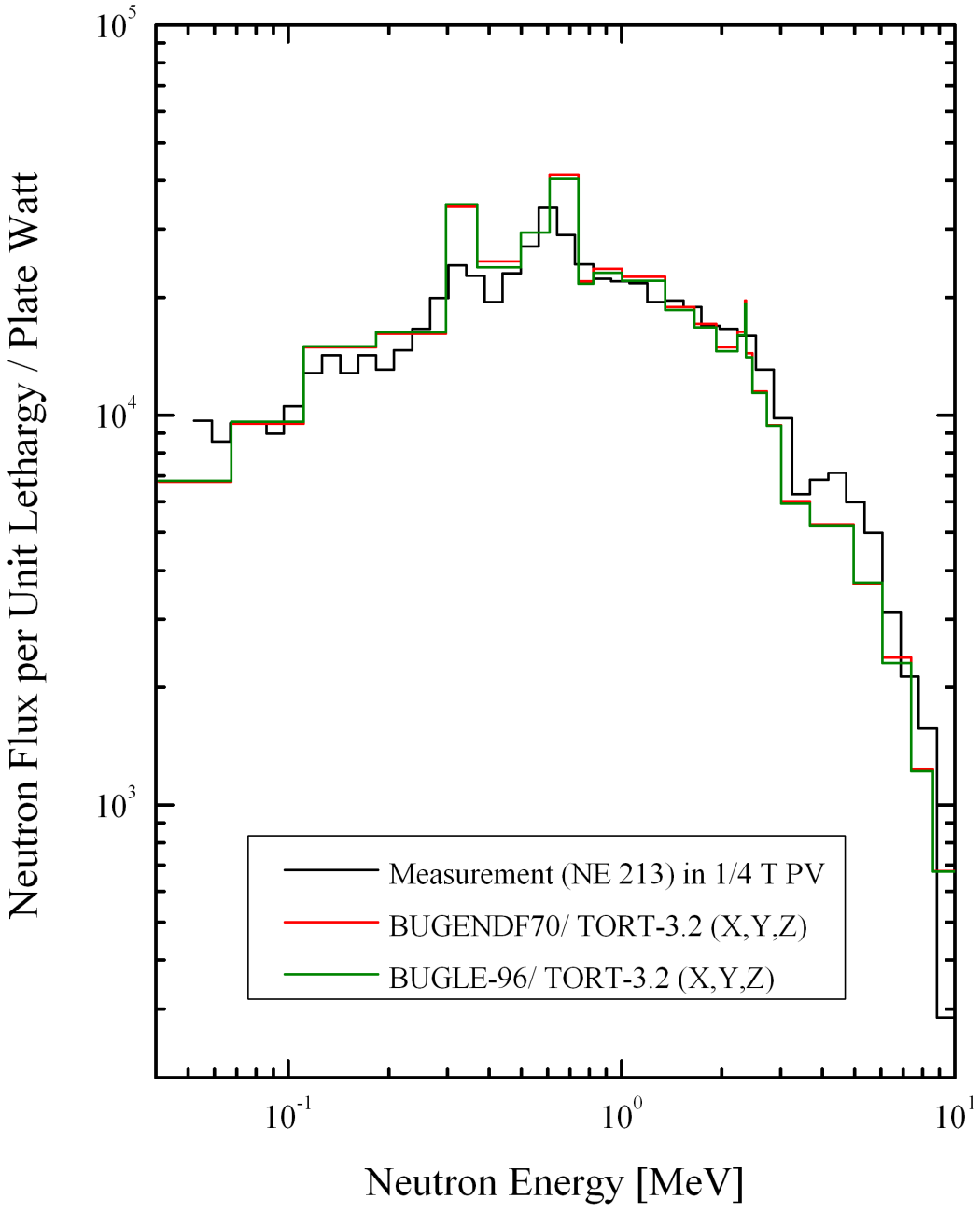

FIG. 4.7

PCA-Replica - Comparison of Experimental and Calculated Neutron Fluxes in the Void Box Position (Air).

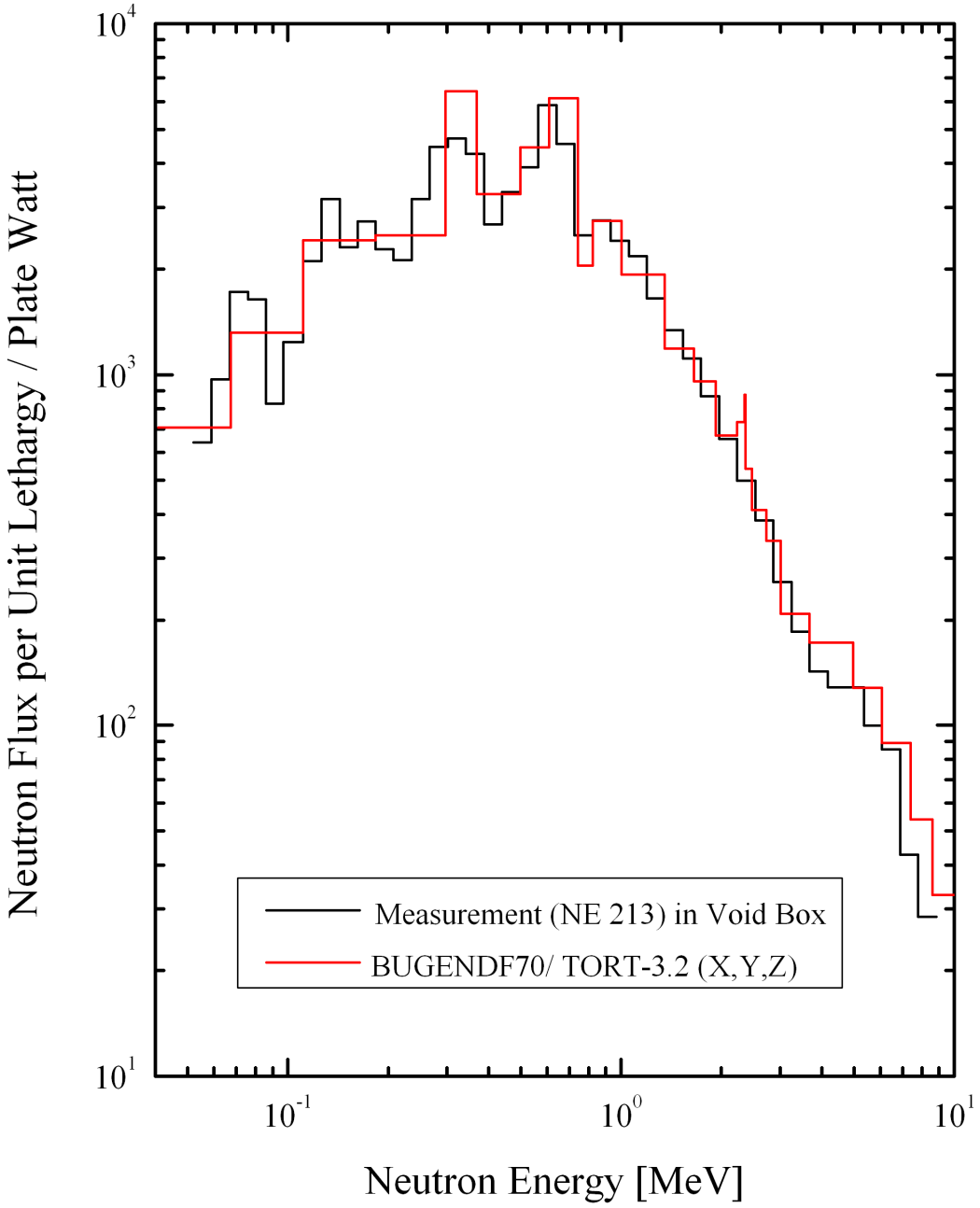

FIG. 4.8

PCA-Replica - Comparison of Experimental and Calculated Neutron Fluxes in the Void Box Position (Air).

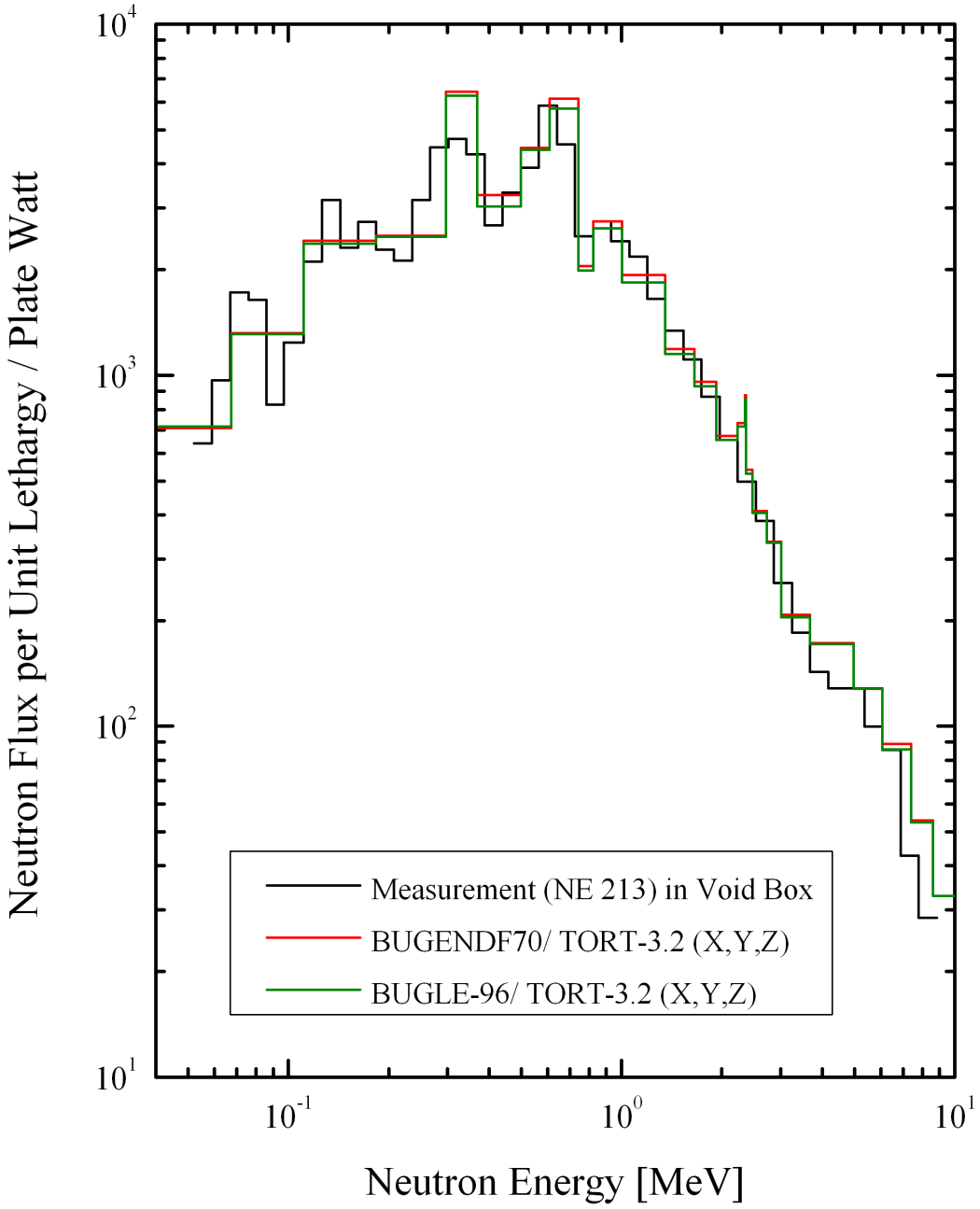

4.2 - VENUS-3 Neutron Shielding Benchmark

4.2.1 - VENUS-3 Experimental Details

The VENUS-3 /27/ low-flux neutron shielding benchmark experiment (Mol, Belgium) is closely related to PWR pressure vessel (PV) safety. It was designed to test the accuracy of the nuclear data and transport codes in the calculation of the neutron radiation damage parameters in stainless steel reactor components, in a context of great precision of the experimental results. Among the available experiments, the VENUS-3 configuration offers the exceptional advantage of exhibiting a realistic radial core shape and a typical PWR neutron spectrum. Typical "17x17" PWR fuel assemblies were employed and a mock-up of the pressure vessel internals, representative of a three-loop Westinghouse power plant, was prepared. VENUS-3 was conceived taking into account that, for some early built reactors, it was proposed to reduce the lead factor at the level of the PV horizontal welding by loading Partial Length Shielded Assemblies (PLSA) at the most critical corners of the core periphery (the shielded part was obtained by replacing part of the fuel length by a stainless steel rod). VENUS-3 was addressed to test this improvement, introducing a PLSA region in the core, and to permit the validation of the analytical methods needed to predict the azimuthal variation of the fluence in the pressure vessel. The VENUS-3 core was designed, in particular, with the following objectives.

1. It had to be representative of typical irradiation conditions of a modern PWR pressure vessel.

2. It had to fit the grid and the vessel geometries of the VENUS facility. This led to a limitation of the core size and of the amount of simulated internals. In particular the second water gap and the pressure vessel of a typical PWR were not simulated.

3. The core loading was projected to obtain a radial power shape factor as low as possible, in order to reach, in the different stainless steel components, fast flux levels high enough to perform accurate measurements. Secondly, the core loading was planned to achieve azimuthal flux variations as high as possible to allow a valuable test of the analytical methods. Finally a quadrangular geometry symmetry was preferred, with two quadrants including both the PLSA fuel region and the unperturbed reference fuel region.

All these objectives were attained with a cruciform-shaped core configuration. The core consisted of three types of fuel pins: 1) stainless-steel-clad $UO_2$ rods (typical of a "15x15" lattice of the early Generation I reactors of Westinghouse plants) containing 4% enriched U-235, 2) zircaloy-clad $UO_2$ rods containing 3.3% enriched U-235 and 3) zircaloy-clad $UO_2$ rods containing 3.3% enriched U-235 over the upper half of their height and zircaloy-clad steel rods over the lower half. The first two types of fuel pins were of uniform composition over their complete height. The 4% enriched rods were positioned in the inner part of the core while the 3.3% enriched rods were located in the arms of the cross configuration together with the PLSA-modified rods. The pin-to-pin pitch for all fuel types was 1.26 cm, typical value of the "17x17" lattices in existing PWR fuel assemblies. In one quadrant of the configuration between 0° and 90° (see the horizontal section in FIG. 4.9 and the vertical section in FIG. 4.10), a mock-up of PWR pressure vessel internals was placed with a total of 639 fuel pins

(including those in the PLSA) and 11 control rods. The other quadrants were loaded with fuel pins "quasi" identical to the fuel pins of the first previous quadrant (due to fuel inventory limitations) and with some absorbing rods for criticality balance adjustment. Starting from the centre, the core quadrant between 0° and 90° may be divided in the following 10 horizontal radial regions:

- the CENTRAL HOLE (water);
- the INNER BAFFLE (stainless steel thickness: 2.858 cm);
- the 4/0 FUEL REGION: 4% enriched uranium fuel rods and 11 pyrex control rods, typical of PWR poison clusters;
- the 3/0 FUEL REGION: 3.3% enriched uranium fuel rods and PLSA rods;
- the OUTER BAFFLE (stainless steel thickness. 2.858 cm);
- the REFLECTOR (water minimum thickness: 2.169 cm);
- the BARREL (stainless steel thickness: 4.99 cm);
- the WATER GAP (water thickness: 5.80 cm);
- the NEUTRON PAD (stainless steel average thickness: 6.72 cm);
- the VENUS environment, i.e., the jacket (air filled), the reactor vessel (stainless steel) and the reactor room (air).

The In-115(n,n')In-115m, Ni-58(n,p)Co-58 and Al-27(n,α)Na-24 threshold dosimeters were employed in the VENUS-3 experiment. The corresponding typical parameters in a light water material testing reactor (MTR) spectrum (see /66/), similar to that of VENUS-3, are reported in TAB. 4.5 to help in the analysis of the obtained calculated results.

TAB. 4.5

VENUS-3 - Dosimeter Parameters in a Light Water MTR Neutron Spectrum.

| Dosimeter | Effective Energy Threshold [MeV] | 90% Response Energy Range [MeV] | Median Energy [MeV] |
|---|---|---|---|
| In-115(n,n') | 1.30 | 1.0 – 5.6 | 2.4 |
| Ni-58(n,p) | 2.60 | 1.9 – 7.5 | 3.9 |
| Al-27(n,α) | 7.30 | 6.5 – 12.0 | 8.6 |

In practice (see also /68/) the results coming from In-115(n,n') are comparable with neutron fluxes above about 1.0 MeV, the results from Ni-58(n,p) with neutron fluxes above about 3.0 MeV and the results from Al-27(n,α) with neutron fluxes above about 8.0 MeV.
In the VENUS-3 experiment the total number of the dosimeters was 386: the In-115(n,n') dosimeters were in 104 positions, the Ni-58(n,p) dosimeters were in 244 positions and the Al-27(n,α) dosimeters were in 38 positions. In other words, each set of dosimeters was placed in a part of the 268 total different spatial locations. Axially, the dosimeters were located at 14 different axial levels between 105.0 cm and 155.0 cm, respectively the lower height and the upper height of the active core region (see FIG. 4.10). The maximum total uncertainty of the

VENUS-3 experimental equivalent fission fluxes corresponding to each of the three dosimeters is ±5% (see /51/, page 31).

FIG. 4.9

VENUS-3 Model with TORT-3.2 (R,Θ,Z), Horizontal Section at Z=114.50 cm.
Dosimeter Locations "×", 111R×113Θ×71Z Spatial Meshes.

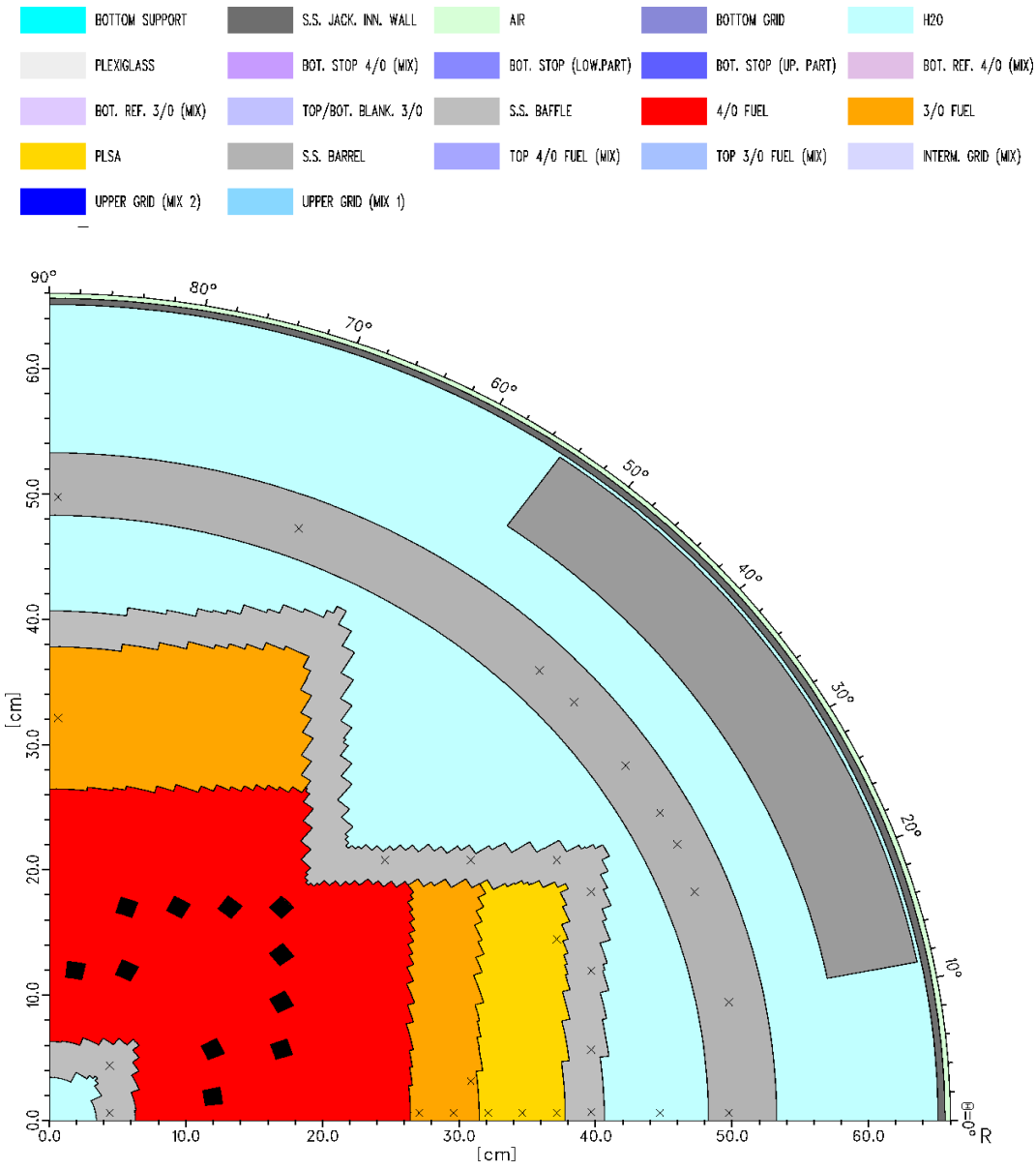

FIG. 4.10

VENUS-3 Model with TORT-3.2 (R,Θ,Z), Vertical Section at Θ=0°.
Dosimeter Locations "×", 111R×113Θ×71Z Spatial Meshes.

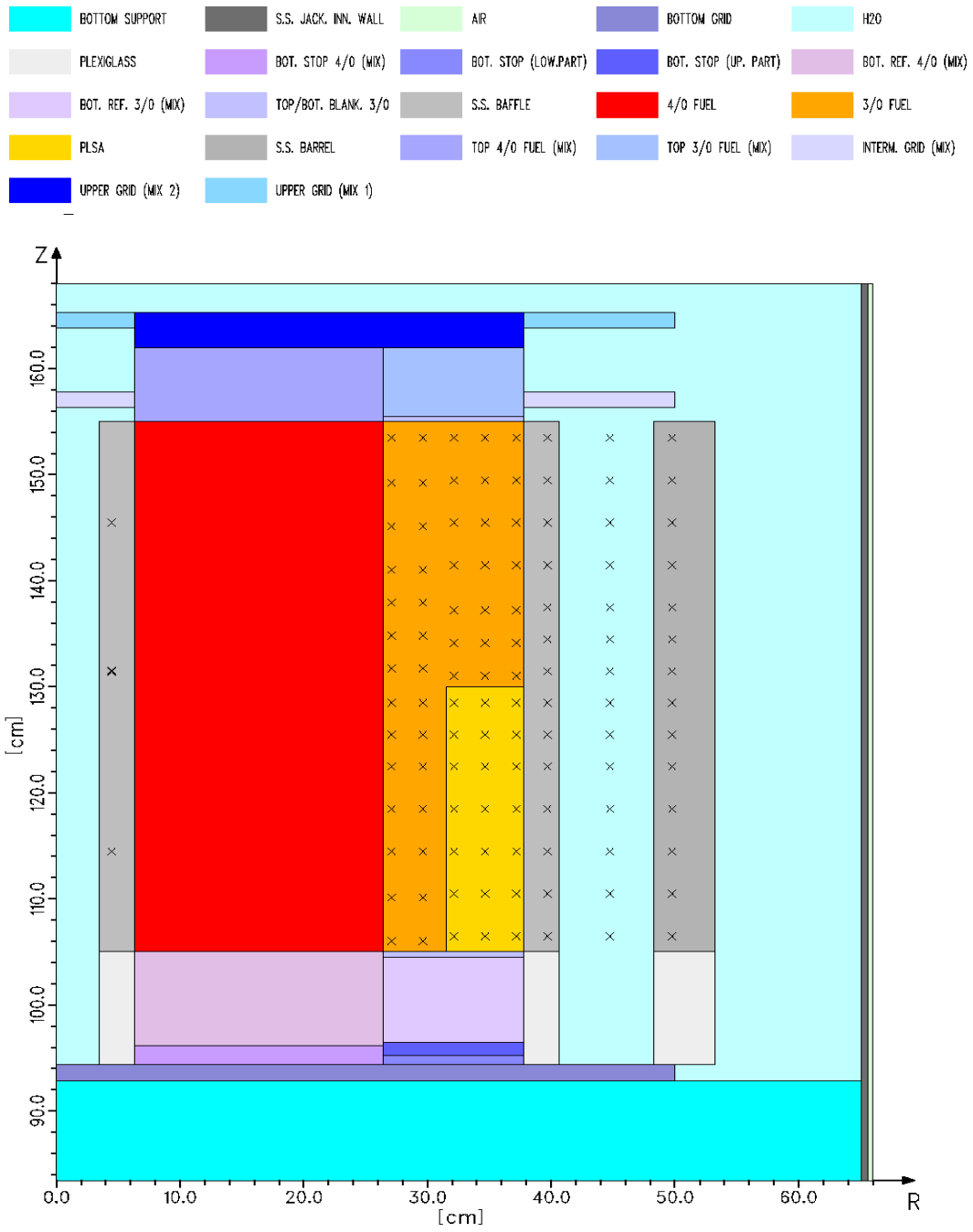

4.2.2 - VENUS-3 Analysis and Results

The BUGENDF70.BOLIB and the BUGLE-96 /8/ libraries were alternatively used to simulate the VENUS-3 /27/ (see also /49/ /50/ and /51/) engineering neutron shielding benchmark experiment. Both infinitely dilute and self-shielded cross sections were selected. In the case, e.g., of Fe-56, in the material mixtures of stainless steel components, the self-shielded cross sections were used. All the calculations were performed only with the 26 neutron groups (see TAB. 3.1) above 1.1109E+05 eV since all the energy thresholds of the employed dosimeters are above this energy value. Three-dimensional calculations in cylindrical (R,Θ,Z) geometry were performed through the TORT-3.2 /10/ discrete ordinates ($S_N$) transport code, included in the ORNL DOORS-3.2 /35/ modular system, using both the previously cited libraries. Fixed source calculations with one source (outer) iteration were performed in the $P_3$-$S_8$ approximation: $P_3$ corresponds to the order of the expansion in Legendre polynomials of the scattering cross section matrix and $S_8$ represents the order of the flux angular discretization. Fully symmetrical quadrature sets were introduced. The theta-weighted difference approximation was selected for the flux extrapolation model. In all the calculations the same numerical value (1.0E-04) for the point-wise flux convergence criterion was employed. The BOT3P-5.3 /12/ system of pre/post-processor programs was used to prepare the automatic generation of the input data for the neutron source and for the geometrical models together with the graphical visualizations. The ADEFTA-4.1 /65/ program was employed for the calculation of the atomic densities of the isotopes involved in the compositional model, on the basis of the atomic abundances reported in the BNL-NNDC database /67/. The (R,Θ,Z) geometrical model is shown in FIG. 4.9 and FIG. 4.10, reproducing respectively the horizontal and the vertical sections. It is underlined that the (R,Θ,Z) model is also usually adopted for the LWR-PV radiation damage transport analyses. In particular a horizontal plane section between 0° and 90° was described (i.e. the first quadrant up to a radius of 66.0 cm, reported in FIG. 4.9) containing the barrel, the neutron pad and the jacket inner wall with a 111R×113Θ×71Z fine spatial mesh grid. The jacket outer wall and the external regions beyond the jacket outer wall were not included since it was considered that they could only slightly affect the results. The following boundary conditions were selected: reflection at the left, inside and outside boundaries and vacuum at the right, bottom and top boundaries.

The distributed (or volumetric) fission neutron sources used in the BUGENDF70.BOLIB and BUGLE-96 calculations and the calculated results in terms of equivalent fission fluxes for the three threshold detectors were obtained using respectively, the BUGENDF70.BOLIB U-235 total (prompt + delayed) neutron fission spectrum (χ) data and the BUGLE-96 U-235 prompt neutron fission spectrum (χ) data (see /8/, page 58, TAB. 3.14), since the total neutron fission spectrum data are not available in the BUGLE-96 library. To determine the volumetric neutron source, the value of $\bar{\nu}$(U-235) = 2.432 for the average number of neutrons produced per U-235 thermal fission was used, as proposed value (see /69/, page 7) for the ENDF/B-VI U-235 processed data file, contained in the BUGLE-96 library.

The calculated dosimeter reaction rates (activities) were divided by the corresponding value of the “flat weighting” dosimeter cross section, averaged on the specific U-235 fission spectrum. The following flat weighting corresponding values (see TAB. 4.6) were used in all the calculations in order to treat simultaneously both water and steel dosimeter locations.

TAB. 4.6

VENUS-3 - IRDF-2002 Dosimeter Cross Sections Averaged on the U-235 Neutron Fission Spectra Respectively Taken from the BUGENDF70.BOLIB and BUGLE-96 Libraries.

| Library | In115(n,n') [barns] | Ni-58(n,p) [barns] | Al-27(n,α) [barns] |
|---|---|---|---|
| BUGENDF70 | 1.8746E-01 | 1.0836E-01 | 7.8151E-04 |
| BUGLE-96 | 1.8853E-01 | 1.0906E-01 | 7.8671E-04 |

A synthesis of the Calculated/Experimental (C/E) results for the In-115(n,n')In-115m, Ni-58(n,p)Co-58 and Al-27(n,α)Na-24 threshold dosimeters, in terms of equivalent fission flux ratios, are respectively reported in FIG. 4.11, FIG. 4.12 and FIG. 4.13.
Deviations contained within ±5% from the 386 dosimeter experimental data were obtained in about 85% of the calculated results with BUGENDF70.BOLIB and in about 88% of the results with BUGLE-96. The calculated equivalent fission fluxes for both the libraries were practically within the desired target accuracy of ±10% (see TAB. 4.7), recommended by OECD-NEA.

TAB. 4.7

VENUS-3 - Percentages[a] of the Calculated (C) Equivalent Fission Fluxes with Deviations Exceeding 5% and 10% the Corresponding Experimental (E) Fluxes.

| Library | In115(n,n') | Ni-58(n,p) | Al-27(n,α) |
|---|---|---|---|
| | \|C-E\| / E > 5% | | |
| BUGENDF70 | 3.8% | 19.7% | 18.4% |
| BUGLE-96 | 3.8% | 12.3% | 28.9% |
| | | | |
| Library | In115(n,n') | Ni-58(n,p) | Al-27(n,α) |
| | \|C-E\| / E > 10% | | |
| BUGENDF70 | 0.0% | 1.2% | 0.0% |
| BUGLE-96 | 0.0% | 1.6% | 2.6% |

([a]) Percentages calculated on the total number of each dosimeter type: 104 for In, 244 for Ni and 38 for Al.

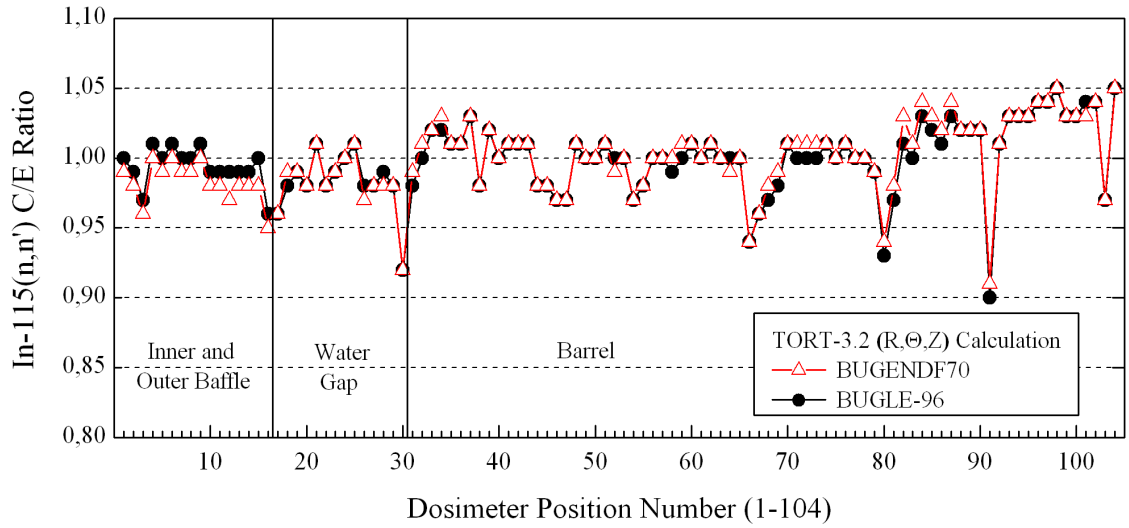


FIG. 4.11 VENUS-3 - In-115(n,n') Equivalent Fission Flux Ratios (Calculated/Experimental).

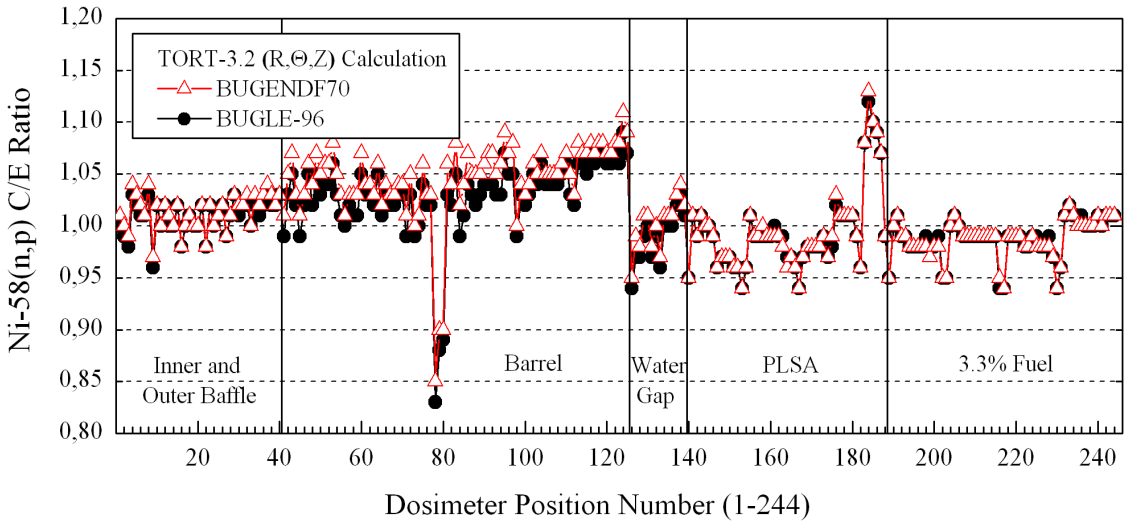


FIG. 4.12 VENUS-3 - Ni-58(n,p) Equivalent Fission Flux Ratios (Calculated/Experimental).

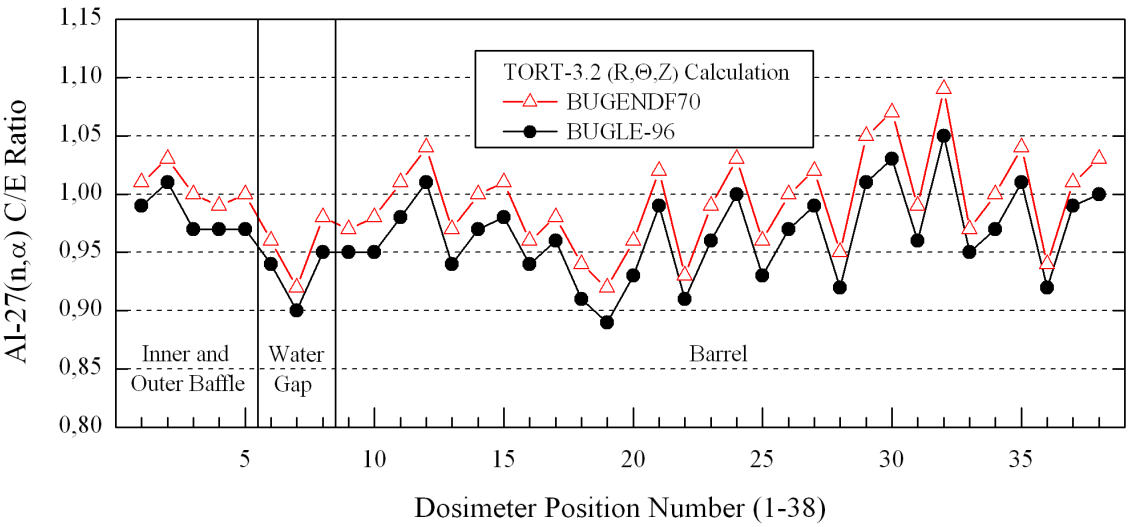


FIG. 4.13 VENUS-3 - Al-27(n,α) Equivalent Fission Flux Ratios (Calculated/Experimental).

## 5 - CONCLUSION

A new coupled neutron and photon broad-group working cross section library for LWR shielding and pressure vessel dosimetry applications was generated with the name BUGENDF70.BOLIB. Two versions of the library in FIDO-ANISN format are available in the dedicated package: BUGENDF70.BOLIB, without upscattering cross sections in the thermal neutron energy region, and BUGENDF70T.BOLIB, including the upscattering cross sections. This library, in the BUGLE-96 neutron and photon energy group structures (47 n + 20 $\gamma$), was obtained through problem-dependent cross section collapsing from the VITENDF70.BOLIB fine-group general-purpose library in AMPX format, based on ENDF/B-VII.0 nuclear data and generated in the VITAMIN-B6 neutron and photon energy group structures (199 n + 42 $\gamma$). The BUGENDF70.BOLIB library was processed with an updated and corrected version of the SCAMPI data processing system, the ENEA-Bologna 2007 Revision, already freely available at OECD-NEA Data Bank and at ORNL-RSICC. The library was preliminarily validated on two engineering neutron shielding benchmark experiments (PCA-Replica 12/13 and VENUS-3), specifically designed for the improvement of the accuracy of the LWR radiation shielding and radiation damage calculations. The calculated results for both the integral experiments are practically within the desired target accuracy value of ±10%. Further validation of the BUGENDF70.BOLIB library will be performed on other integral neutron shielding benchmark experiments.

The possibility is being studied to obtain from the VITENDF70.BOLIB library a new broad-group working library in FIDO-ANISN format with an increased number of thermal neutron energy groups with respect to those included in the BUGLE-96 library. This to permit more accurate analyses of the thermal neutron and photon radiation damage in applications where these contributions to the total damage are not negligible.

It is believed that it should be very important to further promote, at the international level (UNO-IAEA, OECD-NEA, industrial organizations, R&D institutions, etc.), the generation of new working cross section libraries for radiation shielding applications, dedicated to various types of Generation III and IV nuclear fission reactors with different spectral, geometrical and compositional specifications. In fact the availability of these libraries could promote, in particular, the use of the three-dimensional deterministic codes in radiation shielding and radiation damage applications for nuclear safety. This is increasingly requested, due to the fact that these transport codes (TORT, PARTISN, KATRIN, etc.) have now sophisticated possibilities of complex geometry description, through modern dedicated pre/post-processor systems (BOT3P, TORTWARE, etc.) for the automatic generation of the spatial meshes.

In general, the severe nuclear accidents to the PWR unit No. 2 of the Three Mile Island (Harrisburg, US, March 28, 1979) nuclear power plant and, just recently, to the BWR units No. 1, 2 and 3 of the Fukushima Dai-ichi (Japan, March 11, 2011) nuclear power plant, emphasized and confirmed that the structural integrity of the LWR pressure vessel is one of the most relevant key factors within the defence-in-depth approach of the LWR nuclear safety. The RPV structural integrity is particularly important for PWR long term operations, especially when approaching the End-of-Life (EoL) neutron fluence values in the pressure vessel. The monitoring and the evaluation of the degradation of the RPV materials require not only suitable experimental techniques (reactor dosimetry, thermo-mechanical tests on RPV steels, etc.) but also proven calculation tools as, e.g., group working cross section libraries

like BUGLE-96, BUGLE-B7, BUGJEFF311.BOLIB or BUGENDF70.BOLIB which can play a crucial role to quantify accurately the neutron and photon radiation damage to the pressure vessel, during the whole LWR lifetime.

## REFERENCES

/1/ M. Pescarini, V. Sinitsa, R. Orsi, Generation and Preliminary Testing of ENEA-Bologna BUGLE-Type Group Libraries Based on JEFF-3.1 and ENDF/B-VII.0 Nuclear Data for LWR Shielding and Pressure Vessel Dosimetry, Proceedings of the International Conference on the Physics of Reactors (PHYSOR'08) "Nuclear Power: A Sustainable Resource", Interlaken, Switzerland, September 14-19, 2008. ENEA-Bologna Technical Report FPN-P9H6-012, October 3, 2008.

/2/ M. Pescarini, V. Sinitsa, R. Orsi, M. Frisoni, Processing and Validation of JEFF-3.1.1 and ENDF/B-VII.0 Group-Wise Cross Section Libraries for Shielding Calculations, Proceedings of the 3rd International Workshop on Nuclear Data Evaluation for Reactor Applications (WONDER-2012), Aix-en-Provence, France, September 25-28, 2012. ENEA-Bologna Technical Report UTFISSM-P9H6-007, October 3, 2012.

/3/ Computing Radiation Dose to Reactor Pressure Vessel and Internals, State of the Art Report, OECD-NEA Nuclear Science Committee, NEA/NSC/DOC(96)5, 1997.

/4/ W.W. Engle, Jr., A Users Manual for ANISN, A One Dimensional Discrete Ordinates Transport Code with Anisotropic Scattering, ORNL K-1693, Updated June 6, 1973. Available from OECD-NEA Data Bank as CCC-254 ANISN-ORNL.

/5/ M. Pescarini, V. Sinitsa, R. Orsi, M. Frisoni, VITENDF70.BOLIB - An ENDF/B-VII.0 Multigroup Coupled (199 n + 42 γ) Cross Section Library in AMPX Format for Nuclear Fission Applications, ENEA-Bologna Technical Report UTFISSM-P9H6-005, May 25, 2012. Available from OECD-NEA Data Bank as NEA-1870/01 ZZ VITENDF70.BOLIB.

/6/ M.B. Chadwick et al., ENDF/B-VII.0: Next Generation Evaluated Nuclear Data Library for Nuclear Science and Technology, Nuclear Data Sheets, Volume 107, Number 12, pp. 2931-3060, December 2006.

/7/ I.I. Bondarenko, M.N. Nikolaev, L.P. Abagyan, N.O. Bazaziants, Group Constants for Nuclear Reactors Calculations, Consultants Bureau, New York, 1964.

/8/ J.E. White, D.T. Ingersoll, R.Q. Wright, H.T. Hunter, C.O. Slater, N.M. Greene, R.E. MacFarlane, R.W. Roussin, Production and Testing of the Revised VITAMIN-B6 Fine-Group and the BUGLE-96 Broad-Group Neutron/Photon Cross-Section Libraries Derived from ENDF/B-VI.3 Nuclear Data, Oak Ridge, ORNL Report ORNL-6795/R1, NUREG/CR-6214, Revision 1, January 1995. VITAMIN-B6 library available from OECD-NEA Data Bank as DLC-0184 ZZ VITAMIN-B6. BUGLE-96 library available from OECD-NEA Data Bank as DLC-0185 ZZ BUGLE-96.

/9/ P.F. Rose, ENDF/B-VI Summary Documentation, Brookhaven National Laboratory, BNL-NCS-17541 (ENDF-201) 4th Edition, October 1991.

/10/ W.A. Rhoades, D.B. Simpson, The TORT Three-Dimensional Discrete Ordinates Neutron/Photon Transport Code (TORT Version 3), Oak Ridge, ORNL Report ORNL/TM-13221, October 1997.

/11/ J.F. Briesmeister Ed., MCNP - A General Monte Carlo N-Particle Transport Code, Version 4C, Los Alamos, LANL Report LA-13709-M, April 2000.

/12/ R. Orsi, BOT3P Version 5.3: A Pre/Post-Processor System for Transport Analysis, ENEA-Bologna Technical Report FPN-P9H6-011, October 22, 2008. Available from OECD-NEA Data Bank as NEA-1678/09 BOT3P-5.3.

/13/ R. Orsi, The ENEA-Bologna pre-post-Processor Package BOT3P for the DORT and TORT Transport Codes (Version 1.0 - December 1999), JEF/DOC-828, JEFF Working Group Meeting on Benchmark Testing, Data Processing and Evaluations, OECD-NEA Data Bank, Issy-les-Moulineaux, France, May 22-24, 2000.

/14/ R. Orsi, BOT3P: Bologna Transport Analysis Pre-Post-Processors Version 1.0, Nuclear Science and Engineering, Technical Note, Volume 142, pp. 349-354, 2002.

/15/ R. Orsi, BOT3P: Bologna Transport Analysis Pre-Post-Processors Version 3.0, Nuclear Science and Engineering, Technical Note, Volume 146, pp. 248-255, 2004.

/16/ Y. Hirao, K. Ahiko, TORTWARE: Development of an Input-Making Support System for a Three-Dimensional Deterministic $S_N$ Code, TORT, Journal of Nuclear Science and Technology, Volume 47, Number 2, pp. 127-135, 2010.

/17/ R.E. MacFarlane, NJOY-99, "README0", ORNL, RSIC Peripheral Shielding Routine Collection PSR-0480/02, December 31, 1999.

/18/ SCAMPI Collection of Codes for Manipulating Multigroup Cross Section Libraries in AMPX Format, ORNL, RSIC Peripheral Shielding Routine Collection PSR-352, September 1995. Available from OECD-NEA Data Bank as PSR-0352/05 SCAMPI, version of the ORNL SCAMPI system corresponding to the last ENEA-Bologna 2007 Revision (see /19/).

/19/ V. Sinitsa, M. Pescarini, ENEA-Bologna 2007 Revision of the SCAMPI (ORNL) Nuclear Data Processing System, ENEA-Bologna Technical Report FPN-P9H6-006, September 13, 2007.

/20/ The JEFF-3.1.1 Nuclear Data Library, JEFF Report 22, OECD-NEA Data Bank, 2009.

/21/ The JEFF-3.1 Nuclear Data Library, JEFF Report 21, OECD-NEA Data Bank, 2006.

/22/ A.J. Koning, E. Bauge, C.J. Dean, E. Dupont, U. Fischer, R.A. Forrest, R. Jacqmin, H. Leeb, M.A. Kellet, R.W. Mills, C. Nordborg, M. Pescarini, Y. Rugama, P. Rullhusen, Status of the JEFF Nuclear Data Library, Proceedings of the International Conference on Nuclear Data for Science and Technology (ND-2010), Jeju Island, Korea, April 26-30, 2010, Journal of the Korean Physical Society, Volume 59, No.2, pp. 1057-1062, August 2011. ENEA-Bologna Technical Report UTFISSM-P9H6-001, July 8, 2010.

/23/ N.M. Greene, W.E. Ford III, L.M. Petrie, J.W. Arwood, AMPX-77 - A Modular Code System for Generating Coupled Multigroup Neutron-Gamma Cross-Section Libraries from ENDF/B-IV and/or ENDF/B-V, Oak Ridge, ORNL Report ORNL/CSD/TM-283, October 1992. Available from OECD-NEA Data Bank as PSR-0315/01 AMPX-77.

/24/ SCALE: A Comprehensive Modeling and Simulation Suite for Nuclear Safety Analysis and Design, Oak Ridge, ORNL Report ORNL/TM-2005/39, Version 6.1, June 2011. Available from OECD-NEA Data Bank as CCC-0785/01 SCALE-6.1.

/25/ J. Butler, M.D. Carter, I.J. Curl, M.R. March, A.K. McCracken, M.F. Murphy, A. Packwood, The PCA-Replica Experiment Part I Winfrith Measurements and Calculations, UKAEA, AEE Winfrith Report AEEW-R 1736, January 1984.

/26/ J. Butler, The NESTOR Shielding and Dosimetry Improvement Programme NESDIP for PWR Applications, PRPWG/P (82)5, Internal UKAEA Document, November 1982.

/27/ L. Leenders, LWR-PVS Benchmark Experiment VENUS-3 (with Partial Shielded Assemblies) - Core Description and Qualification, Mol, SCK/CEN Report FCP/VEN/01, September 1, 1988.

/28/ Radiation Shielding Integral Benchmark Archive Database (SINBAD), OECD-NEA Data Bank/ ORNL-RSICC, SINBAD REACTOR, NEA-1517, 2009 Edition.

/29/ I. Kodeli, E. Sartori, B. Kirk, SINBAD Shielding Benchmark Experiments Status and Planned Activities, The American Society's 14$^{th}$ Biennial Topical Meeting of the Radiation Protection and Shielding Division, Carlsbad, New Mexico, USA, April 3-6, 2006.

/30/ M. Pescarini, V. Sinitsa, R. Orsi, M. Frisoni, BUGJEFF311.BOLIB - A JEFF-3.1.1 Broad-Group Coupled (47 n + 20 γ) Cross Section Library in FIDO-ANISN Format for LWR Shielding and Pressure Vessel Dosimetry Applications, ENEA-Bologna Technical Report UTFISSM-P9H6-002, May 12, 2011. ENEA-Bologna Technical Report UTFISSM-P9H6-002 Revision 1 published on March 14, 2013. Available from OECD-NEA Data Bank as NEA-1866/01 ZZ BUGJEFF311.BOLIB.

/31/ M. Pescarini, V. Sinitsa, R. Orsi, VITJEFF311.BOLIB - A JEFF-3.1.1 Multi-Group Coupled (199 n + 42 γ) Cross Section Library in AMPX Format for Nuclear Fission Applications, ENEA-Bologna Technical Report UTFISSM-P9H6-003, November 10, 2011. ENEA-Bologna Technical Report UTFISSM-P9H6-003 Revision 1 published on March 14, 2013. Available from OECD-NEA Data Bank as NEA-1869/01 ZZ VITJEFF311.BOLIB.

/32/ J.M. Risner, D. Wiarda, M.E. Dunn, T.M. Miller, D.E. Peplow and B.W. Patton, Production and Testing of the VITAMIN-B7 Fine-Group and BUGLE-B7 Broad-Group Coupled Neutron/Gamma Cross-Section Libraries Derived from ENDF/B-VII.0 Nuclear Data, Oak Ridge, ORNL Report ORNL/TM-2011/12, NUREG/CR-7045, September 2011. Available from OECD-NEA Data Bank as DLC-0245/02 ZZ VITAMINB7/BUGLEB7.

/33/ M. Pescarini, Data Processing and Validation Needs of Group-Wise Working Cross Section Libraries for Nuclear Fission Reactor Shielding and Radiation Damage Applications, Proceedings of the IAEA Technical Meeting in collaboration with NEA on Specific Applications of Research Reactors: Provision of Nuclear Data, IAEA, Vienna, Austria, October 12-16, 2009, IAEA INDC(NDS)-0574, pp. 218-225, July 2010. ENEA-Bologna Technical Report FISNUC-P9H6-001, December 16, 2009.

/34/ American National Standard, American Nuclear Society, Neutron and Gamma-Ray Cross Sections for Nuclear Radiation Protection Calculations for Nuclear Power Plants, ANSI/ANS-6.1.2-1999 (R2009).

/35/ DOORS3.1 One-, Two- and Three-Dimensional Discrete Ordinates Neutron/Photon Transport Code System, ORNL, RSIC Computer Code Collection CCC-650, August 1996. Available from OECD-NEA Data Bank as CCC-0650/04 DOORS-3.2A.

/36/ R.E. Alcouffe, R.S. Baker, J.A. Dahl, S.A. Turner, R. Ward, PARTISN: A Time-Dependent, Parallel Neutral Particle Transport Code System, Los Alamos, LANL Report LA-UR-08-07258, Revised November 2008. Available from OECD-NEA Data Bank as CCC-0760/01 PARTISN-5.97.

/37/ A.M. Voloschenko, S.V. Gukov, V.P. Kryuchkov, A.A. Dubinin, O.V. Sumaneev, The CNCSN One-, Two- and Three-Dimensional Coupled Neutral and Charged Particle Discrete Ordinates Code Package, Proceedings of the International Topical Meeting on Mathematics and Computation, Supercomputing, Reactor Physics and Nuclear and Biological Applications (M&C-2005), Avignon, France, September 12-15, 2005. Available from OECD-NEA Data Bank as CCC-0726/02 CNCSN 2009.

/38/ TRANSX 2.15 Code System to Produce Neutron, Photon, and Particle Transport Tables for Discrete - Ordinates and Diffusion Codes from Cross Sections in MATXS Format, ORNL, RSIC Peripheral Shielding Routine Collection PSR-317, February 1995. Available from OECD-NEA Data Bank as PSR-0317/03 TRANSX-2.15.

/39/ E. Botta, G. Saiu, R. Orsi, M. Pescarini, Westinghouse AP1000 Internals Heating Rate Distribution Calculation Using a 3D Deterministic Transport Method, Proceedings of the 13$^{th}$ International Conference on Nuclear Engineering (ICONE-13), Bejing, China, May 16-20, 2005. ENEA-Bologna Technical Report FIS-P9H6-009, May 19, 2005.

/40/ G. Longoni, S.L. Anderson, Reactor Dosimetry Applications Using RAPTOR-M3G: A New Parallel 3-D Radiation Transport Code, Proceedings of the 13$^{th}$ International Symposium on Reactor Dosimetry (ISRD-13), Akersloot, The Netherlands, May 25-30, 2008.

/41/ F.A. Alpan, S.L. Anderson, A New ENDF/B-VII.0 Based Multigroup Cross-Section Library for Reactor Dosimetry, Proceedings of the 13$^{th}$ International Symposium on Reactor Dosimetry (ISRD-13), Akersloot, The Netherlands, May 25-30, 2008.

/42/ T.A. Wareing, J.M. McGhee, J.E. Morel, ATTILA: A Three-Dimensional, Unstructured Tetrahedral Mesh Discrete Ordinates Transport Code, Transactions of the American Nuclear Society, Volume 75, pp. 146-147, 1996.

/43/ M. Pescarini, V. Sinitsa, R. Orsi, MATJEFF31.BOLIB - A JEFF-3.1 Multigroup Coupled (199 n + 42 $\gamma$) Cross Section Library in MATXS Format for Nuclear Fission Applications, ENEA-Bologna Technical Report FPN-P9H6-014, May 5, 2009. Available from OECD-NEA Data Bank as NEA-1847/01 ZZ MATJEFF31.BOLIB.

/44/ M. Pescarini, V. Sinitsa, R. Orsi, VITJEFF31.BOLIB - A JEFF-3.1 Multigroup Coupled (199 n + 42 $\gamma$) Cross Section Library in AMPX Format for Nuclear Fission Applications, ENEA-Bologna Technical Report FPN-P9H6-007, February 18, 2008. Available from OECD-NEA Data Bank as NEA-1801/01 ZZ VITJEFF31.BOLIB.

/45/ M. Pescarini, V. Sinitsa, R. Orsi, ENEA-Bologna Production and Testing of JEFF-3.1 Multi-Group Cross Sections Libraries for Nuclear Fission Applications, Proceedings of the International Conference on Nuclear Data for Science and Technology (ND-2007), Nice, France, April 22-27, 2007, EDP Sciences, Volume 1, pp. 705-708, 2008. ENEA-Bologna Technical Report FPN-P9H6-005, June 7, 2007.

/46/ M. Pescarini, R. Orsi, T. Martinelli, A.I. Blokhin, V. Sinitsa, ENEA-Bologna Production and Testing of JEF-2.2 Multi-Group Cross Sections Libraries for Nuclear Fission Applications, Proceedings of the International Topical Meeting on Mathematics and Computation, Supercomputing, Reactor Physics and Nuclear and Biological Applications (M&C-2005), Avignon, France, September 12-15, 2005. ENEA-Bologna Technical Report FIS-P9H6-012, October 19, 2005.

/47/ M. Pescarini, R. Orsi, T. Martinelli, A.I. Blokhin, V. Sinitsa, MATJEF22.BOLIB - A JEF-2.2 Multigroup Coupled (199 n + 42 γ) Cross Section Library in MATXS Format for Nuclear Fission Applications, ENEA-Bologna Technical Report FIS-P815-007, June 6, 2004. Available from OECD-NEA Data Bank as NEA-1740/01 ZZ MATJEF22.BOLIB.

/48/ M. Pescarini, R. Orsi, T. Martinelli, A.I. Blokhin, V. Sinitsa, VITJEF22.BOLIB - A JEF-2.2 Multigroup Coupled (199 n + 42 γ) Cross Section Library in AMPX Format for Nuclear Fission Applications, ENEA-Bologna Technical Report FIS-P815-001, April 16, 2003. Available from OECD-NEA Data Bank as NEA-1699/01 ZZ VITJEF22.BOLIB.

/49/ M. Pescarini, R. Orsi, T. Martinelli, Automatic Generation of 3D Fine Mesh Geometries for the Analysis of the VENUS-3 Shielding Benchmark Experiment with the TORT Code, Proceedings of the International Conference on Supercomputing in Nuclear Applications (SNA-2003), Paris, France, September 22-24, 2003. ENEA-Bologna Technical Report FIS-P815-004, October 22, 2003.

/50/ M. Pescarini, R. Orsi, M.G. Borgia, T. Martinelli, ENEA Nuclear Data Centre Neutron Transport Analysis of the VENUS-3 Shielding Benchmark Experiment, ENEA-Bologna Technical Report SIEC-KT-SCG-00013, March 19, 2001. The PDF electronic version of the cited ENEA Technical Report is included in the NEA-1517 SINBAD REACTOR (ORNL-RSICC/ OECD-NEA Data Bank) international database of fission reactor shielding benchmark experiments (see /27/).

/51/ Prediction of Neutron Embrittlement in the Reactor Pressure Vessel: VENUS-1 and VENUS-3 Benchmarks, NEA/NSC/DOC(2000)5, OECD-NEA NSC, 2000.

/52/ M. Pescarini, M.G. Borgia, R. Orsi, T. Martinelli, ENEA-Bologna Validation of the BUGLE-96 ENDF/B-VI Library on the VENUS-1 Neutron Shielding Benchmark Experiment - A Synthesis of the Final Results, ENEA-Bologna Technical Report SIEC-KT-SCG-00005, 1999. JEF/DOC-778, JEFF Working Group Meeting on Benchmark Testing, Data Processing and Evaluations, OECD-NEA Data Bank, Issy-les-Moulineaux, France, April 12-14, 1999.

/53/ M. Pescarini, M.G. Borgia, R. Orsi, VENUS-1 Benchmark Experiment Details and Results of the ENEA-Bologna Calculations, Second Meeting of the OECD-NEA Nuclear Science Committee Task Force on Computing Radiation Dose and Modelling of Radiation-Induced Degradation of Reactor Components (TFRDD), Paris, France, March 3-4, 1998.

/54/ O.Bersillon, L.R. Greenwood, P.J. Griffin, W. Mannhart, H.J. Nolthenius, R. Paviotti-Corcuera, K.I. Zolotarev, E.M. Zsolnay, International Reactor Dosimetry File 2002 (IRDF-2002), IAEA, Vienna, Austria, Technical Reports Series No. 452, 2006.

/55/ R. Orsi, M. Pescarini, V. Sinitsa, IRDF-2002 Dosimetry Cross Section Processing in the BUGLE-96 (47 n) Neutron Group Structure Using Flat and Updated Problem Dependent Neutron Spectra, ENEA-Bologna Technical Report UTFISSM-P9H6-006, May 9, 2012.

/56/ M. Herman (Editor), ENDF-6 Formats Manual: Data Formats and Procedures for the Evaluated Nuclear Data File ENDF/B-VI and ENDF/B-VII, Technical Report BNL-NCS-44945-05-Rev, Document ENDF-102, BNL, June 2005.

/57/ M. Mattes and J. Keinert, Thermal Neutron Scattering Data for the Moderator Materials $H_2O$, $D_2O$ and $ZrH_x$ in ENDF-6 Format and as ACE Library for MCNP(X) Codes, Report INDC(NDS)-0470, IAEA, April 2005.

/58/ M.B. Emmet, The MORSE Monte Carlo Radiation Transport Code System, Oak Ridge National Laboratory, ORNL-4972, February 1975; ORNL-4972/R1, February 1983; ORNL-4972/R2, July1984; ORNL-4972/R3 draft, June 1993. Available from OECD-NEA Data Bank as CCC-0474 MORSE-CGA.

/59/ C.R. Weisbin, R.W. Roussin, J.J. Wagschal, J.E. White, R.Q. Wright, VITAMIN-E: An ENDF/B-V Multigroup Cross-Section Library for LMFBR Core and Shield, LWR Shield, Dosimetry and Fusion Blanket Technology, Oak Ridge National Laboratory, ORNL-5505 (ENDF-274), February 1979. Available from OECD-NEA Data Bank as DLC-0113/VITAMIN-E.

/60/ E. Sartori, VITAMIN-J, a 175 group Neutron Cross Section Library Based on JEF-1 for Shielding Benchmark Calculations, OECD-NEA Data Bank, JEF/DOC-100 Preliminary, October 1985.

/61/ R.W. Roussin, C.R. Weisbin, J.E. White, N.M. Greene, R.Q. Wright, J.B. Wright, VITAMIN-C: The CTR Processed Multigroup Cross Section Library for Neutronics Studies, Oak Ridge National Laboratory, ORNL/RSIC-37, 1980. Available from OECD-NEA Data Bank as DLC-0041/VITAMIN-C.

/62/ International Handbook of Evaluated Criticality Safety Benchmark Experiments (ICSBEP), OECD-NEA Nuclear Science Committee, NEA/NSC/DOC(95)03, September 2004 Edition.

/63/ J.K. Tuli, Nuclear Wallet Cards ($5^{th}$ Edition), National Nuclear Data Centre, Brookhaven National Laboratory, Upton, New York 11973, USA, July 1995.

/64/ D.E. Cullen, PREPRO 2007: 2007 ENDF/B Pre-processing Codes (ENDF/B-VII Tested), LLNL, owned, maintained and distributed by IAEA-NDS, Vienna, Austria, IAEA Report IAEA-NDS-39, Rev. 13, March 17, 2007. Available from OECD-NEA Data Bank as IAEA-1379 PREPRO-2007.

/65/ R. Orsi, ADEFTA Version 4.1: A Program to Calculate the Atomic Densities of a Compositional Model for Transport Analysis, ENEA FPN-P9H6-010, May 20, 2008. Available from OECD-NEA Data Bank as NEA-1708 ADEFTA 4.1.

/66/ J.H. Baard, W.L. Zijp, H.J. Nolthenius, Nuclear Data Guide for Reactor Neutron Metrology, Kluwer Academic Publishers, 1989.

/67/ J.K. Tuli, Nuclear Wallet Cards ($6^{th}$ Edition), National Nuclear Data Centre, Brookhaven National Laboratory, Upton, New York 11973-5000, USA, January 2000.

/68/ G. Hehn, A. Sohn, M. Mattes, G. Pfister, IKE Calculations of the OECD-NEA Benchmarks VENUS-1 and VENUS-3 for Computing Radiation Dose to Reactor Pressure Vessel and Internals, Universität Stuttgart, Institut für Kernenergetik und Energiesysteme, IKE 6 NEA 2, December 1997.

/69/ R.E. Maerker, Analysis of the VENUS-3 Experiments, ORNL/TM-11106, NUREG/CR-5338, August 1989.